



27th

**International Colloquium
on the Dynamics of
Explosions and Reactive Systems**

**Sunday 28th July
–
Friday 2nd August 2019**

Beijing, China



27th International Colloquium on the Dynamics of Explosions and Reactive Systems

July 28 – August 2, 2019 • Beijing, China

Organizer

INSTITUTE FOR DYNAMICS OF EXPLOSIONS AND REACTIVE SYSTEMS

Officers

Nabiha CHAUMEIX (President), Eric PETERSEN (Vice President), Scott I. JACKSON (Treasurer), Kaoru MARUTA (Secretary)

Board of Directors

Luc BAUWENS, Jeff BERGTHORSON, Nabiha CHAUMEIX, Aswhin CHINNAYYA, Gabriel CICCARELLI, Sergei B. DOROFEEV, Scott I. JACKSON, In-Seuck JEUNG, Yiguang JU, Jiro KASAHARA, Francesco MARRA, Kaoru MARUTA, Oleg G. PENYAZKOV, Eric PETERSEN, Uwe RIEDEL, Antonio SANCHEZ, Andrzej TEODORCZYK, Anatoly A. VASIL'EV, Jian-Ping WANG, Ming-Hsun WU

Co-organizers

PEKING UNIVERSITY
NATIONAL NATURAL SCIENCE FOUNDATION OF CHINA
CHINESE SOCIETY OF ENGINEERING THERMOPHYSICS
CHINESE SOCIETY OF MECHANICS
CHINESE SOCIETY OF AERODYNAMICS
CHINESE SOCIETY OF AERONAUTICS AND ASTRONAUTICS
CHINESE SOCIETY OF ASTRONAUTICS

Program Committee

Gabriel CICCARELLI (Chair), Jiro KASAHARA (Co-Chair), Eric PETERSON (Co-Chair), Ben AKIH, Regis BAUWENS, Jeff BERGTHORSON, Yei-Chin CHAO, Nabiha CHAUMEIX, Jeong-Yeol CHOI, Ashwin CHINNAYYA, Andrea COMANDINI, Sergei B. DOROFEEV, Takuma ENDO, Matthew FOTIA, Vadim GAMEZO, Andrew HIGGINS, Kazuhiro ISHII, Scott JACKSON, In-Seuck JEUNG, Francesco MARRA, Salvador NAVARRO-MARTINEZ, Akiko MATSUO, Remy MEVEL, Hoi Dick NG, Matei RADULESCU, Steven SHY, Pierre VIDAL, Bing WANG, Jennifer WEN

Local Advisory Committee

Ping HAO (Chair, President of Peking University), Yilong BAI, Weimin BAO, Maozhang CHEN, Shiyi CHEN, Yong CHEN, Heping CHENG, Juzhi CUI, Weinan E, Weicheng FAN, Daining FANG, Xiaohua GAN, Wen GAO, Song GAO, Qihuang GONG, Liejin GUO, Ru HUANG, Guowei HE, Xiantu HE, Yaling HE, Xiao HOU, Wenrui HU, Lin HUANG, Ru HUANG, Song JIANG, Hongguang JIN, Jialing LE, Chunxuan LI, Jiachun LI, Yinghong LI, Daxiang LIU, Zhongfan LIU, Chung K. LAW, Mu MU, Jinren NI, Jinping OU, Yangqi OU, Zhiming QIU, Wanhua SU, Chengwei SUN, Cong SUN, Shu TAO, Binggang TONG, Enge WANG, Liheng WANG, Zhenguo WANG, Yueguang WEI, Jianzhong XU, Yimin XUAN, Wei YANG, Wei

YANG, Zeyong YIN, Hongru YU, Dongxiao ZHANG, Hanxin ZHANG, Pingwen ZHANG, Weiyang ZHANG, Heng ZHOU, Fengchen ZHUANG, Heng ZHOU

Local Academic Committee

Chunhua BAI, Shulin BAI, Wen BAO, Guobiao CAI, Linqun CHEN, Weifang CHEN, Xiaowei CHEN, Xu CHENG, Yingchun CHEN, Yue CHEN, Chengqi CHEN, Lanhong DAI, Shuiting DING, Yong DING Huiling DUAN, Yuanyuan DUAN, Zhuoyi DUAN, Jianren FAN, Shaolin FAN, Wei FAN, Weijun FAN, Xuejun FAN, Xihui FANG, Chuanbo FANG, Changgen FENG, Xiqiao FENG, Song FU, Qiang GANG, Bo GAO, Ge GAO, Xiang GAO, Chengqi GUAN, Junhong GUO, Kun GUO, Zhaoli GUO, Fei HE, Guoqiang HE, Limin HE, Liming HE, Xiaomin HE, Hong GUO, Liu HONG, Yanji HONG, Haibo HU, Gengkai HU, Zhiyun HU, Fenglei HUANG, Weina HUANG, Zhen HUANG, Yue HUANG, Peixue JIANG, Zhen HUANG, Zuohua HUANG, Jun JI, Peixue JIANG, Zonglin JIANG, Jie JIN, Wenjun KONG, Bin LI, Cunbiao LI, Feng LI, Guangxi LI, Hongxin LI, Jianrong LI, Ming LI, Shuiqing LI, Xiangyuan LI, Xiaojie LI, Xiaoping LI, Xinliang LI, Weina HUANG, Caiyun LIANG, Guozhu LIANG, Jianhan LIANG, Xingang LIANG, Qiang LIAO, Wenhui LING, Fushui LIU, Naian LIU, Sen LIU, Tingyi LIU, Weidong LIU, Xiaoyong LIU, Yongquan LIU, Zhende LIU, Zhirang LIU, Wuqiang LONG, Xingcai LU, Xiyun LU, Ercang LUO, Xisheng LUO, Zhongyang LUO, Longlong MA, Qingguo MENG, Songhe MENG, Jianchun MI, Zeyao MO, Mingjiu NI, Baisheng NIE, Haitao NIE, Wansheng NIE, Fei QI, Hongfu QIANG, Yuxin REN, Changsheng RUI, Shoutang SHANG, Zhensu SHE, Qing SHEN, Weiwei SHEN, Yixiang SHI, Xinxing SHI, Gequn SHU, Shuangwen SONG, Wenyan SONG, Yingdong SONG, Dejun SUN, Xiaofeng SUN, Yonghua TAN, Hao TANG, Shaoqiang TANG, Zhigong TANG, Zhi TAO, Baolin TIAN, Bo WANG, Cheng WANG, Fei WANG, Ge WANG, Jianguo WANG, Jian-Ping WANG, Jianxiang WANG, Jue WANG, Ningfei WANG, Qiuwang WANG, Ruzhu WANG, Taikun WANG, Tianyou WANG, Xiaohong WANG, Zhanxue WANG, Haiqiao WEI, Xiaolin WEI, Quan WEN, Chunsheng WENG, Peifen WENG, Qiang WU, Ji WU, Longxu XIAO, Rui XIAO, Hongyu XIE, Hongyu XIE, Minghou XU, Xu XU, Jianhua YAN, Jiming YANG, Chunde YAO, Hong YAO, Mingfa YAO, Qiang YAO, Daren YU, Qingming ZHANG, Xinyu ZHANG, Yongjiu ZHANG, Yuyin ZHANG, Jianheng ZHAO, Qingjun ZHAO, Lili ZHENG, Longxi ZHENG, Yao ZHENG, Tao ZHI, Huaichun ZHOU, Hui ZHOU, Yichun ZHOU, Junqiang ZHU, Xun ZHU

Local Organizing Committee

Jian-Ping WANG (Chair), Zheng CHEN (Secretary-General), Yue YANG (Academic Affairs), Jianling LI (Public Relations), Juntao CHANG, Gang DONG, Xingang Dong, Yuxin FAN, Qiang GANG, Wei GAO, Ceji FU, Qixiang HAN, Wenhua HAN, Longhua HU, Jie HUANG, Jie JI, Jianzhong LI, Junwei LI, Rong LI, Shuiqing LI, Yuyang LI, Zhihui LI, Huan LIAN, Zhiyong LIN, Dong LIU, Haifeng LIU, Shijie LIU, Yunfeng LIU, Kun LUO, Zhenbing LUO, Hu MA, Tongling MA, Xiaoqi MA, Jianguo PENG, Xiaowen QIN, Hua QIU, Zhuyin REN, Yetao SHAO, Chongbin SHEN, Mingbo SUN, Quanhua SUN, Yuanxiang SUN, Huijun TAN, Honghui TENG, Zhenyu TIAN, Aifeng WANG, Bing WANG, Fei WANG, Jinhua WANG, Ying WANG, Yuhui WANG, Zhi WANG, Zhiwu WANG, Yun WU, Yu YAN, Jiemei YANG, Mohan YANG, Yancheng YOU, Yongliang YU, Huiyan ZHANG, Jianhui ZHANG, Shanshan ZHANG, Huanjuan ZHAO, Qingjun ZHAO, Mengwei ZHENG, Xianxu ZHENG, Zhonghua ZHENG, Rui ZHOU, Weixing ZHOU

Message from the President	1
Message from the Program Committee Chairs	2
Message from the Host Committee Chair	4
Organizers & Sponsors	5
General Information	6
Transportation	8
Presenter Instructions	10
Social Program Information	12
Maps for Reference	15
Program at a Glance	21
Technical Program	22
Monday	22
Tuesday	26
Wednesday	29
Thursday	30
Friday	34
Regular Poster	37
Work-In-Progress Poster	44
Oral Abstracts	49
Monday	49
Tuesday	66
Wednesday	81
Thursday	86
Friday	104
Regular Poster Abstracts	116
WIP Abstracts	141

Message from the President

On behalf of the Board of Institute for Dynamics of Explosions and Reactive Systems (IDERS), I am delighted to welcome you to the 27th International Colloquium on the Dynamics of Explosions and Reactive Systems.

The 27th ICDERS is a continuation in the series of biannual international colloquia that have been held throughout the world since 1967. For the first time, the colloquium is being held in China.

The colloquium would not have been held without the host committee in Beijing chaired by Prof. Jian-Ping WANG and the Program Committee Gabriel CICCARELLI (Chair), Jiro KASAHARA (Co-Chair), Eric PETERSEN (Co-Chair). I would like to express to them my deepest thanks for their wonderful work in organizing the conference that I am sure you will find enjoyable and fruitful.

I hope that you will also find the time to enjoy the cultural activities and take the time after the conference to explore Beijing and the nice surrounding areas.

Welcome to the 27th ICDERS

Nabiha Chaumeix

President, IDERS

Message from the Program Committee Chairs

ICDERS-2019 is the 27th specialist meeting on the dynamical aspects of explosions and reactive systems. This is the first time ICDERS was held in China, a growing presence at this meeting. Submissions were invited on technical areas of relevance to the ICDERS colloquium, ranging from detonations to chemical kinetics, from diagnostics to numerical methods, and from fundamentals to industrial applications. The program committee was chaired by three researchers from diverse technical areas and geographical locations, i.e., North America and Asia. The work of the program chair was supported by the members of the program committee, namely, Ben AKIH, Regis BAUWENS, Jeff BERGTHORSON, Yei-Chin CHAO, Nabihah CHAUMEIX, Jeong-Yeol CHOI, Ashwin CHINNAYYA, Andrea COMANDINI, Sergei B. DOROFEEV, Takuma ENDO, Matthew FOTIA, Vadim GAMEZO, Andrew HIGGINS, Kazuhiro ISHII, Scott I. JACKSON, In-seuck JEUNG, Francesco MARRA, Salvador NAVARRO-MARTINEZ, Akiko MATSUO, Remy MEVEL, Hoi Dick NG, Matei RADULESCU, Steven SHY, Pierre VIDAL, Bing WANG, Jennifer WEN.

This led to acceptance of more than 295 extended abstracts, and 71 abstracts for work in progress posters. All extended abstracts were reviewed by at least two people that were solicited by the program committee members. Due to the large number of papers that were recommended for oral presentation (194 papers) as a result of the peer review process, it was decided to organize five parallel sessions, similar to the 26th ICDERS held in Boston. Additionally, a poster session with 101 papers was held during an extended coffee break with no other parallel sessions. Unfortunately, some researchers with accepted papers had to withdraw their papers because of last minute visa issues.

Four plenary lectures were given reflecting the broad areas of interest to the ICDERS community:

Matei Radulescu, University of Ottawa - The Detonation Structure and its Impact on Detonation Limits Predictions

Bing Wang, Tsinghua University - Recent Research Progress on Rotating Detonation and Its Application in Different Engines

Jiro Kasahara, Nagoya University – Rotating and Pulse Detonation Engines System Development for the Sounding Rocket S520-31 Space Flight Experiment

Ulrich Maas, Karlsruhe Institute of Technology - Mathematical Modelling of Ignition processes

Because of the current interest in rotating detonation engine research, reflected in the large number of papers submitted, a special session on detonation propulsion was organized by Bing Wang. Invited normal length presentations were given by the following leading researchers: Piotr Wolanski, Koichi Hayashi, Venkat Raman, and Ephraim Gutmark.

Message from the Program Committee Chairs

We sincerely express gratitude to the members of the program committee for their help in selecting reviewers and guiding the review process. We thank all the reviewers who spent their valuable time to ensure a high quality program. We especially acknowledge the enormous help of Nabiha Chaumeix with the conference registration program CONFMASTER. We would also like to thank the work of the local organizing committee, especially Jian-Ping Wang and Zheng Chen, for input used for putting together the technical program and putting together the program booklet. All the extended abstracts will be made available to conference registrants during and after the colloquium via the web.

Authors of papers presented at the colloquium are encouraged to submit journal quality versions of their paper to one of the following journals: Shock Waves, Combustion and Science and Technology, Combustion Theory and Modeling. Submitted manuscripts will be peer reviewed according to individual journal standards but will be identified as ICDERS individually or as part of a special issue. Shock Waves will publish two special issues. The traditional special issue, edited by Gaby Ciccarelli, will include papers dealing with detonation phenomena and shock/blast waves, and a second special issue dealing specifically with detonation propulsion will be edited by Ephraim Gutmark.

Finally, if you have any comments on the current program, or suggestions for future ICDERS conferences, please contact us.

The program chairs of the 27th ICDERS

Gaby Ciccarelli, Eric Petersen, Jiro Kasahara

Message from the Host Committee Chair

On behalf of the Local Host Committees, you are most welcome to the 27th International Colloquium on the Dynamics and Reactive Systems (ICDERS2019), organized by Institute for Dynamics of Explosions and Reactive Systems (IDERS), hosted by Peking University, during July 28 – August 2, 2019, Beijing, China.

For more than half century, ICDERS and IDERS are like their hometown for going back every two years, where old members are expecting to see each other again, and new faces are enjoying to find new friends. The close relationship owns to the grateful tradition of our community, benefiting to all members not only in academics but also world-wide view. We pay respect to all people who have been contributed to our community.

We are honored to host this premier colloquium for the first time in mainland China, and we are trying our best to prove the right decision of Site Selecting Committee as well as Board of Directors, IDERS. China has changed since it opened to the world 40 years ago, while still a big delay exists with the frontier of science and technology. Young generations thirst for learning more from the world. ICDERS2019 provides us to be involved in IDERS community deeply and widely, especially in the future. And I believe that Chinese colleagues could contribute more to our community.

As the host, the first principle of us is to serve the colloquium, to provide the condition for all participants to enjoy ICDERS in all aspects. I suppose that you could feel that through the official website, through the announcements, through the sessions, through the social events.

All of those could not be achieved without team works. I am very happy to communicate with Nabiha CHAUMEIX, President of IDERS, and Gabriel CICCARELLI, Chair of Program Committee. I really appreciate the strong support from administration of Peking University (PKU), and that may not be realized without Prof. Ping Hao, President of PKU. Fortunately, we have a very professional colleagues here at PKU and Overseas Exchange Center (OEC). You could feel their existence, Rong LI, Ying WANG and Jiahui ZHANG, through all issues of the present ICDERS. Thanks Profs. Zheng CHEN, Yue YANG, Jianling LI, my colleagues, for devoting them to ICDERS. I also want to thank Jiemei YANG, Jie WU, Meng WANG, and students in my lab, Ming-Yi LUAN for website design and construction, Zhi-Jie XIA for Program assist and mailing, Yan HAO for movie, electron album and kits, et al. I would like to extend our thanks to Local Advisory Committee, Local Academic Committee, Local Organizing Committee, and all co-organizers, sponsors for their indispensable support.

I wish that all participants could spend a fruitful week here in Beijing.

Chair of Host Committee, 27th ICDERS

Jian-Ping Wang, Peking University

Organizer



Co-organizers



Platinum Sponsors



Gold Sponsors



Silver Sponsors



Commercial Sponsors



General Information

Conference Venue

Yingjie Exchange Center, Peking University (北京大学 英杰交流中心)

Registration/ Information Desk and Conference Secretariat

July 28th, 2019

Time: 14:00-20:00

Location: Lobby, the 1st floor of Bldg. 1 of Zhongguanyuan Global Village, PKU
(北京大学 中关村新园 1 号楼 大厅)

July 29th-August 2nd, 2019

Time: 07:30-11:30; 13:30-17:00 (except July 31st & August 2nd)

Location: Lobby, Yingjie Exchange Center, PKU
(北京大学 英杰交流中心 大厅)

Name Badge

For identification purpose and admission to the campus and conference venue, badges are expected to be worn at all times during the conference (July 28th-August 2nd). The strings of badges are color-coded as follows:

- Regular or Student Registration – Blue
- Accompany & Sponsor – Green
- One-day Registration – White
- Staff & Volunteer – Yellow

Internet

Wireless connection is available at conference venue and the account for login will be provided during the conference.

Meals

➤ The following items are the meals that will be offered during the conference. Please be reminded to collect your name badges, coupons and banquet invitation upon on-site registration for admission purposes.

Lunch for Student Attendees

Time: 12:30-13:30, July 29th – July 30th, August 1st - August 2nd

Venue: First floor, Nong Yuan Restaurant, PKU (北京大学 农园餐厅 一层)

Lunch for Regular Attendees

Time: 12:30 - 13:30, July 29th – July 30th, August 1st – August 2nd

Venue: Shao Yuan Restaurant (Building 7), PKU (北京大学 勺园中餐厅)

Lunch Box to Go for all Attendees

Time for Collection: 12:00-12:30, July 31st

Venue for Collection: Lobby, Yingjie Exchange Center

Restaurants

Two popular places with variety of foods near the colloquium venue

Zhongguancun Pedestrian Street (中关村步行街)

This street is located in Zhongguancun, which is a high-tech area of China, and is a place for shopping and eating. Check the 6th map in *Maps for Reference*. Along the street or on the 5th floor of EC Mall, there are many restaurants.

BLE Mall (五道口华联商厦)

This place is located in Wudaokou, with its Nick Name of U-Center where many foreign young people like to gather. It is to the east of the venue, about 2.5 km. Check the 5th map in *Maps for Reference*.

Dress Code

Smart casual is suggested for academic sessions. Casual wear is appropriate for city excursion. T-shirt, short pants, sandals are inappropriate for Banquet.

Currency Exchange

Most banks provide exchange service for foreign currency and traveler's checks. Credit cards such as Unionpay, Master, Visa and JCB are accepted in most hotels, shopping centers and restaurants. However, they may not be accepted at small-scaled shops or restaurants.

Electricity

The voltage is 220V in China.

Tips & Tax

Tipping is not necessary in Beijing. Taxes are already included in the stated prices.

Airport & Flight

It is advised that you leave the hotel 4 hours in advance for international flights, and 3 hours in advance for domestic flights.

Transportation

From Conference Hotels to the Conference Venue:

- For those who stay at Zhongguanyuan Global Village, you may walk to the conference venue (through Southeast Gate of Peking University with conference name badge) which takes 10-15 minutes and the map in the appendix is for your reference.
- For those who stay at Beijing Friendship Hotel, one shuttle bus will be arranged in the morning to Peking University from July 29th to August 2nd. Please refer to the Shuttle schedule below.
- You can also take subway line 4 at Entrance B, Renmin University Station (人民大学站 B 口), which is near to the East Gate of the hotel and get off at East Gate of Peking University Station (北京大学东门站) and exit from D.

Shuttle Schedule			
Date	Starts at	Departure	Arrival
28 th July	17:00	Friendship Hotel	Zhongguanyuan Global Village
	19:30	Zhongguanyuan Global Village	Friendship Hotel
29 th July	07:45	Friendship Hotel	Peking University
	18:00	Peking University	Friendship Hotel
30 th July	08:30	Friendship Hotel	Peking University
	18:30	Peking University	Friendship Hotel
31 st July	08:30	Friendship Hotel	Peking University
	17:00	Peking University	Kairui Yuxiandu Chinese Royal Restaurant
	19:00	Kairui Yuxiandu Chinese Royal Restaurant	Friendship Hotel; Zhongguanyuan Global Village
	20:30	Kairui Yuxiandu Chinese Royal Restaurant	Friendship Hotel; Zhongguanyuan Global Village
1 st August	08:00	Friendship Hotel	Peking University
	17:00	Peking University	Shangri-La Hotel
	20:30	Shangri-La Hotel	Friendship Hotel; Zhongguanyuan Global Village
2 nd August	08:00	Friendship Hotel	Peking University
	19:00	Peking University	Friendship Hotel

Note: Amendment to the schedule above is possible, please refer to notice on-site for updates.

It is convenient to take taxi and subway in Beijing. If you intend to explore the city on your own during the conference, the following transportation information is for your reference.

How It Is Charged When Taking A Taxi:

- Day (05:00—22:59): Starting at 13 RMB if it is less than three kilometers; 2.3 RMB per kilometer if it is more than 3 kilometers and less than 15 kilometers; Additional 50% would be charged per kilometer beyond 15 kilometers.
- Night (23:00—04:59): Starting at 13 RMB if it is less than three kilometers; 2.3 RMB per kilometer if it is more than 3 kilometers and less than 15 kilometers; Additional 50% would be charged per kilometer beyond 15 kilometers; Additional 20% would be charged per kilometer (serving as night driving fee).

Subway

The conference venue, Yingjie Exchange Center, is close to Exit D, Station of East Gate of Peking University (北京大学东门站) on Subway Line 4.

It is recommended to buy the Yi Ka Tong (一卡通, One-Card-Pass), at the ticket office in subway stations, for instance, 100 CNY including 10 CNY deposit. It covers all subway lines and bus lines in Beijing. It can be refunded when you leave Beijing.



Note: It is suggested that you have cash (Chinese currency) with you or exchange money at the airport since the taxi and subway accept cash (Chinese currency) only.

Presenter Instructions

Contents

All of the contents of presentations, including plenary lecture, oral and poster presentations, must be unclassified. The Program Committee and Local Organizing Committee are not responsible for the presented contents. Topics beyond academics are beyond the scope of ICDERS.

Oral Presentations

Presentations should last no longer than 20 minutes to allow 5 minutes for questions and changeover to the next speaker. All screens are in widescreen (16:9) format, except the screen of Sunlight Hall, which displays better 4:3 format.

Each presenter is strongly encouraged to arrive at the assigned conference room a minimum of 10 minutes before the commencement of the session to meet with the session chair.

A Practice Room is available on the 2nd floor (Conference Room 6) for the preparation of presentations.

Audio-Visual Equipment

Presentation rooms are equipped with LED, LCD or projectors for computer-based presentations. Laptops running Windows 7 System with Microsoft PowerPoint and Adobe Acrobat Reader installed. Presenters will be provided with a remote controller, with integrated laser pointer, that can be used to advance slides in PowerPoint.

Speakers are strongly encouraged to have their presentation saved on a USB drive and transferred onto the onsite laptops prior to the start of their sessions.

Slides with movies must be checked for playback on the laptop. At least one hour should be allowed for the technical support staff to solve any arising problems.

A laptop which is the same with those in session rooms, is available in the Practice Room on the 2nd floor (Conference Room 6). All speakers are strongly encouraged to ensure in advance that the presentation displays properly.

Poster Sessions

Posters are presented in the Conference Room 1 and Conference Room 7 on the 2nd floor. Posters are to be printed at the cost of the author(s). Each participant for poster presentation will be provided with tape and one side of a board (90cm in width and 120cm in height). Posters printed in landscape, or larger than the size of provided board, may not be displayed.

Posters assigned to the normal Poster Session (Tuesday 15:30-16:30) can be displayed all day Monday, Tuesday and Wednesday. The poster must be removed by 13:30 on Wednesday. At least one co-author should be available to present the poster on Tuesday 15:30-16:30.

Presenter Instructions

Posters assigned to the WIP Poster Session (Friday 13:20-13:50) can be displayed on Thursday and Friday. The poster must be removed by 15:30 on Friday. At least one co-author should be available to present the poster on Friday 13:20-13:50.

There are several print shops on campus and near to the venue which can be used if necessary.

Social Program Information

Reception Dinner

Time: 17:30-19:30, July 28th

Venue: Time Western Restaurant, Bldg. 2, Zhongguanyuan Global Village
(北京大学 中美新园 2 号楼 时光西餐厅)

Coupon: Regular, Student, Accompany, That day registered Attendees

Young Researchers' Get Together

Time: 18:30-20:30, July 29th

Venue: Sizzler, 5th Floor of EC Mall (See Appendix)
(海淀黄庄 欧美汇购物中心 5 层 时时乐餐厅)

Coupon: Students and PostDocs

Student volunteers would be available for assistance on direction of the venue.

Excursion

Time: 12:30-18:00, July 31st

Depart from: Yingjie Exchange Center (英杰交流中心)

Conference attendee with the intention to participate to the excursion is reminded to collect a coupon at registration desk on the first day of arrival. Due to limited quota, Reservations may also be made onsite if there is availability, but it cannot be guaranteed.

Line 1: Juyongguan Great Wall



Juyongguan, literally "Juyong Pass" (居庸关), is situated in a valley named "Guangou" as long 20 kilometers, which is within Changping District over 50 kilometers north from downtown Beijing. It is one of the three most famous passes of Great Wall in China. The other two passes are Shanhai Pass and Jiayuguan Pass. The Great Wall around the Pass extends over 4 km snaking the ridge of the mountains forming the valley. The natural landscape surrounding the Pass is

extremely beautiful. Juyongguan used to be an ancient military town full of military installations, watch towers, official residences, temples, and other structures. Juyong Pass was first built in Ming Dynasty and received much repair later. It was a very important strategic area linking the inner land and the area close to the northern border of China. The Juyong Pass has been well known for its strategic importance for over 2,000 years.

Line 2: Forbidden City



The Forbidden City is a palace complex in central Beijing. The former Chinese imperial palace from Ming dynasty to the end of Qing dynasty (the years 1420 to 1912), it now houses the Palace Museum. The Forbidden City served as the home of emperors and their households as well as the ceremonial and political center of Chinese government for almost 500 years. It was first built throughout 14 years during the reign of Emperor Chengzu in the Ming Dynasty (1368-1644). Ancient Chinese Astronomers believed that the Purple Star (Polaris) was in the center of heaven and the Heavenly Emperor lived in the Purple Palace. The Palace for the emperor on earth was so called the Purple City. It was forbidden to enter without special permission of the emperor. Hence its name 'The Purple Forbidden City', usually 'The Forbidden City'. It is the world's largest palace complex and covers 74 hectares. Surrounded by a 52-meter-wide moat and a 10-meter-high wall are more than 8,700 rooms. The Forbidden City is listed by UNESCO as the largest collection of preserved ancient wooden structures in the world.

Coupon: Regular, Student, Accompany, That day registered Attendees.

Dinner after Excursion

Time: 18:00-20:00, July 31st

Venue: Beijing Kairui Yuxiandu Royal Cuisine Museum
(四季青桥西南 凯瑞御仙都皇家菜博物馆)

Coupon: Regular, Student, Accompany, That day registered Attendees.

Social Program Information

Entertainment: A big stage with large LED display, Audio-Visual equipment are available. Laptop, mobile phone and USB can be connected to the system. Attendees are encouraged to sing Karaoke, playing instruments.

Banquet

Time: 17:00-20:30, August 1st

Venue: Garden Wing Ballroom, Shangri-La Hotel
(紫竹院桥西北 香格里拉酒店 景阁宴会厅)

Coupon: Attendees who registered with Banquet

Pre-dinner cocktail: 17:00-18:00

Attractions: Folk dance, Sichuan Opera Change Face, Beijing Opera, Acrobatics, Kung Fu, Chinese instruments.

Prize awarding ceremony: N. Manson Medal, A. K. Oppenheim Prize, R. I. Soloukin Award, J. H. S. Lee Young Investigator Award.

Term charge of Borad of Directors

Declaration: Site of 28th ICDERS, Host Chair, Program Chair.

Farewell Dinner

Time: 16:30-19:00, August 2nd

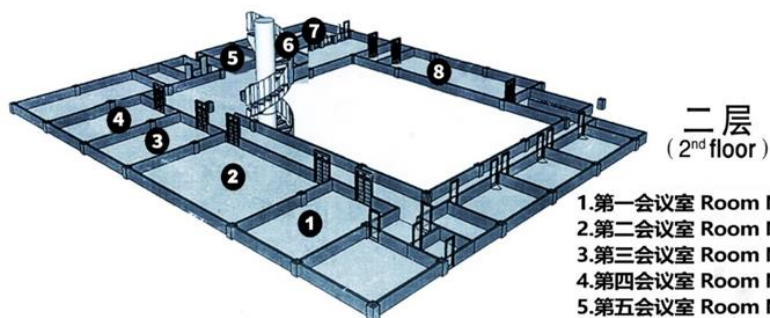
Venue: Shao Yuan Restaurant, PKU (北京大学 勺园中餐厅)

Note: Time of events is subject to change. Please refer to arrangement onsite.

1. Yingjie Exchange Center

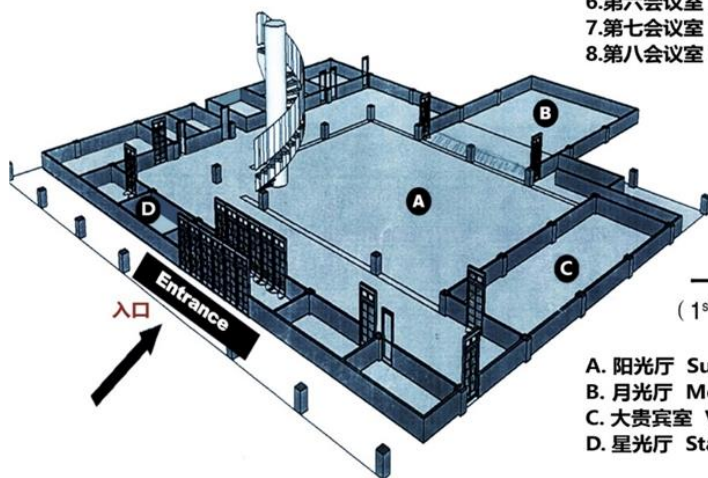
北京大学英杰交流中心会场平面图

Floor plan of Ying Jie Exchange Center, Peking University



二层
(2nd floor)

- 1. 第一会议室 Room No.1
- 2. 第二会议室 Room No.2
- 3. 第三会议室 Room No.3
- 4. 第四会议室 Room No.4
- 5. 第五会议室 Room No.5
- 6. 第六会议室 Room No.6
- 7. 第七会议室 Room No.7
- 8. 第八会议室 Room No.8

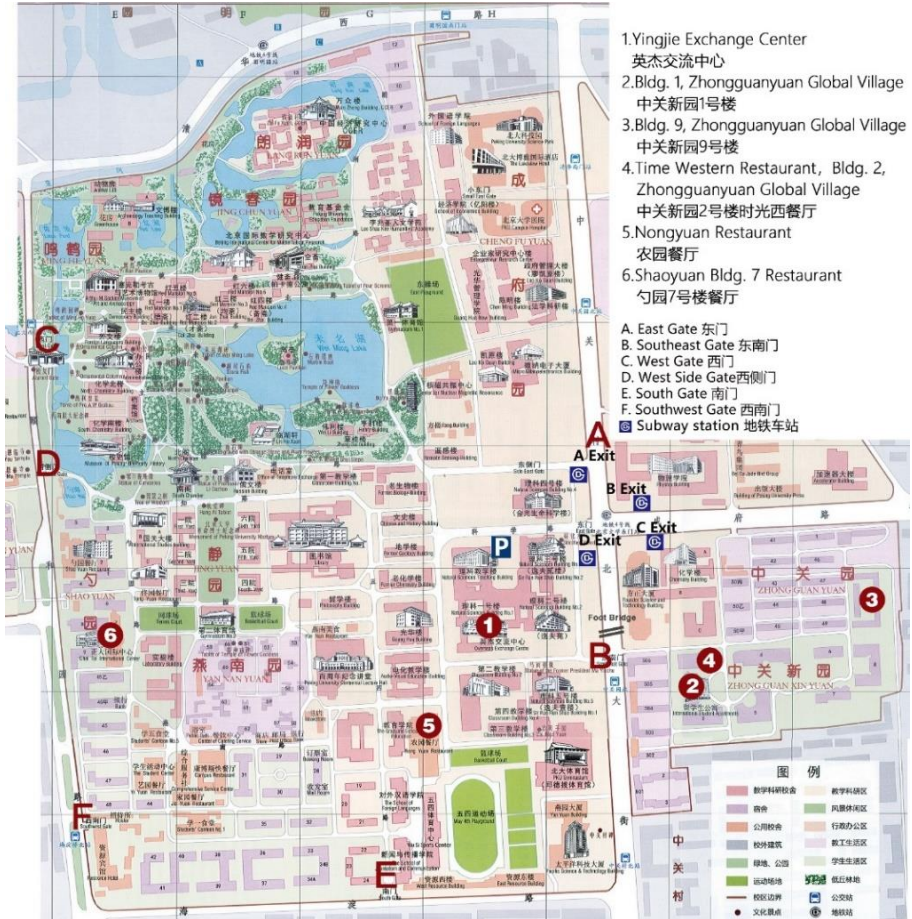


一层
(1st floor)

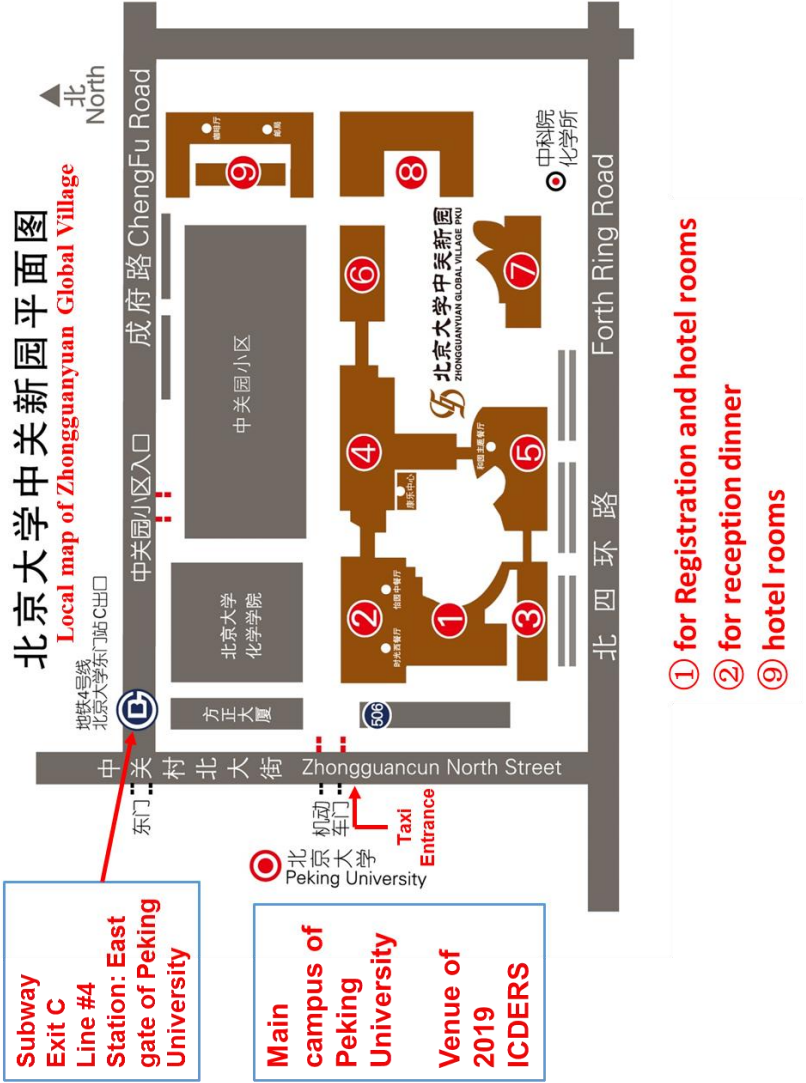
- A. 阳光厅 Sunlight Hall
- B. 月光厅 Moonlight Hall
- C. 大贵宾室 VIP Room
- D. 星光厅 Starlight Hall

Maps for Reference

2. Peking University



3. Zhongguanyuan Global Village, PKU



Maps for Reference

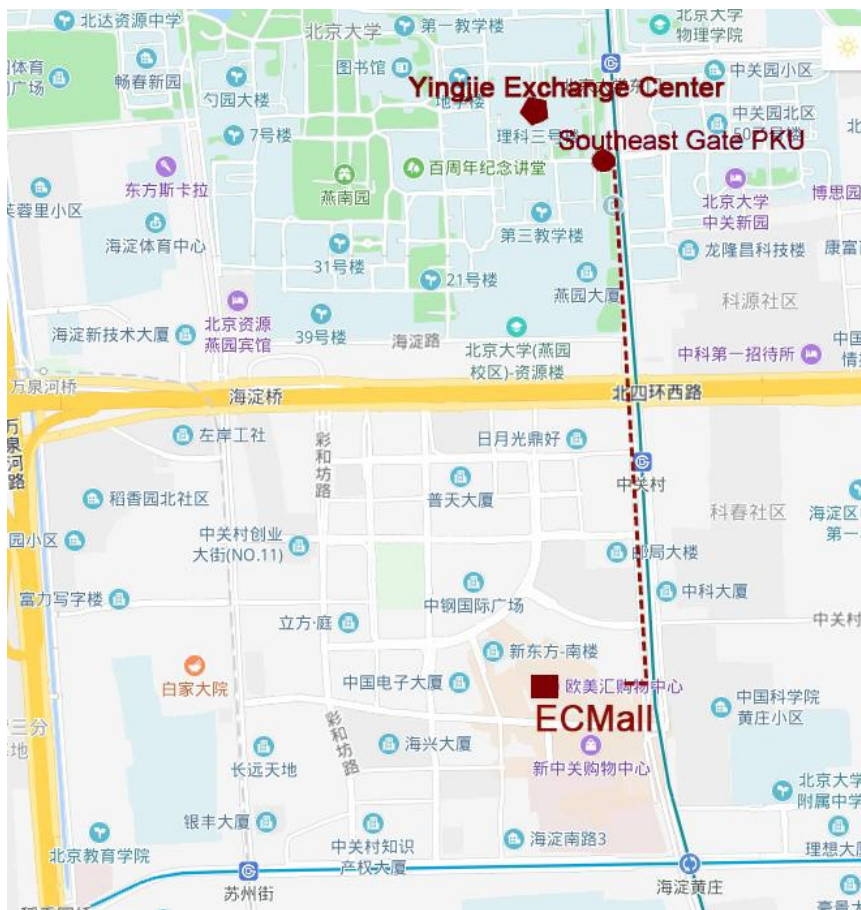
4. Beijing Friendship Hotel



5. BLE Mall

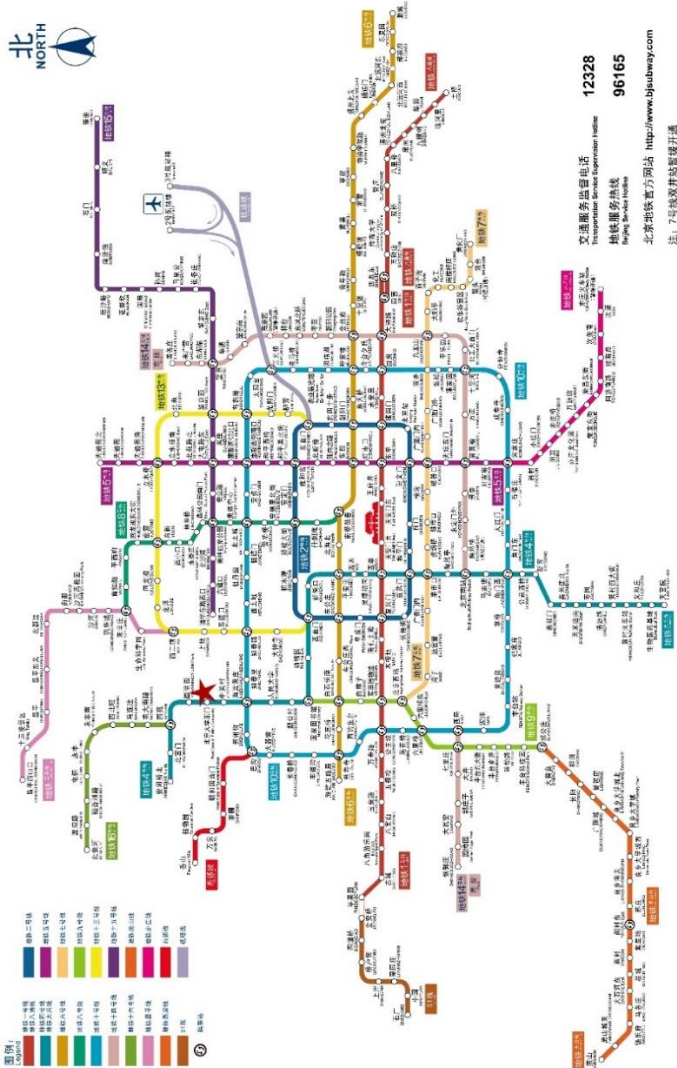


6. Map for “Young Researchers Get Together”



7. Beijing Subway Lines

北京城市轨道交通线图
Beijing Rail Transit Lines



Program at a Glance

Mon. (Jul. 29)		Tue. (Jul. 30)		Wed. (Jul. 31)		Thu. (Aug. 1)		Fri. (Aug. 2)			
08:30	Welcome					08:30	Sessions	08:30	Sessions		
09:00 10:00	Plenary I	09:00 10:00	Plenary II & III	09:00 10:00	Plenary IV	10:10		10:10			
Group Photo & Break		Break		Break		Break		Break			
10:30 12:10	Sessions	10:30 12:10	Sessions	10:20 12:00	Sessions	10:40 12:20	Sessions	10:40 12:20	Sessions		
Lunch 12:30		Lunch 12:30		Lunch 12:00		Lunch 12:30		Lunch 12:30			
				13:20 13:50	WIP Posters						
13:50 15:30	Sessions	13:50 15:30	Sessions	12:30 18:00	Excursion	13:50 15:05	Sessions	13:50 15:30	Sessions		
Break		15:30 16:30	Break & Posert Session			Break		15:30 16:45	Sessions		
16:00 17:40	Sessions	16:30 18:10	Sessions							16:30 19:00	Farewell
18:30 20:30	Young R. G. T.					18:00 20:30	Dinner	18:00 21:00	Banquet		

Technical Program

Monday

8:30	<p>Opening Ceremony Sunlight Hall</p> <p>P. Hao, President of Peking University N. Chaumeix, President of IDERS G. Ciccarelli, Chair of Program Committee W. Yang, President of CSTAM</p> <p><i>Chair: J. P. Wang, Chair of Host Committee</i></p>
9:00	<p>Plenary Lecture 1: Matei Radulescu, University of Ottawa The Detonation Structure and its Impact on Detonation Limits Predictions Sunlight Hall, Chair G. Ciccarelli</p>
10:00	<p>Group Photo & Break</p>

Rooms	Sunlight Hall	Moonlight Hall	Room 2	Room 8	Rooms 3/4
Topic	Detonation Structure <i>G. Ciccarelli</i>	Supersonic Combustion 1 <i>B. Wang</i>	Shock Tubes 1 <i>E. Petersen</i>	Turbulent Flames 1 <i>Y. Ju</i>	Fire 1 <i>S. Dorofeev</i>
10:30	Numerical Investigation on Effect of Dilute Water Spray on Mean Structure for Gaseous Detonation(196) <i>H. Watanabe, A. Matsuo, A. Chinnayya, K. Matsuoka, A. Kawasaki, J. Kasahara</i>	Modal Analysis of Instability Phenomena in Shock-Induced Combustion using Decomposition Techniques(347) <i>P. K. Pavalavanni, J. Choi</i>	Ignition delay-time study of dimethoxymethane/air and CH4/dimethoxymethane/air mixtures over a wide temperature range at high pressure(100) <i>J. Herzler, C. Schulz, M. Fikri</i>	Three-Dimensional Navier-Stokes Simulations of Non-Premixed Reactive Vortex Breakdown(227) <i>J. Chung, X. Zhang, E. Oran, C. Kaplan</i>	Visualization of flow field in narrow space on flame spread along a thin paper disk with fingering combustion(127) <i>H. Tanaka, T. Daitoku, T. Tsuruda</i>
10:55	Numerical Simulation of the Detonation Wave in the Shock-Attached Frame for the Two-Stage Kinetics Model(104) <i>P. Utkin, Y. Poroshyna</i>	High-order accurate hybrid LES/PDF simulation of a supersonic coaxial lifted flame(374) <i>H. Ranadive, B. Savard, E. Hawkes</i>	Study on Ignition Delay Times of Methane/Ethane Mixtures with CO2 and H2O addition(388) <i>M. Braun-Unkhoff, C. Naumann, O. Pryor, U. Riedel, S. Vasu</i>	A level-set formalism for self-ignition fronts(204) <i>X. Wang, C. Strozzi, V. Robin, S. Zhao, K. Q. N. Kha, Z. Bouali</i>	Experimental Investigation of the Fire Spread on Inclined Wooden Rods(154) <i>Y. Lai, H. Zhou, Y. Zhang</i>
11:20	Measurement of Cellular Structure in Methane-Oxygen Detonation by Multiple Ion-Probes(126) <i>T. Yatsufusa, K. Kii, N. Miura, H. Yamamoto</i>	Three-dimensional Numerical Simulation of Detonation Initiation in Supersonic Flows(237) <i>W. Chen, J. Liang</i>	Kinetic Influence of Small Additives of Fe(CO)5 on the Ignition of H2-O2-Ar Mixtures behind Reflected Shock Waves(182) <i>A. Tereza, S. Medvedev, V. Smirnov</i>	Ignition kernel development and subsequent flame propagation in a planar methane/air turbulent jet(159) <i>C. T. d'Auzay, S. Ahmed, N. Chakraborty</i>	Flame spreading in an oxidant flow above burning surface of material(167) <i>V. Tyurenkova, L. Stamov</i>
11:45	Effect of Incident Laser Sheet Orientation on the OH-PLIF Imaging of Detonations(155) <i>K. Chatelain, R. Mevel, J. Melguizo-Gavilanes, A. Chinnayya, S. Xu, D. Lacoste</i>	Structure of Wedge-Induced Oblique Detonations with Small Heat Release(132) <i>D. Martinez-Ruiz, C. Huete, A. L. Sánchez, F. A. Williams</i>	Measurement of Methane Autoignition Delays in Carbon Dioxide Diluent at Supercritical Conditions(94) <i>W. Sun, M. Karimi, B. Ochs, Z. Liu, D. Ranjan</i>	Flame front characterization based on ridge analysis(334) <i>R. Schießl, V. Bykov</i>	Testing a Reduced Model of Flame Spread over a Thin Solid in a Narrow Channel(218) <i>H. Iizuka, K. Kuwana, G. Kushida</i>
12:10					
12:30	Lunch				

Rooms	Sunlight Hall	Moonlight Hall	Room 2	Room 8	Rooms 3/4
Topic	Detonation Initiation <i>H. D. Ng, R. Zitoun</i>	Supersonic Combustion 2 <i>V. Raman</i>	Shock Tubes 2 <i>R. Mevel</i>	Turbulent Flames 2 <i>R. Schiessl</i>	Fire 2 <i>H. Xiao</i>
13:50	Effects of CO2 Dilution on Autoignition and Detonation Development Induced by Hot Spot in n-Heptane/Air Mixtures(40) <i>P. Dai</i>	Experimental and Numerical Analysis of Hydrogen Jet Autoignition in Backward-Facing-Step-Stabilized Model Scramjet Combustor(281) <i>N. Fedorova, M. Goldfeld, Y. Zakharova</i>	Reflected-Shock Non-Idealities in Shock Tubes: The Impact of the Facility-Dependent Effects over a Wide Range of Pressures and Mach Numbers(330) <i>D. Nativel, S. Cooper, T. Lipkowicz, M. Fikri, A. M. Kempf, E. Petersen, C. Schulz</i>	An Experimental Study of Spark Ignition of a Turbulent Biogas Fuel Jet(175) <i>C. T. d'Auzay, S. Ahmed, N. Chakraborty, M. Bassiouny, A. Ebrahemi</i>	Simulations of a Triple Flame and Fire Whirl using the BIC Low-Mach-Number Algorithm(228) <i>X. Zhang, J. Chung, C. Kaplan, E. Oran</i>
14:15	Detonation Onset in Shock Wave Reflected from a Wedge(102) <i>N. Smirnov, V. Tyurenkova, O. Penyazkov, K. Sevrouk, V. Nikitin, L. Stamov</i>	Large-eddy Simulations of a Reactive Jet in Supersonic Cross-Flow based on a Hybrid model of Turbulent Combustion(55) <i>A. Techer, R. Boukharfane, G. Lehmasch, A. Mura</i>	State-to-State Analysis of Chemical Kinetics and Transport Properties in Shock Heated Flow(146) <i>Q. Hong, X. Wang</i>	Experimental Measurements of Flame Structure and Time-averaged Statistics in Turbulent Nonpremixed Cool Flames(74) <i>C. Reuter, O. Yehia, Y. Ju</i>	Effect of Wood Smoke Particles Contamination on Water Droplets Evaporation and Surface Tension(261) <i>A. Albadi, Y. Zhang</i>
14:40	Numerical Study on Detonation Initiation through a Uniform Energy Source(131) <i>D. Chen, J. Ning., J. Li</i>	Simulation of Spray Combustion of n-Heptane in a Model Supersonic Combustor with Pilot Hydrogen(199) <i>Z. Huang, M. Zhao, H. Zhang</i>	Shock Tube Based Diesel Spray Ignition Testing(383) <i>C. Merkel, G. Ciccarelli</i>	Filtered Turbulent Flamelet Model: Analysis and Numerical Test(19) <i>L. Wang, J. Zhang</i>	Generation of Fire Whirls over a Line Fire in a Crossflow: an Experimental Study on the Role of Near-Ground Flow(273) <i>K. Kuwana, Y. Iga</i>
15:05	Numerical and Experimental Investigation of Detonation Initiation in Multifocused Systems(105) <i>P. Utikin, A. Lopato, A. Vasil'ev</i>	Combustion Enhancement in Supersonic Coaxial Jet with an Optimal Forcing Oscillations(287) <i>C. C. Liu, B. Yu, B. Zhang, H. Liu</i>	Facility-Dependent Effects in Shock Tubes(337) <i>S. Cooper, D. Nativel, M. Fikri, C. Schulz, E. Petersen</i>	Computational Study of Turbulent Partially-Premixed Flame with Inhomogeneous Inlets(33) <i>P. Shrotriya, P. Wang</i>	Air Mass Flow Rate Effects on Ignition Front Propagation of Solid Olive Waste in a Fixed-Bed Combustor(316) <i>A. Elorf, B. Sarh, M. Asbik, T. Boushaki, S. Bostyn</i>
15:30	Break				

Rooms	Sunlight Hall	Moonlight Hall	Room 2	Room 8	Rooms 3/4
Topic	Detonation Interface Interaction <i>H. D. Ng, R. Zitoun</i>	Oblique Detonation <i>I. S. Jeung</i>	Shock Tubes 3 <i>J. Herzler</i>	Turbulent Flames 3 <i>U. Maas</i>	Fire 3 <i>Y. Zhang</i>
16:00	Origins of Turbulent Mixing behind Detonation Propagation into Reactive-Inert Gas Interfaces(103) <i>B. Maxwell, J. Melguizo-Gavilanes, R. Mevel</i>	The Role of Activation Energy on the Formation and Stability of Gaseous Oblique Detonation Waves(35) <i>C. Yan, H. Teng, X. Mi, H. D. Ng</i>	A Study of Ethanol Oxidation in High-Pressure Shock Tube: Ignition Delay Time Measurements and High-Speed Imaging of the Ignition Process(386) <i>D. Nativel, J. Herzler, M. Fikri, C. Schulz, P. Niegemann</i>	Reaction-Diffusion-Maniolds for Flame-Wall-Interactions of Stratified Flames(256) <i>C. Strassacker, V. Bykov, U. Maas</i>	How Dripping Flames Ignite a Thin Fuel(377) <i>P. Sun, S. Lin, X. Huang</i>
16:25	Detonation Transmission Across an Inert Layer(174) <i>K. Tang, J. H. Lee, H. D. Ng, X. Mi</i>	Effects of Fluctuating Equivalence Ratios on the Formation of Wedge-Induced Oblique Detonations in Pre-Evaporated Kerosene-Air Mixture(92) <i>Z. Ren, B. Wang</i>	Heat Capacity Effect on Ethanol Preignition in a Shock Tube(297) <i>M. Luong, E. Tingas, H. Im, M. Figueroa-Labastida, A. Sow, F. E. H. Pérez, J. Badra, A. Farooq</i>	Oblique Flame-Wall Interaction in Premixed Turbulent Combustion Under Isothermal and Adiabatic Wall Boundary Conditions(176) <i>U. Ahmed, N. Chakraborty, M. Klein</i>	Analysis of Heat Flux Components and their Influences on Flame Spread over PMMA Walls using a Wall resolved Large Eddy Simulation Approach(309) <i>K. Fukumoto</i>
16:50	Transmission of Cellular Detonation Waves across a Density/Temperature Interface(101) <i>K. Tang, J. H. Lee, H. D. Ng, X. Mi</i>	Effects of Equivalence Ratio on the Characteristics of the Oblique Detonation Wave(39) <i>S. A. Esfehiani, C. Nan, H. Tang</i>	High-Temperature Non-Homogeneous Ignition of Small Alcohols Behind Reflected Shock Waves(21) <i>O. Mathieu, E. Petersen, L. Pinzón, T.ATHERLEY, I. Schoegl</i>	Influence of Fuel Lewis Number on Flame-Wall Interaction for Impinging Turbulent Premixed Flames(283) <i>I. Konstantinou, U. Ahmed, N. Chakraborty</i>	The Potential of Utilizing Near Infrared Spectrum for Fire Detection(166) <i>X. Wang, Y. Zhang</i>
17:15	Dynamics of a Cellular Flame after a Head-on Interaction with a Shock Wave(344) <i>H. Yang, M. Radulescu</i>	Initiation Characteristics of Wedge-Induced Oblique Detonation Waves in a H₂-O₂ Mixtures with Ar dilution(188) <i>C. Tian</i>	n-Heptane Ignition: High-Speed Imaging in a High-Pressure Shock Tube(9) <i>D. Davidson, R. Hanson, J. Shao, R. Choudhary, A. Suta</i>	Experimental Study of the Diluent Influence (N₂, He, Ar) on Stable Premixed Methane Flame in a Quartz Micro Flow Reactor(321) <i>C. Chauveau, F. Halter, G. Dayma, H. Chouraqui, P. Dagaut</i>	FREE
17:40	Adjourn				
18:30	Young Researchers' Get Together				
20:30	<i>Sizzler, 5F, EC Mall</i>				

Tuesday					
9:00	Plenary Lecture 2: Bing Wang, Tsinghua University Recent Research Progress on Rotating Detonation and Its Application in Different Engines Sunlight Hall, Chair E. Gutmark				
9:30	Plenary Lecture 3: Jiro Kasahara, Nagoya University Rotating and Pulse Detonation Engines System Development for the Sounding Rocket S520-31 Space Flight Experiment Sunlight Hall, Chair E. Gutmark				
10:00	Break				
Rooms	Sunlight Hall	Moonlight Hall	Room 2	Room 8	Rooms 3/4
Topic	Detonation Diffraction <i>M. Radulescu</i>	Detonation Propulsion Special Session <i>B. Wang</i>	Ignition 1 <i>F. Marra</i>	Dynamics & Stability 1 <i>B. J. Lee</i>	Energetic Materials 1 <i>C. L. Tang</i>
10:30	Experimental D(κ) Relationships for Unstable Detonations(97) <i>Q. Xiao, M. Radulescu</i>	RDE Research and Development in Poland <i>P. Wolanski</i>	Autoignition of n-Decane and Multi-Component Surrogates of Kerosene in an Optical Rapid Compression Machine(349) <i>C. Strozzi, J. Sotton, M. Bellenoue, H. Ossman, K. Tsuzuki</i>	Flame Topology and Combustion Instability Limits of Lean Premixed Hydrogen Enriched Flames(385) <i>I. Chtereve, I. Boxx</i>	Ignition Temperature of CS2- Explosive Atmospheres in Dependence on Spatial Orientation of the Hot Surface(314) <i>M. Beyer, P. Raval</i>
10:55	Detonation Behaviors Downstream of a Perforated Plate with Large Hole Diameters(376) <i>W. Lin, K. Guo, H. Zhao, Y. Zhu, Z. Zhong, J. H. Lee</i>	Numerical Analysis on Disc- Type RDE <i>K. Hayashi</i>	Ignition Delay Time Model based on a Deep Neural Network(65) <i>A. Jach, A. Teodorczyk, M. Zbikowski, K. Malik</i>	Effects of Hydrogen Addition on the Stabilization of Lean Premixed Swirl Flames(115) <i>W. Zhang, J. Wang, W. Lin, B. Lin, Y. Wu, M. Zhang, Z. Huang</i>	Non-Shock Ignition Simulation for PBXs based on Combined Microcrack and Microvoid Hotspot Mechanisms(82) <i>K. Yang, Y. Wu, F. Huang</i>
11:20	Effect of Cellular Instabilities on the Detonation Transmission of Weakly Stable Detonations(238) <i>L. Shi, K. C. K. Uy, C. Y. Wen</i>	Computational Tools for Rotating Detonation Engines <i>V. Raman</i>	Effect of Low Initial Pressures on Ignition Properties of Methane/O2/N2 Mixtures for Laser Induced Breakdown(275) <i>B. Molière, S. Rudz, J. Dougal, P. Gillard, M. William-Louis</i>	Mode Transition of Interacting Flickering Flames(49) <i>A. Bunkwang, T. Matsuoaka, Y. Nakamura</i>	Propagation of Reactive Cracks in Pressed HMX-Based Pbx and Reaction Violence of Explosive System in Thick Wall Confinement(356) <i>T. Li, H. Hu</i>
11:45	An Experimental Investigation of a Detonation Characteristic Length Scale Relevant to Critical Diffraction(301) <i>A. Kawasaki, J. Kasahara</i>	Rotating Detonation Research at the University of Cincinnati <i>E. Gutmark</i>	Study of Synthesis Gas Auto- Ignition Process by using GQL and QSSA Model Reduction Approaches(263) <i>C. Yu, V. Bykov, U. Maas</i>	Response of a Low Swirl Premixed Flame to Velocity Perturbations(143) <i>M. Shahsavari, B. Wang, M. Farshchi, D. Zhao</i>	Clustering Effect of Hot Spots on Shock-to-Detonation Transition (SDT) in Nitromethane with Air-Filled Cavities(183) <i>X. Mi, N. Nikiforakis, A. Higgins, L. Michael</i>
12:10					
12:30	Lunch				

Rooms	Sunlight Hall	Moonlight Hall	Room 2	Room 8	Rooms 3/4
Topic	Detonation Failure/Limits <i>A. Chinnayya, L. Bauwens</i>	RDE 1 <i>K. Hayashi, A. Matsuo</i>	Ignition 2 <i>S. Alturaifi, S. Cooper</i>	Dynamics & Stability 2 <i>B. J. Lee</i>	Energetic Materials 2 <i>J. W. Li</i>
13:50	Critical Ignition in Detonation Cells due to Expansion Cooling(319) <i>K. Cheevers, R. Murugesan, F. Giroux, W. Morin, A. Dion-Dallaire, M. Radulescu</i>	Characterization of Detonation Wave Heat Release and Rotating Detonation Engine Mode Selection(351) <i>J. Burr, K. Yu</i>	Rapid Compression Machine (RCM) Studies on the Production of Unsaturated Hydrocarbons from Methane(257) <i>S. Drost, R. Schießl, U. Maas</i>	Large Eddy Simulations of Turbulent Premixed Flame Stabilization by Pulsed Plasma Discharges(171) <i>Y. Bechane, N. Darabiha, V. Moureau, C. Laux, B. Fiorina</i>	A Spectroscopic Method for Assessing the Degree of Oxidation of Zirconium-based Pyrotechnic Initiators(112) <i>J. Ryu, J. Yoh</i>
14:15	Propagation Limit of Gaseous Detonations Governed by Yielding Confinement and Arrhenius Kinetics(359) <i>L. Zhou, X. Mi, H. D. Ng, Y. Zhang, H. Teng</i>	Detonation Propagation in a Linear Representation of a Rotating Detonation Engine(384) <i>C. Metrow, G. Ciccarelli</i>	Effects of NTC Region on end-Gas Combustion Modes under Temperature Stratification(266) <i>T. Nogawa, H. Terashima</i>	Numerical Studies of the Flame Dynamics in a Novel, Ultra-Lean, Non-Premixed Model GT Burner using PDF-ESF Method(76) <i>S. Yu</i>	The Changes of Thermodynamic Reactions of a NASA Standard Initiator due to Hygrothermal Aging(113) <i>J. Oh, Y. Park, J. Yoh</i>
14:40	Experimental Study on Deflagration-to-Detonation Transition Shortening by Nanosecond Pulsed Laser Ignition(240) <i>T. Sato, K. Matsuoka, A. Kawasaki, J. Kasahara</i>	Effect of Parasitic and Commensal Combustion on Rotating Detonation Combustors(362) <i>F. Chacon, M. Gamba, A. Feleo</i>	Analysis of the Vibrational Non-equilibrium Characteristics in Hydrogen-Oxygen Auto-Ignition using DSMC Method(160) <i>C. Yang, Q. Sun</i>	Multi-Dimensional Numerical Analysis on Flames with Repetitive Extinction and Ignition in a Heated Micro Channel(300) <i>K. Akita, Y. Morii, H. Nakamura, T. Tezuka, K. Maruta</i>	Aluminized and Non-Aluminized AP/HTPB-Composite Propellant Burning Rates at Very-High Pressures(339) <i>C. Dillier, E. Petersen, T. Sammet, F. Rodriguez, E. Petersen, J. Thomas</i>
15:05	Near-Limit Dynamics of Gaseous Detonations: Distinguishing Tube Scale and Initial Pressure Effects(48) <i>B. Zhang, H. D. Ng</i>	OH* Chemiluminescence Investigation of Rotating Detonation Wave Structure(212) <i>J. Jodele, E. Gutmark, A. Zahn, V. Anand</i>	A Parametric Validation of Auto-Ignition Numerical Studies on Compact Rapid Compression Machine(205) <i>P. Kumar, S. Nakaya, M. Tsue</i>	Ultra-Lean Hydrogen-Air Flame Kernels Large-Scale Dynamics in Terrestrial Gravity Conditions(187) <i>A. Kiverin, V. Golub, M. Anton, I. Yakovenko, V. Vladislav, M. Kseniya</i>	Updated Three-Flame Modeling of Composite AP/HTPB Propellants(363) <i>J. Thomas, E. Petersen</i>
15:30	Break & Regular Poster Session				

Rooms	Sunlight Hall	Moonlight Hall	Room 2	Room 8	Rooms 3/4
Topic	Detonation Modeling <i>A. Chinnayya, L. Bauwens</i>	RDE 2 <i>K. Hayashi, A. Matsuo</i>	Ignition 3 <i>N. Chaumeix</i>	Dynamics & Stability 3 <i>O. H. Sun</i>	Energetic Material 3 <i>C. Wang</i>
16:30	Steadily-Rotating Overdriven Detonation : Experiments vs. GSD Modeling(95) <i>C. Jourdain, V. Rodriguez, P. Vidal, R. Zitoun</i>	Chemistry Modeling Effects on the Interaction of a Gaseous Detonation with an Inert Layer(320) <i>S. Taïleb, J. Melguizo-Gavilanes, A. Chinnayya</i>	Effects of Low-Temperature Chemistry on Hot-Particle Ignition in a Premixed Fuel/Air Mixture(139) <i>Y. Wang, Z. Chen</i>	Swirl Flames Diagnostics Using Diode Laser Absorption Tomography with High Temporal-Spatial Resolution(271) <i>F. Li, L. Xin</i>	Effect of Acoustic Excitation on Ammonium Perchlorate Decomposition and Combustion(253) <i>L. Han, J. Li</i>
16:55	A 3-D Pseudo-Arc-Length Method for Numerical Simulation of Detonation Wave Propagation(50) <i>M. Tianbao, Z. Jinqing, N. Jianguo</i>	Detonation Diffraction and Failure of Gaseous Detonations Bounded by an Inert Gas(193) <i>R. Houim, B. Roque, H. Li</i>	Premixture Ignition of Jet-A Kerosene and Some of its Surrogates in Flowing Conditions(233) <i>R. L. Dortz, C. Strozzi, J. Sotton, M. Bellenoué</i>	Propagation Speeds and Kinetic Analysis of Premixed Heptane/Air Cool Flames at Large Ignition Damköhler Numbers(366) <i>T. Zhang, Y. Ju</i>	A copper Oxide based Metal-Organic Framework: Effect on Combustion of Ammonium Nitrate and Magnesium Composition(329) <i>M. Atamanov, R. Shen, Z. Yelemessova, K. Kamunur, A. Imangazy, B. Lesbayev, Z. Mansurov</i>
17:20	Two-Dimensional Numerical Simulations on Unstable Propagation of Propane/Oxygen Detonation using a Detailed Chemical Mechanism(268) <i>N. Takeshima, K. Ozawa, N. Tsuboi, K. Hayashi, Y. Morii</i>	The Numerical Investigation of Hydrogen Detonation Propagating in Semi-Confined Layers(138) <i>S. Shigeoka, A. Matsuo, A. Kawasaki, J. Kasahara, K. Matsuoka</i>	Autoignition Studies of Unsaturated Methyl Ester: Methyl Crotonate(250) <i>S. K. Vallabhuni, B. Shu, X. He, K. Moshammer, R. X. Fernandes</i>	Premixed Methane/Air/Hydrogen Flame Oscillations in Horizontal Open End Tubes(164) <i>H. Jiang, N. A. b. Amaludin, R. Woolley, Y. Zhang</i>	Thermal Decomposition of Nitromethane: Experiments and Model Validation(53) <i>Y. Meng, Z. Xu, Z. Gao, C. Tang, E. Hu, Z. Huang</i>
17:45	Statistical Analysis of the Reaction-Zone Characteristics of Unstable Gaseous Detonations(180) <i>X. Mi</i>	Analytical and Numerical Study of the Expansion Effect on the Velocity Deficit of Continuous Detonation Waves(311) <i>M. Y. Luan, S. J. Zhang, Z. J. Xia, S. B. Yao, J. P. Wang</i>	Network Community Detection based Combustion Reaction Mechanism Coarse Graining method(259) <i>L. Ji, J. Gao</i>	Effect of Boundary Conditions on Thermo-Acoustic Instability of Flames Propagating in Tubes(84) <i>A. Dubey, O. Fujita, Y. Koyama, N. Hashimoto</i>	FREE
18:10	Adjourn				

Wednesday					
9:00	Plenary Lecture 4: Ulrich Maas, Karlsruhe Institute of Technology Mathematical Modelling of Ignition processes Sunlight Hall, Chair Peterson				
10:00	Break				
Rooms	Sunlight Hall	Moonlight Hall	Room 2	Room 8	Rooms 3/4
Topic	Detonation Miscellaneous 1 <i>O. Penyazkov</i>	Micro Reactors <i>H. Nakamura</i>	Detonation Analog/Model <i>A. Kasimov</i>	Sprays & Droplets 1 <i>J. C. Thomas</i>	Explosion Safety 1 <i>R. Bauwens</i>
10:20	Detonation Propagation through Inhomogeneous Fuel-Air Mixtures(361) <i>S. Prakash, V. Raman</i>	Reactivity of CO/H₂/CH₄/Air Mixtures derived from In-cylinder Fuel Reformulation Examined by a Micro Flow Reactor with a Controlled Temperature Profile(258) <i>Y. Murakami, H. Nakamura, T. Tezuka, G. Asai, K. Maruta</i>	Detonation Model using Burgers Equation and a Pulsed Reaction(315) <i>S. Lau-Chapdelaine, M. Radulescu</i>	A Numerical Investigation of the Behaviour of the Minimum Ignition Energy for Turbulent Droplet-Laden Mixtures(156) <i>V. Papapostolou, G. O. Erol, N. Chakraborty, C. T. d'Auzay</i>	Numerical Study on the Process of Fixed-axis Rotation of Object Under Action of Shock Waves(38) <i>Q. Liu, J. Lei, J. Yin</i>
10:45	Patterns of Detonation Decay and Combustion of Hydrogen-Air Mixture in Porous Layer(305) <i>S. Golovastov, G. Bivol</i>	Very Rich Methanol-Air Combustion in Microchannel-based Reactors to Produce Hydrogen-Rich Syngas(165) <i>D. Fernandez-Galisteo, E. F. Tarrazo, C. Jiménez, V. Kurdyumov</i>	Analog Modeling of Detonation in a Periodic Medium(168) <i>A. Kasimov, A. Gonchar</i>	Increased Combustion Interactions of Closely Packed Diesel Droplets Caused by Soot Contamination(194) <i>A. F. b. A. Rasid, S. Hanriot, Y. Zhang</i>	Thermal Explosions in Alkenes Epoxidation Processes(70) <i>G. Pio, E. Salzano</i>
11:10	Numerical Investigation of Shock Waves as Detonation Initiator(306) <i>S. Bengoechea, J. Reijß, M. Lemke, J. Sesterhenn</i>	Study on Reactivities of Refrigerants R32, R125 and R410A using a Micro Flow Reactor with a Controlled Temperature Profile(269) <i>S. Takahashi, H. Nakamura, T. Tezuka, S. Hasegawa, K. Maruta</i>	Non-Equilibrium Effects in Detonations Initiation using Hard Spheres(346) <i>R. Murugesan, N. Sirmas, M. Radulescu</i>	Subcritical to Supercritical Transition of Fuel Mixtures in High Temperature and Pressure Environment(324) <i>S. Chakraborty, L. Qiao</i>	Effect of Gap Width on the Flame Propagation in a Millimeter-Scale Closed Chamber(209) <i>J. Huo, H. Su, L. Jiang</i>
11:35	The Effect of Ozone Addition on DDT for Ethylene-Oxygen Mixtures in Macro-Scale Tube(203) <i>Y. Cai, W. Han, C. Wang, Y. Cui, W. Ma, Y. Wu</i>	FREE	Discrete Boltzmann Modelling of Compressible Reactive Flows(56) <i>C. Lin, K. Luo</i>	FREE	Effect of Rock-Dust Height on Suppression of Coal-Dust Entrainment by Shock Waves(47) <i>S. Lai, R. Houim, E. Oran</i>
12:00	Lunch				
12:30	Excursion				
	Route 1: Juyongguan Great Wall Route 2: Forbidden City (Depart from Yingjie Exchange Center at 12:30)				
17:30	Dinner				
20:30	Yv Xian Du Royal Cuisine Museum				

Thursday

Rooms	Sunlight Hall	Moonlight Hall	Room 2	Room 8	Rooms 3/4
Topic	1D Detonation Stability <i>R. Deiterding</i>	RDE 3 <i>P. Wolanski, J. P. Wang</i>	Chemical Kinetics 1 <i>R. Hanson</i>	Laminar Flames 1 <i>M. Braun-Unkoff</i>	Explosion Safety 2 <i>J. Wen, T. Skjold</i>
8:30	Nonlinear Stability of Square Wave Detonations and the Zaidel Paradox(342) <i>A. Olmo-Velazquez, L. Bauwens</i>	Critical Height for Rotating Detonation Wave based on the Modified ZND Model(99) <i>L. Deng, M. Wang</i>	Effect of Oxygen Atom Precursors Addition on LTC-affected Detonation in DME-O2-CO2 Mixtures(15) <i>R. Mevel, Y. He</i>	Comparative Study of Laminar Burning Velocity Measurement between Confined and Unconfined Spherical Flames Methods for Methane/Air and n-Decane/Air Premixed Flames(254) <i>R. L. Dortz, C. Strozzi, J. Sotton, M. Bellenoue</i>	Numerical Study of the Influence of Gas Expansion on the Acceleration of outwardly Expanding Flames(221) <i>R. Feng, R. Zhang, D. Valiev</i>
8:55	Effect of Longitudinal Concentration Gradient on 1-D Double-Period Detonation(59) <i>W. Han</i>	Numerical Investigation on Multi-Wave Propagation Mode of Rotating Detonation Waves(125) <i>P. Yang, Z. Jiang, H. Teng</i>	Methane Combustion Dynamics in Diabatic PSRs with Detailed Reaction Mechanisms at Low and High Pressures(328) <i>F. S. Marra, L. Acampora</i>	Measurements of Laminar Burning Velocity in a Shock Tube(10) <i>A. Susa, D. Davidson, R. Hanson, A. Ferris</i>	Influence of Wall Boundary Condition on the Dynamics of Premixed Flames Propagating in a Closed Channel(52) <i>X. Li, H. Xiao, J. Sun</i>
9:20	One-Dimensional Stability Analysis of Vibrational Nonequilibrium Effect on Detonation Neutral Stability(241) <i>C. K. Uy, L. Shi, C. Y. Wen</i>	One Inducing Factor of the Operational Mode Transition in a Rotating Detonation Engine(46) <i>Z. Lei, X. Yang, J. Ding, P. Weng</i>	Role of Low-Temperature Chemistry on the Onset of Detonation behind an Incident Shock Wave(117) <i>W. Han, R. Mevel, D. Ning, W. Liang, C. K. Law</i>	Laminar Flame Speed Measurements from Chemiluminescence of OH* and CH* in Spherically Expanding CH4-Air Flames(332) <i>M. Turner, T. Paschal, P. Parajuli, W. Kulatilaka, E. Petersen</i>	Understanding How Mixture Composition Affects Flame-Acoustic Interactions in Large-Scale Vented Explosions(350) <i>C. R. Bauwens, L. Boeck, S. Dorofeev</i>
9:45	Stability of Non-Adiabatic Shocks(77) <i>C. Huete, A. Cuadra, M. Vera</i>	Effects of Isothermal Wall Boundary Conditions on Continuous Detonation Chamber(298) <i>L. F. Zhang, K. Q. Wu, J. P. Wang</i>	Experimental and Numerical Study on Fuel-NOx Formation in Oxy-Fuel Processes in a Jet Stirred Reactor(234) <i>K. Wang, L. Pengfei</i>	Thermoacoustic Analysis of Lean H2-Air Premixed Flames in Thin Layers(169) <i>F. Veiga-Lopez, D. Martínez-Ruiz, M. Sánchez-Sánz, M. Kuznetsov</i>	Numerical Investigation of Venting through Roof for an ISO Containers(343) <i>J. Wen, V. C. M. Rao</i>
10:10	Break				

Rooms	Sunlight Hall	Moonlight Hall	Room 2	Room 8	Rooms 3/4
Topic	Flame Acceleration & DDT 1 <i>S. Frolov, K. Ishii</i>	RDE 5 <i>E. Gutmark, Z. Chen</i>	Chemical Kinetics 3 <i>D. Nativel</i>	Laminar Flames 3 <i>C. Keesee</i>	Explosion Safety 4 <i>V. Molkov, F. Tamanini</i>
13:50	High-Speed Imaging of DDT in a Round Tube(71) <i>P. Krivosheyev, O. Penyazkov, A. Sakalou</i>	Dynamic Mode Decomposition Analysis of Rotating Detonation Waves(5) <i>R. Bluemner, M. D. Bohon, C. O. Paschereit, E. Gutmark</i>	A Theoretical Study on the Isomerization and Dissociation Kinetics of Methyl Decanoate Radicals(147) <i>Q. Meng, Y. Chi, L. Zhang, P. Zhang, L. Sheng</i>	Analysis of Synthetic Flames(365) <i>S. Coronel, R. Mevel, J. E. Shepherd</i>	Experimental and Simulation Studies on the Influence of Hydrogen Addition on the Lean Flammability Limits of Methane/Air Mixtures(295) <i>C. Wu, C. Yu, R. Schießl</i>
14:15	Hot Spots Formation at DDT in Cylindrical Tube(252) <i>Y. Baranyshyn, P. Krivosheyev, O. Penyazkov, K. Sevrouk</i>	Effect of Secondary Waves on Detonation Wave Properties in a Rotating Detonation Engine(333) <i>F. Chacon, M. Gamba</i>	Theoretical Kinetics Analysis for OH Radical Addition to 1, 3-Butadiene and Related Reaction on the C₄H₇O Potential Energy Surface (34) <i>C. Zhou, J. Bai</i>	Effects of Water Droplet Vaporization on Propagation of Premixed Spherical Flames(140) <i>Y. Zhuang, H. Zhang</i>	Problems of Detonation Wave Suppression in Hydrogen-Air Mixtures by Clouds of Inert Particles in One- and Two-Dimensional Formulation(148) <i>D. Tropin, I. Bedarev</i>
14:40	Deflagration-to-Detonation Transition in Laser-Ignited Explosive Gas Contained in a Smooth-Wall Tube(135) <i>T. Endo, W. Kim, T. Johzaki, K. Okada, S. Kuwajima, D. Shimokuri, A. Miyoshi, S. Namba</i>	Mode Switching in 2-Dimensional Continuous Detonation Chambers with Discrete Injectors(284) <i>Y. L. Chen, X. Y. Liu, J. P. Wang</i>	A Parameter Study of NSD Plasma Assisted Pyrolysis and Oxidation of CH₄ in a Temperature-Dependent Flow Reactor(289) <i>C. Guo, Q. Chen</i>	Pressurized MILD and Oxy-Fuel Combustion in Counter-Flow Configuration: Emissions of NO and CO(230) <i>K. Wang, L. Pengfei</i>	Theoretical Estimation of Concentration Limits for Water Steam Capability to Suppress Flame Acceleration in Hydrogen-Air Mixtures(310) <i>I. Kirillov, N. Kharitonova, A. Lebedev, S. Nikiforov, V. Plaksin</i>
15:05	Break				

Rooms	Sunlight Hall	Moonlight Hall	Room 2	Room 8	Rooms 3/4
Topic	Detonation Miscellaneous 2 <i>S. Frolov, K. Ishii</i>	RDE 6 <i>E. Gutmark, Z. Chen</i>	Chemical Kinetics 4 <i>C. Zhou</i>	Sprays & Droplets 2 <i>C. Diller</i>	Explosion Safety 5 <i>V. Molkov, F. Tamanini</i>
15:30	Model for CJ Deflagrations in Open Ended Tubes with Varying Vent Ratios(186) <i>W. Rakotoarison, M. Radulescu, Y. Vilende</i>	Effects of a Radial Strip Injection Pattern on a Continuous Detonation Chamber using Navier-Stokes Equations(303) <i>L. Zhang, Y. Hao, J. Wang</i>	Comparison of the Experimental and Kinetic Study of two Aviation Surrogate Fuels(51) <i>Y. Liu, B. Wang, Z. Tian</i>	Effects of Oxygen and Buffer Gas Concentration on Diesel Spray Flame Characteristics(129) <i>W. Yi, H. Liu</i>	Estimation of the Critical Conditions for Suppression of the Combustion and Detonation Waves(66) <i>A. Vasil'ev</i>
15:55	The Effects of Compressibility on the Propagation of Premixed Deflagration(367) <i>A. Fecteau, J. McDonald, M. Radulescu</i>	Numerical Study of Rotating Detonation Onset in Engines(173) <i>E. Mikhhalchenko, V. Nikitin, Y. Filippov, L. Stamov</i>	Theoretical Kinetics Study on the Reactions of 1, 3-Butadiene +HO₂ (30) <i>Y. Zhu, C. Zhou</i>	On the Low Temperature and Low Pressure Regime Diagram of n-Heptane Droplet Burning in Microgravity(373) <i>W. Zhang, Y. Liu</i>	Effects of Fuel Decomposition on the Minimum Ignition Energy of n-Decane/Air(85) <i>X. Chen, Z. Chen, Y. Wang</i>
16:20	Effect of Inverse Reactions on One-Dimensional Detonation Simulated by DSMC(292) <i>D. Ding, H. Chen, B. Zhang, B. Zhang, H. Liu</i>	Minimum Mass Flow Rate Predictions for Rotating Detonation Engines Operating on Mixtures of H₂-O₂-N₂, C₃H₈-N₂O and C₂H₄-N₂O(338) <i>S. Connolly-Boutin, C. B. Kiyanda, H. D. Ng, A. Higgins</i>	Laminar Flame Speed and Laser Absorption Measurements of Conventional and Alternative Kerosene-Based Liquid Fuels(80) <i>C. Keese, E. Petersen, B. Guo</i>	FREE	FREE
16:45	Adjourn				
18:00	Banquet, <i>Shangri-La Hotel</i> , Beijing Cocktails starts at 17:00				
21:00	Buses depart from <i>Yingjie Exchange Center</i> at 17:00 Dress code: no T-shirt, short pants, sandals				

Friday					
Rooms	Sunlight Hall	Moonlight Hall	Room 2	Room 8	Rooms 3/4
Topic	Detonation Propagation in Rough Wall Duct <i>E. Oran, M. Kuznetsov</i>	Micro Combustor <i>J. Kasahara, P. Vidal</i>		Turbulent Flames 4 <i>J. L. Li</i>	Dust Combustion 1 <i>T. Endo</i>
8:30	Change in Quasi-Detonation Wave Propagation Mechanism with Obstacle Blockage(91) <i>Q. Li, M. Kellenberger, G. Ciccarelli, C. Wang, S. Lu</i>	Combustion Instability Analysis in a Subscale Rocket Chamber with a Single Injector and Two Injectors(62) <i>Y. Wang, J. Son, C. H. Cho, C. H. Sohn</i>	FREE	Experimental Study of EGR Dilution and O2 Enrichment Effects on Turbulent Non-Premixed Swirling Flames(360) <i>T. Boushaki, H. Zaidaoui</i>	Radiation Heat Loss and Solid Combustion Products Characterisation of Premixed Al-Air Flames(323) <i>P. Laboureur, C. Chauveau, F. Halter, R. Lomba, C. Dumand</i>
8:55	Computational Study of Gaseous Detonation Diffraction and Re-Initiation by Small Obstacle Induced Perturbations(41) <i>X. Yuan, X. Mi, H. Xu, J. Zhou, H. D. Ng</i>	Standalone Portable Micro Power Generator using Stepped Micro Combustor(226) <i>B. Aravind, R. Varghese, S. Kumar, K. Hiranandani</i>	FREE	Measurements of High-Pressure/Temperature Turbulent Burning Velocities of Lean and Rich Iso-Octane/Air Mixtures and Their Various General Correlations(235) <i>M. T. Nguyen, Y. Chen, S. Shy</i>	Effects of Particle Size Distribution on Cell Size Prediction in Al-Air Detonation(265) <i>Z. Zhang</i>
9:20	Propagation of Near-Limit Gaseous Detonations in Rough Walled Tubes(335) <i>Y. Yan, T. Ren, J. H. Lee, H. D. Ng</i>	A Numerical Investigation on Non-Premixed Catalytic Combustion of CH4/Air in a Symmetrical Planar Micro-Combustor(90) <i>L. Li, A. Fan</i>	FREE	Characterization of Soot in a Co-annular Ethylene Diffusion Flame when Submitted to a DC Electric Field(317) <i>A. S. Kassem, P. Gillon, M. Idir, V. Gilard</i>	Comparison on Laser Ignition and Combustion Characteristics of Nano- and Micron-sized Aluminum(206) <i>X. Huang, X. Jin, S. Li</i>
9:45	Flame Acceleration in the Hydrogen-based Microfoams(211) <i>B. Kichatov, A. Kiverin, I. Yakovenko, A. Korshunov</i>	Numerical Simulation of the Influence of Propellant Mixture Ratio on High Frequency Combustion Instability in a Kero/LOX Liquid Rocket Engine(299) <i>K. Guo, W. Nie, Y. Liu, T. Shi</i>	FREE	FREE	Flame Inhibition of Aluminum Dust Explosion by Sodium Bicarbonate with Different Particle Size(192) <i>W. Gao, H. Jiang</i>
10:10	Break				

Rooms	Sunlight Hall	Moonlight Hall	Room 2	Room 8	Rooms 3/4
Topic	Flame Acceleration & DDT 2 <i>E. Oran, M. Kuznetsov</i>	RDE 7 <i>J. Kasahara, P. Vidal</i>	Explosion Safety 6 <i>R. Bauwens</i>	Turbulent Flames 5 <i>G. Dong</i>	Dust Combustion 2 <i>Yun Wu(Y. Wu)</i>
10:40	Detonability Limits in H₂-Air Mixture in a Tube Filled with Obstacles(277) <i>W. Rudy, A. Teodorczyk</i>	Effects of Combustor Size on Behavior of Rotating Detonation Waves(251) <i>K. Ishii, H. Kawana, W. Kurata, K. Ohno, D. Ikema</i>	Towards Descriptive Scenario of a Burning Accident in an Obstructed Mining Passage: An Analytical Approach(369) <i>F. Kodakoglu, V. Akkerman, S. Demir, D. Valiev</i>	Statistics of Two-Phase Coupling in Turbulent Spherically Expanding Flames in Mono-sized Fuel-Droplet Mists(78) <i>G. O. Erol, J. Hasslberger, N. Chakraborty</i>	Experimental Study on the Ignition Temperature of Combustible Dust Clouds with the Effect of CH₄/CO/H₂(133) <i>X. Tan, W. Huang, M. Schmidt, D. Wu</i>
11:05	Effects of Unequal Blockage Ratio and Obstacle Spacing on Wave Speed and Overpressure during Flame Propagation in Stoichiometric H₂/O₂(45) <i>C. B. Ahumada, M. S. Mannan, E. Petersen</i>	Experimental Research of Liquid Fueled Continuously Rotating Detonation Chamber(185) <i>P. Wolanski, W. Balicki, W. Perkowski, A. Bilal</i>	Ignition Temperature of Combustible Liquids in Mixtures of Air with Oxygen or Dinitrogen Oxide(73) <i>S. Zakei, E. Brandes, M. Mitu, W. Hirsch</i>	Numerical Simulation of Turbulent Flame Propagation in a Fan-Stirred Combustion Bomb at Elevated Pressures(64) <i>F. Zhang, T. Zirwes, P. Habisreuther, H. Bockhorn, N. Zarzalis, D. Trimis</i>	Numerical study on a shock wave through dusty-gas layers with different particles(86) <i>J. Yin, X. Yu</i>
11:30	Deflagration-to-Detonation Transition in Mixtures of the Pyrolysis Products of Polypropylene with Air(172) <i>S. Frolov, V. Zvegintsev, V. Aksenov, I. Bilera, M. Kazachenko, I. Shamshin, P. Gusev, M. Belotserkovskaya</i>	Mixed Detonation-Deflagration Behavior of Hydrocarbon-based Rotating Detonation Engines(353) <i>T. Sato, V. Raman</i>	Simulations of blast wave propagation in open space that require adaptive mesh refinement(111) <i>T. Roh, J. Yoh</i>	Experimental and numerical determination of Lewis number and Markstein lengths for a multi-component jet fuel surrogate and air mixtures(239) <i>R. L. Dortz, C. Strozzi, J. Sotton, M. Bellenoue</i>	Dynamics, Spectra, and Temperatures of Silicon Combustion in the pSi-CO₂ System(177) <i>V. Mironov, O. Penyazkov, Y. Baranyshyn, P. Krivosheyev</i>
11:55	Two-Dimensional Numerical Simulation of Flame Acceleration and Deflagration-to-Detonation Transition in Channels with Obstacles: Effects of Blockage Ratio and Chanel Size(267) <i>K. Iwasaki, A. Ago, N. Tsuboi, K. Ozawa, K. Hayashi</i>	Propulsive Performance of Rotating Detonation Engines in CH₄/O₂ and C₂H₄/O₂ for Flight Experiment(245) <i>K. Goto, A. Kawasaki, K. Matsuoka, J. Kasahara, A. Matsuo, D. Nakata, R. Yokoo, J. Kim, I. Funaki, M. Uchiumi</i>	An adaptive flame-tracking shock-capturing scheme for industry-scale explosion simulations(63) <i>J. Hasslberger, T. Sattelmayer, S. Ketterl</i>	FREE	Pyrolysis and Ignition of Branched-Chain Amino Acid Powders(128) <i>W. Kim, T. Soga, T. Johzaki, T. Endo, T. Kato, K. Choi</i>
12:20					
12:30	Lunch				
13:20	Work in Progress posters all afternoon				

Rooms	Sunlight Hall	Moonlight Hall	Room 2	Room 8	Rooms 3/4
Topic	Flame Acceleration & DDT 3 <i>N. Smirnov</i>	RDE 8 <i>C. Kiyanda</i>			
13:50	Flame Acceleration and Transition to Detonation in Methane-air Mixtures with Composition Gradients(43) <i>W. Zheng, C. Kaplan, R. Houim, E. Oran</i>	Numerical Study on two-Dimensional Detonation Propagation across Inert Layers(68) <i>Y. Wang, C. Huang, R. Deiterding, Z. Chen</i>	FREE	FREE	FREE
14:15	Numerical Analysis of Flame Acceleration and Onset of Detonation in Homogenous and Inhomogeneous Mixture(341) <i>J. Wen</i>	Experimental Research of Performance of Combined Cycle Rotating Detonation Rocket-Ramjet Engine(181) <i>P. Wolanski, M. Kawalec</i>	FREE	FREE	FREE
14:40	Flame acceleration and transition to detonation in a channel with triangular obstacles(197) <i>H. Xiao, E. Oran</i>	Chemical and Thermal-Chemical Non-Equilibrium Calculation of FIRE-II Vehicle(36) <i>N. Hu</i>	FREE	FREE	FREE
15:05	Numerical Investigation of DDT Mechanism in Cross-Section Abrupt Detonation Tube(25) <i>X. Jia, N. Zhao, H. Zheng, X. Chen</i>	FREE	FREE	FREE	FREE
15:30	Adjourn				
16:30	Farewell				
19:00	<i>Shao Yuan Restaurant</i>				

Session 1: Detonations Room 1	
RP-1	Coupled Shock Cluster-Reaction Front Structures during Detonation Transition in Narrow Channels Filled with Ethylene/Oxygen Mixtures(280) <i>M. Wu, H. Ssu, W. Su, Y. Tseng</i>
RP-2	The Impact of Spark-igniting Configuration on Detonation Onset in a Rapid Compression Machine(7) <i>Y. Wang, W. Liu, Y. Qi, Z. Wang</i>
RP-3	Effect of Initiation on Detonation Cells for a Three Step Chain-Branching Scheme(389) <i>H. Qiu, L. Bauwens, C. Xiong</i>
RP-4	Numerical Investigation of the Direct Initiation Mechanism of Double Point Laser Ignition(24) <i>G. Hongbo, N. Zhao, H. Zheng, Z. Li, C. Sun</i>
RP-5	Numerical Studies on the Effects of Ozone Addition on Flame Acceleration and Deflagration-to-Detonation Transition for Hydrogen/Oxygen Mixtures(137) <i>W. Kong, D. Ning</i>
RP-6	Effect of Molar Ratio of H₂ to O₂ on Gaseous Detonation Synthesis of Graphene Quantum Dots(114) <i>C. He, X. Wang</i>
RP-7	Detonation Cellular Structure with Inner Tube of CH₄-O₂ Pre-mixed Mixture(29) <i>H. Zhao, Y. Yan</i>
RP-8	Propagation Mechanism of Quasi-Detonation in Annularly Rough Tube(248) <i>J. Ning, J. Li, T. Yang</i>
RP-9	Flame Evolution in Shock Accelerated Flow under Different Reactive Gas Mixture Distributions(93) <i>Y. Zhu, L. Gao, K. Luo, J. Pan, Z. Pan, P. Zhang</i>
RP-10	Numerical Investigation of Cylindrical Detonation using a Multiscale Adaptive Reduced Chemistry Solver (MARCS)(255) <i>H. Liang, L. Wang</i>
RP-11	Parallel Chemistry Acceleration Algorithm with Table Size Control Method for Gaseous Detonation Simulations(67) <i>J. Wu, G. Dong</i>
RP-12	Study on Simplified Model of Detonation Based on Wave Front Curvature(378) <i>Y. Sun</i>
RP-13	Theoretical Study on the Deflagration to Detonation Transition Process(37) <i>W. Zhang, Y. Liu</i>
RP-14	Research on Detonation of Liquid Hydrogen-Oxygen by Numerical Simulation(242) <i>Y. He</i>

Session 2: Explosions Room 1	
RP-15	Evaluation of the Effects of Coated Walls on Flame Stability of C1-C3 Alkane/Air Mixtures in a Slit Burner(58) <i>F. Li, H. Yang, D. Zhao, X. Wang</i>
RP-16	Finger Flame over the Heat Absorbing Surface(215) <i>G. Viktor, V. Volodin, A. Gavrikov, A. Mikushkin, V. Petukhov</i>
RP-17	Experimental Study on Active Deflagration Suppression Technology in an Open Tube(60) <i>W. Fan, H. Wu, Y. Huo</i>
RP-18	Energy of the Explosion of Unit 3 Reactor Building of Fukushima Daiichi(14) <i>T. Tsuruda</i>
RP-19	Effect of Impurities on Thermal Hazard of Dimethyl 2, 2'-azobis (2-Methylpropionate) (AIBME) in Industrial Application(151) <i>A. Yu, X. Pan, M. Hua</i>
RP-20	Determination of the Explosion Characteristics of Methanol -Air Mixture in a 20-l Sphere(107) <i>H. Yu, X. Zang, X. Pan</i>
RP-21	Exhaust Gas Components and Hazardous Effect of Coal Dust Explosion(260) <i>B. Nie</i>
RP-22	Relation between the Ignition Point of the Flame and the Jet Behavior in the Gas Explosion(122) <i>K. Jindai, T. Tsuruda, T. Daitoku</i>

Session 3: Energetics Room 1	
RP-23	Propagation of the Explosion of a Solid Propellant in a Partitioned Structure(8) <i>J. M. Pascaud</i>
RP-24	The Effect of Relative Humidity on Aging of Zirconium-based Energetic Materials(208) <i>B. Han, Y. Park, J. Yoh</i>
RP-25	Study on Ignition and Combustion Characteristics of Zirconium-Containing Solid Propellant(72) <i>Q. Liu</i>
RP-26	A Highly Integrated Conjoined Single Shot Switch and Exploding Foil Initiator Chip Based on MEMS Technology(286) <i>C. Xu, Q. Zhang, Z. Yang, P. Zhu, R. Shen</i>
RP-27	Experimental Study on The Reaction Evolution of Pressed Explosives in Long Thick Wall Cylinder Confinement(357) <i>H. Hu, T. Li</i>
RP-28	Radiation Imaging Based Temperature Measurement Method for Aluminum Particles in NEPE Propellant Combustion(136) <i>L. Huang, Z. Xia</i>
RP-29	Thermal Decomposition and Microscopic Characterization of 8701 Explosive Subjected to Thermal Load(288) <i>Z. Shao, Y. Wu, F. Huang, P. Jiang</i>

RP-30	High-Resolution Numerical Simulation of Dead Zones in the Insensitive Explosive Detonation(83) <i>T. Ma, F. Ma, J. NING</i>
-------	---

Session 4: Fire Room 1	
-----------------------------------	--

RP-31	A Numerical Analysis on the Shedding Mechanism of Dripping Flame(152) <i>X. Huang, C. Xiong, P. Sun, Y. Jiang</i>
RP-32	Modelling the Propagation of One-End-Burning Cylindrical Firebrands based on the Measured Regression Rates(345) <i>H. Zhou, Y. Lai, Y. Li, Y. Zhang</i>
RP-33	Experimental Investigation on the Flame Characterization and Temperature Profile of Single/Multiple Pool Fire in Cross Wind(198) <i>Z. Chen, X. Wei, T. Li</i>
RP-34	Heat and Mass Transfer of Flame Spread along a Combustible Slope(200) <i>T. Daitoku, K. Hiyama, T. Tsuruda</i>
RP-35	Thermal Stability of Chemicals under Fire Conditions: the Case of Hydroxylamine Sulphate(130) <i>E. Danzi, G. Pio, E. Salzano, L. Marmo</i>
RP-36	Study on Characteristics of Ship Engine Room Fires(290) <i>L. Cong</i>
RP-37	AutoCAD inspired Level-Set Algorithm for 3D Simulation of Industrial Fire and Explosion(119) <i>H. J. Kim, J. Yoh</i>

Session 5: Kinetics and Flames Room 1	
--	--

RP-38	Nonlinear Large-Eddy Simulation of a Cambridge Stratified Swirling Flame(278) <i>X. Qian, H. Lu, C. Zou</i>
RP-39	Study of Oil Droplet Ignition and its Induction for Pre-ignition under Different Environmental Conditions(20) <i>S. Fei, Y. Qi, Y. Wang, Z. Wang, H. Zhang</i>
RP-40	Composition and Outlet Distribution of Pre-Combustion Pyrolysis Products(28) <i>F. Song, Y. Wu, D. Jin, X. Chen, S. Xu</i>
RP-41	Genetic Algorithm Applied in Optimizing Reaction Mechanism Based on Reduced Reaction Mechanism(118) <i>R. Yang</i>
RP-42	Two-Dimensional Frequency Analysis of a Diffusion Methane Jet Flame under Transverse Acoustic Excitations(264) <i>J. Wang, X. Mei, Q. Wang</i>
RP-43	Numerical Study of OH*, CH* and C2* Radicals in a New Reduced Ethanol Kinetics(79) <i>J. Zhng, Y. Zhang</i>
RP-44	Effect of Hydroxyl Radical Precursors Addition on LTC-affected Detonation in DME-O2-CO2 Mixtures(16) <i>Y. He, R. Mevel</i>

RP-45	Kinetic Study on Nitromethane and its Application as Power Booster in Engines(69) <i>K. P. Shrestha, F. Mauss, L. Seidel, T. Franken, T. Zeuch</i>
RP-46	Advanced Dimension Reduction Methods for the Identification of Intrinsic Low-Dimensional Manifolds in Composition Space(162) <i>Y. Xia, Y. Jiang</i>
RP-47	Effect of Hydrogen Addition on Ignition of Methane-Hydrogen-Air Mixtures over a Hot Surface(247) <i>S. Kumar, R. K. Velmati, S. Shashidharan</i>
RP-48	Velocity Measurement Comparison of Traditional and Schlieren-Equation Based Optical Flow Methods(243) <i>H. Cheng, Y. Wu, X. Mei, Q. Wang</i>
RP-49	Effects of Nitrogen on the Flammability Limits of Dimethyl Ether at Different Temperatures(232) <i>Y. Zhang, Y. Liu</i>
RP-50	A Study of Combustion Characteristics of Heterogeneous Combustion Field by Impinging Injection and Multiple Fuel Injection(201) <i>J. Liu, H. Aoki, T. Kawakami</i>
RP-51	Burning of Fuel Droplets Incorporating Solid Carbon Particles(170) <i>V. Nikitin, V. Tyurenkova, N. Smirnov</i>
RP-52	Structure and Dilatation of Perturbed Flame Interface during the Reactive Richtmyer-Meshkov Instability(370) <i>D. Wang, G. Dong</i>
RP-53	A New Cylindrical Converging Shock Tube(222) <i>D. Zheng, X. Luo, Z. Zhai</i>
RP-54	Experimental Study on the Lower Flammability Limits of Ammonia/Methanol/Air Mixtures at Elevated Pressures and Temperatures(13) <i>W. Ji, Y. Wang, J. Yu, X. Yan</i>
RP-55	Experimental and Numerical Study of Excited-State Radicals in Methane-Air Jet Diffusion Flames(75) <i>Y. Liu, J. Tan, L. Zhang</i>
RP-56	Characteristics of Sub-Standard Liquid hydrocarbons Combustion when Interacting with Superheated Steam Jet(145) <i>E. Kopyev, I. Anufriev, O. Sharypov, A. Tsepenok</i>
RP-57	Experimental Study of Substandard Liquid Hydrocarbons Spraying by Shadow Photography Method(141) <i>I. Anufriev, E. Shadrin, E. Kopyev, O. Sharypov, Y. Osintsev, M. Mukhina</i>
RP-58	RANS Simulation of Turbulent Non-Premixed H₂/Air Combustion(4) <i>H. Dong, J. Liu, X. Bai, Y. Wei</i>
RP-59	Investigation of Characteristics of Diesel Fuel Atomization by Steam Jet(144) <i>O. Sharypov, I. Anufriev, E. Shadrin, E. Kopyev, V. Leschevich</i>
RP-60	Further Investigation of Hydrogen Flame Colour(355) <i>M. Pan</i>
RP-61	Effect of CO₂ Dilution on Combustion Characteristics of a Liquid Fuel-Fired Flameless Combustor(214) <i>S. Sharma, S. Kumar, H. Lal, A. Chowdhury</i>
RP-62	Study of Ignition Delay in Mixtures of Diesel, Biodiesel and Ethanol(195) <i>S. Hanriot, D. Guimarães, O. Valente</i>

RP-63	Kinetic Modeling for PAH Formation in a Counterflow Diffusion Flame of Isobutane(308) <i>W. Chiu, H. Tao, K. C. Lin</i>
RP-64	Numerical Studies of Hydrogen-Enriched Partially Premixed Combustion on a Model Gas Turbine Combustor(110) <i>J. Nam, J. Yoh</i>
RP-65	A Numerical Investigation of Combustion Characteristics of Biogas Fuel in a Spark Ignition Engine(179) <i>M. Bassiouny, A. Ebrahemi, S. Ahmed</i>
RP-66	High Efficiency and Clean Combustion of Converter Gas(32) <i>Y. Zhai, S. Li</i>
RP-67	Dynamics of the Low-Temperature Autoignition Kernels in Turbulized Hydrogen-Air Mixture(158) <i>S. Medvedev, S. Khomik, O. Maximova, G. Agafonov, A. Tereza, A. Betev, H. Olivier</i>
RP-68	Multiphase LES Analysis on Kerosene/H₂O₂ Combustion of a Slit Injector(87) <i>J. Kang, Y. Yoo, H. Hwang, H. Sung</i>

Session 6: Dust Room 7	
RP-69	Analysis of Explosion Dynamics from Dust Cloud Metal Particle using Thermal Infrared Imaging(6) <i>S. B. Tombet, F. Marcotte, A. Huot, L. Yi</i>
RP-70	Study on Heating Process of Micro-Sized Aluminum Particles in Planar Flame(375) <i>J. Li, X. Gu</i>
RP-71	Combustion Behavior of Acoustically Levitated Biomass Particle(272) <i>T. Matsuoka, Y. Nakamura, T. Kajimoto</i>
RP-72	Explosion Characteristics of Coal Dust with Different Metamorphism Degrees(262) <i>B. Nie</i>
RP-73	Mechanisms of Silicon Combustion in the pSi-O₂ and pSi-NaClO₄·H₂O Systems(304) <i>V. Mironov, O. Penyazkov, P. Krivosheyev, E. Golomako</i>
RP-74	TG-FTIR Study on Effects of Titanium Dioxide Nanoparticles on the Decomposition of HAN Aqueous Solutions(313) <i>M. Wu, H. O. Yang, C. You, J. Chin</i>
RP-75	Ignition and Combustion of Individual Aluminum Particles below 10μm at Different Laser Heating Rates(244) <i>X. Huang, F. Hou</i>
RP-76	Determination of Burning Rate of Gas Generator Compositions based on Sodium Nitrate(331) <i>M. Atamanov, Z. Mansurov, S. Tursynbek, D. Bayseitov, F. Abdrakova, M. Tulepov</i>
RP-77	Propagation of a Strong Shock Wave in a Random Bed of Metal Particles(120) <i>S. Choi, J. Yoh</i>

Session 7: RDE Room 7	
RP-78	Effect of Wall Viscosity on Flow Structures in 3-D Rotating Detonation Wave(11) <i>P. Liu</i>
RP-79	Numerical Prediction of the Detonation Wave Number(23) <i>Q. Meng, N. Zhao, H. Zheng, J. Yang, L. Qi</i>
RP-80	Effect of Expansion Outlet on Continuous Rotating Detonation Combustor(26) <i>C. Sun, N. Zhao, H. Zheng, J. Yang, H. Guo</i>
RP-81	Investigation for Delay Time of Rotating Detonation Fueled by Hydrocarbon-Hydrogen Mixture(27) <i>Y. Zhong, Y. Wu, D. Jin, X. Chen, X. Yang</i>
RP-82	An Analysis of the Performance of a Continuous Rotating Detonation Engine(44) <i>S. Huang</i>
RP-83	Numerical Simulation of Reactive Gas Mixes Flows in the Detonation Engine(57) <i>M. Sergey</i>
RP-84	Experimental Investigation of Pulse Compression Detonation System(61) <i>K. Korytchenko, O. Sakun, C. Senderowski, D. Dubinin, V. Nikoluk, B. Maxwell</i>
RP-85	Numerical Simulations of Compression and Detonation Strokes in a Pulse Compression Detonation System(98) <i>B. Maxwell, K. Korytchenko, O. Shypul</i>
RP-86	Numerical Investigation of a Non-premixed Rotating Detonation Engine with Different Number of Fuel Injectors(109) <i>J. Sun, J. Zhou</i>
RP-87	Numerical Investigation on Non-Premixed Rotating Detonation Engine with Different Exhaust Nozzle Configurations(116) <i>S. Xue</i>
RP-88	Numerical Investigation of Effect of Wall Curvature on Detonation Propagation in an Annular Cylinder(124) <i>M. Gui, H. Cui, H. Zhang</i>
RP-89	Frequency Locking of Global Unstable Lean Premixed Bluff Body Stabilized FlamewithAcoustic Excitation(149) <i>P. Liu, J. Feng, X. Lv</i>
RP-90	Influence of the Combustion Wave Velocity in a Mixture on the Thrust of a Pulsed Detonation Combustor(161) <i>M. Assad, O. Penyazkov, I. Chernuho</i>
RP-91	Investigation on Self-Sustaining Mechanism of Wedge Supported Oblique Detonation Waves for Equilibrium Flow(178) <i>A. Wang</i>
RP-92	Experimental Research on Ignition and the Stabilization Process in Rotating Detonation Chamber(229) <i>Z. Ma, Y. Hao, S. Zhang, J. Wang</i>
RP-93	Wave Direction Studies in Rotating Detonation Engine(246) <i>M. Kawalec</i>

RP-94	Numerical Simulation of the Rotating-Detonation Process with Nonpremixed Injection of Hydrogen and Air(249) <i>D. Li, Y. Zhang, G. Liang</i>
RP-95	The Comparison of Detonation Diffraction and Re-initiation in the Static and Supersonic Inflow(276) <i>L. Hongbin, J. Li, W. Fan</i>
RP-96	3D Simulations of a Non-Premixed Continuous Rotating Detonation Ramjet Engine Fueled by Hydrogen(294) <i>D. Xiong, M. Sun, H. Wang, S. Liu</i>
RP-97	Adaptive Mode Switching Process of Rotating Detonation Engine(296) <i>S. B. Yao, M. Y. Luan, J. P. Wang</i>
RP-98	Number Change of Detonation Waves in Hollow Continuous Detonation Chamber(302) <i>Z. J. Xia, M. Y. Luan, S. J. Zhang, Z. Ma, J. P. Wang</i>
RP-99	Numerical Simulation of Detonation Propagation in the Branch Tubes of the Detonation Wave Ignition System(307) <i>H. Guo</i>
RP-100	Control of Detonation Combustion of Hydrogen-Air Mixture in Plane Channels(312) <i>V. Levin, T. Zhuravskaya</i>
RP-101	Analysis of Fuel Mixing Characteristic in Supersonic Combustor with Injection Pressure and Existence of Cavity using Modal Decomposition Method(327) <i>S. Jeong, J. Choi</i>
RP-102	Experimental Study on 100 N-scale C2H4/GO2 Small RDE(352) <i>H. Han, J. Choi</i>

Work-In-Progress Poster
Friday 13:20

Session 1: Detonations/Explosions
Room 1

WP-1	Investigation on Self-Sustaining Mechanism of Wedge Supported Oblique Detonation Waves for Equilibrium Flow(178) <i>A. Wang</i>
WP-2	Investigation on Damage Norm and Criterion of the Shock Wave in Underwater Explosion(407) <i>J. Zhang, S. Wang</i>
WP-3	Numerical Study on the Oblique Shock Wave in a Surrounding Fluid and Detonation in a Cylindrical PETN(410) <i>Y. Sugiyama, T. Homae, T. Matsumura, K. Wakabayashi</i>
WP-4	Experiment and Numerical Analysis for H₂-air Rotating Detonation Engine with Water Cooling System(414) <i>W. Koido, E. Dzieminska</i>
WP-5	A Study on Operating Conditions of Disk-Type Rotating Detonation Engine(415) <i>H. Kawana, W. Kurata, K. Ohno, K. Ishii, A. K. Hayashi, N. Tsuboi, K. Ozawa, T. Obara, S. Maeda, E. Dzieminska, T. Mizukaki</i>
WP-6	Effect of bluff bodies on DDT(416) <i>L. Wang</i>
WP-7	Influence of Transversely Supersonic Inflow Condition on the Diffraction and Re-initiation Process for Regular and Irregular Detonation Wave(417) <i>H. Li, J. Li</i>
WP-8	Numerical Simulations of Induction Fronts with Nearly-Constant Propagation Speed(419) <i>V. Robin, A. Chinnayya, S. Taileb, A. Karan</i>
WP-9	Safety Characteristics of Hybrid Mixtures for Explosion Protection-Determination Methods Capable for Standardization (NEX-HYS)(420) <i>W. Hirsch, U. Krause, M. Schmidt, S. Zakel, E. Askar, D. Gabel, J. Kleinert, A. Krietsch, J. Meistes, A. Sachtleben, V. Schröder</i>
WP-10	Proper Orthogonal Decomposition (POD) Analysis of CFD Data for Two-Dimensional Cellular Detonations(422) <i>M. Kim, X. Mi, H. D. Ng</i>
WP-11	Flame Acceleration in Presence of Polyurethane Foam on the Channel Walls(424) <i>G. Bivol, S. Golovastov</i>
WP-12	Analysis of Coupling Characteristics between RDE Nozzle and Combustion(425) <i>H. Xia, Y. Huang</i>
WP-13	Numerical Simulations on Ignition using NRPD under High-Speed Flow Conditions(426) <i>Y. Morii, H. Nakamura, K. Maruta</i>
WP-14	Study on Flame Development using the External Excitation in Baffled Combustion Chamber(427) <i>W. Song, J. Koo</i>
WP-15	A Low Cost Microwave Detonation Velocity Measurement System(428) <i>F. Viot</i>

WP-16	Numerical Simulation of Reactive Gas Mixes Flows in the Detonation Engines(432) <i>M. Sergey</i>
WP-17	Simulation of a Detonation Propagation in a Two-phase Gas/Liquid Cross Flow Injection(435) <i>N. Jourdain, N. Tsuboi, K. Hayashi, X. M. Tang, K. Ozawa</i>
WP-18	Generation of Shock Wave in a Tube by Detonation of Spherical High Explosive(436) <i>E. Anderzhanov, S. Medvedev, A. Tereza, S. Khomik, B. Khristoforov</i>
WP-19	Lower Explosion Points of Selected Reference Substances under Non-Atmospheric Conditions(437) <i>A. Lucassen</i>
WP-20	Experimental Investigation and Modeling of Oxidizer Size and Concentration Effects on Composite AP/HTPB Propellant Burning Rates(440) <i>J. Thomas, C. Dillier, E. Petersen, G. R. Morrow</i>
WP-21	Performance Enhancement of HTPB Fuels burning in Gaseous Oxygen by Metallic Additives(441) <i>J. Thomas, F. Rodriguez, E. Petersen, A. J. Tykol</i>
WP-22	Burning Rate Characterization of Ammonium Perchlorate Pellets Containing Energetic and Catalytic Additives(442) <i>F. Rodriguez, E. Petersen, J. Thomas, C. Dillier, E. Petersen</i>
WP-23	A Review of the Effect of Particle Size and Particle Concentration on Burning Velocity Calculation in FLACS-DustEx: a Simplified Approach(444) <i>M. Ghaffari, T. Skjold, K. v. Wingerden, A. Hoffmann, R. Eckhoff</i>
WP-24	Effect of Impurities on Thermal Hazard of Dimethyl 2, 2'-Azobis (2-Methylpropionate) (AIBME)(451) <i>A. Yu, X. Pan, M. Hua</i>
WP-25	Determination of the Explosion Characteristics of Methanol-Air mixture in a 20-l Sphere(452) <i>H. Yu, X. Zangö</i>
WP-26	Experimental Study on the Detonation Propagation Behaviors through a Single Orifice Plate in Hydrogen-Air Mixtures(456) <i>X. Sun, Q. Li, S. Lu, L. Wang</i>
WP-27	Experimental Study of the Spray Characteristics of Liquid Jets in Supersonic Crossflow(459) <i>C. Li, Q. Li</i>
WP-28	Comparison of OH-PLIF Visualization of the Supersonic Combustion in Partly Premixed and Diffusion Hydrogen-Air Hlow(460) <i>Q. Yang, X. Xu</i>
WP-29	Effects of Fluidic Jet Angle on Detonation Propagation in Rotating Detonation Engines(462) <i>Z. Luan, Y. Huang</i>
WP-30	Effect of Molar Ratio of H₂ to O₂ on Gaseous Detonation Synthesis of Graphene Quantum Dots(470) <i>C. He, X. Wang</i>
WP-31	Theoretical Study on the Deflagration to Detonation Transition Process(471) <i>W. Zhang</i>

Session 2: Kinetics/Flames Room 7	
WP-32	Propagation of Symmetric and Non-symmetric Flames in Channels(392) <i>V. Kurdyumov, C. Jiménez, A. Dejoan</i>
WP-33	Investigation of Flame Measurement Characteristics on Multiple Ion-Probes(393) <i>N. Miura</i>
WP-34	Effects of Projection Length and Diameter of Ion-Probe on Flame Detecting Characteristics in 2-Stroke Gasoline Engine(394) <i>R. Kamei, T. Yatsufusa</i>
WP-35	Effects of Flame Detection Performance on Wire Diameter of Ion-Probe(395) <i>H. Yamamoto</i>
WP-36	Laminar Flame Propagation and Instability Investigations of Transportation Fuels in a High-Pressure Constant-Volume Cylindrical Combustion Vessel(396) <i>Y. Li</i>
WP-37	A Study of Oxy-Combustion of Palm Empty Fruit Bunch with Coal(397) <i>F. H. Wu, G. B. Chen, H. Lin, Y. C. Chao, C. Peng</i>
WP-38	Numerical Study of the Propagation of Lean Hydrogen-Air Flames in Hele-Shaw Cells(401) <i>A. Dejoan, D. Fernandez-Galisteo, V. Kurdyumov, J. Meguizo-Gavilanes</i>
WP-39	Effects of the Different Injection Delay on the Combustion Characteristics for the Propagation Flame in a Tube(404) <i>Z. Luoyu, T. Kawakami, A. Yukiya</i>
WP-40	Influence of Low Hydrocarbon Fuel Addition on Exhaust Characteristics for Small Gas Engines(406) <i>Y. Hong, T. Kawakami, H. Matsunaga</i>
WP-41	RANS Simulation of Turbulent Non-Premixed H₂/Air Combustion(408) <i>H. Dong</i>
WP-42	Ignition by Electrical Discharges - Interaction of the Hot Gas Kernel with Self-Generated Vortices(409) <i>J. Kummer, S. Essmann, D. Markus, U. Maas, H. Grosshans</i>
WP-43	Optimizing Mixture Properties for Accurate Laminar Flame Speed Measurement from Spherically Expanding Flame: Application to H₂/O₂/N₂/He Mixture(411) <i>Y. Zhang</i>
WP-44	Micro-Explosion Effect of Bio-Oil Spray Combustion(412) <i>S. Yang</i>
WP-45	High Efficiency and Clean Combustion of Converter Gas(413) <i>Y. Zhai, S. Li, W. Yan</i>
WP-46	Assessment of Chemical Improvers for the Oxidation of Heavy Fuels(421) <i>A. M. Rayaleh, A. Comandini, S. D. Persis, N. Chaumeix, S. Abid</i>
WP-47	Minimum Ignition Temperature of Hybrid Mixtures(423) <i>D. Gabel, U. Krause, Z. Abbas</i>
WP-48	Experimental Research about Combustion of Multi-Hole Pintle Injector using LO_x/GCH₄(429) <i>K. Lee, J. Koo, J. Nam</i>

WP-49	Unsteady Dynamics of Impinging Jet with Swirl and Premixed Combustion Studied by PIV and PLIF(430) <i>L. Chikishev, V. Dulin, L. Aleksei, R. Tolstoguzov, D. Sharaborin</i>
WP-50	Structure of Premixed Flames of H₂/CO Mixtures at Atmospheric Pressure: Experimental and Numerical Study(431) <i>D. Knyazkov, A. Dmitriev, T. Bolshova, A. Shmakov, V. Dulin</i>
WP-51	An Adaptive Multiresolution Framework Applied to Turbulent Compressible Reacting Flows(433) <i>M. Sroka, J. Reiff</i>
WP-52	A New Miniature Shock Tube for Kinetic Studies(438) <i>S. Abid, N. Chaumeix, A. Comandini, S. Nagaraju, R. Tranter</i>
WP-53	Entropy and Exergy Analysis of Syngas Premixed Flames with a Detailed Mechanism(439) <i>L. Acampora, F. Marra</i>
WP-54	Spontaneous Combustion of Hydrogen/Oxygen Mixtures in Nanobubbles(446) <i>S. Chakraborty, L. Qiao, S. Jain</i>
WP-55	A Detailed Computational Model of a Wood-Fired Cookstove for Determining the Effect of Geometric Parameters on Thermal Efficiency and Emissions(447) <i>R. K. Velmati, V. Sankar, C. Tighe, M. Serrar</i>
WP-56	Methane Number Model based on a Deep Neural Network(448) <i>A. Jach, K. Malik, M. Zbikowski, A. Teodorczyk, Ł. Kapusta</i>
WP-57	Experimental Study of Combustion Syngas released from Gasification of Agriculture Waste in a Downdraft Gasifier(449) <i>B. Sarh</i>
WP-58	A Study on the Combustion Characteristics of Non Class 1E Cables with Accelerated Deterioration(450) <i>M. Kim, H. J. Seo, E. H. Jang, M. C. Lee, S. K. Lee, Y. S. Moon</i>
WP-59	Flickering of Momentum-driven Jet Diffusion Flames(453) <i>X. Xia, Y. Gao</i>
WP-60	Large Eddy Simulation of the Response of Turbulent Non-premixed Flame to Acoustic Perturbation(454) <i>Y. Cheng, K. Luo</i>
WP-61	Experimental Study on Intrinsic Thermoacoustic Instability from a Lean-Premixed Swirl Combustor with Tunable Acoustic Liners(455) <i>L. Xu, S. Wang, J. Zheng, G. Wang, X. Liu, L. Li, F. Qi</i>
WP-62	A New Aerosol Shock-Tube Facility for the Study of Mixtures with Large Hydrocarbons(457) <i>S. Cooper, O. Mathieu, E. Petersen, B. Guo, J. Hargis</i>
WP-63	Effect of Char Combustion Reactions on Drag Force Coefficient(458) <i>H. Zhang, K. Luo, T. Jin, J. Fan</i>
WP-64	Single-Pulse Shock Tube Investigation on the Pyrolysis of n-Heptane and Benzene(463) <i>S. Abid, N. Chaumeix, A. Comandini, A. Hamadi, W. Sun</i>
WP-65	Droplets Autoignition Simulations of Ethanol Mixtures with a Reduced Kinetic Mechanism(464) <i>A. M. Merino, E. F. Tarrazo, M. Sánchez-Sánchez, F. A. Williams</i>

WP-66	<p>High-Speed OH* and CH* Chemiluminescence Imaging and OH-PLIF Diagnostics in Spherically Expanding Flames(465) <i>P. Parajuli, M. Turner, E. Petersen, W. Kulatilaka, T. Paschal, Y. Wang</i></p>
WP-67	<p>Effect of a DC Electric Field on the Flame Stability and Soot Emissions in an Ethylene Diffusion Flame(467) <i>A. S. Kassem, P. Gillon, M. Idir, V. Gilard</i></p>
WP-68	<p>A GPU Accelerated Filtered Density Function Discontinuous Galerkin Large Eddy Simulator(468) <i>A. Kaltayev, M. Inkarbekov</i></p>
WP-69	<p>Exploring Flame Dynamics of Lean, Dliuted Hydrogen Mixtures(477) <i>N. Chaumeix, N. Kouame, L. Wartski</i></p>

9:00 Plenary Lecture 1**PL1 - The Detonation Structure and its Impact on Detonation Limits Predictions***Matei Radulescu, University of Ottawa*

All gaseous detonations take on a cellular structure with large departures from the steady 1D laminar ZND model. The present talk outlines the current understanding on how the departure from the steady model influences the dynamics of detonations with boundary losses and ultimately their limits. It is argued that there are two wide classes of detonation behavior. Detonations in which all gas reacts rapidly by auto-ignition behind the different elements of the cellular front are well predicted by the ZND model neglecting the non-steady cellular structure. We refer to these as piece-wise laminar detonations. In the second class, for more sensitive chemistry, the gas escapes auto-ignition via unsteady expansion behind the non-steady lead shocks and turbulent diffusive burning controls the burning rate. Large departures are found from the ZND model predictions for these turbulent detonations. We review the mechanisms controlling the generation of turbulence in detonations in the latter class, associated with the Mach reflections of strong shocks in low isentropic exponent gases.

10:30 Detonation Structure**196 - Numerical Investigation on Effect of Dilute Water Spray on Mean Structure for Gaseous Detonation***H. Watanabe, A. Matsuo, A. Chinnayya, K. Matsuoka, A. Kawasaki, J. Kasahara*

In this study, the mean structure of gaseous detonation with dilute water spray is analyzed by 2D numerical simulations. The mean structure of gaseous detonation with dilute water spray share similar structure with gaseous detonation without water spray, and the hydrodynamic thickness of the detonation is changed due to the interaction with water spray. The global two-phase exchanges (mass, momentum and energy exchanges) induce a decrease of the detonation velocity within the hydrodynamic thickness. Droplet breakup occurs downstream of the induction zone and in our case, the water vapor from the evaporation of water spray does not affect the reactivity of gaseous detonation. The characteristic lengths of detonation and interphase exchanges have been ordered under the present simulation conditions and have been shown to be intimately intertwined.

104 - Numerical Simulation of the Detonation Wave in the Shock-Attached Frame for the Two-Stage Kinetics Model*P. Utkin, Y. Poroshyna*

The computational algorithm was proposed for the simulation of detonation wave propagation using two-stage kinetics model in the shock attached frame. The algorithm was applied for the simulation of four regimes of detonation propagation, namely very high frequency, high frequency, low frequency and transient regimes. Very high frequency and high frequency regimes correlate well with the data from (Leung et al., Phys. Fluids, 2010). There are discrepancies in amplitude and period of pulsations in low frequency and transient regimes in comparison with (Leung et al., Phys. Fluids, 2010). The obtained results were confirmed in simulations with variation of computational domain length and rear boundary conditions.

126 - Measurement of Detonation Front Structure in Methane-Oxygen Detonation by Multiple Ion-Probes*T. Yatsufusa, K. Kii, N. Miura, H. Yamamoto*

Multiple ion-probe method is the specialized method to capture the movement of propagating flame front along the wall surface of combustion vessel by using plural ion-probes. This method is able to capture not only the propagation velocity along the wall surface, but also propagating direction and instantaneous shape of flame front. Ion-probe itself is physically and thermally strong. In addition, ion-probe allows fast data sampling rate. These features of ion-probe make this method possible to apply to the measurement on explosive combustion, such as detonation and engine knocking. In this work, well matured detonation of stoichiometric methane-oxygen mixture was precisely measured by multiple ion-probe method. Convexo-concave of the flame front and fluctuation of local propagation velocity that may be caused by detonation cellular structure were found in captured data by this method.

155 - Effect of Incident Laser Sheet Orientation on the OH-PLIF Imaging of Detonations*K. Chatelain, R. Mevel, J. Melguizo-Gavilanes, A. Chinnayya, S. Xu, D. Lacoste*

Planar Laser-Induced Fluorescence of OH radical (OH-PLIF) is a common technique used to characterize the geometry of the reaction zone in weakly and highly unstable detonations. Depending on the selected laser orientation (transverse or head-on relative to the detonation front), different results might be obtained from this visualization technique. To enable direct comparison between the experimental PLIF images and 2-D numerical simulations, a LIF model that considers these two orientations is required. The goal of the present study is to investigate the effect of the incident laser light sheet orientation on the OH-PLIF imaging of the reaction zone of detonation waves. We limited our investigation to a weakly unstable detonation propagating in hydrogen-oxygen mixtures highly diluted with argon to enable direct comparison with the experimental OH-PLIF images available in the literature. Thus, an updated LIF model has been developed and validated using steady one-dimensional (1-D) and unsteady two-dimensional (2-D) numerical simulations. A comparison of two numerical OH-PLIF images obtained with the aforementioned laser orientations is performed to highlight the advantages and drawbacks of the two configurations.

10:30 Supersonic Combustion 1

347 - Modal Analysis of Instability Phenomena in Shock-Induced Combustion using Decomposition Techniques

P. K. Pavalavanni, J. Choi

Shock-Induced Combustion (SIC) is a phenomenon in which the leading shock wave aerodynamically compresses the combustible mixture and self-ignites. In the ballistics experiments, unsteady modes of combustion were observed when the projectiles are fired near CJ Mach number. In the unsteady case of Lebris experiment [1], regularly oscillating combustion regimes were also observed. Numerical simulation involves various challenges such as effectively capturing the discontinuities, selection of reaction mechanisms. In our previous paper [2], we have reported that even with the modern reaction mechanisms, the flowfield develops a disturbance in the regularly oscillating case and slowly grows into a low-frequency instability phenomenon like that of the Large disturbance regime (LDR) for regular regime case. Investigation of the source and characteristics of these instabilities is crucial in understanding the complex combustion instability phenomena. Robust decomposition techniques [3] were developed in the recent times through which the coherent structures from any non-linear flow field can be extracted and the flow physics can be analyzed. Among various decomposition techniques, Proper Orthogonal Decomposition (POD) was widely studied in which the coherence structures are extracted and ranked based on the accumulated energy content. Recently Dynamic Mode Decomposition (DMD) has gained attention because of its robustness and its ability to extract the spatial coherent structure mapped to its temporal characteristics which is fluctuating frequency. In this study, these two decomposition techniques were used to analyze the instabilities in the unsteady Shock-Induced Combustion.

374 - High-order accurate hybrid LES/PDF simulation of a supersonic coaxial lifted flame

H. Ranadive, B. Savard, E. Hawkes

In this work, a newly developed LES/PDF solver is assessed on an experimental supersonic lifted flame. The implementation features high-order tightly coupled temporal integration of the deterministic and stochastic equations that govern the Eulerian and the Lagrangian solvers respectively. High-order accurate schemes are also used for the spatial discretisation and particle mean estimation and interpolation algorithms. Overall, the statistics show good agreement with the experimental data at different axial stations. The flame lift-off height and the flame ignition near the jet centreline were slightly under-predicted as compared to the experiment.

237 - Three-dimensional Numerical Simulation of Detonation Initiation in Supersonic Flows

W. Chen, J. Liang

In this study, three-dimensional reactive Euler equations with one-step two-species chemistry model are solved using adaptive mesh refinement method to investigate the detonation initiation in both square tube and circular tube in supersonic combustible mixtures. The different shape of the tubes cause the different reflection effects of the shock waves, resulting in different effects of the hot jet detonation. In square tube, the corner regions where the two tube faces intersect, the reflected shock surfaces interact, so that the shock wave strength is further increased, and the detonation occurs in the corner region. In the circular tube, the bow surface of the bottom of the tube has the strongest

reflection, and the Mach stem near the bottom region first induces detonation, initiating the combustible mixtures.

132 - Structure of Wedge-Induced Oblique Detonations with Small Heat Release

D. Martínez-Ruiz, C Huete, A. L. Sánchez, F. A. Williams

A simplified formulation is given for the computation of weakly exothermic oblique detonations with supersonic post-shock flow, for which the small relative variations of velocity and thermodynamic properties across the reaction region can be described with the linearized Euler equations written in characteristic form, supplemented with the linearized Rankine-Hugoniot jump conditions across the leading shock. The problem reduces to the integration of ordinary differential equations along fixed characteristic lines of constant known slope (i.e. the streamlines and the two Mach lines), providing a useful computational framework for the investigation of the structure and dynamics of oblique detonations in many different configurations of interest. The formulation can incorporate any chemistry description, with the corresponding conservation equations for chemical species integrated along the streamlines. Results are given for an Arrhenius irreversible reaction, with the dimensionless product A of the large activation energy and the small heat of reaction taken to be of order unity, resulting in order-unity changes of the reaction rate across the reaction layer. The model is used to investigate the structure of wedge-induced oblique detonations. The calculations reveal changes in the character of the resulting solution associated with increasing values of the activation energy A , from smooth transitions to the formation of a triple point at the leading shock.

10:30 Shock Tubes 1

100 - Ignition delay-time study of dimethoxymethane/air and CH₄/dimethoxymethane/air mixtures over a wide temperature range at high pressure

J. Herzler, C. Schulz, M. Fikri

Dimethoxymethane (DMM) is the smallest oxygenated methyl ether (OME). OMEs (CH₃-CO-C(CH₂-CO)_n-CCH₃) can be used as Diesel fuel or as additives to Diesel fuel. Studies in internal combustion engines have shown that the addition of OMEs can reduce soot emissions, increases the efficiency, and has a positive influence in the context of the soot-NO_x tradeoff. DMM as pure fuel in Diesel engines exhibits the same advantages as Diesel/DMM mixtures. OMEs are produced from syngas in a gas-to-liquid process with methanol as intermediate. Syngas required for this process can be produced from methane, coal, biomass, or CO₂/H₂ mixtures (with H₂ produced by electrolysis of water, power-to-liquid (PtL), e-fuel).

388 - Study on Ignition Delay Times of Methane/Ethane Mixtures with CO₂ and H₂O addition

M. Braun-Unkhoff, C. Naumann, O. Pryor, U. Riedel, S. Vasu

In this study, ignition delay times of RefGas, a natural gas surrogate consisting of 92% methane (CH₄) and 8% ethane (C₂H₆) [7], will be examined under oxy-fuel conditions including addition of H₂O, for the first time, to the best of our knowledge. In the past, the effects of CO₂ on methane in an oxy-fuel environment has been studied focusing on flame speeds of nitrogen diluted mixtures to CO₂ mixtures and on ignition delay times [8-10]. For example, it was found that CO₂ addition reduces the flame speeds compared to air due to the difference in the heat capacity compared to N₂ [8] and due to the competition between CO₂ and oxygen (O₂) for H radicals reducing the radical pools and inhibiting the overall reaction rate. A more detailed overview is given in [11].

182 - Kinetic Influence of Small Additives of Fe(CO)₅ on the Ignition of H₂O₂/Ar Mixtures behind Reflected Shock Waves

A. Tereza, S. Medvedev, V. Smirnov

The effect of small additives of iron pentacarbonyl on the ignition of hydrogen/air mixtures was investigated by the reflected shock waves technique. It has been established that small additives of Fe(CO)₅ inhibits the process of ignition of H₂/O₂/Ar mixtures. With increasing temperature and Fe(CO)₅ concentration in the H₂/O₂/Ar mixture, the inhibitory effect of Fe(CO)₅ additives decreases. The detailed kinetic mechanism developed in this work made it possible to satisfactorily describe the observed effect of inhibition and to identify the main reactions that determine its kinetics.

94 - Measurement of Methane Autoignition Delays in Carbon Dioxide Diluent at Supercritical Conditions*W. Sun, M. Karimi, B. Ochs, Z. Liu, D. Ranjan*

The directly fired supercritical carbon dioxide (sCO₂) power cycle has high efficiency while allowing nearly complete carbon dioxide (CO₂) capture. The operating condition of sCO₂ power cycle (100 to 300 bar) combustors is dramatically different from conventional gas turbine combustors. However, combustion properties such as autoignition delay are not well understood at these conditions. This study reports methane autoignition delay measurements for diluted carbon dioxide environments at 100 and 200 bar and temperature within the range of 1139° C/1433 K using a high pressure shock tube. The experimental data is then compared with calculations using different chemical kinetics models. For the conditions of this study, predictions of the Aramco Mech 2.0 shows the overall best agreement with experimental measurements while predictions of the GRI 3.0 kinetic model have the largest (by a factor of 3) deviation with experiments. Sensitivity and reaction pathway analyses reveal that methyl (CH₃) recombination to form ethane (C₂H₆) and oxidation of CH₃ to form methoxide (CH₃O) are the most important reactions controlling the ignition behavior at temperatures greater than approximately 1250 K. However, at temperatures below approximately 1250 K, an additional reaction pathway for methyl radicals is found through CH₃+O₂+M=CH₃O₂+M which leads to formation of methylperoxy (CH₃O₂). This reaction pathway plays a distinct role in dictating the ignition trends at lower temperature conditions.

10:30 Turbulent Flames 1**227 - Three-Dimensional Navier-Stokes Simulations of Non-Premixed Reactive Vortex Breakdown***J. Chung, X. Zhang, E. Oran, C. Kaplan*

Vortex breakdown is an instability in columnar vortices that results in abrupt changes in the vortex structure leading to complex three-dimensional flow structures. It was first observed and primarily studied in nonreactive flows, but is also used in premixed swirl combustors to anchor and stabilize flames. In this work, we study the interaction of vortex breakdown and combustion in a non-premixed reactive system. A compressible swirling flame subject to vortex breakdown is simulated by solving the full three-dimensional, unsteady Navier-Stokes (NS) equations with a low-Mach-number correction that removes the acoustic limit on the integration time step. The simulations model a laboratory-scale cubical domain with an open boundary at the top and a non-slip wall at the bottom. A constant flux of air is forced in through four slits along the corners of the non-slip side walls, and fuel is introduced at the center of the bottom wall with a constant flux in a specified diameter. During the early development of the swirling flame, there is a series of breakdown modes similar to those seen in nonreactive flows. A bubble mode forms first near the fuel source at the bottom wall. A second bubble mode later develops above it. The burning occurs entirely within a cup-like shape along the lower-half of the bubble. The flame structure is analyzed and results suggest the formation of a triple flame structure.

204 - A level-set formalism for self-ignition fronts*X. Wang, C. Strozzi, V. Robin, S. Zhao, K. Q. N. Kha, Z. Bouali*

The well known G-equation that is level-set approach to track flame front is revisited to propose a strategy able to deal with self-ignition fronts. Such phenomenon plays a key role in various applications where heterogeneous mixtures (composition and temperature) are involved as rapid compression machine or turbulent non premixed flames (Jet-in-hot-coflow-burner). The original definition of the level-set function introduced involves a normalized time that accounts for local effects on the ignition process via these of tabulated self-ignition times. The new equation derived is applied to two representative test cases: self-ignition in a diffusion layer and self-ignition of an homogeneous mixture submitted to a compression. This approach avoids the use of Arrhenius laws during the computation but provides excellent results to track self-ignition in heterogeneous mixtures. Preliminary results of a LES of a constant volume combustion chamber that includes self-ignition/deflagration interactions are eventually presented.

159 - Ignition kernel development and subsequent flame propagation in a planar methane/air turbulent jet*C. T. d'Auzay, S. Ahmed, N. Chakraborty*

The localised forced ignition and subsequent flame propagation in a planar turbulent methane jet in ambient air has been simulated using Direct Numerical Simulation (DNS) with a modified single-step chemistry. Two different ignition locations were considered using identical energy deposition parameters (duration, width, total energy). The kernels formation and subsequent growth leading to either flame propagation or quenching were analysed. The current DNS framework captures these two outcomes reasonably well. Following ignition, and after a short time in which the kernel growth is driven by the large temperature gradient resulting from the energy deposition, it is found that the flame presents a tribrachial structure in which the triple-point propagates along the stoichiometric iso-surface. At early times, the convection dominates the movement of the flame kernel leading edge, resulting in the flame being advected downstream. If a self-sustained flame state is to be obtained in which the flame is stabilised, the propagation of the flame leading edge locally needs to reach an equilibrium with the local stream-wise velocity. Finally, the key role played by the scalar dissipation rate (SDR) is highlighted by showing that the quenching of the first kernel results from the mean SDR along its edge flame front being above the extinction limit.

334 - Flame front characterization based on ridge analysis

R. Schießl, V. Bykov

We introduce a novel approach for characterizing the reaction zone in turbulent combustion. The method is highly generic with respect to the kind of fuel/oxidizer-combination, the premixing state (non/partially/fully premixed), the degree of homogeneity within the reaction zone, and the level of flow-turbulence interaction. It requires a suitable field representing the local reaction strength, like heat release rate, chemical entropy production rate, or similar. The concept of ridge analysis is then applied to the reaction field in order to identify the reaction zone center, local orientation and its shape. Three-dimensional direct numerical simulation (DNS) of a turbulent non-premixed flame are analysed and statistics of the reaction front structure is presented and discussed. It is found that, beside the conventional flame sheet, the filament- and patch-type paradigms are also represented in the data set. Conditional statistics show that a significant part of the combustion occurs in these filament- or patch-shaped zones, rather than in flame sheets.

10:30 Fire 1

127 - Visualization of flow field in narrow space on flame spread along a thin paper disk with fingering combustion

H. Tanaka, T. Daitoku, T. Tsuruda

An example of a flame spreading accident in a narrow space is a fire caused by ignition of a curing sheet used for repair work. If there is a narrow space on the sheet, floor, or wall, a high temperature heat source, such as chips generated during welding and melting can fall and a fire may occur. Therefore, it is considered necessary to clarify the mechanism of flame spread in a narrow space to take fire prevention measures. Takahashi et al. reported the phenomenon of flame spreading like fingers when thin flammable solids combust in a narrow space under natural convection. This phenomenon is called fingering. In previous studies, we analyzed the velocity field of the vertical section of a flame spreading in a narrow space. But from the horizontal direction it was impossible to visualize the flow field between the fingers splitting the flame and the flame. In this study, the fingering was observed from above, and smoke generated by combustion was visualized using laser light. By analyzing this smoke, we attempt to elucidate the flow field in the fingering.

154 - Experimental Investigation of the Fire Spread on Inclined Wooden Rods

Y. Lai, H. Zhou, Y. Zhang

The flame propagation rate of a burning rod, as one of the most important properties, is dependent on numerous factors including inclined angle, oxygen concentration and moisture content. Among those, the inclined angle of fuel surface could be the dominant factor which affects the flame propagating rate. As a new study, the fire propagation rate of a single wood rod without side walls is investigated by using a high-speed Schlieren imaging system. As a great advantage, the Schlieren imaging system can be utilized to visualize the fire induced heated flow which cannot be observed by direct imaging. Furthermore, a wood rod is easily controlled under certain experimental conditions, which could be helpful for the understanding of real circumstances. In this paper, a sequence of oak wood rods with different diameters has been ignited at various angles to investigate the effects of inclined angle on the fire propagation rate and burning lifetime. A high-speed imaging system with a CMOS camera has

been used to capture the images of burning rods, as well as a Schlieren system has been utilized for visualising the fire induced flow around the wood rods.

167 - Flame spreading in an oxidant flow above burning surface of material

V. Tyurenkova, L. Stamov

Numerical simulations of three-dimensional flow of a gas mixture with chemical reactions over a flat thermally destructing material surface are presented. To create an effective numerical model, two ways of determining the heat removal are considered, and a comparison with the analytical solution obtained within the frame of the boundary layer approximation is represented. As an example, the numerical simulations of three-dimensional flow in combustion chamber of hybrid rocket are performed. The temperature maps and molar fraction of fuel within the chamber for different times are shown.

218 - Testing a Reduced Model of Flame Spread over a Thin Solid in a Narrow Channel

H. Iizuka, K. Kuwana, G. Kushida

Understanding flame-spread characteristics near the extinction limit is important from the fire-safety viewpoint. A tiny flame is usually formed under a near-limit condition, possibly leading to a different flame-spread mechanism. An example of near-limit flame-spread phenomenon is that in a narrow channel. The experiment by Zik and Moses has been a subject of later modelling studies. Most models adopted reduction techniques to reduce originally 3-D (or 2-D) governing equations into 2-D (or 1-D) under the expectation that such reduction does not cause significant errors because of the narrowness of the control volume. However, it has been rarely tested whether the reduced models yield similar results to the original ones. The objective of this study is to test the validity of a reduced 1-D model. A 2-D model is first developed, which is then reduced to 1-D. Predictions of the 1-D model are compared with those of the 2-D model under various conditions to test the validity of the former. The range of conditions under which the reduction technique is valid is then discussed.

13:50 Detonation Initiation

40 - Effects of CO₂ dilution on autoignition and detonation development induced by hot spot in n-heptane/air mixtures

P. Dai

Diluted combustion is widely used in advanced internal combustion engines (ICEs). The thermal efficiency of ICEs is constrained by knock and super-knock due to end-gas autoignition and detonation development. Therefore, the effects of CO₂ dilution on autoignition modes induced by a hot spot in n-heptane/air mixture are numerically investigated in this study. It is found that the increase of CO₂ dilution can greatly increase the excitation time and reduce volumetric energy density. Therefore, the propensity of detonation development becomes lower since the pressure wave and its interaction with chemical reaction both become weaker under more diluted condition. Non-dimensional parameters are introduced to quantitatively describe different autoignition modes including detonation development. The detonation development regimes for n-heptane and dimethyl ether at different conditions are obtained and compared.

102 - Detonation Onset in Shock Wave Reflected from a Wedge

N. Smirnov, V. Tyurenkova, O. Penyazkov, K. Sevrouk, V. Nikitin, L. Stamov

The paper presents results of numerical and experimental investigation of mixture ignition and detonation onset in shock wave reflected from inside a wedge. Contrary to existing opinion of shock wave focusing being the mechanism for detonation onset in reflection from a wedge or cone, it was demonstrated that along with the main scenario there exists a transient one, under which focusing causes ignition and successive flame acceleration bringing to detonation onset far behind the reflected shock wave. Several different flow scenarios manifest in reflection of shock waves all being dependent on incident shock wave intensity: reflecting of shock wave with lagging behind combustion zone, formation of detonation wave in reflection and focusing, and intermediate transient regimes.

131 - Numerical Study on Detonation Initiation through a Uniform Energy Source

D. Chen, N. Jianguo, J. Li

Detonation initiation through a homogeneous energy source is studied using one-dimensional simulations. The initial temperature and pressure which are uniform in the reactants of a energy source are varied to provide different auto-ignition delay time and strength of the leading shock.

Detailed chemical reaction mechanism is used for a stoichiometric hydrogen/oxygen mixture diluted by 70% Argon. According to the length of energy source and initial thermodynamic parameters, three different regimes of detonation initiation were found in the present study, namely supercritical, critical, and subcritical regimes. The initiation process is essentially a Riemann problem (shock tube problem) nonlinearly coupled with a constant-volume explosion. Depending on the auto-ignition delay time, the above two processes can be decoupled roughly. The critical internal energy in the driver section used to initiate a detonation is also analyzed. It was found that, with a short energy source, the detonation initiation energy is less than the blast energy, and the critical internal energy keeps constant as the driver length decreases below a critical value. In contrast, for cases with a large driver length, the critical internal energy is proportional to the driver length, indicating a same energy utilization ratio. In addition, the energy of different initial temperature at same energy source was studied. It is found that the scaled critical energy is independent of the energy source length, indicating no length scale effect is involved in the detonation initiation process with the present model. However, the scaled critical energy heavily affected by the initial temperature.

105 - Numerical and Experimental Investigation of Detonation Initiation in Multifocused Systems

P. Utkin, A. Lopato, A. Vasil'ev

The mechanisms of detonation initiation in the multifocused systems of two types ° C with two semi-elliptical reflectors with the part of flat wall and with five adjoin semi-elliptical reflectors ° C are investigated. Mathematical model is based on two-dimensional Euler equations and one-stage chemical kinetics model. Simulations are carried out on fully unstructured computational grids. The spatial diversity of the reflectors and the presence of a flat wall part for the geometry of the first type gives different modes of initiation for the larger (without interference) and the smaller (with interference) Mach numbers of the incident wave. For the lowest considered Mach number $M = 2.4$ the initiation didn't occur during the time of simulations. For $M = 2.5$ both multifocused systems provides initiation. For $M = 2.6$ the geometry with two reflectors works better. The numerics are in correspondence with the experimental data: $M_{crit} = 2.48$ for the geometry with five reflectors and $M_{crit} = 2.44$ for the geometry with two reflectors.

13:50 Supersonic Combustion 2

281 - Experimental and numerical analysis of hydrogen jet autoignition in backward-facing-step-stabilized model scramjet combustor

N. Fedorova, M. Goldfeld, Y. Zakharova

The results of numerical and experimental investigations of hydrogen mixing and ignition processes in a supersonic combustion chamber with backward facing steps located on the channel walls are presented. The study is focused on determining the conditions for self-ignition of hydrogen in the combustion chamber with the Mach number at the entrance equaled to 4. Another task consisted in determination the effective fuel supply model for self-ignition and flame stabilization, and prevention of the channel choking. The experiments are carried out at the hotshot with tunnel IT-302M. 3D numerical simulations are conducted by means of ANSYS FLUENT 18.0 on the RANS based approach under the conditions of the experiments. The flow structure is analyzed in details and the influence of the jet injection angle and fuel-air equivalence ratiowere shown. The satisfactory agreement between experimental and numerical data by static pressure distributions on a channel walls was received. The results can be used for optimization of supersonic combustor chamber parameters and choosing injection schemes.

55 - Large-eddy simulations of a reactive jet in supersonic cross-flow based on a hybrid model of turbulent combustion

A. Techer, R. Boukharfane, G. Lehnasch, A. Mura

Since it provides efficient mixing and combustion stabilization in high-speed regimes, the jet in supersonic cross-flow (JISCF) is considered as a geometry of reference for scramjet applications. However, despite significant progresses made in the experimental analysis of this configuration, the understanding of the corresponding turbulent reactive flows still remains incomplete from a quantitative viewpoint. The detailed experimental characterization of such a complex three-dimensional flow topology indeed poses severe difficulties for diagnostics and it exhibits quite a significant sensitivity to the variations of flow parameters, e. g. , nozzle pressure ratio (NPR) and

momentum flux ratio. For instance, the latter is known to influence jet penetration and trajectory as well as the global structure of the stabilization zone. As a consequence, high-fidelity numerical simulations offer an interesting and complementary alternative to experiments so as to improve our understanding of such complicated flowfields.

199 - Simulation of Spray Combustion of n-Heptane in a Model Supersonic Combustor with Pilot Hydrogen

Z. Huang, M. Zhao, H. Zhang

Liquid hydrocarbon fuels are more preferred in practical hypersonic propulsion systems, e. g. in supersonic combustion ramjets (scramjets) or scramjet-based combined-cycle engines, due to the advantages of easy storage and the potential of being a coolant [1,2]. However, combustion of liquid hydrocarbon fuels generally involves complex physical-chemical processes, such as injection, atomization, droplet breakup, evaporation, mixing, ignition, and flame stabilization. Presently, there are limited studies about the spray combustion characteristics under supersonic conditions. The ignition delay time of hydrocarbon fuels is much longer than that of hydrogen, while the flame speed of the former is smaller. Therefore, flame stabilization of liquid hydrocarbon fuels in supersonic flows is challenging. Flame stabilization of hydrocarbon fuels can be enhanced by increasing the characteristic scale of the flame stabilization device [3], by using swirl atomizers [4], and by providing a pilot flame [5], etc. In this study, hydrogen is used as a pilot flame to stabilize a spray n-heptane (C7H16) jet in a model supersonic combustor. The combustor only with hydrogen injection was experimentally investigated by Waidmann et al. at the German Aerospace Center (DLR) [6]. For brevity, we termed this burner as DLR combustor hereafter in this paper. The focus of our work is to numerically investigate the combustion and stabilization characteristics of spray n-heptane flames in this supersonic DLR combustor.

287 - Combustion enhancement in supersonic coaxial jet with an optimal forcing oscillations

C. c. Liu, B. Yu, B. Zhang, H. Liu

Due to the low growth rate of high convective Mach number mixing layer, building the fuel-rich injection environment is the normal strategy to compensate the poor mixing and combustion in scramjet engine. In present study, a nominally lean-fuel injection with high combustion efficiency in a Mach number $Mc = 0.6$ coaxial H₂ jet flame at high Damkohler number ($Da = 17$) is achieved by exert the adequate impulse forcing oscillations through the numerical experiment. The results indicate that the maximum reaction production per unit mass of fuel of all forcing period (from forcing period $T/2 = 10\mu s$ to $50\mu s$) is increased near six times than the one of no forcing scenario. Moreover, the forced fuel injection is much more stable exhausted in short period forcing ($T/2 < 30\mu s$). Under high Da number condition, combustion is mainly controlled by equivalent mixing which is closely related to the continuous large-scale vortex flow structures. The limiting formation of vortex from each impulse forcing is found the cause of the superior behavior comparing to the no forcing jet.

13:50 Shock Tubes 2

330 - Reflected-Shock Non-Idealities in Shock Tubes: The Impact of the Facility-Dependent Effects over a Wide Range of Pressures and Mach Numbers

D. Nativel, S. Cooper, T. Lipkowitz, M. Fikri, A. M. Kempf, E. Petersen, C. Schulz

In an ideal shock-tube experiment, the incident and the reflected shock waves would be planar and move at a constant velocity, creating a homogeneous zone of stagnant, high-temperature and high-pressure test gas behind the reflected wave. In real shock tubes, however, additional phenomena affect the experiment and cause deviations from the ideal behavior. Shock attenuation by interaction of the gas flow with the boundary layer due to slow or asymmetric rupture of the diaphragm, and finite formation time of the shock wave can affect the ideality of a shock. These non-ideal effects are influenced by the shock-tube geometry and design, so results (e. g. ignition delay times) may vary between different shock tubes. In this study, facility-dependent effects on pressure were studied using four shock tubes from two different laboratories (Texas A&M University and the IVG at the University of Duisburg-Essen). Pressure rise behind the reflected wave (e. g. dp^*/dt) measurements were performed for a wide range of Mach-numbers and pressures ($\sim 2.1^\circ C_4$, 1 and $2^\circ C_{30bar}$, respectively) for pure argon and pure nitrogen mixtures. A correlation ($dp^*/dt = e26.82p^{10.05T1-5.53M13.60\Gamma 1.44d-0.96}$) was established to help rationalize facility-dependent effects for the

shock tubes. Additionally, boundary-layer thickness calculations were obtained by an in-house code and compared to the experimental dp^*/dt .

146 - State-to-state analysis of chemical kinetics and transport properties in shock heated flow

Q. Hong, X. Wang

Shock heated flows are always in the situation of high temperature, causing internal energy excitation and chemical reactions. These thermo-chemical processes are usually completed in different time scales, and some of the relaxation times may be comparable to the flow time in certain situation, which makes the flow non-equilibrium. A simple and efficient means to include non-equilibrium effects in flow is to adopt multi-temperature models in which empirical parameters are calibrated using experimental and other validated data. However, multi-temperature model cannot obtain the detailed and accurate distribution of non-equilibrium internal energy state. In recent years, the direct state-to-state calculation, which can accurately obtain the evolution law of the internal energy mode and chemical kinetics in the non-equilibrium flow, has been utilized to investigate the vibrational kinetics in shock heated flows and nozzle flows. It is known that transport coefficients of gas mixtures are critical to high temperature flows. However, these studies mainly focus on the non-equilibrium process, the transport coefficients of gas mixtures are not sufficiently investigated. In the current study, in order to analyze the detailed chemical kinetics of the shock heated non-equilibrium air flows, the state-to-state calculation with the available latest state-specific reaction rates data are accomplished. Totally, 46 vibrational states of O₂, 61 vibrational states of N₂ and 48 vibrational states of NO are considered, and the vibrational distribution of these molecules are carefully compared with the Boltzmann distribution. After that, based on the flow parameters, the transport coefficients is also obtained and analyzed through the state-to-state approach.

383 - Shock Tube Based Diesel Spray Ignition Testing

C. Merkel, G. Ciccarelli

Modern diesel engines use common rail injectors, splitting the fuel addition into a short duration pilot injection to reduce the shortcomings of traditional diesel engines. Also, dual fuel engines use diesel pilot injection to act as an ignition source for a premixed natural gas air primary charge. Dual-fuel engines are increasingly receiving attention because of the low cost of natural gas and their clean burn. There is plenty of data on diesel spray ignition but nothing on diesel spray ignition in a premixed natural gas (or methane) air mixture. It would be expected that the presence of methane mixed in with cylinder air would affect the diesel spray ignition time since the methane takes the place of some of the oxygen and can interfere in the diesel ignition kinetics. The objective of this study is to use a shock tube approach, where the premixed methane-air is shock heated before diesel injection. Diesel fuel was injected at the endplate of an optically accessible shock tube test-section following shock reflection. To the best of our knowledge such shock tube experiments have never been performed. Experiments were carried out with diesel-only into air and premixed methane-air with no diesel injection in order to get baseline ignition delay data. High-speed regular and schlieren photography were used to capture the fuel spray formation and ignition process. The results are discussed in the context of the goal of performing experiments involving diesel injection into methane-air.

337 - Facility-Dependent Effects in Shock Tubes

S. Cooper, D. Nativel, M. Fikri, C. Schulz, E. Petersen

Gas dynamic effects during shock-tube experiments cause deviation from ideal shock-wave behavior. In theory, the incident shock wave propagates down the driven section of a shock tube at a constant velocity. However, in real shock-tube experiments, the incident shock-wave velocity is attenuated by the growth of the boundary layer. Once the shock is fully developed in the driven section, the attenuation, in general, causes a linear decrease in velocity as the shock propagates down the tube. Another non-ideal gas-dynamic effect observed in real shock tubes is a steady pressure rise behind the reflected shock wave due again to the boundary layer growth behind the incident shock wave. This generally linear pressure increase is defined as the pressure increase over time normalized by the initial test pressure, p_5 , and is referred to as dp^*/dt . Correlations between these effects and test conditions (Mach number, ratio of specific heats, test conditions, etc.) have been made previously. However, specific facility-dependent parameters, such as shock-tube dimension, design, and operation, are important factors not accounted for in existing correlations.

13:50 Turbulent Flames 2**175 - An Experimental Study of Spark Ignition of a Turbulent Biogas Fuel Jet***C. T. d'Auzay, S. Ahmed, N. Chakraborty, M. Bassiouny, A. Ebrahemi*

Spark Ignition of turbulent flames is a very important topic and is widely used in engines and industrial applications. However, the effect of CO₂ dilution on the ignition behavior of turbulent non-premixed flames has not been investigated yet. Therefore, the present work aims to study the ignition of biogas fuel with different CO₂ percentages. The spark ignition of turbulent biogas fuel jets with different CO₂ concentrations in the fuel, ranging from 10 ° C 40% by volume, has been studied experimentally. Visualization with high-speed imaging showed that the ignition and flame propagation behavior of the biogas jet flame is similar to that of the standard methane jet. However, the redness of the flame decreases due to the reduction in the flame temperature with high CO₂ ratio. In addition, the ignition probability as well as the flame stability reduces as the CO₂ ratio increases. It was not possible to ignite the biogas jet and obtain a stable flame if CO₂ percentage in the fuel exceeds 30%. However, initiating a flame kernel after the spark without obtaining a stable flame was possible up to 40% CO₂ concentration in the fuel.

74 - Experimental measurements of flame structure and time-averaged statistics in turbulent nonpremixed cool flames*C. Reuter, O. Yehia, Y. Ju*

Turbulence, low-temperature chemistry, and their interactions in the form of turbulent cool flames are critical to understanding and controlling ignition in advanced engines. While some computational studies have provided insight into the qualitative role of cool flames in turbulent environments, there have been few experimental investigations of isolated turbulent cool flames. To address this, a Co-flow Axisymmetric Reactor-Assisted Turbulent (CARAT) burner with well-defined boundary conditions is developed for the study of turbulent nonpremixed DME cool flames. Measurements are made using the formaldehyde planar laser-induced fluorescence (PLIF), acetone PLIF, and planar Rayleigh scattering techniques. The acetone PLIF signals are converted into mixture fraction values, and quantitative time-averaged temperature measurements are derived from the Rayleigh scattering signals by taking advantage of the inherent reactant leakage in cool flames. It is found through the formaldehyde PLIF measurements that the turbulent cool flame structure is corrugated but unbroken at the reported experimental condition. Additionally, the time averaged maximum flame temperature is located considerably on the lean side of the stoichiometric mixture fraction. The present investigation offers a well-defined experimental platform for the detailed study of turbulence-chemistry interactions at low temperatures.

19 - Filtered turbulent flamelet model: analysis and numerical test*L. Wang, J. Zhang*

A new approach of turbulent combustion modeling for large eddy simulation of nonpremixed turbulent reacting flows is developed. The modeling idea is to solve the turbulent flamelet equation, which was derived based on the filtered governing equations (L. Wang, *Combust. Flame* 175(2017) 259-269), instead of solving species transport equations with source term closure or using the flamelet/progress-variable approach with assumed probability density functions. Favorably the scalar dissipation term for tabulation can be directly computed from the flow field; meanwhile the chemical sources are closed by scaling relations. Based on tracking the temperature and mass fraction of chemical species over time, model predictions of the bluff-body flame have sufficiently better agreement with experimental measurements, compared with the results from the progress-variable model.

33 - Computational Study of Turbulent Partially-Premixed Flame with Inhomogeneous Inlets*P. Shrotriya, P. Wang*

This paper presents computational study of two turbulent partially-premixed flame cases, FJ200-5GP-Lr75-103 (FJ103) and FA200-5GP-Lr75-45 (FA45) with inhomogeneous inlets via large eddy simulations (LES) using Reaction-Diffusion Manifold (REDIM) technique combined with Presumed Filtered Density Function (PFDF). REDIM technique reduces detailed chemistry into a two-dimensional chemistry table, with the mass fraction of CO₂ and N₂ as the reduced coordinates. REDIM-PFDF sub grid scale combustion model is implemented with two presumed FDF shape: top-hat FDF shape for probability distribution of N₂ and clipped Gaussian shape for CO₂ probability

distribution. A periodic inflow condition is used to obtain fully developed turbulence inside the jet pipes, hence to obtain the correct mixing of fuel and air inside the main jet. It is demonstrated that at upstream locations FA45 case exhibits higher shear stress values compare to FJ103 case, which cause uniform mixture fraction field near the jet exit plane in the FA45 case. Furthermore, two flame cases are compared with experimental results which shows the good performance of the REDIM-PDF model.

13:50 Fire 2**228 - Simulations of a Triple Flame and Fire Whirl using the BIC Low-Mach-Number Algorithm**

X. Zhang, J. Chung, C. Kaplan, E. Oran

In this work, we simulate a triple flame and fire whirl to demonstrate the ability of the BIC low-Mach-number algorithm to simulate complex reacting flowfields. To do this, we extend the recently published BIC algorithm to include chemistry and describe the integration of other physical processes. A 2D methane-air triple flame is simulated within a 16 mm wide square domain with varying stoichiometry at the inflow. The results show that BIC can compute complex flame structures containing diffusion flames as well as rich and lean premixed flames. A 3D unsteady heptane fire whirl is also simulated within a 30 by 30 cm square enclosure, open at the top and closed at the bottom. Circulation is imposed by forcing air in at the corners through 6 cm wide slits. The bottom wall has a constant flux of heptane in a specified diameter at the center. The results show the formation of a columnar vortex with solid body rotation within the thermal core and irrotational flow outside of it. The hot gas generated by the combustion forms a jet-like profile due to buoyancy. The radial profiles of temperature, tangential velocity, and axial velocity at different heights show qualitative agreement with other experimental measurements.

261 - Effect of Wood Smoke Contamination on Water Droplet Evaporation and Surface Tension

A. Albadi, Y. Zhang

In this paper, an experimental investigation was conducted on water droplet surface contaminated by smoke particles. Droplets were evaporated by external heating to show the effect on one of the primary four mechanisms of fire extinguishment. When water is sprayed over a fire plume, it serves to extinguish it by various mechanisms. Primary mechanisms are heat extraction and air displacement [1]. Heat is extracted from flames or the combustible surface by droplet evaporation. Evaporation leads to water vapour which in turn displaces air and reduces oxygen concentration. These mechanisms are all affected by the interaction of water spray and fire, which starts with water droplets passing through a smoke layer. Experimental investigations on water interaction with fire have been conducted in large scale setups, chambers, and real scale rooms. Experiments mainly focused on water suppressing efficiency [1, 2]. In practice, water spray is contaminated by smoke particles during fire quenching. The main aim of this paper is to show the significance of smoke contaminants can have on water droplet evolution and surface tension. [1] Grant G, Brenton J, Drysdale D. (2000). Fire suppression by water sprays. *Prog. Energy Combust. Sci.* [2] Zhang P, Tang X, Tian X, et al. (2016). Experimental study on the interaction between fire and water mist in long and narrow spaces. *Appl. Therm. Eng.*

273 - Generation of Fire Whirls over a Line Fire in a Crossflow: an Experimental Study on the Role of Near-ground Flow

K. Kuwana, Y. Iga

The generation mechanism of fire whirls over a line fire in a crossflow has been studied with a particular focus on the influence of near-ground flow. A wind tunnel was used to provide a crossflow of velocity U , and a blocking board was placed to cover the wind-tunnel exit and adjust its opening height, h . Evolution of flame height was measured for various values of U and h , from which the frequency of fire-whirl formation was obtained. The frequency of fire-whirl formation for $h=5$ cm was found to be greater than that for $h=10$ cm. A near-ground flow is necessary to generate fire whirls, but strong crossflow far above the ground tends to weaken their intensity. When h was too small at 3 cm, strong enough near-ground flows could not be maintained, resulting in a small frequency of fire-whirl formation. Finally, it was demonstrated that formation of fire whirls could be effectively prevented by blocking near-ground flow.

316 - Air mass flow rate effects on ignition front propagation of solid olive waste in a fixed-bed combustor

A. Elorf, B. SARH, M. Asbik, T. Boushaki, S. Bostyn

The aim of this paper is to study experimentally fixed-bed solid olive waste combustion. The effects of the air mass flow (AMF) rate on significant physical parameters especially, mass ignition rate (MIR), maximum temperature, ignition front velocity (IFV) and bed height, are highlighted. Comparison with experimental results available in the literature was realized and a good agreement is recorded. Furthermore, the increasing of the AMF values accelerates the combustion process and hence reduced the time spent in it. On the other hand, the increasing of the air mass flow rate generates three different phases: the acceleration phase, convective cooling phase, and the reaction-limited phase. Supplementary tests with different bulk density and additional biomass (such as Argan nut shell and Wood pellets) are in progress and will be presented in the final version of paper.

16:00 Detonation Interface Interaction**103 - Origins of turbulent mixing behind detonation propagation into reactive-inert gas interfaces**

B. Maxwell, J. Melguizo-Gavilanes, R. Mevel

The interactions of mildly irregular detonation waves with sharp interfaces, separating combustible mixtures from inert gas, were modelled numerically. In past experiments of Liebermann and Shepherd, such interactions resulted in the transmission of a shock-Turbulent Mixing Zone (TMZ) complex as the reactive wave travelled through the interface of fuel rich ethylene-oxygen mixtures into nitrogen. Although Kelvin-Helmholtz (K-H) instability was proposed as a mechanism contributing to the formation of the TMZ, this work aims to determine to what extent K-H plays a role, and to determine whether other sources of instability contribute to the observed TMZ development. Thus, the objectives of this study are two-fold: first (i) to validate the CLEM-LES approach for detonation propagation into sharp interfaces following past experiments of Liebermann and Shepherd; and (ii) to examine the source of instabilities in the resulting turbulent mixing zone that forms upon the interaction of a detonation wave with a sharp reactive-inert gas interface. Results indicated that full-scale simulations, using the CLEM-LES, were found to recover well the observed experimental flow features. Upon re-casting the simulations in the frame of reference of the node, where the reactive wave meets the interface, and by removing cellular instability from the reactive wave front, it was found that shear growth rates of the TMZ were insignificant. Then, by perturbing the detonation front pressure, in a controlled manner, it was found that the observed TMZ growth is actually heavily influenced by instabilities originating at the front.

174 - Detonation Transmission Across an Inert Layer

K. Tang, J. H. Lee, H. D. Ng, X. Mi

In this study the transmission of a gaseous detonation wave across an inert layer is computationally simulated in both one and two dimensions. The incident one-dimensional detonation has the ZND detonation structure with a trailing unsteady expansion wave. In two-dimensions, the incident detonation has an unsteady cellular structure. The inert layer is characterized by its thickness. Downstream from the layer the detonation may re-establish the intrinsic structure corresponding to the mixture's chemical and thermodynamic properties within a finite distance. In one dimension the wave amplification process closely resembles other detonation initiation phenomenon such as direct initiation. However, there is some critical thickness of the inert layer beyond which the detonation fails to be re-initiated downstream. This critical thickness is characteristic of the reactive mixture. It is highly dependent on and decreases with the temperature sensitivity of the induction zone. Preliminary two-dimensional simulations indicate that the critical thickness is an order of magnitude larger in two-dimensions than in one-dimension.

101 - Transmission of Cellular Detonation Waves across a Density/Temperature Interface

K. Tang, J. H. Lee, H. D. Ng, X. Mi

In a previous study, the transmission of a planar ZND detonation across a density/temperature interface was investigated numerically. Due to the finite thickness of the ZND detonation, a finite relaxation zone exists downstream of the interface. Subsequent to this, the downstream state of the transmitted detonation is achieved asymptotically. These transient processes in the relaxation zone involve the non-linear coupling of the chemical reactions with the gas dynamic flow. However, real detonation

waves possess a multi-dimensional cellular structure. Therefore, in the present study a two-dimensional cellular detonation is considered. The relaxation process is found to depend mostly on the downstream thermodynamic condition, quantified as the downstream effective activation energy. For low downstream activation energy, such as a density decrease or small density increase, the detonation is fairly stable downstream. The relaxation process is smooth. As downstream activation energy is increased, changes in the relaxation process and relaxation length become apparent. There is a transition to a case where the detonation fails downstream and localized explosions cause re-initiation. The relaxation length is also increased.

344 - Dynamics of a cellular flame after a head-on interaction with a shock wave

H. Yang, M. Radulescu

The present paper seeks to quantify the increase of the flame surface area and burning velocity caused by the interaction of a shock with a cellular flame. The experiments focused on stoichiometric hydrogen-air flames, which are prone to Landau-Darrieus hydrodynamic instability. Following the passage of the incident shock, the flame cusps were flattened and reversed backwards into the burnt gas due to the Richtmyer-Meshkov (RM) instability. A one-dimensional model was built to reconstruct the flow field in order to infer the turbulent burning velocity of the flame. The burning velocity was found 6 times larger than the laminar value at local conditions after the interaction, and 16 times larger than the laminar burning velocity of the original flame. At later times, the flame front was found to thicken and transitioned to a detonation after a re-shock. The irregular rough flame surface characterized by small scale perturbations and the emergence of the fine structures were attributed to RM instability based on time scale analysis of perturbation growth. Nevertheless, the influence of boundary layers at later times could not be excluded.

16:00 Oblique Detonation

35 - The Role of Activation Energy on the Formation and Stability of Gaseous Oblique Detonation Waves

C. Yan, H. Teng, X. Mi, H. D. Ng

High-fidelity numerical simulations are performed using an idealized model with reactive Euler equations and a one-step Arrhenius kinetics to investigate oblique detonations induced by a two-dimensional, semi-infinite wedge. The novelty of this work analyzes particularly the role of high activation energy E_a at different inflow Mach number regime M_0 and wedge angles on the two types of oblique detonation formation, namely, the abrupt onset with a multi-wave point and a smooth transition with a curved shock. The conditions for these two formation types are described quantitatively by the obtained boundary curves in M_0 - E_a space. At low M_0 , the critical $E_{a,cr}$ for the transition is independent of the wedge angle. At high flow Mach number regime, the boundary curves for the three wedge angles deviate from each other. The overdrive effect by the wedge becomes the controlling factor on the transition type. At very high E_a limit, interesting salient flow features in the vicinity of the initiation region are observed and their effect on the unstable oblique detonation surface are discussed.

92 - Effects of fluctuating equivalence ratios on the formation of wedge-induced oblique detonations in pre-evaporated kerosene-air mixture

Z. Ren, B. Wang

Two-dimensional numerical simulations of wedge-induced oblique detonation in pre-evaporated kerosene-air mixtures are presented. The unsteady inflow is modeled by a continuous sinusoid equivalence ratio disturbance, and the effects of fluctuating aptitude and wave number on the formation of oblique detonation wave (ODW) are simulated and discussed. Based on a typical initiation structure with smooth transition with a curved shock, the increase of wave number makes the detonation surface more unstable with the cellular structures and the increasing fluctuating aptitude results in the unsteady dynamics for the ODW formation. The results indicate that for some conditions the ODW structure can re-adjusts itself with local unstable features and tend to be resilient to the inflow disturbances.

39 - Effects of equivalence ratio on the characteristics of the oblique detonation wave

S. A. Esfehiani, C. Nan, H. Tang

This paper studies the effect of the equivalent ratio on the characteristics of the induction zone, in an attempt to explore the inner mechanism of the characteristics variation in the induction zone of the oblique detonation wave with two-dimensional Euler equation with the detailed chemical reaction model of H₂/O₂. The result shows that with the increase of the equivalence ratio, the length of the induction zone is U-shaped, and the temperature plays a key role in this process. By studying the pressure distribution at the induction zone, it is found that the compression wave intensity at the end of the induction zone is the decisive factor affecting the transition form of the induction zone. When the equivalent ratio is between 0.6 and 2.5, the compression waves intensity is strong, and the transition form is abrupt; out of this range, the compression waves intensity is weak, and the transition form is smooth. In addition, combined with the theory of constant volume combustion (CVC), the change of the induction zone length with an equivalent ratio under different flow pressures is analyzed. Comparison between numerical and analytical results demonstrates that the major factor which affects the length of induction zone is the chemical reactions.

188 - Initiation characteristics of wedge-induced oblique detonation waves in a H₂-O₂ mixtures with Ar dilution

C. Tian

Two types of combustible mixtures, H₂-O₂-Ar and H₂-O₂-N₂, are widely used in detonation research, but only the latter is employed in the oblique detonation wave (ODW) studies before. In this study, ODWs in H₂-O₂-Ar are simulated to investigate their structure characteristics, using the reactive Euler equations with a detailed chemistry model. Similar to the ODWs in H₂-O₂-N₂ mixtures, two kinds of the structures are observed dependent on incident Mach numbers. However, it is further found that in the mixtures of 2H₂+O₂+7Ar, the structures are sensitive to inflow static pressure P₀, different from the structures in H₂-O₂-N₂ mixtures. Based on the analysis of the flow fields, the ratio of induction and heat release zone lengths RL, is proposed to model the difference induced by the dilution gas. Generally, RL is found to be large in N₂ diluted mixtures, while small in Ar diluted mixtures. When the dilution gas changes from N₂ to Ar gradually, the ratio RL increases slowly first and then decreases rapidly to approach a constant. The variation rule of RL is analyzed, demonstrating how different dilution gases determine the ODW structures.

16:00 Shock Tubes 3

386 - A Study of Ethanol Oxidation in High-Pressure Shock Tube: Ignition Delay Time Measurements and High-speed Imaging of the Ignition Process

D. Nativel, J. Herzler, M. Fikri, C. Schulz, P. Niegemann

Non-ideal effects in shock tubes have a non-negligible impact on the study of fast chemical processes. In particular, uncertainties in the determination of the rate constants as well as premature ignition (or pre-ignition) at lower temperatures were observed. For the combustion community, understanding pre-ignition has become a major task in the last decade. Among other hydrocarbons, ethanol was found to be prone to have a high pre-ignition tendency. From an engineering point of view, the importance of studying pre-ignition stems from the development of engines with higher energy density where pre-ignition can lead to particularly severe peak pressures oscillation that damages the engine. For this study, new ignition delay times were measured for dilute and non-dilute ethanol stoichiometric mixtures at ~20 bar from 800 to 1250 K. Additionally, high-speed imaging using two high-repetition-rate cameras on different positions around the shock tube (end-wall and side wall) provided important information about the ignition process, permitting to distinguish between homogeneous and inhomogeneous ignition in time and space.

297 - Heat capacity effect on ethanol preignition in a shock tube

M. Luong, E. Tingas, H. Im, M. Figueroa-Labastida, A. Sow, F. E. H. Pérez, J. Badra, A. Farooq

The effect of heat capacity on the preignition propensity of ethanol mixtures under shock tube conditions is examined using direct numerical simulation (DNS). An imposed ignition source is introduced to reproduce a hot spot that might encounter in a shock tube. The sensitivity of ignition delay time of ethanol mixtures to different imposed ignition sources is systematically investigated. Four different ethanol mixtures are considered as in a recent shock tube study by M. Figueroa-Labastida et al. [1] by keeping a fixed 5% ethanol mole fraction and varying (i) the bath gas of containing either Ar or N₂, and (ii) equivalence ratio of 0.5 and 1.0. It was experimentally observed that under the same condition, the ignition delay times of Ar cases are significantly advanced compared

with the corresponding N₂ cases [1]. The main reason is found to be attributed to the heat capacity of Ar much smaller than N₂ such that Ar cases are more sensitive to the hot spots. With the same ignition-source strength imposed, the temperature increment of Ar cases is higher than that of N₂ cases which in turn enhances the H₂O₂ decomposition reaction, $\text{H}_2\text{O}_2 + \text{M} \rightarrow \text{OH} + \text{OH} + \text{M}$, thereby promoting the system to reach the autoignition point quicker. As a result, Ar cases exhibit higher propensity to preignition than N₂ cases if exposed to the hot spots, which is consistent with the experimental findings.

21 - High-Temperature Non-Homogeneous Ignition of Small Alcohols Behind Reflected Shock Waves

O. Mathieu, E. Petersen, L. Pinzón, T. Atherley, I. Schoegl

The ignition of methanol and ethanol was studied for various equivalence ratios, pressures, dilution levels, and using different bath gas (for ethanol) for test times shorter than 2 ms. Results are in agreement with the literature, but inhomogeneous ignition was detected at around 13 atm for fuel-lean and stoichiometric mixtures with Ar as bath gas. The inhomogeneous ignition translated into ignition delay times significantly shorter than expected. While inhomogeneous ignition behavior has been recorded with methanol and ethanol in the literature, under similar equivalence ratios, fuel concentrations, and pressure conditions, these were observed for longer test times/colder temperatures, and no inhomogeneous ignition was observed within the temperature range investigated herein. This difference with the literature seems to be due to the use of Ar as bath gas in the present study, instead of N₂ in the literature. The use of N₂ allows for a larger flame thickness than Ar, which could prevent hot spots from developing into flame kernels that lead to inhomogeneous ignition.

9 - n-Heptane Ignition: High-Speed Imaging in a High-Pressure Shock Tube

D. Davidson, R. Hanson, J. Shao, R. Choudhary, A. Susa

Conventional distillate fuels are complex hydrocarbon mixtures. Understanding the low-temperature, high-pressure chemistry of these fuels and their surrogate components is critical to understanding auto-ignition and knocking behavior in real engines. Simple modeling of ignition behind reflected shock waves assumes that these processes are zero-dimensional. However, there is growing evidence of inhomogeneous ignition processes occurring under certain conditions in these facilities. Conventional methods of studying these processes in shock tubes, i.e. using pressure transducers, emission, and line-of-sight laser absorption, may not be sufficient to distinguish between inhomogeneous and homogeneous ignition modes, necessitating more sophisticated methods to identify homogeneous ignition. In this study, we implemented high-speed imaging of reactive n-heptane mixtures behind reflected shock waves in a high-pressure shock tube, using a modified shock tube endwall to investigate homogeneous and inhomogeneous ignition behavior.

16:00 Turbulent Flames 3

256 - Reaction-Diffusion-Manifolds for Flame-Wall-Interactions of Stratified Flames

C. Strassacker, V. Bykov, U. Maas

In this study, the REDIM method is applied for stratified flame regimes with flame-wall-interactions. In previous works regarding flame-wall-interactions with the REDIM method, two-dimensional REDIMs for laminar flat and premixed flames of homogeneous mixtures were generated. In order to enable accurate reduced computations for practically relevant combustion regimes, an approach that allows the construction of a REDIM that is able to handle stratified flames with flame-wall-interactions is proposed in this work. It is possible to recapture those scenarios within the REDIM method, but here, a two-dimensional REDIM is not sufficient. This is due to the fact, that the thermochemical states of these flames are not always part of the same two-dimensional subspace, but they are part of higher-dimensional subspaces, especially for computations with different starting solutions (slight change in mixture compositions at the different locations in the computational domain). Therefore, the dimension must be increased and three-dimensional REDIMs are generated. An approach to construct these REDIMs is suggested and demonstrated in this work. Afterwards, different three-dimensional REDIMs are constructed and compared to each other.

176 - Oblique Flame-Wall Interaction in Premixed Turbulent Combustion Under Isothermal and Adiabatic Wall Boundary Conditions

U. Ahmed, N. Chakraborty, M. Klein

Two different V-flame simulations in a fully developed turbulent channel flow have been performed at $Re_{tau}=110$ under adiabatic and isothermal wall conditions. Mean quantities such as turbulence kinetic energy, and its dissipation rate, mean reaction rate, flame surface density and scalar dissipation rate have been investigated. It is found that the location of the oblique flame-wall interaction is slightly altered by the choice of the wall boundary condition. Variations in the mean values of progress variable, temperature, density and reaction rate have been observed for the two cases. Some features of aerodynamic quenching have been observed for the V-flame under adiabatic conditions, which occurs due to the low $SL/utau$ ratio considered in this work. Furthermore, mean flame surface density and scalar dissipation rate statistics have also been calculated and it is found that the reaction rate closures based on these quantities need to be modified for the conditions considered in this work.

283 - Influence of fuel Lewis number on flame-wall interaction for impinging turbulent premixed flames

I. Konstantinou, U. Ahmed, N. Chakraborty

In this work, the influence of non-unity fuel Lewis number, Le_F , on the statistical behaviour of flame-wall interaction for statistically planar turbulent premixed flames impinging on isothermal inert walls has been investigated by performing Direct Numerical Simulations. Statistical behaviours of the wall heat flux, wall-normal strain rate and dilatation rate have been analysed for different values of Le_F and turbulence intensities under isothermal wall boundary conditions. The critical quenching distance has been found to decrease with increasing Le_F in this configuration. By contrast, the maximum wall heat flux magnitude remains comparable for all Le_F values considered here. No strong correlation is found between the wall heat flux and the wall-normal strain rate with varying Le_F . The distribution of the wall heat flux in regions of non-zero wall-normal strain rate is altered at different turbulence intensities. The joint PDFs between dilatation rate and wall-normal distance have been marginally affected by the variation of Le_F , with the overall trend remaining qualitatively similar for different turbulence intensities.

321 - Experimental Study of the Diluent Influence (N₂, He, Ar) On Stable Premixed Methane Flame in a Quartz Micro Flow Reactor

C. Chauveau, F. Halter, G. Dayma, H. Chouraqui, P. Dagaut

The current strong interest in the miniaturization of electromechanical systems (MEMs) is related to an increasing demand on portable power generation devices with high-density energy. One solution investigated to address this issue is to exploit the high-density energy of hydrocarbon fuels. The driving idea is that, even with low energy efficiency, devices using the combustion of hydrocarbon fuels will provide more energy than the most powerful current batteries. Power generation devices requiring to be as small as possible, reactors used in micro scale combustion have an inner diameter that is typically smaller than the quenching diameter. At this scale, characteristic flame behaviors have been experimentally and numerically observed such as flames with repetitive extinction and ignition (FREI), weak flames and stable flames depending on the inlet velocity. Previous studies investigated fuel/air mixtures but since application to micro scale combustion are numerous, a deep understanding of flame behaviors in different environments is required. Therefore, the present work focuses on the influence of different diluent on premixed stable CH₄ flame in order to point out physico-chemical properties that have an impact on stable flame in micro-flow reactor. New experiments were performed in He/He/N₂, and Ar and the influence of heat capacities, viscosities, thermal conductivities, and mass diffusivities was investigated.

16:00 Fire 3

377 - How dripping flames ignite a thin fuel

P. Sun, S. Lin, X. Huang

Dripping flame refers to the burning and molten thermoplastic fuel whose gravity can overcome its surface tension and then produce drips with flame. Dripping phenomena have been widely observed in electrical wire fires and the building facade fires. Although dripping plays an important role in the development of fire, very limited researches have addressed the dripping-ignition process. In this work, we study how these dripping flames ignite the thin fuel in the lab-scale experiment. Uniform drips with four different masses, ranging from 2.6 mg to 6.2 mg, are produced from burning polyethylene tubes. Three types of print paper with different thicknesses, ranging from 0.07 mm to 0.32 mm, are ignited by various numbers of continuous drips to determine the ignition probability and

the limiting ignition conditions. Experimental results show as the thickness of the paper is increased, both the required number of drips and the total mass of ignition are increased, i.e., satisfying the classical thermally-thin ignition theory. Moreover, the required number of drips for ignition is found to be almost insensitive to the mass of a single drip. The analysis shows that for different drip size, the equivalent heat flux to the paper is almost the same, resulting in a similar heating intensity.

309 - Analysis of heat fluxes and their influences on vertical flame spread over PMMA walls by a large eddy simulation

K. Fukumoto

The present study aims to obtain further understandings of vertical fire spreading phenomena by analysing individual heat flux components on PMMA walls using an in-house version of FireFOAM 2.2.x, which has recently undergone specific development and validation for flame spread studies by the authors. The code is based on wall-resolved large eddy simulation (LES) techniques. It includes pyrolysis, combustion, radiation and soot treatments as well as appropriate for different regimes from laminar through transition to fully turbulent in the near wall region as well as the effects of in-depth radiation and solid surface regression. Numerical simulations have been conducted for middle and large scale flame spread configurations to facilitate detailed analysis of the individual heat flux components on the walls, their respective fractions in the total heat flux and relevant importance in the different regions of the upward spreading flame. The ratio between radiative and total heat flux changed from approximately 20 to 60% as a flame spread from 0.1 to 1.0 m.

166 - The Potential of utilizing Near Infrared Spectrum for fire detection

X. Wang, Y. Zhang

Traditional fire detection in buildings usually uses heat detectors, smoke detectors, carbon monoxide or combined multi-sensor detectors. Those types of fire detection notoriously suffer from very slow response time and high rate of false alarm. The advancement of machine learning in recent years has offered a new promising approach to develop fire detection systems. However, most vision-based fire detection algorithms are developed with features extracted from visible spectrum, which can be easily tricked by artificial fire, art work, advertising posters, etc. With IR cameras operating a selected NIR spectrum (850 to 1100nm), only real fire is observed because of high temperature IR emission. Moreover, based on experimental observation, the use of NIR imager greatly simplifies region-of-interest, which is notably a challenge for objection detection algorithms. This paper presents the potential use of NIR spectrum for fire detection regarding to these two aspects.

9:00 Plenary Lecture 2**PL2 - Recent Research Progress on Rotating Detonation and Its Application in Different Engines**

Bing Wang, Tsinghua University

Propulsion devices based on rotating detonation have been proposed, and hot tests have been performed over the past 60 years. With a historical overview of research highlights, this presentation focuses on recent research progress on unstable combustor phenomena, the combustion mode identification and the associated physical mechanism. Research indicates that multiple factors can influence rotating detonation instability and most of them can be linked to the reactants injection condition and combustor geometry. A series of instabilities can be identified in the combustor by either changing the mass flow rates and the equivalence ratios, or adopting a different injection configuration. The mechanisms for the effects of injection conditions are investigated by means of flow visualization and flame diagnosis. With respect to the effects of the combustor geometry, the minimum combustor channel has been accepted as a key criterion for the stable rotating detonation, but other geometrical factors have also been suggested to influence the instabilities, such as, the length of combustor, the hollow combustor and the exit size of throat. Both experimental and numerical simulations have been carried out in our laboratory investigating this problem. In particular, we experimentally investigated the mechanisms and the control method of the instabilities of rotating detonation, and an explanation based on the combustor acoustic modes has been proposed to illustrate the occurrence of unstable phenomena. Future prospects for rotating detonation engines are provided.

9:30 Plenary Lecture 3**PL3 - Rotating and Pulse Detonation Engines System Development for the Sounding Rocket S520-31 Space Flight Experiment**

Jiro Kasahara, Nagoya University

A research group consisting of Nagoya University, Keio University, Japan Aerospace Exploration Agency Institute of Space and Astronautical Science (JAXA/ISAS), and Muroran Institute of Technology is developing a space flight rotating detonation engine demonstrator using the JAXA/ISAS sounding rocket S520-31. Development of the engine is ongoing with the goal of launch in the summer of 2020. The sounding rocket will be equipped with two rotating detonation engines and one pulse detonation engine as a second stage system. This flight experiment will demonstrate that a detonation engine can function as a high-performance rocket engine for space propulsion and a reaction control system engine. In this talk the recent experimental results and the total system of the second stage are presented.

10:30 Detonation Diffraction**97 - Experimental $D(\kappa)$ Relationships for Unstable Detonations**

Q. Xiao, M. Radulescu

Experiments of unstable detonations in mixtures of $\text{CH}_4/2\text{O}_2$, $\text{C}_2\text{H}_4/3\text{O}_2$, and $\text{C}_2\text{H}_6/3$. SO_2 have been conducted inside the exponentially diverging channels (exponential horns) with constant area divergence rates, which were very recently proposed by Radulescu and Borzou for experimentally investigating the gaseous detonation dynamics and its modelling by the simple one-dimensional (1D) models. The results showed that, well above the limit, quasi-steady detonations can be reasonably assumed with a constant mean mass divergence. By appropriately constructing the characteristic $D(\kappa)$ relationships, the boundary layer induced mass divergence rates were derived for each mixture, and their calibrated $D/DCJ\text{-}K_{\text{eff}}^i$ and $D/DCJ\text{-}\lambda K_{\text{eff}}^{\text{curves}}$ were correspondingly obtained. The comparisons between these experimentally obtained characteristic relationships and the theoretical predictions, made with the steady 1D ZND model by using the San Diego chemical mechanism (Williams 2014), demonstrated that the generalized ZND model with lateral mass divergence can predict quite well the dynamics of detonations in most mixtures except the highly unstable $\text{CH}_4/2\text{O}_2$ and $\text{C}_3\text{H}_8/5\text{O}_2$ ones.

376 - Detonation behaviors downstream of a perforated plate with large hole diameters

W. Lin, K. Guo, H. Zhao, Y. Zhu, Z. Zhong, J. H. Lee

The detonation behaviors downstream of perforated plates placed perpendicular to the propagation direction were investigated by using ionization probes to record velocity trajectories and smoked foils to determine cellular evolution. A 1.91 mm millimetric thick staggered perforated plates with

relatively large hole diameters $d=12.5$ mm, a ratio of hole spacing over diameter ($l/d=1.376$) were tested, providing ordinal blockages of 52 %. The stable mixture $C_2H_2+2.5O_2+70\%Ar$ and unstable mixture $C_2H_2+5N_2O$ were used. It is determined that for either stable or unstable mixture, there exists a pressure limit below which no decay occurs downstream of the given perforated plate. However, for pressure comparable with or slightly higher than this limit, detonation may transmit the orifices and maintain lower propagation mode downstream, but finally fail even after a propagation of tens of tube diameters. It implies that the perforated plate has a role in filtering the detonation propagation mode. Increasing pressure results in detonation re-initiation within several tube diameters downstream of the perforated plate. At relatively high pressure, detonation downstream doesn't fail, since detonation cellular structure travel across the orifices.

238 - Effect of Cellular Instabilities on the Detonation Transmission of Weakly Unstable Detonations

L. Shi, K. C. K. Uy, C. Y. Wen

When a detonation wave propagates from a channel into an unconfined space, the detonation could extinguish if the size of the channel reduces below a critical value. This value is defined as the critical channel height. In the present paper, the 2D simulations with high numerical resolution are performed to determine the critical channel heights for planar/cellular detonation diffraction. It is found that for the planar detonation diffraction, re-initiation happens inside the shocked-unreacted zone. In the cellular cases, the transmission is greatly determined by the effective collisions of transverse waves with multiple randomly distributed hot sites, rather than only one hot bubble in the planar cases.

301 - An Experimental Investigation of a Detonation Characteristic Length Scale Relevant to Critical Diffraction

A. Kawasaki, J. Kasahara

For stoichiometric $C_2H_4-CO_2$ mixtures with or without Ar dilution, the processes of detonation diffraction have been investigated in a two-dimensional setup through high-speed schlieren imaging, with the characteristic length and the stability of detonation varied by regulating the initial pressure and argon mole fraction of the mixture. In particular, a length relevant to the process of supercritical diffraction (i.e., distance from the channel end corner to reflection point of the transverse detonation on the channel end face, reflection point distance in short) was deduced from obtained sequential schlieren images and analyzed. The reflection point distance can be idealized for the infinitely wide donor channel, and thus, it can be a parameter in which properties intrinsic to each detonable mixture are manifested. Experimental results showed that the reflection point distance was roughly inversely proportional to the initial pressure for identical mixtures and independent of the width of the donor channel at high initial pressures. For a certain combination of the fuel and oxidizer, correlations between the reflection point distance and the initial partial pressure of fuel were very similar regardless of the argon mole fraction. Critical conditions of the diffraction problem could be given for the ratio of the reflection point distance to the channel width, and it was suggested that the critical value lies in a range of 3-C5 and does not significantly depend on the stability of the mixture.

10:30 Ignition 1

349 - Autoignition of n-decane and multi-component surrogates of kerosene in an optical rapid compression machine

C. Strozzi, J. Sotton, M. Bellenoue, H. Ossman, K. Tsuzuki

Gas phase auto ignition of single and multi-component kerosene surrogates is characterized at low temperatures in an optical rapid compression machine. Different pressures (7-15 bar), equivalence ratios (0.5 and 1) and temperatures are considered for n-decane, Dagaut and MURI2 multi-component surrogate fuels. Optical diagnostics bring insights into the understanding of the auto-ignition process for the two stages of ignition. The delay measurements either provide new data, confirm or complement the databases already published. Significant differences in ignition delays are observed between the different surrogates. Furthermore the data are compared to kerosene ignition delays published in the literature: MURI2 surrogate is found to best represent the kerosene behavior in the investigated conditions.

65 - Ignition delay time model based on a deep neural network

A. Jach, A. Teodorczyk, M. Zbikowski, K. Malik

The ignition delay time (IDT) is one of basic properties describing any flammable mixture and it is very important in process safety management. IDT is usually modeled with detailed reaction mechanisms (DRMs), however those calculations might be very time consuming and DRMs are still being developed and refined. The authors of the recent paper accumulated around 1800 IDTs from shock tube experiments for various C1-C7 hydrocarbon-O₂-Ar mixtures. This amount of points becomes sufficient for deployment of one of Machine Learning algorithms - a deep neural network (DNN). Machine Learning is widely used in numerous aspects of life, for instance: self-driving cars, handwriting recognition, anti-spam filtering, web search and rating systems. Now it is becoming more popular in science as well. A DNN is based on an artificial neural network which is inspired by the biological neural networks. The biggest advantage of DNNs is high predictive power and flexibility of application. According to authors' best knowledge IDTs have not been yet modeled with a DNN. Hence, the goal of the recent paper is to introduce a new ignition delay time model based on the DNN technique.

275 - Effect of low initial pressures on ignition properties of methane/O₂/N₂ mixtures for laser induced breakdown

B. Molière, S. RUDZ, J. Dougal, P. GILLARD, M. William-Louis

Laser ignition presents several advantages over usual electrical ignition. The most preeminent one is a better energy deposition control which is of particular interest to the aerospace industry. At the same time, new fuel/oxidizer combinations are explored by these companies to reduce their environmental footprint while keeping high performances. This paper is investigating the ignition energy for the couple methane/synthetic air below atmospheric pressure, by mean of non-resonant laser breakdown. Both incident and absorbed energies were controlled. The combination of laser ignition and the new couple methane/oxygen needs to be studied specifically, notably for low pressures representative of the flight altitudes. The ignition energy is affected by both the pressure and the equivalence ratio. Moreover, an energy deposition model previously proposed for decane/air mixtures has been validated once again for the couple methane/air.

263 - Study of synthesis gas auto-ignition process by using GQL and QSSA model reduction approaches

C. Yu, V. Bykov, U. Maas

In this work, an automatic model reduction method for chemical kinetics, the so-called Global Quasi-Linearization (GQL) method, is implemented to reduce homogeneous systems for ignition in the synthesis gas combustion system. The GQL approach has been developed as a robust, automatic and scaling invariant method, allowing global analysis of the system timescale hierarchy. This method is compared with one conventional reduction method, namely with the quasi-steady state approximation (QSSA). It is shown that although using the standard QSSA the same reduced model dimension (5D) as with GQL can be obtained, predictions of the ignition delay times of the latter approach are more accurate than these of the QSSA. Furthermore, the GQL performs much better with respect to species profiles both in time and in the state space.

10:30 Dynamics & Stability 1

385 - Flame Topology and Combustion Instability Limits of Lean Premixed Hydrogen Enriched Flames

I. Chtere, I. Boxx

The operation of a technically premixed, swirl stabilized atmospheric laboratory burner based on the PRECCINSTA with high hydrogen fuel mixtures is demonstrated at various operating conditions across different thermal powers, equivalence ratios and H₂/CH₄ volume fractions up to 50%. The stable and unstable operating conditions are experimentally determined in terms of equivalence ratio and thermal power, and the peak frequencies and amplitudes of thermoacoustically excited cases are measured. This work finds (as expected) that hydrogen addition significantly affects the flame shape and combustion instability limits. Specifically, the flame is made more compact and the flame is observed to change from M to V-shaped at fuel lean conditions, both of which impact combustor thermal loading. Furthermore, hydrogen addition raises the peak frequencies by 5-25%, and modifies the thermoacoustic amplitude.

115 - Effects of hydrogen addition on the stabilization of lean premixed swirl flames

W. Zhang, J. Wang, W. Lin, B. Lin, Y. Wu, M. Zhang, Z. Huang

This paper described an experimental study on the effects of hydrogen addition on the stabilization of ultra-lean premixed CH₄/H₂/air flames. The flames were stabilized with a bluff-body and swirl burner. Flame structure and flow characteristics were investigated with simultaneous measurements of OH-PLIF and PIV. It is observed that, the hydrogen addition promotes the flame towards the main flow and the direct distortion from shear layer vortexes is decreased. The flamelet conditioned straining shows different patterns of flow shear forces. Especially, the resistance to the straining near flame attachment with hydrogen addition is probably the vital step for the hydrogen to stabilize the lean flames.

49 - Mode Transition of Interacting Flickering Flames

A. Bunkwang, T. Matsuoka, Y. Nakamura

Flame flickering is one of typical buoyancy-induced instability phenomena and rich literatures are available on this regard [e. g. ,1-2]. Nevertheless most of the existing works have been devoted to the dynamic behavior of the single fire and effect of their interaction is quite limited. The present work is motivated on this regard through investigation of the effect of interaction of multiple separated fires systematically. To model on the target phenomena, jet-diffusion flames are used for the present purpose. Thermocouple mounted at the flame base of the burner exit can tell the periodic motion of the flame behavior. Better understanding of the buoyancy-driven instability in a precise manner is the main target on this work. Although the presence of in-phase and anti-phase flickering behavior depending on the burner separation distance has been observed in past works [3-5], all of them were phenomenological, and less quantitative discussions have been provided. To clarify this issue, we have developed the well-controllable experimental system previously [6-7]. In this study, in order to examine the transition mechanism in scientific way, key parameters, namely, fuel flowrate, burner diameter, and burner separation distance, are systematically modified and key modeling strategy is then obtained.

143 - Response of a Low Swirl Premixed Flame to Velocity Perturbations

M. Shahsavari, B. Wang, M. Farshchi, D. Zhao

In this study, large eddy simulations with dynamically thickened flame combustion model are used to study effects of acoustic excitations on low swirl flow and flame features. Obtained results show that external excitations induce perturbations in swirl number upstream of the flame front, which in turn change the coherent structures and the temporal recirculation zone features. Moreover, results show that combination of such changes in the flow field induces heat release fluctuations. The Rayleigh index is calculated at various phases of the excitations to investigate the thermoacoustic couplings. Phase-locked results show that the Rayleigh index is positive at the center of the flame at phase angles of 0 and 180. However, at phase angles of 90 and 270, the Rayleigh index can be both positive and negative at the central region. Furthermore, the boundary of the flame experiences both damping and driving processes at all phase angles of the excitations. Finally, low swirl flame transfer function is calculated to further identify effects of the excitations on the flame dynamics.

10:30 Energetic Materials 1

314 - Ignition Temperatures of Explosive Atmospheres of CS₂ in Dependence on Spatial Orientation of the Hot Surface

M. Beyer, P. Raval

The hot surfaces are an important ignition source that can cause explosions and fires in industry. It must be safely mastered in equipment for use in potentially explosive atmospheres. The temperatures that cause ignition can be originated by various sources such as electrical currents, optical radiation, ultrasound or mechanical friction. The aim of this work is to investigate the ignitability of hot surfaces as a function of their temperature and their spatial orientation. The term associated with ignition by a hot surface is the safety characteristic AIT (autoignition temperature). It is determined by standard test methods (ISO/IEC 80079-20-1). It is the lowest temperature using the standard procedure, at which an explosive atmospheric mixture of vapors or gases with air is ignited. AIT is used for classification of substances and of equipment into temperature classes (T1 to T6 acc. to IEC 60079-0)). But it has limited application in a practical situation as the actual ignition temperatures (IT) are, except some specific cases, always higher than the AIT. In most of the investigations small heating bodies are used in vertical and horizontal positions. There is lack of data for larger hot surfaces as they may appear in

electrical or mechanical equipment. This will be covered here, by using a hemispherical heating body of $d = 100$ mm in five different orientations of the heating body. The results shall be used for validation, modelling and future studies by numerical simulation.

82 - Non-shock Ignition Simulation for PBXs based on Combined Microcrack and Microvoid Hotspot Mechanisms

K. Yang, Y. Wu, F. Huang

A multiscale damage-ignition model incorporating two micro-defects related hotspot mechanisms, namely, shear-crack friction and void collapse, has been developed to evaluate non-shock ignition of polymer-bonded explosives (PBXs). For an uncovered PBX9501 charge punched by a flat-front rod, the simulated results show that shear-crack friction heating plays a critical role on ignition under low-velocity impact (<400 m/s). Under high-velocity impact (>400 m/s), the heating due to void collapse becomes to dominate ignition because time-to-ignition of void hotspots (~ 1 μ s) is shorter than the time of crack hotspots (~ 10 μ s). At the beneath of rod, the cracks are stable governed by friction-locked stress state and void collapse becomes a dominant hotspot mechanism. At the periphery of rod, both the shear-crack and void collapse hotspots have strong influences on ignition.

356 - Propagation of Reactive Cracks in Pressed HMX-Based Pbx and Reaction Violence of Explosive System in Thick Wall Confinement

T. Li, H. Hu

High temperature gas products of conductive reaction on explosive surface can penetrate into preformed crack inside explosive bulk under high pressure to form so-called convective reaction which behaviors as rapid transportation of hot gas products along crack and the initiation of local conductive reaction on the preformed crack surface with a time delay for thermal induction. The high rising gas products pressure of the convective reaction in turn will create cracks inside the continuum explosive bulk to form new channels for convective reaction and more reaction surface for combustion. The propagation of such kind of reactive cracks inside a confined 110mm spherical explosive of one pressed HMX-based PBX with non-shock initiation on center point was recorded and evaluated with the total reaction violence growth behavior characterized by reaction pressure and confinement wall velocity profile. The early stage evolution of crack inside explosive sphere is invisible (Stage I) and the crack system after the crack break through to the spherical surface (Stage II) shows a 4 fold symmetric crack pattern which is deduced to be related with outer layer confinement conjunction manner. The violence evolution experienced a sustaining low pressure growing rate stage which lasted about 100 μ s before the confinement movement stage and a rapid burst during the confinement wall movement stage (Stage III) in about 10 μ s up to over GPa which leading to a typical explosion outcome with 20%-30% air blast over pressure level relative to detonation event. The velocity of 20mm steel wall has reached 500m/s at the moment of confinement wall rupture (the beginning of Stage IV).

183 - Shock-to-detonation transition in nitromethane with spatially non-uniform distributions of air-filled cavities

X. Mi, N. Nikiforakis, A. Higgins, L. Michael

Liquid nitromethane (NM) can be sensitized to shock initiation via the addition of hollow micro-balloons. This sensitizing effect is attributed to the formation and development of localized high-temperature regions, or hot spots, as cavities collapse upon the arrival of an incident shock wave. To further elucidate the underlying mechanisms, GPU-accelerated, meso-resolved simulations wherein a large number (i.e., more than 100) of air-filled cavities are explicitly described are performed to probe the sensitizing effect on the overall shock-to-detonation (SDT) behavior in liquid NM. The simulation results show that, in a mixture of NM with a uniformly random distribution of cavities, the sensitizing effect, i.e., the reduction in the detonation overtake time, is less pronounced than the corresponding experimental data. A non-uniformly random distribution of cavities may give rise to clusters of closely neighbouring hot spots, namely, hot spots of hot spots, and thus, leads to a more significant sensitization to shock initiation. This hypothesized mechanism will be examined in this study via controlling the spatial distribution of cavities and compare the SDT behaviors resulting from ensembles of simulations. Statistical analysis is performed to demonstrate the clustering effect of hot spots.

13:50 Detonation Failure/Limits**319 - Critical Ignition in Detonation Cells due to Expansion Cooling***K. Cheevers, R. Murugesan, F. Giroux, W. Morin, A. Dion-Dallaire, M. Radulescu*

Gaseous detonation waves are characterized by a cellular structure, during which the lead shock continuously decays until its re-amplification caused by triple shock reflections. The present study addresses the ignition behind the decaying lead shocks. We analyze experimentally obtained cellular dynamics in CH_4+2O_2 and $2\text{H}_2+\text{O}_2+7\text{Ar}$. Using the experimental records of shock decay and shock curvature, the expansion cooling along the particle paths is evaluated using the shock change equations. Ignition calculations along the particle paths using full chemistry and the local volumetric expansion inferred from the shock dynamics permitted us to reconstruct the ignition history along particle paths and identify the conditions for quenching of the ignition process. In both mixtures, the ignition is quenched before the shock has travelled half the cellular cycle, and occurs earlier in the methane system. For both mixtures, the role of shock curvature was found to play a comparable role to the shock unsteadiness in controlling the Lagrangian volumetric expansion along particle paths for the first half of the cellular cycle, the curvature effects becoming negligible in the second half.

359 - Propagation limit of gaseous detonations governed by yielding confinement and Arrhenius kinetics*L. Zhou, X. Mi, H. D. Ng, Y. Zhang, H. Teng*

Two-dimensional computational simulations have been performed to model the dynamics of a detonation wave propagating in a layer of reactive gas under the confinement of an inert layer. For single-step kinetics with a sufficiently large activation energy and two-step kinetics, a critical thickness of the reactive layer below which the detonation wave propagation cannot be self-sustained has been captured. Qualitatively opposite relationships between the critical thickness and the stability of the reactive mixture have been obtained from the simulations with single-step Arrhenius kinetics and two-step induction-reaction kinetics. More in-depth investigation into these intriguing results will be done in future effort.

240 - Experimental Study on Deflagration-to-Detonation Transition Shortening by Nanosecond Pulsed Laser Ignition*T. Sato, K. Matsuoka, A. Kawasaki, J. Kasahara*

In considering DDT shortening and direct initiation of detonation together, based on the criterion, it is indispensable to clarify the critical Mach number and the critical radius of the blast wave as well as to predict the relation between the absorbed energy and the Mach number of the blast wave. In this paper, first of all, oscillator's emission energy and the characteristics of the variable beam splitter used for the breakdown observation are evaluated. Secondly, using Schlieren method, a spherical blast wave is observed in the air. Thirdly, Mach number is calculated based on the diameter of the blast wave. Fourthly, with Lee's surface energy model, the criteria for direct initiation by laser ignition is discussed. Finally, the absorption rate of the emission energy was calculated by measuring the transmitted laser's energy.

48 - Near-limit dynamics of gaseous detonations: Distinguishing tube scale and initial pressure effects*B. Zhang, H. D. Ng*

In this study, the near-limit propagation dynamic behavior of gaseous detonations with varying tube inner diameter and mixture initial pressure was investigated. Stoichiometric methane-oxygen detonations in tubes with different inner diameter ($D = 36$ mm, 25 mm, 20 mm and 13 mm) and low initial pressure from 3.5~18 kPa were studied. Smoked foils were employed to observe the evolution of the detonation cellular structure for various initial conditions. An alternate length scale is examined, L_{dcs} , which is the maximum length from the beginning of the test section after which cellular patterns can no longer be observed. Simultaneous local velocity measurements were obtained by photodiodes to complement the L_{dcs} results. The purpose of this study is to explore relation between the near-limit detonation dynamics, the tube geometry, and the thermodynamic properties of the mixture. The results indicate that past the failure limit, L_{dcs} decreases with decreasing mixture initial pressure for a given tube diameter, and L_{dcs} decreases faster in a smaller diameter tube. In the $D = 13$ mm tube, galloping detonation mode is observed, and the length of the galloping cycle is reduced with an increase in initial

pressure. To further understand the near-limit detonation behavior, a scaling analysis of Ldc's with tube inner diameter (D) and detonation cell size (λ) was performed.

13:50 RDE 1**351 - Characterization of Detonation Wave Heat Release and Rotating Detonation Engine Mode Selection**

J. Burr, K. Yu

In this paper, high-quality visualization images of various detonation waves propagating inside a channel geometry similar to an unwrapped RDE combustor flowfield are provided. The corresponding schlieren and chemiluminescence images are used to establish the structure of the detonation waves propagating through the model injector flowfield. Also, the average timing of the local pressure change and heat release fluctuations associated with the detonation waves is deduced from the high-frequency-response pressure transducer data, CH^*/OH^* radical chemiluminescence, and time-resolved general luminescence data. The results are used to characterize the fluctuating pressure and heat release fields in the wake of the detonation wave. Lastly, the reacting flowfield is modeled with a reduced-dimension approximate analysis to quantify the expected CJ detonation wave speed and demonstrate the mode selection process. Some of the data obtained in our linear rig experiments can be compared with the approximate analysis results.

384 - Detonation Propagation in a Linear Representation of a Rotating Detonation Engine

C. Metrow, G. Ciccarelli

In recent years, there has been a dramatic increase in research interest concerning Rotating Detonation Engines (RDEs). The detonation mode of combustion offers the potential for high thermal efficiency and power to weight ratio. In an RDE, the fuel and oxidizer are injected separately into an annular cylindrical combustion chamber through a base-plate. The fuel and oxidizer are injected separately to prevent flashback. A detonation is initiated in a pre-detonator and then propagates continuously around the annulus. The high-pressure behind the detonation front is significantly larger than the manifold pressure, and as a result the fuel and oxidizer mass flow is arrested. As the products expand behind the detonation wave, pressure in the manifold once again surpasses the base-plate pressure and fresh reactants flow into the chamber to sustain the propagation of the detonation. Detonation wave phenomena is typically studied by schlieren photography. However, since schlieren photography relies on parallel light transmission, it is not applicable for an annular RDE. In this study an optically accessible linear RDE is developed that is connected to a similar cross-section detonation channel that introduces a steady CJ detonation wave. Preliminary experiments were carried out with the injection of premixed hydrogen-oxygen into argon through a series of holes fed by a plenum in the base plate. Schlieren video shows the propagation of a detonation along the injection plate at a constant velocity of 2000 m/s. Flashback in the plenum eventually leads to DDT, the expansion of the products from the plenum detonation produces an oblique shock ahead of the channel detonation wave.

362 - Effect of Parasitic and Commensal Combustion on Rotating Detonation Combustor Properties

F. Chacon, M. Gamba, A. Feleo

Secondary combustion modes present in rotating detonation combustors are investigated in both high speed video and point wise measurements. In particular a distinction is drawn between secondary combustion before and secondary combustion after the wave due to the differing impact the two non idealities have on the properties of the detonation wave. Some initial quantification of the phenomena suggest as much as 50% of reactions in RDCs is associated with non ideal combustion.

212 - OH^* Chemiluminescence Investigation of Rotating Detonation Wave Structure

J. Jodele, E. Gutmark, A. Zahn, V. Anand

A rotating detonation combustor (RDC) is investigated in order to determine the impact of equivalence ratio, mass flow rate, and channel sizing on a rotating detonation wave. High speed chemiluminescence is used in order to visualize the detonation wave as it propagated through the combustor. Centered images of the detonation wave are aligned and averaged in order to determine the characteristics of the detonation front per test case. Average detonation wave intensities and wave heights are then calculated. The standard deviation is then calculated and divided by the average combustion intensity in order to determine the normalized deviation from the average. It was

determined that detonation waves that propagated at a global equivalence ratio of 1 experienced the highest average intensity. Increasing the mass flow rate of the engine also resulted in a reduced normalized deviation; however, this trend is not expected to continue endlessly.

13:50 Ignition 2**257 - Rapid compression machine (RCM) studies on the production of unsaturated hydrocarbons from methane**

S. Drost, R. Schießl, U. Maas

In this paper, we investigate the conversion of methane to other substances, notably unsaturated hydrocarbons, by pyrolysis under engine-like conditions in a rapid compression expansion machine (RCEM). The RCEM allows to study the conversion process under similar conditions like in a motored piston engine, but with better controlled initial- and boundary conditions. The aim of this study is to understand the formation and yield of higher valuable and energetic species that can be created in an internal combustion engine. We investigate the influence of temperature, pressure and reaction time. It is shown that the conversion in the RCEM under the conditions of our study reaches a quasi steady state after 50 ms. The highest conversion is found for a high diluted mixture. The main product is hydrogen. The conversion is almost independent of pressure, however, the yield of C₂H₂ slightly drops with increasing pressure.

266 - Effects of NTC region on end-gas combustion modes under temperature stratification

T. Nogawa, H. Terashima

Effects of NTC characteristics on end-gas combustion modes under temperature stratification are numerically investigated. The compressible Navier-Stokes equations are solved with detailed chemical kinetics mechanisms of n-heptane/air and n-butane/air mixtures. The result shows that smaller temperature gradients in a reactor lead to higher pressure peaks along with the generation of a developing detonation mode. On the other hand, pressure peaks associated with end-gas autoignition are significantly reduced in the case of larger temperature gradients, where a successive end-gas autoignition mode is observed. A comparison between the results of n-heptane and n-butane/air mixtures demonstrates that the NTC characteristics affect end-gas autoignition behavior through the non-monotonic spatial distribution of ignition delay times. The NTC characteristics may increase a possibility of a developing detonation mode.

160 - Analysis of the Vibrational Non-equilibrium Characteristics in Hydrogen-Oxygen Auto-ignition using DSMC method

C. Yang, Q. Sun

The thermal-chemical non-equilibrium coupling in H₂-O₂ auto-ignition process is numerically studied using the DSMC method. The vibrational favor characteristic of the 3-step chain reactions is analyzed with the TCE reaction model, and it is found that the molecules of H₂ and O₂ consumed by chain reactions are at a strong vibrational non-equilibrium state. The DSMC simulation result of H₂-O₂ auto-ignition shows that the vibrational temperature of H₂ and O₂ gradually decreases during the induction period while the vibrational temperature of H₂O is much higher than the translational temperature. Theoretical and numerical analysis shows that the variation of vibrational temperatures of H₂ and O₂ are mainly affected by the consumption and production of forward and reverse reactions, while thermal relaxation effect is not important unless the initial temperature is relatively low.

205 - A Parametric Validation of Auto-ignition Numerical Studies on Compact Rapid Compression Machine

P. Kumar, S. Nakaya, M. Tsue

In this study, an analytical model is developed based on CRCM thermodynamics incorporated essential physics assuming no chemical heat release to investigate the heat loss. Moreover, a 2D axisymmetric model is developed to model the autoignition process using reduced mechanism for n-butane combustible mixtures. Analytical and axisymmetric models are validated against the experimental pressure time history obtained from the CRCM. Furthermore, Ignition delay obtained using 2D axisymmetric model is validated against the zero-dimensional study using detailed reaction mechanism. The fuel considered in this study shows the negative temperature coefficient (NTC) in which ignition delay increases with increasing temperature [13]. Moreover, near to the turnover states[7], it is difficult to predict two-stage ignition from pressure trace. Therefore, two-stage ignition

is investigated based on OH formation near to the turnover states in the numerical simulation.

13:50 Dynamics & Stability 2

171 - Large Eddy Simulations of turbulent premixed flame ignition and stabilization by pulsed plasma discharges

Y. Bechane, N. Darabiha, V. Moureau, C. Laux, B. Fiorina

The more and more severe environmental norms on pollutant emission impose a technological breakthrough to combustion-related industries. An efficient solution to reduce pollutant formation is to maintain a relatively low flame temperature. However low-temperature flames are subject to instabilities and extinction, causing safety issues. A promising technology is to stabilize the flame by Nanosecond Repetitively Pulsed (NRP) discharges. A plasma, generated at the flame basis, produces active species and local heating sufficient to sustain the combustion. Despite this proven efficiency demonstrated experimentally, the mechanisms of plasma assisted combustion are not understood, highlighting the need of numerical simulations. The numerical simulations of interactions between NRP discharges and turbulent flames has yet never been performed and are the final objective of this project. This simulation will be possible by using a novel, recently published, semi-empirical plasma model, designed to capture the influence of NRP discharges on the flame properties. This strategy is used to include for the first time plasma discharges in LES of flames. These simulations give a formidable new insight in the understanding of plasma-assisted combustion.

76 - Numerical studies of the flame dynamics in a novel, ultra-lean, non-premixed model GT burner using PDF-ESF method

S. Yu

The flame dynamics in a novel, ultra-lean non-premixed model GT burner flame was numerically studied using LES (Large Eddy Simulation) coupled with PDF (Probability Density Function) based on the ESF (Euler stochastic field) method. One non-reacting case and three reacting cases with global equivalence ratio $\phi_{\text{glob}}=1.0, 0.6, 0.3$ were simulated. Comparison of mean flow fields and OH distributions between numerical and experimental results was conducted. Flame dynamics including flame stabilization, structures and transitions of combustion modes were investigated. The simulation results were in close agreement with the experimental measurements showing the PDF-ESF LES model capable of predicting the flame behaviors. At higher ϕ_{glob} , the fuel jet velocity was higher, which yielded higher scalar dissipation rate, χ , near the burner exit, leading to local extinction and flame lifted-off. In the extinction region, a series of low to medium temperature reactions were active, providing favorable conditions for re-ignition downstream where $\chi < \chi_{\text{crit}}$. In addition, with ϕ_{glob} decreasing, the flame height decreased due to a smaller jet velocity and χ , and thus the mechanism of flame stabilization changed from the swirl-stabilized to the bluff-body stabilized.

300 - Multi-dimensional numerical analysis on flames with repetitive extinction and ignition in a heated micro channel

K. Akita, Y. Morii, H. Nakamura, T. Tezuka, K. Maruta

Research on the ignition and combustion characteristics plays an important role for the development of high-efficiency internal combustion engines. This study aims to clarify the ignition and extinction phenomena, FREI, in consideration of multi-dimensional effects using the two-dimensional numerical simulation for stoichiometric CH₄/air mixture. Two-dimensional numerical simulation results indicate that the ignition occurs at the central axis of the tube and the flame is separated into the opposite direction, and in the extinction phase, the distance of two heat release peaks which produced from CO reaction is larger than that of one-dimensional simulation.

187 - Ultra-lean hydrogen-air flame kernels large-scale dynamics in terrestrial gravity conditions

A. Kiverin, V. Golub, M. Anton, I. Yakovenko, V. Vladislav, M. Kseniya

The paper is devoted to the experimental study of the ultra-lean flame kernels development in hydrogen-air mixture inside large-scale volume in terrestrial gravity conditions. Main stages of the flame kernel evolution during its convective motion are defined and physical mechanisms determining peculiarities of ultra-lean combustion in presence of natural convection are proposed. Experimental results were compared with numerical modeling carried out earlier that allowed to demonstrate the correctness of the numerical results and physical mechanisms revealed on its basis. It is shown that

the key role in the process of flame propagation in ultra-lean mixture belongs to the convective rise of the flame kernel due to the terrestrial gravity field. Herewith, kernel rising velocity is much higher than the laminar burning velocity of the ultra-lean mixture. Considered processes may result in emergency situations and should be taken into account when elaborating robust fire and explosion safety technologies.

13:50 Energetic Materials 2**112 - Advanced Spectroscopic Approachs for Assessing the aging level for Zirconium-based Pyrotechnic Initiator**

J. Ryu, J. Yoh

Solid mixtures have long been used as pyrotechnic materials in military or private sectors due to its high energy through instant combustion. This study is aimed to estimate the thermal performance of pyrotechnic initiator (Zr/KClO₄), which is composed of Zr fuel and KClO₄ oxidant, according to hygro-thermal aging through spectroscopic analyzes. LIBS and XPS studies were performed on accelerated aged samples under various humidity and heat conditions. In LIBS study, the oxidation level of Zr was determined based on the difference in ZrO molecular signal relative to the amount of ZrO₂. Meanwhile, the decomposition amount of KClO₄ into KClO₃ and KCl with respect to aging was determined by quantitative XPS analysis. Then, NASA CEA (chemical equilibrium with application) code was used to predict the thermal performance based on composition, which is estimated from spectral analyzes. In addition, we verify the feasibility of spectroscopic analysis results with DSC experiments. Performance prediction technique based on spectroscopic analyzes has been proposed to determine the performance of pyrotechnic materials.

113 - The changes of thermodynamic reactions of a NASA standard initiator due to hygrothermal aging

J. Oh, Y. Park, J. Yoh

When energetic materials are in storage for a long period of time, their performance degradation may occur due to various factors such as oxidization, hydrolysis, chemical or structural deformations. The authors also provide surface analysis that shows chemical variations in both fuel (Zr) and oxidants (KClO₄) by utilizing X-ray photoelectron spectroscopy (XPS). Moreover, the thermal analysis and reaction kinetics are extracted from differential scanning calorimetry (DSC). The extracted reaction kinetics is also utilized in simulating a trend of reaction progress for ZPP aged under various conditions. The simulation result matches well with the conducted experimental results. Thus, it can be derived that high-RH conditions induces significant performance degradation of ZPP materials.

339 - Aluminized and Non-Aluminized AP/HTPB-Composite Propellant Burning Rates at Very-High Pressures

C. Dillier, E. Petersen, T. Sammet, F. Rodriguez, E. Petersen, J. Thomas

Recent advancements in chemical synthesis techniques have allowed for the production of improved solid rocket propellant nano-scale additives. These additives show larger burning rate increases in composite propellants compared to previous generations of additives. In addition to improving additive effectiveness, novel synthesis methods can improve manufacturability, reduce safety risks, and maximize energy efficiency of nano-scale burning rate enhancers. Burning rate increases as high as 67. 7% at additive mass loadings of less than 0. 5% were seen in non-aluminized, ammonium perchlorate-based propellants over the pressure spectrum of 500 psi to 2250 psi. To further characterize these additives, a new very high-pressure strand burner was designed and implemented at Texas AM University. While many strand burner facilities are capable of determining propellant burning rates, most only test regularly up to 15. 5 MPa (2250 psi). Few burning rate data exists for higher pressures and almost none for pressures exceeding 34. 5 MPa (5000 psi). Therefore, aluminized and non-aluminized AP/HTPB-composite propellants were tested at very high pressures in the present study, up to 68. 9 MPa (10,000 psi). The paper presents the results of these new data, with emphasis on ballistic curve exponent changes at these extreme pressures.

363 - Updated Three-Flame Modeling of Composite AP/HTPB Propellants

J. Thomas, E. Petersen

The Beckstead-Derr-Price (BDP) model for the steady-state burning of ammonium perchlorate composite propellants (APCP) is based on multiple flames above the propellant surface and has been

widely utilized for purposes of modeling the complicated, heterogeneous combustion of APCPs. However, APCP burning rate data that have been previously utilized to validate various versions of the BDP model have not spanned adequate propellant formulations (AP particle size and concentration) and combustion pressure. The authors have recently developed an experimental database of unimodal APCP burning rates that includes AP particle sizes of 20-500 μm , AP mass concentrations of 70-87.5%, and combustion pressures up to 15.5 MPa (2250 psia). In the current study, a BDP model framework is outlined and updated to built-in, variable flame temperatures and combustion product transport properties determined from combustion equilibrium analyses (CEA). Model parameters are initially taken from previous literature and are tuned to the burning rate data that have been recently published.

16:30 Detonation Modeling

95 - Steadily-rotating overdriven detonation : experiments vs. GSD modeling

C. Jourdain, V. Rodriguez, P. Vidal, R. Zitoun

This experimental and numerical work reports on detonation dynamics in a curved chamber without center body after diffraction of a Chapman-Jouguet (CJ) detonation from a straight channel tangent to the chamber outer wall. In the experiments, the upper and lower faces of the chamber receive either soot foils for recording the history of the transmission dynamics, or optical windows for high-speed shadowgraphy. Tests were carried out with the stoichiometric propane-oxygen mixture at initial temperature 288 K and initial pressures p_0 ranging between 8 kPa and 15 kPa. The primary observation is the existence of an initial pressure range (8 kPa - 12 kPa) for which, after diffraction transients, a Mach front rotates normal to the outer wall with a constant angular velocity and a normal velocity at the wall and its close vicinity larger than the CJ value. Below the lower limit of this p_0 range, detonation quenches, above the upper limit, detonation re-initiates in the whole chamber without rotating.

50 - A 3-D Pseudo-Arc-Length Method for Numerical Simulation of Detonation Wave Propagation

M. Tianbao, Z. Jinqing, N. Jianguo

In this paper, we propose a robust pseudo-arc-length moving mesh scheme for detonation wave propagation in three dimensions, which involves governing equations evolution and mesh-redistribution. Second-order finite-volume schemes are used for governing equation evolution, while mesh-redistribution is an iterative procedure that includes mesh point redistribution and cell average conservative interpolation. Since the grids are distorted, the numerical algorithm is non-convergence in three-dimensional space. Then the combination of block reconstruction and integral calculation strategy is adopted in the algorithm design process. Finally, several numerical examples are presented to demonstrate the accuracy and effectiveness of the pseudo arc-length method.

268 - Two-dimensional Numerical Simulations on Unstable Propagation of Propane/Oxygen Detonation Using a Detailed Chemical Mechanism

N. Takeshima, K. Ozawa, N. Tsuboi, K. Hayashi, Y. Morii

The final goal of our research is to clarify the cause of cell size inhomogeneity and velocity oscillation of propane/oxygen detonation, which is considered to be more unstable than hydrogen/oxygen detonation and highly diluted detonations. As the first step, we perform two-dimensional analysis and investigated the propagation behavior of unstable propane/oxygen detonation for different channel width using a detailed chemical kinetic mechanism and Euler equations. As the result of maximum pressure histories, the cell length was nearly equal in a narrow channel ($d = 1.5 \text{ mm}$), but in a wide channel ($d = 3.0 \text{ mm}$) irregular cell pattern was seen and the maximum pressure is higher than that of a narrow channel case.

180 - Statistical Analysis of the Reaction-Zone Characteristics of Unstable Gaseous Detonations

X. Mi

A framework of statistical analysis is proposed and performed to describe the reaction-zone characteristics of unstable gaseous detonations. The probability of the occurrence of a certain amount of gas reacting at a rate and a distance relative to the location of the leading shock front is calculated. The probability functions of reaction rate resulting from two-dimensional simulations are compared with those of the corresponding ZND solution. For simulations based on the inviscid Euler equations,

the statistical results provide a quantitative measurement of how much material undergoes a significantly slow reaction. The diffusive effects on the statistical nature of the detonation reaction-zone dynamics will be probed within the complete scope of this study. The effective diffusivity in the simulations can be varied via changing the physical diffusivity in a model based on the Navier-Stokes equations or refining the computational grid of a simulation based on the Euler equations.

16:30 RDE 2
320 - Chemistry Modeling Effects on the Interaction of a Gaseous Detonation with an Inert Layer

S. Taileb, J. Melguizo-Gavilanes, A. Chinnayya

Two-dimensional simulations are conducted to assess the effect of chemistry modeling on the detonation structure and quenching dynamics of detonations propagating into a semiconfined medium. Two different simplified kinetic schemes are used to model the chemistry of stoichiometric H₂-O₂ mixtures: single-step and three-step chain-branching chemistry. Results show that although the macroscopic characteristics of this type of detonations (e. g. detonation velocity and cell size irregularity) are very similar for both models tested, their instantaneous structure is found to be very different upon interaction with an inert layer. Notably, the minimum reactive layer height capable of sustaining detonation propagation is larger when a more realistic description of the chemistry is used.

193 - Detonation Diffraction and Failure of Gaseous Detonations Bounded by an Inert Gas

R. Houim, B. Roque, H. Li

Two-dimensional numerical simulations of detonation propagation through a semi-confined layer of stoichiometric ethylene and oxygen bounded by high-temperature products are presented. The reactant layers were variable in height to approximate a scenario where the thrust of a rotating detonation engine is suddenly increased by increasing the reactant mass flow rate into the combustor. Details such as fuel jets and turbulent mixing were neglect. The computed results show that the detonation maintains a quasi-steady structure if the transition in the reactant layer height is very gradual. The detonation loses its quasi-steady structure if the transition in the detonation layer height is rapid. In these scenarios the detonation diffracts and partially fails. The extreme limit of a step change from h₁ to h₂ produces stochastic behavior based on the location of the step. In some cases the diffraction of the detonation around the step causes complete failure, while in others a chance interaction of shocks reignites the mixture.

138 - The Numerical Investigation of Hydrogen Detonation Propagating in Semi-confined Layers

S. Shigeoka, A. Matsuo, A. Kawasaki, J. Kasahara, K. Matsuoka

Hydrogen detonation in semi-confined layers is numerically investigated utilizing detailed chemical kinetics. Considering hydrogen leakage in a building as one accidental situation, hydrogen is accumulated under the ceiling because of the low density. In the other words, the combustible mixture layer is produced between a rigid wall and inert air. This system is called as semi-confined layers, and the combustible and inert gases in this study are set as 2H₂+ O₂+ 1.5N₂ and O₂+ 1.5N₂ respectively. Simulations are carried out in two combustible layer heights (h) which are 152 and 182 times as high as half reaction length (l_{1/2}). In h= 182 l_{1/2} case, detonation propagates over 3000 l_{1/2} because some transverse waves are successfully reflected at the interface between combustible and inert layers. However, in h= 152 l_{1/2} case, detonation fails after 1000 l_{1/2}. The averaged velocity deficit from CJ velocity is about 1.5 % in h= 182 l_{1/2} case. Near the rigid wall, chemical exothermic reaction completes within the sonic line and the detonation front has no curvature. Ideally, detonation near the wall does not have the velocity deficit. However, near the interface, H₂ remains behind the sonic line and the detonation front inclines. It comes from the failed reflection of transverse waves. Eventually, the detonation is weakened near the interface, but sustained near the wall, with the slight velocity deficit.

311 - Analytical and numerical study of the expansion effect on the velocity deficit of continuous detonation waves

M. Luan, S. Zhang, Z. Xia, S. Yao, J. Wang

A quasi-one-dimensional ZND model of detonation considering expansion process perpendicular to the detonation propagating direction is extended to continuous detonation chamber (CDC) to

investigate the influence of expansion on the detonation waves in the CDCs. This model is first used in more general cases of one-dimensional detonation waves, coupled with the one- and two-step kinetics models for the stoichiometric hydrogen-air mixtures. The expansion has an effect on reducing the detonation propagating speed, which is the result of two influencing factors. One is the extra work during expansion and the other one is the lost heat released behind the sonic point. And which one plays a more important role depends on the kinetics models. For the one-step kinetic model, the deficit of the detonation velocity is mainly controlled by the expansion. However, for the two-step kinetic model, the deficit is mainly affected by the chemical equilibrium, which is in better agreement with real situations. Finally, a set of numerical simulations of CDCs are performed for comparison with the theoretical model. It shows that the expansion process in CDCs reduces the speed of the detonation wave by approximately 5%, which is an important factor of the detonation velocity deficit in two-dimensional simulations.

16:30 Ignition 3

139 - Effects of low-temperature chemistry on hot-particle ignition in a premixed fuel/air mixture

Y. Wang, Z. Chen

The hot particle, such as mechanical sparks in manufacturing and mining operations, is one of the typical thermal ignition sources. Scientific understanding and characterizing of hot-particle ignition plays an important role on accessing and reducing the risk of accidental ignition of flammable mixture in industry and aviation. In the literature there are many studies on hot-particle induced ignition. However, few studies considered the role of low-temperature chemistry (LTC) which is closely related to the two-stage ignition behavior for fuels with negative temperature coefficient (NTC). The present study aims to investigate the effect of LTC on hot-particle ignition in a premixed DME/air mixture. The LTC is demonstrated to play an important role in hot-particle induced ignition. Since the temperature in the thermal boundary layer around the hot particle is within the NTC region, LTC ignition happens first at some distance away from the particle surface and it initiates a cool flame propagating outwardly. A hot flame is eventually initiated by HTC ignition and it catches up and merges with the leading cool flame. The LTC can greatly accelerate the hot-particle induced ignition. Therefore, LTC should be considered for hot particle ignition of large fuels.

233 - Premixture ignition of Jet-A kerosene and some of its surrogates in flowing conditions

R. L. Dortz, C. Strozzi, J. Sotton, M. Bellenoue

Ignition process is critical in innovative constant-volume combustion chambers dedicated to aeronautical propulsion: the ignition kernel must be able to expand while the presence of high velocities (several tens of meters per second) at ignition point. Few data are available in literature concerning ignition of aeronautical jet fuel in presence of a flow at ignition point. Data concerning ignition of its surrogates are also essential to understand this phenomenon but the representativity of these surrogates are not evaluated. This paper studies the comparison between Jet A and several surrogates concerning the ability to represent experimentally the ignition behavior of Jet A in lean (equivalence ratio equal to 0.7) and flowing conditions (mean velocity equal to 25 m/s). Experimental measurements are performed also at ambient initial pressure and initial temperature equal to 400 K. The minimum ignition energies of Jet A and its surrogates in these conditions are determined statistically. The surrogates do not reproduce correctly the ignition behavior of the commercial kerosene, but the more the surrogate is complicated, the best the surrogate is reproducing the commercial kerosene.

250 - Autoignition Studies of Unsaturated Methyl Ester: Methyl Crotonate

S. K. Vallabhuni, B. Shu, X. He, K. Moshhammer, R. X. Fernandes

Biofuels, including biodiesel have high potential to completely replace conventional diesel fuel for low-temperature combustion (LTC) engine applications and to improve their performance. Furthermore, it is a promising approach to reduce greenhouse gases and particulate matter. Other advantages include its cleaner burning nature, its renewability, easy adaption and its indigenous availability. However, the combustion kinetics, engine performance and emission characteristics of biofuels are expected to be different from fossil fuels due to differences in the composition and properties. This study examines the effect of unsaturation on the combustion of fatty acid methyl ester (FAME). Methyl crotonate, a biodiesel surrogate fuel with short chain lengths and known physical chemical properties was chosen for this chemical kinetic study. Methyl crotonate oxidation

experiments were performed in a rapid compression machine (RCM) facility at pressures of 20 and 40 bar under diluted conditions over a temperature range between 870 and 1080 K, and at different equivalence ratios ($= 0.25, 0.5$ and 1.0). The obtained data are useful to study the ignition behavior over a wide range of operating conditions for modern engines. Furthermore, the obtained experimental data were compared to preliminary modeling results in order to get a deeper insight into the combustion chemistry of methyl crotonate in the intermediate temperature regime.

16:30 Dynamics & Stability 3

271 - Swirl Flames Diagnostics Using Diode Laser Absorption Tomography with High Temporal-Spatial Resolution

F. Li, L. Xin

Tunable Diode Laser Absorption Spectroscopy (TDLAS) has been one of the most powerful techniques for combustion diagnostics in different kinds of burners. Combined with Hyperspectroscopy Tomography (HT), TDLAS can improve its spatial resolution. This study reports a TDLAS-tomography system and its application in a swirl burner. The diagnostics system composed of forty-two beams (21X21, 21 parallel beams and 21 vertical beams). Four water vapor absorption lines, 7185.6 cm⁻¹, 7444.3 cm⁻¹, 7466.3 cm⁻¹, and 6807.8 cm⁻¹, were utilized in each beam using time-division-multiplexed (TDM) method at total measuring frequency of 2.5 kHz. A reconstruction routine based on simulated-annealing algorithm was used to deduce distributions of temperature T and water partial pressure PX. Demonstration experiments were performed at cross-sections of different height.

366 - Propagation Speeds and Kinetic Analysis of Premixed Heptane/Air Cool Flames at Large Ignition Damköhler Numbers

T. Zhang, Y. Ju

The auto-ignition assisted laminar cool flame speeds at different ignition Damköhler numbers under elevated temperatures and pressures are numerically modeled in a broad range of equivalence ratios with detailed chemistry. The results show both fuel lean and fuel rich cool flame speeds increase dramatically with the increase of the ignition Damköhler number. At higher pressure, the flame speed becomes smaller but more sensitive to the ignition Damköhler number change. Furthermore, the results show that at the same ignition Damköhler number, with the increase of the initial mixture temperature, there is a strong non-monotonic dependence of flame speeds on temperature due to the Negative Temperature Coefficient (NTC) effect. The peak speed appears around the turnover temperature. The results also show that flame speed decreases immediately once a cool flame transits to a hot flame after the NTC region. A comprehensive analysis of the controlling reaction modes for cool flame propagation is performed using the CSP method under G-scheme framework.

164 - Premixed Methane/Air/Hydrogen Flame Oscillations in Horizontal Open End Tubes

H. Jiang, N. A. b. Amaludin, R. Woolley, Y. Zhang

In combustion studies, emissions from the excited species formed during chemical reactions are known as flame chemiluminescence. Flame chemiluminescence measurements have received increasing attention from researchers as they can provide emission information on the combustion process. Huang and Zhang explored C₂* chemiluminescence intensities utilizing RGB colour channels [11]. Then Yang et al applied this method to flame propagation in tube, described the impact of pressure fluctuations using flame chemiluminescence [12]. However the important pressure oscillation information is not available in their study. In this study, a fuel rich = 1.2 methane-hydrogen-air (RH 0.2) flames have been filmed propagating within a 1200mm long horizontal tube of 20 mm internal diameter quartz tube. The flame propagation was monitored by post-processed C₂* chemiluminescence captured using a high speed colour camera and a pressure sensor was used to simultaneously capture the pressure history so that their coupling effect can be investigated.

84 - Effect of Boundary Conditions on Thermo-Acoustic Instability of Flames Propagating in Tubes

A. Dubey, O. Fujita, Y. Koyama, N. Hashimoto

In this work, we present a theoretical analysis to explain the role and occurrence of thermo-acoustic instability in tubes subject to various boundary conditions. The goal is to explain why thermo-acoustic instability happens only under certain boundary conditions. It is found that fundamental mode is

completely/mostly stable when flame is ignited near the closed end of an open-closed/closed-closed tube. Open-open tube shows instability when flame is in the upper two third of the tube but is stable when flame is in the lower one third of tube. Smaller pressure fluctuations cannot be ruled out due to pressure coupling as it is destabilizing irrespective of boundary conditions, but is unlikely to cause significant flame instability. The theoretical results are consistent with experiments.

16:30 Energetic Material 3**253 - Effect of Acoustic Excitation on Ammonium Perchlorate Decomposition and Combustion***L. Han, J. Li*

The experimental study on the combustion decomposition of ammonium perchlorate (AP) particles under different external acoustic excitation is carried out with a methane planar burner. The results show that the decomposition time, average maximum amplitude, self-excitation amplitude and oscillation amplitude of AP combustion are influenced by the frequency and amplitude of external acoustic excitation. Low frequency and medium-amplitude external excitation conditions can accelerate the combustion decomposition of AP and shorten the decomposition combustion time, but it is easy to cause additional higher amplitude of acoustic pressure oscillation. The combustion and decomposition process of AP will attenuate the amplitude corresponding to the external excitation, and the attenuation is positively correlated with the excitation amplitude.

329 - A copper oxide based metal-organic framework: Effect on combustion of ammonium nitrate and magnesium composition*M. Atamanov, R. Shen, Z. Yelemessova, K. Kamunur, A. Imangazy, B. Lesbayev, Z. Mansurov*

In order to obtain a better understanding of the combustion characteristics of ammonium nitrate (AN) and carbon (C) mixtures (AN/C), burning tests and Differential Scanning Calorimetry (DSC) were performed. Ammonium nitrate is widely used in rocket fuels, in explosives and gas generators as an oxidant. However, several major drawbacks have reduced the scope of the application. In order to improve these disadvantages of AN in the composition of composites, energy materials are used activated carbon with metal oxides as a metal organic frameworks (MOFs). In addition, the influence of copper oxide on the combustion of compositions and its thermal characteristics was studied. Compositions were combusted at the pressure of 1 MPa, 2 MPa, 3 MPa and 3,5 MPa in the combustion chamber and the burning rates were determined. With the addition of a metal oxide burn rate has increased two-three times. The thermal characteristics of compositions have been investigated on a Differential Scanning Calorimeter at different heating rates, and the activation energy of the system is also calculated.

53 - Thermal decomposition of nitromethane: Experiments and model validation*Y. Meng, Z. Xu, Z. Gao, C. Tang, E. Hu, Z. Huang*

The thermal decomposition experiment of nitromethane is investigated at pressure of 1 atm, fuel concentration of 1% and resident time of 2 s by using a jet-stirred reactor (JSR). Eight important species concentration profiles are obtained at the temperature range 675-1225 K. In addition, the detailed discussions about the mole fraction profiles are also presented. Results show that at $T = 750$ K, the nitromethane begins to decompose. Then it decomposes sharply as the temperature increasing. At $T = 900$ K, the pyrolysis of nitromethane finishes completely. In addition, the recent model of Mathieu et al. is validated using the JSR experimental data in this work. It can be seen that the current model of nitromethane exists some problems and need to be improved.

10:20 Detonation Miscellaneous 1**361 - Detonation Propagation through Inhomogeneous Fuel-air Mixtures***S. Prakash, V. Raman*

Rotating detonation engines (RDEs) provide a practical route to pressure gain combustion. However, to realize the potential of these devices, it is necessary to use non-premixed fuel-air injection, which introduces significant fuel stratification inside the combustor. Furthermore, following the passage of a detonation wave, incompletely mixed fuel and air streams prematurely burn due to deflagration within the annulus. The primary objective of this work is to increase understanding of the interaction between the detonation wave and the fuel-air mixture inhomogeneity. Past numerical and experimental work has shown that poor mixing and inert gases result in irregular detonation cell structures and diminish mixture detonability. To this end, the direct numerical simulation approach is used to evaluate the influence of mixture pre-burning on the detonation wave structure and behavior. The fuel-air stratification length scale is varied and its effect on the detonation wave structure is realized. Using a fixed stratification of fuel and oxidizer within a channel, four levels of pre-burning of the fuel and oxidizer mixture, up to the fully-burnt equilibrium state, are studied. The effects of fuel-air stratification and mixture pre-burning on the properties of the detonation wave are thoroughly discussed.

305 - Patterns of Detonation Decay and Combustion of Hydrogen-Air Mixture in Porous Layer*S. Golovastov, G. Bivol*

A processes of decay of the detonation wave in hydrogen-air mixture during propagation along a porous surface were considered. Propagation and evolution of the flame front was investigated in a rectangular cross-section channel with a polyurethane porous coating. The width of the channel was 20 mm, the thickness of the porous layer was 10 mm. A stationary detonation wave was formed before the entering the adsorbing section with the porous walls. Dynamics of the flame were recorded using a high-speed camera both in the centre of the gaseous stream and inside the porous coating. Pressure under the porous covering was measured by piezoelectric pressure transducers. Pressure impulses were determined in dependence on pore size. Four types of polyurethane foam with a number of pores per inch ranging from 10 to 80 covering two opposite channel walls were used for detonation attenuation. A non-monotonic influence of the parameters of the porous coating on the evolution of the detonation wave in the channel was observed.

306 - Numerical Investigation of Shock Waves as Detonation Initiator*S. Bengoechea, J. Reiß, M. Lemke, J. Sesterhenn*

Pulse detonation engines (PDEs) are quasi-isochoric and offer an efficiency gain compared with well-established constant-pressure combustors [1]. However, the direct initiation of detonations requires a substantial amount of energy in a short time, so that an indirect initiation via deflagration-to-detonation transition (DDT) is desired. One realization is via deflagration-induced shock waves. These ignite the detonation at the focal point, as was demonstrated by [2,3]. The present study numerically investigates in detail the detonation initiation at the focal point of the imploding shock wave. The combustion chamber under consideration is a circular pipe with one convergent-divergent axisymmetric obstacle [3]. The nozzle-shaped geometry, sketched in Figure 1, has a blockage ratio (BR) of 75%, a converging angle of 45 and a diverging angle of 131. The results describe the aspects of the onset of detonation via focusing shock waves. The sensitivity of DDT to the obstacle shape is analysed as a first attempt to optimize the geometry.

203 - The Effect of Ozone Addition on DDT for Ethylene-Oxygen Mixtures in Macro-Scale Tube*Y. Cai, W. Han, C. Wang, Y. Cui, W. Ma, Y. Wu*

The experiment used a 1.5m stainless steel channel with a square of 20-20cm in cross section. The present experimental results indicate that the addition of a certain amount of ozone has an accelerating effect on DDT in macro-scale channel. However, compared with the micro-pipeline, its impact is relatively weaker. In the macro-scale channel, turbulence combustion has a major role on the detonation run-up distance, the effect of ozone kinetics on macro DDT is minor. The ozone addition changes slightly detonation velocity, showing that the addition of ozone hardly affects the rate of chemical reaction heat release during the detonation phase.

10:20 Micro Reactors**258 - Reactivity of CO/H₂/CH₄/air Mixtures derived from In-cylinder Fuel Reformation Examined by a Micro Flow Reactor with a Controlled Temperature Profile***Y. Murakami, H. Nakamura, T. Tezuka, G. Asai, K. Maruta*

Reactivity of CO/H₂/CH₄/air mixtures were examined by a micro flow reactor with a controlled temperature profile (MFR) at atmospheric pressure. In target mixtures of the present study, H₂ fractions were replaced with CH₄ fractions every 5% while CO fractions were fixed as constant (50%). Weak flames of stoichiometric CO/H₂/CH₄/air mixtures were observed in the reactor at atmospheric pressure and the mixture flow velocity of 3 cm/s. The maximum wall temperature of the reactor wall was set to 1300 K. One-dimensional computations simulating MFR system were also conducted with several chemical reaction models. Experimental and computational results showed that flame locations shifted to higher temperature (downstream) side of the reactor as H₂ fraction decreased and CH₄ fraction increased, which interprets the reactivity of the CO/H₂/CH₄/air mixture decreased. Ignition delay times of the same CO/H₂/CH₄/air mixtures at atmospheric pressure were also calculated using a zero-dimensional homogeneous reactor model. The results showed that ignition delay times increased consistently as H₂ fraction decreased and CH₄ fraction increased in the temperature range over 900C1300 K, where weak flames of CO/H₂/CH₄/air mixtures stabilized. For further investigations on the decrease in the mixture reactivity, rate-of-production analysis was performed for OH radicals in each case of MFR computations. Based on the analysis, for CO/H₂ mixtures, OH radicals are mainly consumed by H₂ and CO. Subsequently, H radicals are produced through H₂+OH=H+H₂O and CO+OH=H+CO₂. However, once CH₄ is included in CO/H₂ mixtures, CH₄ starts consuming OH radicals through CH₄+OH=CH₃+H₂O and produces CH₃ radicals. The consumption rate of OH radicals by CH₄ becomes larger than that by H₂ and CO especially at early stage of reactions as CH₄ fraction increases. Therefore, primary factor of the significant reduction of reactivity of CO/H₂/CH₄/air mixtures seems to be the increase of OH consumption by CH₄ and CH₃ production rate due to the increase of CH₄ fractions.

165 - Very rich methanol-air combustion in microchannel-based reactors to produce hydrogen-rich syngas*D. Fernandez-Galisteo, E. F. Tarrazo, C. Jiménez, V. Kurdyumov*

We examine very rich methanol-air combustion in a microchannel-based reactor consisting of multiple counter-current channels of finite length separated by thin solid conducting walls. Within the framework of the narrow-channel approximation, this problem can be formulated as a one-dimensional model for a single channel with an extra term representing heat transfer from hot stream products to fresh reactants in adjacent channels. The heat recirculation enables superadiabatic temperatures and promotes the oxidation of the fuel far beyond the conventional rich limit of flammability, resulting in a feasible thermal partial oxidation that produces hydrogen without the need for a catalyst. We present an analysis of the stationary model burner performance with detailed gas-phase kinetics in terms of operating variables such as the equivalence ratio and the gas inflow velocity, and for different physical parameters such as the length of the reactor and the conductivity of the wall material. The model predicts a hydrogen yield between 50 and 60% for a range of equivalence ratios between 3 and 6 and a wide range of reactant flow rates.

269 - Study on Reactivities of Refregirants R32, R125 and R410A using a Micro Flow Reactor with a Controlled Temperature Profile*S. Takahashi, H. Nakamura, T. Tezuka, S. Hasegawa, K. Maruta*

We examined the weak flames of R32(CH₂F₂), R125 (C₂HF₅) and R410A (CH₂F₂/C₂HF₅) by a micro flow reactor with a controlled temperature profile. For a mixed refrigerant (R410A) and pure refrigerants (R32, R125), Computational results showed the detailed reaction mechanism developed by NIST group qualitatively reproduced the experimental results. From experiments and computations, it was found that position of the weak flames shifted to the high temperature side as the proportion of C₂HF₅ in the mixed fuels increase up to 50 wt%. When the proportion of C₂HF₅ exceeds 50 wt%, the weak flame position shifted to the low temperature with the increase of C₂HF₅. Analysis of flame structures and CO production rates of R32, R125 and R410A revealed that unreacted CO increased with the addition of C₂HF₅ and contributes greatly to the heat release at high temperature region. This reduction of CO consumption rate is due to H radical reduction by HF formation at lower temperature region.

10:20 Detonation Analog/Model

315 - Detonation model using Burgers equation and a pulsed reaction*S. Lau-Chapdelaine, M. Radulescu*

A simplified detonation model is used to investigate the behaviour of pulsating detonations. Burgers equation is used with a reaction that periodically consumes all shocked gas. The resulting pulsating detonation travels at an average speed equal to the Chapman-Jouguet velocity. The pulsations are characterized by two decay periods. A characteristic investigation reveals that characteristics originating from the head of an expansion created by a pulsation take approximately one-and-a-half periods to reach and attenuate the detonation front, while characteristics from the tail take up to two-and-a-half periods. The leading characteristics are amplified twice by passing through subsequent reaction interfaces, before arriving at the front, whilst the weaker trailing characteristics are amplified three times. The two distinct portions of lead shock decay, characterized by two different decay rates, may be responsible for the period doubling bifurcations of real detonations obtained when the dynamics of pulsating detonations approach the singular limit treated in the current work. A closed-form solution is found for the dynamics.

168 - Analog modeling of detonation in a periodic medium*A. Kasimov, A. Gonchar*

We analyze the dynamics of one-dimensional detonations in smooth periodic heterogeneous media within the framework of reactive Burgers analog. We find that heterogeneity influences both the stability of solutions and the nature of unstable pulsating solutions. In particular, various mode interactions leading to the generation of new frequencies or mode locking are observed. In addition, the interaction can lead to a resonant amplification of the pulsations.

346 - Non-Equilibrium Effects in Detonations Initiation using Hard Spheres*R. Murugesan, N. Sirmas, M. Radulescu*

The present communication addresses the role of non-equilibrium effects in detonation waves where the shock relaxation and chemical reactions overlap. We investigate this problem with the aid of molecular dynamics simulations in a system of reactive hard spheres (3D), where the shock wave is generated by a constant piston velocity. The model we consider is a single binary exothermic reaction of the form $A + B \rightarrow C + C$. Molecular dynamics calculations are performed using event-driven molecular dynamics algorithm (EDMD) involving 40,000 particles in a dilute ideal gas regime with a packing factor of 0.01. The calculations are performed for an activation energy of 19RT and heat release of 8RT and 38RT. Ensemble average of 10 calculations for each set of parameters permitted to determine ignition delay, along with the measure of stochasticity of the process. The results for all the values of Q and EA are found to initiate a detonation wave propagating approximately with the Chapman-Jouguet velocity. For high heat release case, the ignition delay time was found to be smaller than the low heat release case because of the molecular instabilities, which scales up with increase in activation energy and heat release. The MD results indicate a super-diffusive nature of detonation wave, in which the reaction zone overlaps with the compression shock. This study also emphasizes the importance of non-equilibrium effects in detonation problems by quantifying our present molecular dynamics calculations with the existing continuum models used for detonation waves to treat problems with strong non-equilibrium effects.

56 - Discrete Boltzmann modelling of compressible reactive flows*C. Lin, K. Luo*

Reactive flows are ubiquitous in nature, and play a key role in human life and society. At present, it still remains a challenge to study complex reactive flows, especially when compressible, hydrodynamic and thermodynamic coupling effects are under consideration. As a kinetic model, discrete Boltzmann method (DBM) provides a versatile tool to simulate and investigate complex fluid flows. In this work, we develop a novel DBM for compressible reactive flows with various nonequilibrium effects beyond traditional hydrodynamic models. It has been demonstrated that the present DBM is physically accurate, computationally efficient, and numerically robust.

10:20 Sprays & Droplets 1

156 - A numerical investigation of the behaviour of the minimum ignition energy for turbulent droplet-laden mixtures

V. Papapostolou, G. O. Erol, N. Chakraborty, C. T. d'Auzay

The minimum ignition energy (MIE) for uniformly dispersed n-heptane droplet-laden mixtures in homogeneous isotropic decaying turbulence has been numerically evaluated for three different initial turbulence intensities, droplet diameters and overall equivalence ratios. The findings of the present study indicate that the size and number (global equivalence ratio) of droplets affect MIE in a complicated manner. The present study has found two key effects. A smaller initial droplet diameter or a higher initial global equivalence ratio, reduces the MIE requirement and is beneficial towards successful ignition and subsequent self-sustained propagation. The effects of increasing initial turbulence intensity have also been analysed and the MIE has been found to increase with increasing turbulence intensity but a significant increase of the MIE was observed for large turbulence intensities. Additionally, it was shown that the MIE required for droplet laden mixtures, is higher than the relevant MIE required for a corresponding homogeneous mixture, due to the extra energy required to evaporate the droplets.

194 - Increased Combustion Interactions of Closely Packed Diesel Droplets Caused by Soot Contamination

A. F. b. A. Rasid, S. Hanriot, Y. Zhang

The contamination process of interacting high carbon fuel droplet combustion was investigated experimentally for the first time. Diesel with high soot and bioethanol with low soot emission were used to demonstrate their differences in the combustion stability. Three horizontally arranged droplets were used and lower volatility fuel shown to have higher interaction effects. It was observed that strong interacting conditions of closely packed diesel droplet tends to be contaminated by soot released by its neighboring droplets. This reduced the lifetime of linear regressions of squared droplet diameter and transitioned it to disruptive phase that occupied up to 20% of its total lifetime. Strong puffing and atomisations were observed to be increased as the soot contaminated droplet interacts. Liquid-phase visualisation on the droplet shows earlier onset of disruptive behaviour, shifting all onset of puffing and atomisations earlier throughout the combustion. The agglomeration of soot particles on the surface of the droplet hinders the liquid phase diffusion from the center of the droplet to the surface thus reduced the evaporation rate. It was found that the contamination of soot during a group combustion of high carbon fuel droplet is possible which in turn highly destabilised the combustion phases. These insights are of significance for understanding the effect of droplet interaction, with various conditions of volatility and soot emission during combustion.

324 - Subcritical to Supercritical Transition of Fuel Mixtures in High Temperature and Pressure Environment

S. Chakraborty, L. Qiao

The study investigates the evaporation transition from subcritical to supercritical for alkane fuel mixtures using Molecular Dynamics (MD) simulations. This work emphasized on the ambient conditions required for the transition from classical two-phase evaporation to diffusion-controlled mixing supercritical evaporation for multi-component mixtures. The subcritical and supercritical evaporation characteristics were analyzed and compared for different mixtures with same or various mean molecular weights. The results show that at subcritical conditions, a distinct gas/liquid interface and surface tension exist throughout the entire evaporation process. Evaporation was first dominated by the lighter species and then heavier species. However under supercritical conditions, the gas/liquid interface disappears and surface tension vanishes at some point; the evaporation then becomes diffusion-dominated, one-phase mixing. Lighter and heavier species dominated the evaporation concurrently. The dissolution of nitrogen into fuel is significant. Mixture alkane fuels presented similar evaporation behaviors as the single component fuel with similar molecular weight. The pressure in the transition diagram at low temperature increases with the increasing of mixture mean molecular weight.

10:20 Explosion Safety 1

38 - Numerical Study on the Process of Fixed-axis Rotation of Object Under Action of Shock Waves

Q. Liu, J. Lei, J. Yin

When the explosions occur, the force is applied to the peripheral objects by the shock wave and causes the movement of objects. However, the object motion in flow field is a large-displacement transient process, in which the coupling problem between object motion and flow field is also considered. Even when the object being studied interacts with other objects, various constraints need to be considered. In this paper, the numerical study of fixed-axis rotation of object on the ground under action of shock waves is carried out. The weak coupling algorithm is used to solve the coupling problem between flow field and object motion, and the displacement constraint is applied to object to achieve the constraint between object and ground. The force and object motion at different height of gravity center and positive pressure time are analyzed, and the flow field around object is studied. The results show that the variation laws of rotation speed of object at different height of gravity center are consistent, and the laws under different positive pressure time have some similarities. It is also the case with aerodynamic forces of object along the direction of inflow and perpendicular to ground.

70 - Thermal Explosions in Alkenes Epoxidation Processes

G. Pio, E. Salzano

A significant number of petrochemical accidents are still ascribed to the thermal explosion (runaway reaction). Several criteria based on either simplified or detailed kinetic models can be adopted for the individuation of quick, safe and fair process conditions. Conditions relevant for ethylene oxide and propylene oxide production were analysed. It was found that detailed kinetic models have the potential to evaluate the generic reactivity of homogeneous mixtures in details and may include the heterogeneous/catalytic phenomena. The utilization of accurate kinetic models suitable for process conditions can lead to increased selectivity and reactor design optimization because of the simultaneous evaluation of safety aspects and products distributions.

209 - Effect of Gap Width on the Flame Propagation in a Millimeter-scale Closed Chamber

J. Huo, H. Su, L. Jiang

The laminar flame propagating behaviors are studied experimentally and numerically in a narrow closed disc-shape chamber of millimeter scale. The effect of gap width on the flame propagation velocity of premixed n-butane/air mixture is presented. The gap widths are varied from 2.0 mm to 5.0 mm in the experiment whose results show that the flame speed have a non-monotonic relation with the gap width of which the optimal value is 3.0 mm. Two-dimension transient numerical computations with consideration of conductive heat loss are carried out to clarify the mechanism. It is found that heat loss becomes dominant for the gaps narrower than 3.0 mm while flame staining has a significant effect for larger gaps. The flame propagation in millimeter-scale chamber is strongly influenced by the combined effect of them.

47 - Effect of Rock-Dust Height on Suppression of Coal-Dust Entrainment by Shock Waves

S. Lai, R. Houim, E. Oran

Simulations of a shock wave passing over two layers of dust containing rock and coal particles were performed to investigate the effect of applying a layer of rock dust on suppressing of coal-dust entrainment by shock waves. The simulations solve the Euler equations of fluid dynamics and granular flow, and accounts for different particle types using a binning approach. The rock-layer thickness of 1, 2, and 3 mm were considered, and the coal-dust layer underneath had a thickness of 4 mm. The results suggest that placing a 1-mm thick rock layer fails to suppress the coal particles from being lifted. With increased rock-layer thickness, the coal dust rises more slowly. A 3-mm thick of rock dust is needed to meet the 80% total incombustible content requirement.

8:30 1D Detonation Stability**342 - Nonlinear Stability of Square Wave Detonations and the Zaidel Paradox***A. Olmo-Velazquez, L. Bauwens*

Linear stability of square wave detonations was originally studied by Zaidel, resulting in a spectrum in which higher frequency modes are more unstable, which appears unphysical. Likewise, because the inverse Fourier transform does not exist for its spectrum, the stability initial value problem is ill-posed. It is proposed that the explanation for these observations is that the thin reaction zone in the square wave structure is subject to non-linear breakdown. For a mixture described as an ideal gas, the Riemann problem for boundary conditions matching the jump across thin reaction zone admits a second solution which is non-reactive, made up of two expansion waves moving in opposite directions, and obviously a contact surface separating unburnt and burnt fluid. For other gas models, it is conceivable that the breakdown solution, while still existing, might include a shock on the downstream side. The linear perturbation model of Zaidel is clearly unable to represent such a process, which entails changes at leading order, thus providing an explanation for it being ill-posed.

59 - Effect of Longitudinal Concentration Gradient on 1-D Double-Period Detonation*H. Wenhui*

The present work carried out simulations to study the propagation of a 1-D detonation in the media with periodical concentration gradient and to address the effects of longitudinal concentration gradient on a 1-D double-period detonation. It is found that the periodical and longitudinal gradient in terms of concentration disturbance will cause the propagation mode to change. The reestablished mode depends on the frequency of the gradient. As the frequency of gradient increases, the influence on the detonation behavior weakens and the front structure does not change significantly. It is found that the periodical gradient leads to the deficit of propagation velocity and the lower frequency leads to more deficit of detonation velocity

241 - One-dimensional stability analysis of vibrational nonequilibrium effect on detonation neutral stability*C. K. Uy, L. Shi, C. Y. Wen*

Single-step chemistry coupled with vibrational relaxation mechanism is considered in hydrogen-related detonation stability analysis. The present study aims to numerically investigate the shift of neutral stability range at the fixed activation energy under different time scale ratio of the chemical time scale to the vibrational time scale. Activation energy at mildly unstable state under thermal equilibrium assumption are selected in the present study. Cases at different time ratio are simulated and compared with the benchmark case at thermal equilibrium. Results show that with the decrease of the time ratio, corresponding to the case when vibrational relaxation effect is significant, the magnitude of ignition pulse increases. Moreover, the smaller amplitude and lower frequency of pulsation under smaller time ratio suggests that the detonation instability is suppressed under increasing vibrational nonequilibrium. Furthermore, the simulated temporal variation of peak pressure at time ratio of two shows decay in contrast with the other cases. This implies that a shift of neutral stability boundary to a higher activation energy value will take place when vibrational relaxation is substantial. The possible time ratio range for the shift is less than four and requires further investigation.

77 - Stability of non-adiabatic shocks*C. Huete, A. Cuadra, M. Vera*

Adiabatic steady shocks moving through a perfect gas have been proven stable against weak perturbations. As firstly predicted by D'yakov and Kontorovich, certain nonideal gases, can make the shock oscillate permanently in the so-called DK-regime. The present work reports that DK-instability can also occur in isolated steady shocks moving in perfect gases when non-adiabatic effects take place. In particular, the reactive shock may exhibit constant-amplitude oscillations in exothermic configurations when the amount of heat release is positively-correlated to the shock strength. The opposite highly-damped oscillating regime may occur in endothermic configurations. These scenarios may be representative of thermonuclear detonations, nuclear dissociating, ionizing and radiative shocks.

8:30 RDE 3**99 - Critical Height for Rotating Detonation Wave Based on the Modified ZND Model***L. Deng, M. Wang*

A modified ZND model is applied to determine the critical height of rotating detonation wave suffers from the lateral expansion. The predicted critical height is closely related to the reaction mechanism, however, the differences among the results are small. A critical height around 0.011 m is obtained with the stoichiometric H₂/Air mixtures at 1.0 bar and 293 K. It shows that the critical height decreases with the increase of initial temperature and pressure. The predicted critical height at equivalence ratio of 1.1 is least compared to other equivalence ratios. A non-dimensional parameter, the critical height over the cell width, is applied to evaluate the general critical height of RDW at different initial conditions. It shows that the ratio varies from 1.0 to 5.0 based on the initial conditions with an average value of 3.0, which is similar to the critical propagation of detonation in a yielding tube and the recently published experimental data of RDE. Thus, it is better to set the detonation height as 5 cell widths in the design of RDE.

125 - Numerical Investigation on Multi-Wave Propagation Mode of Rotating Detonation Waves*P. Yang, Z. Jiang, H. Teng*

Two-dimensional rotating detonation waves were simulated to investigate the wavelet pattern varying the inflow stagnation temperature, the initiation pattern and the heat release rate. Using the two-step induction-reaction model, we perform the generalizing dependences of rotating detonation wave number on some thermodynamic parameters and analyze the instability of multiple rotating wave. Two-dimensional rotating detonation waves were simulated to investigate the wavelet pattern varying the inflow stagnation temperature, the initiation pattern and the heat release rate. Using the two-step induction-reaction model, we perform the generalizing dependences of rotating detonation wave number on some thermodynamic parameters and analyze the instability of multiple rotating wave. By increasing the stagnation temperature T_t , it is found that there exists various forms of flow field, like single wave, double waves and treble waves. Besides, the flow structures are quasi-steady and the detonation wave height and intensity can keep one constant over time. However, an interesting distinct detonation phenomenon appears, which indicates the importance of coupling of flow and heat release on the instability of rotating detonation flow field. Decreasing k_R , the triple points of detonation surface weaken and disappear gradually, but the entire rotating detonation waves become more unstable than high k_R . To investigate the possibility of multi-pattern induced by initiation, three different ignition zone are chosen at different stagnation temperature. The present results show that, generally speaking, the greater ignition energy is more conducive to forming multiple rotating detonation waves.

46 - One Inducing Factor of the Operational Mode Transition in A Rotating Detonation Engine*Z. Lei, X. Yang, J. Ding, P. Weng*

A numerical study on the rotating detonation engine is presented to investigate the relationship between the number of detonation waves and the evolution process of the flow field. The simulations are based on the Reynolds-averaged Navier-Stokes equation with a detailed chemistry reaction model. For the given engine model, the unstable evolution of the flow field is observed when the number of detonation waves is one. New detonation waves are spontaneously formed and cause operational mode changes from single-wave mode to four-wave mode. When the number of detonation waves is two or three, the subsequent evolution of the flow field is quasi-steady. Under this condition, all existing detonation waves propagate stably, the number of detonation waves and the propagation direction of detonation waves are fixed. Further study reveals that the newly-formed detonation wave results from the acceleration of chemical reaction occurring on the contact face of detonation products and the reactive mixture. Based on the "requirements" detonation waves can propagate stably, the parameter so called "NL" is proposed. By comparing the value of NL and the number of detonation waves in the combustor, the evolution of the flow field can be predicted. If the number of detonation waves is equal or greater than NL, the subsequent evolution is quasi-steady. Otherwise, the subsequent evolution is unstable. This article may provide some help for operational mode control in rotating detonation engine experiments.

298 - Effects of isothermal wall boundary conditions on continuous detonation chamber

L. Zhang, K. Wu, J. Wang

The present study focuses on the effects of isothermal walls on a CDC, employing the Navier-Stokes equations with the one-step reactive chemical model. It is found that in the cases of isothermal walls of 600 K and 900 K, the heat flux peaks at the detonation wavefront and is about 6.0 MW/m² and 7.4 MW/m². The average peak heat flux is about 2.8 times of the average heat flux. The detonation wave undergoes a process of quenching, reinitiation, and stable propagation in the CDC with the isothermal walls of 900 K.

8:30 Chemical Kinetics 1

15 - Effect of Oxygen Atom Precursors Addition on LTC-affected Detonation in DME-O₂-CO₂ Mixtures

R. Mevel, Y. He

In the present work, in order to reduce the induction zone length and enable experimental observation or multi-dimensional numerical simulation of LTC-affected detonation, the effects of ozone (O₃) or nitrogen dioxide (NO₂) as oxygen atom precursors on the characteristic length-scales of LTC-affected detonation propagating in DME-O₂-CO₂ mixtures were investigated using ZND model. The effect of these two additives on the energy release dynamics and chemical kinetics have been also discussed in details. Ozone strengthens the LTC which induces a decrease of the induction zone length along with an increase of the energy release rate. The addition of NO₂ provides chemical pathways which induce a by-pass of the intermediate-temperature chemistry and a decrease of the separation distance between the first and the second steps of energy release. An increase of the ERR is also observed for the two first peaks. Ozone appears as a promising additive to experimentally observe LTC-affected detonation with multi-stage energy release.

325 - The Effects of Low Temperature Chemistry on DDT Transition in Microchannels through Ozone addition to DME

A. Rouso, W. Kong, Y. Ju, T. Chen, S. Liu

117 - Role of Low-Temperature Chemistry on the Onset of Detonation Behind an Incident Shock Wave

W. Han, R. Mevel, D. Ning, W. Liang, C. Law

The effect of low-temperature chemistry (LTC) on flame acceleration and detonation onset has been investigated using high-resolution one-dimensional unsteady numerical simulations performed with detailed chemistry. A stoichiometry propane-oxygen mixture diluted with 85% by mole of CO₂ was considered with initial pressure and temperature of 300 K and 507 kPa, respectively. For case 1, LTC was kept active in the reaction model, whereas for case 2, four LTC reactions were deactivated to by-pass the LTC oxidative pathways. The temperature, pressure and species mole fraction profiles were analyzed for both cases. In a physical space, the LTC induces a much faster ignition of the reactive mixture and transition to detonation occurs at a shorter time than without LTC. However, in a space normalized by the induction distance of the main ignition event, the onset of detonation is taking place after a shorter time. It is concluded that, in the specific case we have studied, the LTC does not generate conditions particularly favorable to flame acceleration and detonation onset. This is because, following the cool flame, a quasi-equilibrium is reached with weak chemical activity, which results in a weak temperature gradient. On the contrary, the induction zone for case 2 is characterized by a continuous chemical activity which results in a stronger temperature gradient and favors flame acceleration and detonation onset.

234 - Experimental and numerical study on fuel-NO_x formation in oxy-fuel processes in a jet stirred reactor

K. Wang, L. Pengfei

New experimental results on fuel-NO_x formation in oxy-fuel processes are obtained in a jet stirred reactor. In the present work, effects of CO₂ (0–97.4%), temperature (873–1323 K) and equivalence ratio (0.56–1.61) on fuel-NO_x in oxy-fuel processes are experimentally and numerically researched. NH₃ is selected as the N element source. The predicted results by the PG2018 mechanism (Progress in Energy and Combustion Science, 67, 31–68, 2018) are consistent with the experimental results. Compared with N₂ diluted conditions, CO₂ increases in diluents can reduce NO formation in fuel-lean conditions and HCN formation in fuel-rich conditions. Under fuel-lean conditions, the NO

formation path: $\text{NH}_3\text{-NH}_2\text{-HNO-NO}$ weakens with the increase of CO_2 concentrations. Under the fuel-rich conditions, HCN is abundantly produced and reduced with the increase of CO_2 . Moreover, the N_2O formation is basically insensitive to the CO_2 concentration.

8:30 Laminar Flames 1

254 - Comparative study of laminar burning velocity measurement between confined and unconfined spherical flames methods for methane/air and n-decane/air premixed flames

R. L. Dortz, C. Strozzi, J. Sotton, M. Bellenoue

Laminar burning velocity (LBV) is a fundamental parameter needed to characterize the combustion process and the behavior of a premixed flame. Different methodologies have been developed to estimate this parameter from a spherical constant-volume combustion chamber. This study focuses more specifically on the comparison between confined (3 different techniques) and unconfined (2 different techniques) methodologies. These methodologies are respectively based on the pressure-time evolution and on the optical visualization of the flame front during combustion process. Two mixtures are tested here over a large panel of equivalence ratios (between 0.6 and 1.6): methane/air at normal temperature and pressure conditions, and n-decane/air at initial temperature $T_0 = 400\text{ K}$ and initial pressure $P_0 = 0.1\text{ MPa}$. In main cases, deviations of LBV can be noted between unconfined and confined methodologies. There is no important differences between the techniques of unconfined methodology. Also, one technique from confined methodology is able to reproduce results from unconfined methodology.

10 - Measurements of Laminar Burning Velocity in a Shock Tube

A. Susa, D. Davidson, R. Hanson, A. Ferris

The speed at which a laminar flame consumes an unburned, flammable mixture represents one of the most important quantities in combustion science. Premixed flames appear in many of the combustion systems upon which society relies. One ubiquitous occurrence of these flames is in spark ignition (SI) engines, where an understanding of flame propagation at elevated temperatures is critical not only for maximizing performance, but also for preventing inadvertent, abnormal effects such as engine knock. Due to difficulties in preparing flammable mixtures at elevated-temperature conditions in traditional, static-bomb flame speed experiments, very little flame speed data exists at engine-relevant temperatures. Here, we present the first measurements of laminar burning velocities (u_0) of n-heptane and iso-octane at engine-relevant, negative temperature coefficient (NTC) regime temperatures using high-speed imaging in a shock tube. The findings provide direct experimental evidence to support the presence of an NTC regime in the laminar burning velocities of flames propagating at temperatures associated with NTC behavior in ignition delay times, as had been predicted through direct numerical simulations (DNS). These findings highlight the value of continued study of high-temperature flame phenomena, both through the application of novel experimental methods and the DNS methods established in the literature.

332 - Laminar Flame Speed Measurements from Chemiluminescence of OH^* and CH^* in Spherically Expanding CH_4 -Air Flames

M. Turner, T. Paschal, P. Parajuli, W. Kulatilaka, E. Petersen

An experimental study of laminar flame speed of spherically expanding methane-air flames measured from chemiluminescence of OH^* at 306 nm and of CH^* at 430 nm is presented for the first time. Chemiluminescence of intermediate radicals is indicative of the high-temperature reaction zone of the flame, and can be used to measure laminar flame speed in a similar fashion to the widely used schlieren imaging technique. Flame speeds for one atmosphere and room temperature methane-air flames were measured for equivalence ratios of 0.7 to 1.3 in increments of 0.1. There was no significant difference between flame speeds measured from different wavelengths of chemiluminescence. The averaged flame speed measurements ranged from 15.7 cm/s at $\phi = 0.7$ to 36.7 cm/s at $\phi = 1.1$. The new data are in good agreement with spherically expanding flame data from the literature, indicating that chemiluminescence can be used to extract accurate laminar flame speed measurements from spherically expanding flames.

169 - Thermoacoustic analysis of lean H_2 -air premixed flames in thin layers

F. Veiga-Lopez, D. Martínez-Ruiz, M. Sánchez-Sánchez, M. Kuznetsov

An experimental study of lean hydrogen-air premixed flames propagating in a confined combustion chamber is presented in this paper. The combustion chamber has a rectangular prismatic shape of 900 x 200 x 10 mm (length x width x thickness). The thickness of the channel can be varied from 10 to 4 mm in order to study the effect of this parameter on the flame propagation. The hydrogen flames travel vertically from the top of the chamber, which is open to the ambient, to its closed bottom. First, the dependency on the mixture equivalence ratio is analyzed by keeping a constant thickness (10 mm) of the combustion chamber. Two main regimes are found for the range of lean hydrogen-air mixtures analyzed (9.5% to 15% in volume of hydrogen). For mixtures up to 13% of hydrogen, the flame propagates with a violent oscillatory motion of a frequency around 85 Hz, driven by the acoustic pressure waves present in the chamber.

8:30 Explosion Safety 2

221 - Numerical study of the influence of gas expansion on the acceleration of outwardly expanding flames

R. Feng, R. Zhang, D. Valiev

The role of Darrieus-Landau instability in wrinkling the initially smooth freely propagating expanding flame front has been studied by solving the two-dimensional Navier-Stokes equations with one step irreversible Arrhenius reaction. Numerical simulation of the radially expanding flames indicates a power law temporal dependence of mean radius after a certain critical time instant. Influence of gas expansion ratio on power-law exponent and flame surface dimension is the focus of this research. It is shown that the expansion coefficient has a considerable effect on fractalization behavior of the flame, confirming the assumption that fractal dimension is not a universal parameter.

52 - Influence of Wall Boundary Condition on the Dynamics of Premixed Flames Propagating in a Closed Channel

X. Li, H. Xiao, J. Sun

Understanding the dynamics of unsteady flames propagating in confined regions is important for explosion safety and combustion applications. This paper presents simulations of flame dynamics in a tube under three different types of wall boundary conditions: adiabatic free-slip wall, adiabatic no-slip wall and isothermal wall. Two-dimensional reactive Navier-Stokes equations are solved with high-order algorithms and adaptive mesh refinement (AMR). The objective of this work is to interpret the effect of wall boundary condition on the formation and evolution of distorted tulip flame. The result shows that wall boundary condition has an important influence on the properties of pressure waves and the flame dynamics in the later stages. The significant effect of wall boundary condition on the strength of pressure waves generated and oscillating flame behavior provides further evidence of the importance of pressure waves on the dynamics of distorted tulip flame. Details of generation and characteristics of pressure waves and their interactions with flame front will be described in the presentation.

350 - Understanding How Mixture Composition Affects Flame-Acoustic Interactions in Large-Scale Vented Explosions

C. R. Bauwens, L. Boeck, S. Dorofeev

In this study, previously obtained experimental pressure data was analyzed to determine the frequencies that develop during vented explosions over a range of fuels and equivalence ratios for two test geometries. Two primary classes of acoustics were observed: lower frequency standing waves that traverse the entire enclosure, and high-frequency acoustics created by local interactions between the enclosure and the flame. It was found that rich propane-air explosions generated strong high-frequency acoustics that increased with equivalence ratio. A similar trend was observed for methane-air mixtures; the resulting acoustics, however, were much weaker for all frequencies, and only increased slightly with concentration. For hydrogen-air mixtures, the acoustics generated were strongly biased toward higher frequencies, and minimal low-frequency response was observed. In a closed vessel, rich propane-air mixtures were found to generate strong high-frequency oscillations, while venting introduced a wide range of lower frequency acoustics. These results demonstrate how different mixtures can present significantly different trends for the variation of frequency response with equivalence ratio for the same enclosure and can be used in future studies to gain insight into when flame-acoustic interactions must be considered in real-world scenarios.

343 - Numerical Investigation of Venting Through Roof for an ISO Containers*J. Wen, V. C. M. Rao*

In the present study, turbulent deflagration in premixed hydrogen-air cloud enclosed in a 20-foot container of 20 x 8 x 8.6 are investigated numerically. Numerical simulations have been performed using HyFOAM, a dedicated solver developed in-house for vented hydrogen deflagration processes within the framework of the opensource computational fluid dynamics (CFD) code OpenFOAM toolbox. The flame area wrinkling combustion model is used for modelling turbulent deflagrations. Additional sub-models have been added to account for lean combustion of hydrogen-air mixtures. The numerical predictions are performed for venting through roof scenario. Overpressures for venting through roof are also validated against the available recent experiments carried out by Gexcon as part of the HySEA project supported by the Fuel Cells and Hydrogen 2 Joint Undertaking (FCH 2 JU) under the Horizon 2020 Framework Programme for Research and Innovation. The numerical simulations are performed to establish the modelling approach. Further aid in filling the experimental knowledge gaps and the effects of congestion within the containers on the generated overpressures are also investigated.

10:40 DDT**274 - Gradient mechanism on the onset of detonation in the deflagration to detonation transition***X. Tang, E. Dzieminska, K. Hayashi, N. Tsuboi*

The onset of detonation, which is one of the central roles in deflagration to detonation transition (DDT), has been explained by the gradient mechanism of reactivity suggested by Meyer, Oppenheim, Zeldovich and Lee. In this work, to discuss the gradient mechanism of reactivity on the onset of detonation, the reactive flow in narrow tubes filled with hydrogen-oxygen mixture are numerically solved by the 2D fully compressive Navier-Stokes equation with 9 species. Adaptive mesh refinement (AMR) method is employed together with a detailed chemical reaction model. Briefly two kinds of autoignition arise in the tube which are the mild and strong ignitions reported in Oppenheim's experiments. The spatial gradient of induction time τ for the first autoignition which is in the boundary layer is not small enough. The spontaneous reaction wave propagates through the mixture but it cannot catch up with the shock. Therefore the onset of detonation cannot be triggered this time, while the second autoignition occurs with quite small spatial τ gradient. This time the spontaneous reaction wave can propagate at a high velocity along the spatial τ gradient valley. The high reaction wave velocity allows the reaction wave to catch up with the shock wave. In this mechanism a coherent coupling of the traveling shock wave with the chemical energy release is achieved and the onset of detonation is triggered. Afterwards this local detonation leads to the DDT in the tube. With analysis on the reactive flow, especially on these two different types of autoignition, the gradient mechanism is substantiated and more details are embodied. Moreover, the critical condition that an active hot spot requires is surfaced.

322 - Role of gasdynamic wave fluctuations in shock induced ignition and transition to detonation: the hotspot cascade mechanism*W. Wang, J. McDonald, M. Radulescu*

We address the problem of shock-induced ignition in the presence of mechanical fluctuations. We study the influence of these perturbations on the transition to detonation. The problem is studied in one dimension. The magnitude and frequency of the perturbations behind the leading shock are driven by an oscillating piston. We numerically integrate the 1D non-steady problem using an in-house code coupling the Lagrangian gasdynamic evolution with the chemical evolution calculated for full chemistry. The calculations focused on the hydrogen-oxygen system close to the weak-strong ignition boundary. Different ignition behavior were observed at different magnitudes of forcing frequencies. For perturbations periods longer the nominal ignition delay time, the classical ideal strong ignition behavior was recovered. When the perturbation period was intermediate between the induction and much shorter reaction time, a series of hotspots were created. Two enhancing mechanisms were observed. The first mechanism of hotspot creation and generation of subsequent hotspots was from the interaction of the pressures waves emitted by a first hotspot to the lead shock, resulting in a cascade of hotspots. The second mechanism was the enhancement of compression waves travelling through a series of hotspots in phase with its motion.

121 - On the Gasdynamic Mechanisms of Reaction Wave Development in Shock Tube

A. Kiverin, I. Yakovenko

The paper studies the process of ignition and detonation onset behind the shock wave propagating through the channel filled with reactive gaseous mixture. On the base of numerical analysis it is shown that the origins of ignition events behind the shock waves in channels and tubes are related to the gasdynamical behavior of the compressed test mixture. In particular, an important role belongs to the roller vortices formed already on the linear stage of boundary layer development. The most probable position of first ignition kernel is the intersection of contact surface and boundary layer where locally higher values of temperature and reaction progress are achieved. The ignition develops in the form of spontaneous combustion wave with maximal initial speed equal to the shock wave speed relative the moving compressed gas. Since this value is subsonic the spontaneous wave forms the unstable complex consisting of combustion wave behind the outrunning compression wave. In such conditions the combustion wave accelerates finally forming the detonation. In case of mixtures diluted with monomolecular gas the boundary layer on the developed stage occurs to be rather thin that determines almost continuous process of detonation formation. In case of gas consisting of larger amount of molecules the boundary layer is thicker that determines discrete manner of spontaneous wave propagation in the form of spatially separated kernels.

381 - Characterization of a narrow channel to study flame propagation and DDT

Y. Ballossier, J. Melguizo-Gavilanes, F. Virost

Stoichiometric H₂-Air flame propagation experiments are conducted using a 10 x 10 mm square cross-section channel of 449 mm in length. The effect of ignition source and the presence of a dead volume behind the electrodes on flame propagation is assessed using direct observation of the visible light emitted by the front. Using schlieren at the end of the channel, the effect of flame-acoustic interactions induced by the accelerating flame are characterized. Results show that the number of arcs present in the ignition source have a negligible impact on the overall evolution within the range of electric energy tested, whereas the presence of a dead volume has a noticeable effect. The puffs at the channel exit result in an inflow of air that changes the mixture composition which sometimes leads to flame quenching. Future work will include extending the range of conditions (i.e. less diluted H₂-Air mixtures), as well as a thorough analysis of the front evolution, its acceleration and characterization of the observed oscillations through improved visualization of the flame evolution inside the channel.

10:40 RDE4

12 - Detonation combustion of a hydrogen-oxygen gas mixture in a plane-radial chamber with exhaustion toward the periphery

F. Bykovskii, S. Zhdan, E. Vedernikov, A. Samsonov, E. Popov

Regimes of continuous spin detonation of a hydrogen-oxygen mixture were obtained in a plane-radial combustor with an inner diameter of 100 mm and exhaustion toward the periphery including in the oxygen ejection mode. Upon the forced flow of oxygen first discovered the continuous multifront detonation. The structure of detonation waves was considered. For continuous spin detonation, the transverse detonation waves and the flow in the vicinity of these waves in the PRC plane were reconstructed. It was demonstrated that the detonation wave is significantly curved owing to the increase in the tangential component of velocity along the combustor radius. It was found that the scale effect is manifested only in terms of the number of rotating waves. However, the velocity of these waves increases with an increase in the PRC size because of the smaller influence of centrifugal forces acting on the products and reducing the pressure behind the detonation front. The mechanism of oxygen absorption in the mode of its ejection is revealed.

293 - Numerical Study of Counter-rotating Waves in Hollow Rotating Detonation Chamber

X. Liu, Y. Chen, Z. Xia, J. Wang

The continuous detonation chamber (CDC) is a concept engine chamber using detonation as power source. Experimental researches have been done widely around the world by Wolanski et al. [1], Rankin et al. [2] and Bykovskii et al. [3]. Numerical simulations of CDC with annular chamber were performed by Shao et al. [4], Schwer et al. [5] and Frolov et al. [6]. To resolve the problem of overheating of the inner cylinder in co-axial annular combustor model, a new model with hollow combustor was proposed by Tang et al. [7]. Various number of detonation fronts was observed under different fuel injection area ratios. To get closer to experimental conditions, Yao's simulation [8] used array-hole injection model which was close to actual injection structure. Multiple detonation fronts

were observed in his simulation which was consistent with the multi-head experimental results. This paper adopts the model of injection via array-hole in 3D numerical simulations of CDC with hollow combustor using the premixed stoichiometric hydrogen-air mixture. The calculation is based on the Euler equations coupled with a one-step Arrhenius chemistry model. The array-hole injection method is more practical than previous conventional simulations where ideal full-area injection model is used. Counter-rotating waves exist in flow field which are composed of obverse-rotating wave (ORW) propagating clockwise and reverse-rotating wave (RRW) propagating anticlockwise. Wave collision mode of these counter-rotating waves are investigated in this paper.

157 - The effect of Cavity Location on Continuous Rotating Detonation Wave fueled by ethylene-air

H. Peng, W. Liu, S. Liu, H. Zhang

Designed for flame stabilization, an annular combustor with the cavity in the inner cylinder is proposed. Ethylene-air CRD has been achieved in the annular combustor with cavity. The flame stabilization in the cavity is a key factor contributing to the ethylene-air CRD wave propagation. For $LC = 0$ or 20 mm, ethylene-air CRD waves propagate as two-waves in homo-rotating mode with larger operating range and higher outlet pressure. When ER is 1.02 and $LC = 20$ mm, the propagation velocity of CRD wave is 1234.81 m/s accounting for 67.5% of corresponding CJ velocity. For $LC = 40$ or 60 mm, CRD waves propagate as two-waves in hetero-rotating mode with smaller operating range and lower outlet pressure. Through analysis from the high-speed photography images, the flame luminance in re-circulation zone gradually decreases with the cavity moving downstream.

318 - Rotating Detonation in Annular Gap

V. Levin, I. Manuylovich, V. V. Markov

The problem of a three-dimensional nonstationary flow with a rotating detonation wave arising in the annular gap of an axisymmetric device between two parallel planes perpendicular to its axis of symmetry is investigated. It is assumed that a homogeneous combustible propane-air mixture, resting in a reservoir with predetermined braking parameters, enters the annular gap through its outer cylindrical surface towards the axis of symmetry and its parameters are determined by the pressure in the reservoir and the static pressure in the gap. The detonation products flow out of the gap into space, bounded on one side by an impenetrable wall—the continuation of the side of the gap. Through the hole in the other side of the gap and the conical exit section with the half-angle 45 degrees, the gas flows out of the device into the outer space.

10:40 Chemical Kinetics 2

81 - REDIM simplified chemistry for the simulation of counter-flow diffusion flames with oscillating strain rates

C. Yu, F. Minuzzi, U. Maas

In many practical combustion devices such as gas turbines and internal combustion engines, combustion always occurs under transient conditions. Over the last decades, many efforts have been made to investigate the transient behavior of flames. Among these investigations is the transient behavior under harmonic time-dependent strain rates. In this work, the Reaction-Diffusion Manifolds (REDIM) reduction method, is applied to simplify the chemical kinetics. In this method, the dynamics of system is constrained to a low-dimensional attracting slow manifold in the composition space. We investigate the applicability of REDIM reduced chemistry to counter-flow diffusion flames with oscillating strain rates, showing that REDIM reduced chemistry can indeed represent the response of flames to oscillating strain rates.

259 - Network community detection based combustion reaction mechanism coarse graining method

L. Ji, J. Gao

A brand-new network community detection based coarse-graining representation method for combustion reaction mechanism is proposed. The detailed kinetic mechanism was first translated into a complex weighted network, whose nodes are reactants and edge weights integrate dynamic information. Then, community structures were found by the Louvain network unfolding algorithm. The grouping information obtained in H₂ explosion system agrees well with previous detailed mechanism and kinetic investigations under a variety of conditions, which suggests that the proposed

method is feasible for coarse-graining the combustion mechanism. Under our framework, it is also possible to extract the non-equilibrium characteristics by describing the reaction with entropy growth rate, thermal dissipation rate and other thermodynamic parameters. The network constructed by the time-dependent unsteady reaction flow may be useful for the investigation of turbulent combustion. Besides, the hierarchy exploration function of the Louvain algorithm allows users to employ suboptimal partitions under the different resolutions, thus making it possible to achieve desirable multi-scale expression.

202 - CO₂ effects on NO reburning by methane in a jet-stirred reactor: Experiments and modeling

L. Wenhao, L. Pengfei

New experimental results on the NO reduction by CH₄ in both N₂ and CO₂ atmospheres are obtained in a jet-stirred reactor. Experiments are conducted in the temperature range of 600 - 1323 K at 1 atm. The experiments are simulated using an updated reaction mechanism and the simulations are highly consistent with the experiments. The NO-reburning in the CO₂ atmosphere is reduced by 40% - 60%, relative to that in the N₂ atmosphere. The inhibition of methane oxidation under high CO₂ concentrations is responsible for the decrease of the NO reduction efficiency. The main reaction pathways of the NO reduction in the N₂ atmosphere are: NO (HCNO) HCN NCO N₂ and NO HNCO NH₂ NNH N₂, while the primary path in the CO₂ atmosphere is: NO (H₂CN) HCN CH₃CN NCO N₂ due to the chemical effect of CO₂.

380 - A Comprehensive Chemical Kinetic Model of 2,6,10-trimethyl Dodecane

X. Gou, Y. Yu

As a promising renewable fuel, 2,6,10-trimethyldodecane has received extensive attention. In order to deeply understand the combustion process of this fuel, a detailed chemical reaction mechanism for 2,6,10-trimethyl dodecane has been developed by using the reaction class method. The verification results of the detailed reaction mechanism on the ignition delay time show that the addition of the new reaction path can improve the prediction accuracy on the low temperature region. At the same time, the concentration of important components of the flow reactor and the velocity of laminar flame propagation were also verified. The good agreement between the simulated values and the experimental values proves the validity of the chemical reaction mechanism construction process. It brings an opportunity to study the reaction flow process by simulation.

10:40 Laminar Flames 2

224 - Effect of Hydrogen Addition on Burning Velocity of LPG-Air Mixtures at Elevated Temperatures

J. Ev, R. K. Velmati

The present work reports the investigations on the effect of hydrogen addition in the laminar burning velocity (LBV) of LPG-air mixture at elevated temperatures. The experimental measurement of LBV (Su) is performed using a diverging channel in which planar flame stabilizes. The burning velocities were measured for 20% and 40 % hydrogen addition on the pure LPG-air mixture, for various equivalence ratios, ranging from 0.7 to 1.3. Using the present experimental setup, LBV was measured up to an elevated temperature 450 K of the unburnt gas mixture. The present work reports the investigations on the effect of hydrogen addition in the laminar burning velocity (LBV) of LPG-air mixture at elevated temperatures. The experimental measurement of LBV (Su) is performed using a diverging channel in which planar flame stabilizes. The burning velocities were measured for 20% and 40 % hydrogen addition on the pure LPG-air mixture, for various equivalence ratios, ranging from 0.7 to 1.3. Using the present experimental setup, LBV was measured up to an elevated temperature 450 K of the unburnt gas mixture.

368 - Experimental n-Hexane-Air Expanding Spherical Flames

S. Coronel, R. Mevel, N. Chaumeix, J. E. Shepherd, S. Lapointe

The effects of initial pressure and temperature on the laminar burning speed of n-hexane-air mixtures were investigated experimentally and numerically. The spherically expanding flame technique with a nonlinear extrapolation procedure was employed to measure the laminar burning speed at atmospheric and sub-atmospheric pressures and at nominal temperatures ranging from 296 to 422 K. The results indicated that the laminar burning speed increases as pressure decreases and as temperature increases.

The predictions of three reaction models taken from the literature were compared with the experimental results from the present study and previous data for n-hexane-air mixtures. Based on a quantitative analysis of the model performances, it was found that the most appropriate model to use for predicting laminar flame properties of n-hexane-air mixtures is JetSurF.

236 - Laminar Burning Velocities of Methane-Air Mixtures at Elevated Pressures and Elevated Temperatures

R. Varghese, H. Kolekar, B. Aravind, S. Kumar

Extensive research is carried out on the evaluation of the high-pressure dependence of laminar burning velocity, but studies on the combined effect of elevated pressures and temperatures are limited. Preheated diverging channel method, a potential approach which determines laminar burning velocities at elevated temperatures has been extended to elevated pressures. The laminar burning velocity of methane-air mixtures at 2 atm and elevated temperatures (300 - 650 K) are presented for a range of equivalence ratio ($\phi = 0.7 - 1.4$). There is an excellent agreement with the present results and comparisons with numerical simulations and few literature sources available. Temperature exponents are calculated from the measured burning velocities, and the comparison with GRI 3.0 is presented. Flame structure of major species and temperatures in the reaction zone are also presented. A slight increase in the adiabatic flame temperature at stoichiometric mixtures of 2 atm deserves an exhaustive study of molecular properties for a reasonable explanation.

371 - Stabilization of Laminar Hydrocarbon Jet Diffusion Flames in Earth's and Micro-gravity

L. Smith, D. Souza, F. Takahashi

Liftoff and blowout stability limits of laminar jet diffusion flames have been studied further in Earth's gravity (1g) and compared with the data obtained in microgravity (mg) previously within the Microgravity Science Glovebox aboard the International Space Station. The fuels used include C1 - C4 gaseous hydrocarbons (methane, ethane, ethene, propane, butane, and 1-butene) and selected fuels diluted with nitrogen (70 % methane and 20 % ethene). The fuel issues from a fuel tube with an inner diameter between 0.4 mm and 3.2 mm into a co-flowing air duct (76 mm * 76 mm square cross-section) with the mean air velocity between 10 cm/s and 70 cm/s. The fuel jet is ignited at low fuel and air velocities to form a stable burner rim-attached flame. The fuel or air velocity is gradually increased until the flame lifts off the burner rim and then blows out. The dynamic flame lifting phenomena are recorded with color video and digital still cameras. The critical liftoff/blowout jet velocities are, in general, larger in mg than in 1g. The gravity effect decreases for fuels with high critical fuel and air velocities (e.g., ethene). For the lighter-than-air fuel (methane), there seems to be an additional gravity effect. For small fuel jet diameters, a rapid dilution of the fuel by air seems to reduce the critical jet velocity at the stability limit. For the fuel with nitrogen dilution, the lower reaction rates also result in lower flame stability. On the other hand, higher reaction rate fuels (alkenes alkanes) have the higher stability limits. This work was supported by the NASA Space Life and Physical Sciences Research and Applications Division (SLPSRA).

10:40 Explosion Safety 3

190 - Effect of Venting on Flame-Acoustic Instability in Large-Scale Propane-Air Explosions

L. Boeck, C. R. Bauwens, S. Dorofeev

Explosion venting is a passive method to protect an enclosure by reducing the overpressure related to confined accidental explosions. Vented gas explosions can exhibit multiple pressure peaks, each of which depends on several factors, such as the enclosure geometry, obstructions, reactive mixture, and characteristics of the vent itself, such as vent size, geometry, and deployment dynamics. Predicting the magnitudes of these peaks is critical for the determination of the required vent size. In addition to the pressure peaks related to vent deployment, external explosion, and maximum flame surface area, it has been shown that also flame-acoustic instability can generate a pressure peak which typically appears near burn-out. The present experimental study contributes to the understanding of flame-acoustic instabilities in large-scale explosions. Experiments were performed in an 8-m³ vessel with propane-air mixtures, both for closed-vessel and vented configurations. The effects of venting and mixture composition on the development of flame-acoustic instability and mean explosion parameters are characterized, and the mechanisms that trigger the onset of instability are identified. The experiments reveal distinct effects of venting on the development of flame-acoustic instability: In a closed vessel, flame-acoustic instability only occurs for rich propane-air mixtures. With venting,

however, lean mixtures also exhibit instability. The magnitude of acoustic pressure depends strongly on the measurement location in the vessel. Peak rates of pressure rise are consistently higher in vented explosions, compared to closed-vessel explosions, and venting leads to earlier burn-out. In a closed vessel, flame-wall interactions trigger instability, whereas onset of instability in vented explosions without vent panels was related to flame-exit from the vent and the external explosion.

3 - Effect of initial temperature and temperature gradient on H₂/Air flame propagation in confined area

R. Grosseuvres, A. Bentaïb, N. Chaumeix

During severe accident in Pressurized Water Reactor (PWR), the interaction between the fuel rod and steam leads to the build-up of an explosive atmosphere inside the containment building [1]. This atmosphere is mainly composed of hydrogen, oxygen, nitrogen and water vapor. A gradient of both temperature and hydrogen concentration is usually generated from the primary circuit leak to the top part of the containment building. In case of an ignition by an energy source (electrical discharge spark, hot surface, etc.), a flame occurs and is capable to threaten the containment building. The flame propagation in such environment depends on geometrical configuration, turbulence level and initial mixture composition. The evaluation of the pressure loads which can be damaging are evaluated by using combustion models implemented in CFD and LP codes. These models have to be faced with reliable experiments. This paper aim is to present new data on H₂/Air flame propagation in a new facility through homogeneous and heterogeneous conditions of temperature and hydrogen concentration. The experimental work has been conducted over conditions relevant to severe accident in PWR: hydrogen molar fraction from 8 to 15, homogeneous initial temperature (298, 363, 413 K) and gradient of temperature (from 363 to 298K and from 298 to 363K).

358 - Structural response of 20-foot shipping containers during vented hydrogen deflagrations

T. Skjold, H. Hisken, L. Bernard, A. G. Hanssen

It is common practice to install equipment for hydrogen energy applications in shipping containers. Fires and explosions represent a significant hazard for such installations, and specific measures are generally required for reducing the risk to a tolerable level. Explosion venting is often used for mitigating the consequences of hydrogen deflagrations in confined systems. Whereas empirical correlations for the design of explosion venting systems in international standards focus on the maximum reduced explosion pressure, it is equally important to consider the structural response and integrity of the enclosure. The dynamic response of the structure is particularly relevant for relatively weak structures, such as buildings and shipping containers. Pressure-impulse (PI) diagrams are often used for assessing the damage of structural components. This paper presents results from structural response measurements conducted for a series of vented deflagration experiments in 20-foot shipping containers, and describes the construction of a P-I diagram for the structural response of 20-foot shipping containers subjected to internal pressure loads from vented hydrogen deflagrations. Although there is significant uncertainty associated with the results, most of the available data points fall within well-defined areas in the diagram.

18 - Contribution of combustion to the blast wave strength after high-pressure hydrogen tank rupture in a fire

V. Molkov, D. Cirrone, V. Shentsov, W. Dery, D. Makarov

Fuel cell vehicles store hydrogen onboard at pressure either 70 MPa (bikes, cars and trucks) or 35 MPa (buses). Tank volume is 10-140 litres. More than 1/3 of CNG car tank ruptures in a fire are due to pressure relief device failure. The quantitative risk assessment of hydrogen onboard storage [1] has demonstrated that the acceptable level of risk 10⁻⁵ fatalities/vehicle/year can be achieved if storage tank has fire resistance rating above 47 min. This is based on the non-zero probability of thermally activated pressure relief device (TPRD) failure. The consequences of tank rupture in a fire are blast wave, fireball, projectiles. To underpin hydrogen safety engineering the underlying physical phenomena should be understood first. The aim of this study is to understand if there is a contribution of combustion into the blast wave strength.

13:50 Flame Acceleration & DDT 1

71 - High-speed imaging of DDT in a round tube

P. Krivosheyev, O. Penyazkov, A. Sakalou

To date there is no unambiguous understanding of the deflagration to detonation transition (DDT) event. In particular, the question remains about the structure and shape of the flame, the reasons for its acceleration and the conditions and place of the onset of detonation sites. In this investigation we used high-speed (210 000 fps) visualization to study final stage of fast flame propagation and onset of explosion under DDT process in a smooth transparent long tube. It was shown that the flame shape similar to the cone (or a bell) which is strongly extended along a tube axis. The base of such cone has an irregular shape, is also deformed and elongated along the tube axis. The length of the flame front cone reaches 3-4tube diameters. It was found that explosion mainly occurs in the gas layer in the vicinity of the tube walls. Analysis of the data obtained showed that for studied mixtures (acetylene/oxygen with 50% argon or nitrogen dilution) only in 14% of cases the explosion occurred directly at the flame front. In 86% of cases ignition first occurred in front of the main flame, and only then one or several explosions occur leading to the formation of a detonation wave.

252 - Hot spots formation at DDT in cylindrical tube

Y. Baranyshyn, P. Krivosheev, O. Penyazkov, K. Sevrouk

There is still no complete theory that can clearly describe the observed experimental data on deflagration to detonation transitions (DDT) in gases and accurately predict its behavior at certain conditions. That is why experimental studies of DDT are still actually. Furthermore, DDT is very complex and unsteady phenomenon, which is sensitive to local interplay between gasdynamics and chemical reactions at different flow and boundary conditions. The study of hot spot occurrence and distance of induction zone at deflagration to detonation transition in gases is important fundamental and practical problem. Understanding and accurate description of this complex gasdynamics and chemical reactions process can help to predict onset of detonation in specific conditions and its application in detonation propulsion systems. This work is a continuation of our experimental study of DDT in smooth-walled cylindrical tube at low energy ignition mode. We carried out high speed video observations of self-luminescence at DDT in stoichiometric C₂H₂CO₂ mixture with Ar and N₂ dilution and induction time study in shock tube for close initial conditions. This allowed us to estimate the observed local temperature for hot spots formation at DDT in studied mixtures and compare it with ideal values calculated for experimental post-shock conditions.

135 - Deflagration-to-Detonation Transition in Laser-Ignited Explosive Gas Contained in a Smooth-Wall Tube

T. Endo, W. Kim, T. Johzaki, K. Okada, S. Kuwajima, D. Shimokuri, A. Miyoshi, S. Namba

Explosive gas: 0. 87[(1/4)C₂H₄+(3/4)O₂]+0. 13N₂ was ignited by 1064-nm 12-ns laser at 8 or 88. 8 mm from the closed tube end connected to the gas-feeding pipe, where the incident laser energy was varied as 40, 80, and 120 mJ. When the gas was ignited at 8 mm from the tube end, although laser ignition promoted DDT, it was not significant. This is because the scenario of DDT was essentially the same as the typical one. When the gas was ignited at 88. 8 mm from the tube end, two scenarios of DDT were observed. The first scenario was the typical one. In the second scenario, the detonation onset was induced in the abnormally early phase by a shock wave following the flame front. Significant DDT promotion was realized in the second scenario by the laser ignition with larger energy. The shock wave inducing the detonation onset was probably created by the end-gas autoignition near the tube end or inside the gas-feeding pipe. As a result of the analysis on the shock wave, the mixing of the unburned and burned gases induced by Richtmyer-Meshkov instability at the flame front is the most plausible mechanism for initiating micro-explosions inducing the detonation onset.

13:50 RDE 5

5 - Dynamic Mode Decomposition Analysis of Rotating Detonation Waves

R. Bluemner, M. D. Bohon, C. O. Paschereit, E. Gutmark

Rotating Detonation Combustors (RDCs) have been shown to be able to stabilize a variety of steady operating modes with multiple co- or counter-rotating waves, and longitudinal waves. These wave patterns were observed to lead to complex pressure fluctuations in the combustor annulus, which makes the detailed analysis of these modes challenging. In previous studies, high-speed aft end videos were used to determine the wave mode based on simple visual analysis. However, in complex situations, the data contained in the video by visual inspection alone has difficulty to explain the pressure spectra obtained in the RDC annulus. Towards this goal, the Dynamic Mode Decomposition (DMD) technique was applied to these videos to extract the dominant dynamic behavior captured in

the sequence. Three different global operating modes with different numbers of counter-rotating waves were analyzed. The DMD modes confirmed the existence of a variety of superposition modes as a result of wave interaction, the existence of a longitudinal wave mode driven by the combustor length, and the dependence on the relative strengths of two intersecting waves. The DMD analysis has proven to be a valuable tool to analyze RDC operation.

333 - Effect of Secondary Waves on Rotating Detonation Combustor Properties

F. Chacon, M. Gamba

Rotating Detonation Engine flows have been observed to contain secondary waves travelling in the annulus both in this work and in previous studies for a variety of injection schemes and operating conditions. The source of these secondary waves are not currently known. However their presence has been associated with a measurable impact on detonation properties in particular reduced detonation speed and increased pressure oscillations.

284 - Mode Switching in 2-Dimensional Continuous Detonation Chambers with Discrete Injectors

Y. Chen, X. Liu, J. Wang

In this paper, numerical simulations for Continuous Detonation Chambers (CDCs) with separate injectors are carried out and mode switching is realized by raising the inlet total temperature. It is found that there is a series of reversed compression waves. They play an important part in mode switching in CDCs. A reversed compression wave can develop into a detonation wave after passing through a distance where unburnt gas and burnt gas distribute alternatively or bumping against another compression wave. When the inlet total temperature increases, a compression wave is easier to develop into a detonation wave and result in mode switching.

13:50 Chemical Kinetics 3

147 - A theoretical study on the isomerization and dissociation kinetics of methyl decanoate radicals

Q. Meng, Y. Chi, L. Zhang, P. Zhang, L. Sheng

The isomerization and dissociation reactions of methyl decanoate (MD) radicals were theoretically investigated by using high-level theoretical calculations based on a two-layer ONIOM method, employing the QCISD(T)/CBS method for the high layer and the M06-2X/6-311++G(d,p) method for the low layer. Temperature- and pressure-dependent rate coefficients for involved reactions were computed by using the transition state theory and the Rice-Ramsperger-Kassel-Marcus/Master-Equation method. The structure-reactivity relationships were explored for the complicated multiple-well interconnected system of ten isomeric MD radicals. Comparative studies of methyl butanoate (MB) and MD were also performed systematically. Results show that the isomerization reactions are appreciably responsible for the population distribution of MD radicals at low and intermediate temperatures, while the β -scission reactions are dominant at higher temperatures. Although the rate constants of MB specific to methyl esters are close to those of MD in certain temperature ranges, MB is unable to simulate most of dissociation reactions due to its short aliphatic chain. Significant differences of rate constants for isomerization reactions were observed between the calculated results and the literature data, which were estimated by analogy to alkane systems, but the rate constants of β -scissions show generally good agreement between theory and experiment. The current work extends kinetic data for isomerization and dissociation reactions of MD radicals, and it serves as a reference for the studies of detailed combustion chemistry of practical biodiesels.

34 - Theoretical Kinetics Analysis for H Radical Addition to 1,3-Butadiene and Related Reaction on the C4H7O Potential Energy Surface

C. Zhou, J. Bai

The chemical reaction kinetics of 1,3-butadiene is significant to understand the role of polyunsaturated hydrocarbons in combustion and soot formation. The important reactions of 1,3-butadiene and H radical and their subsequent reactions have been investigated in this work. The geometry optimizations and vibrational frequency are calculated at BH HLYP/6-311++G(d,p) level of theory. Electronic energy for stationary points on the potential energy surface related to the primary reactions are calculated at ROCCSD(T)/CBS and G4 level of theory. Discussion of the different configurations of trans and cis structures for reactants and intermediates are also given. Based on the comparison of

barrier heights, terminal addition is the dominating pathway, $\text{CH}_2=\text{CHCH}_2\text{CH}_2$ and $\text{CH}_2=\text{CHCHCH}_3$ are two important intermediates, and $\text{CH}_2=\text{CHCHO} + \text{CH}_3$, $\text{CH}_2=\text{CHCH}_2 + \text{HCHO}$ are important bimolecular products. A significant three-membered ring intermediate (IT7) is found to be important in both terminal and central addition reactions. Pressure- and temperature-dependent rate constants and thermodynamic properties for the H radical addition to 1,3-butadiene are also investigated using the Master Equation System Solver (MESS). The calculated kinetics and thermodynamics properties of the title reaction will be helpful to understand the 1,3-butadiene oxidation in their model development.

289 - A Parameter Study of NSD Plasma Assisted Pyrolysis and Oxidation of CH₄ in a Temperature-Dependent Flow Reactor

C. Guo, Q. Chen

The present work reports the quantitatively experimental results in a temperature-controlled He/CH₄/O₂ laminar flow reactor, showing the temperature-dependent and parameter-dependent kinetics in plasma assisted methane pyrolysis and oxidation. At first, the comparison in experimental plots shows that plasma can significantly increase fuel consumption and product concentration by kinetic pathway other than thermal pathway at lower temperature. Typically, methane consumptions reach maximums of only 7.7% and 8.6% in thermal enhanced pyrolysis and oxidation experiment at 1373 K. However, application of plasma in methane pyrolysis and oxidation can dramatically increase the conversion rates of up to 80.7% and 82.5% at 1173 K. Then, the effects of NSD parameters including discharge voltage, discharge frequency and pulse width in plasma assisted CH₄ conversion kinetics as a function of temperature, are well compared in a temperature-dependent reactive system. The most effective parameter is the applied voltage, followed by the repetition frequency and pulse width. The higher the voltage and frequency are applied, the higher the conversion rates of methane pyrolysis and oxidation are achieved. The pulse width is however opposite.

13:50 Laminar Flames 3

365 - Analysis of Synthetic Flames

S. Coronel, R. Mevel, J. E. Shepherd

A methodology was developed for fitting nonlinear models of laminar flame propagation to radial time history data for spherically expanding flames. The performance of the methodology was examined by analyzing synthetic data with various levels of noise. Calculations were used to obtain uncertainties in the burning speed and Markstein length due to uncertainty in radial time histories. The results indicated that for accurate determination of the flame speed and Markstein length, a minimum of 50 points is needed in the data set (flame radius vs. time) and a minimum range of 48 mm in the flame radius for data with 1% added Gaussian noise. If the number of points increases, the the minimum range needed for determination of the flame speed and Markstein length decreases.

140 - Effects of water droplet evaporation on propagation of premixed spherical flames

Y. Zhuang, H. Zhang

In this study, we develop a theoretical model for flame propagation in premixed gas mixture containing water droplets, by considering droplet vaporization in the post-flame zone. Analytical correlations between flame propagating speed (U), flame front temperature (T_f), flame radius (R_f), front of onset and completion of evaporation are derived to investigate the spherical flame propagation behavior, with emphasis on the effects of initial mass loading on spherical flames. It is found that there exists a single stable flame branch or two stable and one unstable flame branch for spherical flame, depending on initial mass loading. Within the strong stable steady-state (i.e. high speed flame regime), U, T_f and is almost unchanged with initial mass loading, but decreases with. In the weak stable branch (i.e. low speed regime), the droplets with larger are more effective in reducing U and T_f but increasing and.

230 - Pressurized MILD and oxy-fuel combustion in counter-flow configuration: Emissions of NO and CO

K. Wang, L. Pengfei

Both the MILD combustion and oxy-fuel combustion technologies have received significant attention as clean combustion technologies. However, the majority of previous investigation is limited at atmospheric pressure condition. This paper systematically investigates the effect of pressure on the

NO and CO emissions from counter-flow combustion under MILD and oxy-fuel conditions. After comprehensive validation of the modeling, the effects of pressure on the formation of nitrogen oxides (NO_x) and CO are investigated in detail. Note that the terms T-N₂, T-CO₂, MILD-N₂ and MILD-CO₂ combustion adopted hereafter represent the traditional combustions diluted by N₂ and CO₂, and MILD combustions diluted by N₂ and CO₂, respectively. As the pressure increases from 1 atm to 10 atm under T-N₂ or T-CO₂, the temperature raises by approximately 300 K and the NO emission drastically increased by 10 times. However, for MILD-N₂ or MILD-CO₂, the temperature raises by only 150 K. More interestingly, although both the pressure and reaction temperature increase, the NO emission from MILD combustion first increases but then decreases with the peak NO emission obtained at 3 atm, regardless of N₂ or CO₂ dilution. This unexpected NO reduction phenomenon at high pressure is caused by the competition between the chain reaction ($H+O_2 \leftrightarrow O+OH$) and recombination reaction ($H+O_2(+M) \leftrightarrow HO_2(+M)$). Further analysis found that the prompt NO route controls the NO formation in pressurized MILD-N₂ combustion, while the N₂O-intermediate route dominates the NO production in pressurized MILD-CO₂ combustion. The importance of N₂O-intermediate route increases significantly when the strain rate is lower than 10 s⁻¹ at 5 atm. "

13:50 Explosion Safety 4

295 - Experimental and simulation studies on the influence of hydrogen addition on the lean flammability limits of methane/air mixtures

C. Wu, C. Yu, R. Schießl

Flame extinction is a crucial issue in fuel-lean combustion system. The addition of hydrogen seems to be an option to improve the flammability limit of methane/air mixture. In our work, we present both experimental and simulation studies on the influence of hydrogen addition on the lean flammability limit of methane/air mixtures under both laminar and turbulent conditions. Experiments are repeatedly performed in a constant-volume combustion bomb with variation of fuel/air equivalence ratio and turbulence. The maximum pressure is extracted to decide between flame propagation and flame extinction. Premixtures of methane/air and methane/hydrogen/air with CH₄/H₂=9/1 (mol/mol) are used as fuel. Model simulations of flame initiation and propagation were performed using the in-house code INSFLA. The simulation used a premixed counterflow configuration to compute the behavior of a small sample of fuel/air mixture. The results of the experiments and simulations show that hydrogen addition shifts the lean flammability limit to smaller equivalence ratios by about 0.05. Meanwhile, the mixture with same equivalence ratio can be ignited at higher turbulence. The addition of hydrogen to lean methane/air mixtures has a great effect for a larger flammability limit range and a more stable flame.

148 - Problems of Detonation Wave Suppression in Hydrogen-Air Mixtures by Clouds of Inert Particles in One- and Two-dimensional Formulation

D. Tropin, I. Bedarev

The interaction of a plane (one-dimensional) and cellular (two-dimensional) detonation wave with a semi-infinite cloud of inert particles was calculated. The detonation flow modes were obtained. The integral dependences of the detonation wave velocity deficit for various volume concentrations and particle diameters were calculated. Volume concentrations and corresponding particle diameters, resulting to detonation wave failure in a hydrogen-air mixture were obtained. Comparison of one-dimensional and two-dimensional approaches showed a quantitative similarity of the integral dependences of the velocity deficit and the correspondence of the values of volume concentration and particle diameters at which detonation failure is occurs.

310 - Theoretical Estimation of Concentration Limits for Water Steam Capability to Suppress Flame Acceleration in Hydrogen-Air Mixtures

I. Kirillov, N. Kharitonova, A. Lebedev, S. Nikiforov, V. Plaksin

This paper is focused on - 1) non-empiric, computationally inexpensive method for conservative estimation an ultimate value of steam concentration, which can totally suppress the flame acceleration for the given initial conditions (gas mixture temperature and pressure). Method uses only the fundamental kinetic and thermodynamic parameters of the hydrogen-air-steam mixtures; 2) dependence of the ultimate steam concentration upon temperature (373 - 813 K) at normal pressure (100 kPa), computed according to the proposed K-T model.

15:30 Detonation Miscellaneous 2**186 - Model for Chapman-Jouguet deflagrations in open ended tubes with varying vent ratios***W. Rakotoarison, M. Radulescu, Y. Vilende*

Turbulent flames accelerating and propagating in tubes at high speeds could generate a shock ahead of it, to form a shock-flame complex that propagates at supersonic velocities. Such configuration has been investigated in the formulation of the double-discontinuity model by Chue et al. (1993) involving a shock followed by a Chapman-Jouguet deflagration, applied to tubes with a closed end wall downstream of the flame. The present work proposes an extension of this model, applied to tubes with an open or partially open wall to the atmosphere, downstream of the flame. Results obtained reproduce properly the results of Chue's model for a tube with a closed end. It also is able to provide flow properties for a partially open end wall with a known section area.

367 - The Effects of Compressibility on the Propagation of Premixed Deflagration*A. Fecteau, J. McDonald, M. Radulescu*

Numerical simulation of fast flame propagation using a restrictive domain width is compared with quasi-isobaric flames using a 2-D Navier-Stokes solver with adaptive mesh refinement to understand the effects of compressibility on deflagration. This study demonstrates that a pre-compression region appears in the flame profile of cellular flames at the Chapman-Jouguet (CJ) velocity affecting the burning velocity of fast flames. It is also demonstrated that, in compressible deflagrations, the flame surface area does not correctly predict the flame burning velocity. To conclude, an analysis of the vorticity production of the cellular flame shows that the baroclinic vorticity source term is the primary source of vorticity in such flames.

292 - Effect of Inverse Reactions on One-dimensional Detonation Simulated by DSMC*D. Ding, H. Chen, B. Zhang, B. Zhang, H. Liu*

The detonation of gas mixtures is an interesting phenomenon which has been widely studied. In this paper we apply the direct simulation Monte Carlo method to study the microscopic structure of the one-dimensional detonation. A simplified reversible reaction model which consists only two species is concerned. Most of the cases with different activation energies E^* for inverse reactions result in stable detonation waves whose propagation velocities are a little larger than C-J velocities. The non-equilibrium reaction zone is clearly distinguished and measured by calculating molecular reaction frequency and analyzing microscopic structures of the detonations. It is concluded that the lower the threshold for inverse reactions, the faster the detonation wave propagate relative to the C-J velocity. The non-equilibrium reaction zone will also become longer until it is too long to keep the detonation wave moving, when no stable detonation exists.

15:30 RDE 6**303 - Effects of a radial strip injection pattern on a Continuous Detonation Chamber using Navier-Stokes equations***L. Zhang, Y. Hao, J. Wang*

Most of current numerical simulations on the continuous detonation chamber (CDC) are based on Euler equations and a simple fuel-injection pattern is usually used. In this study, the Navier-Stokes (N-S) equations coupled with the one-step chemical reaction model are used for CDC simulations. Besides, a radial strip injection pattern is adopted. It is found that the injection set-up affects the number of detonation waves in the CDC. The transition process from the single-wave mode to the double-wave mode is discussed.

173 - Numerical Study of Rotating Detonation Onset in Engines*E. Mikhaltchenko, V. Nikitin, Y. Filippov, L. Stamov*

3D numerical modeling of a rotating detonation engine (RDE) combustion chamber is performed based on the original code. The RDE is a new type of engines capable to create higher thrust than the traditional ones based on the combustible mixture deflagration process. The dynamical process of combustion in the RDE is more than 100 times faster than in case of usual slow combustion. This type of an engine has more efficient thermal dynamics. The combustion chamber under consideration is a co-axial hollow cylinder. The fuel is injected from one side, either premixed with the oxidizer, or from separate injectors. It is ignited in the chamber near the injectors, and this invokes the self-sustaining

detonation wave which is then rotates consuming the combustible mixture. The burnt gases are expanded in the central part of the chamber where the internal hollow body changes from cylinder to cone and then vanishes. After the expansion, they leave the chamber from the side opposite to the injectors. The primary ignition is modeled by an energy source strong enough to produce an instant detonation wave. The calculations are based on the Navier - Stokes system of equations along with the equations for turbulence modeling and the chemical kinetics. The computational domain used a regular mesh of uniform cubic elements. The time-critical program parts were parallelized using the OpenMP technique. Our calculations were made at APK-5 with a peak performance of 5.5 Tera Flops.

338 - Minimum Mass Flow Rate Predictions for Rotating Detonation Engines Operating on Mixtures of H₂-O₂-N₂, C₃H₈-N₂O and C₂H₄-N₂O

S. Connolly-Boutin, C. B. Kiyanda, H. D. Ng, A. Higgins

Rotating detonation engines are annular combustor continuously fed by a detonable mixture and in which one or more detonation waves propagate in a circumferential manner. These engines present a lower operating bound in terms of mass flow rate. For given reactant total pressure and temperature and a given engine geometry, there exists a minimum mass flow rate below which the engine cannot sustain a successful, steady operation. An analytical model is formulated, based on 1D isentropic flow and normal shock relations that reproduces this limit. Cell size and detonation velocity are determined experimentally for mixtures of interest and the model is tested against those mixtures.

15:30 Chemical Kinetics 4

51 - Comparison of the experimental and kinetic study of two aviation surrogate fuels

Y. Liu, B. Wang, Z. Tian

The comparison of pollutants reveals that 3-C surrogate is a cleaner surrogate fuel which could generate less aromatic and aldehyde pollution than 2-C surrogate. The mechanisms of two surrogate fuel are considered in this work. The mechanisms predict the oxidation and ignition experimental results reasonably, and successfully predict the NTC region in these results. The comparison of ignition delay times indicates that 2-C surrogate mechanism could well predict under low temperature and 3-C surrogate mechanism gives better simulated result at high temperature, and reveals the focus area for further modification of mechanisms. These conclusions will be benefit for the understanding of combustion kinetic of jet fuel and the further studies of surrogate and jet fuels combustion.

30 - Theoretical Kinetics Study on the Reactions of 1,3-butadiene + H₂

Y. Zhu, C. Zhou

The reaction system of 1,3-butadiene + H₂ was investigated in this study. Electronic chemical calculations were carried out on possible entrance channels and subsequent reaction paths for 1,3-butadiene + H₂, at ROCCSD(T)/CBS//BHandHLYP/6-311++G(d,p) level of theory. Potential energy surfaces (PES) were obtained based on the zero-point corrected relative energies. It was found that H₂ addition to 1,3-butadiene forming C₄H₇-OO₃ and C₄H₆-3OOH₄ are two energetically favoured entrance channels. C₄H₇-OO₃ undergoes -scission reaction to the formation of the bimolecular products C₄H₇-3 and O₂, and C₄H₆-3OOH₄ undergoes the ring closure reaction to form the bimolecular products of C=C(CYCO) and H radical are the most important reaction pathways. Whilst, C₄H₆-4OOH₃ undergoing the cyclization reaction to form HOO(CYCC)C, and C₄H₇-OO₄ cyclizing to (CYCOOC)C and CYCOCC are the important products channels. The calculations of the rate constants for all reaction channels studied are underway.

15:30 Sprays & Droplets 2

129 - Effects of Oxygen and Buffer Gas Concentration on Diesel Spray Flame Characteristics

W. Yi, H. Liu

Oxygen and buffer gas concentration have been shown to have an important impact on combustion and emission process. Therefore, effects of oxygen and buffer gas concentration on diesel spray flame ignition and development process were investigated by high-speed imaging techniques in a constant volume vessel under wide oxygen concentrations ranging from 10% to 70% with different buffer gases (Ar, N₂ and CO₂). The findings can be summarized as follows: 1. As the oxygen concentration increases, the natural flame luminosity of diesel spray flame becomes stronger, the width and length of soot flame reduce in size, a stronger fluctuation of soot head vortex occurs in the flame tips. 2. Comparing three different buffer gases, the thermal effects of CO₂, N₂ and Ar influence natural flame

luminosity in a decreasing order. The weakest natural flame luminosity of O₂-CO₂ can be explained by the thermal effect. The severer fluctuation of O₂-CO₂ mixture in the flame head is observed at 30% oxygen concentration. 3. Under low oxygen concentrations (less than 21%), natural flame luminosities using N₂ as the buffer gas are much weaker than that of Ar. An extremely weak combustion process occurs at 10%O₂+90%N₂ case which can only be captured at the biggest aperture ($f/1$). 4. A faint blue chemiluminescence is observed at initial stage of combustion.

373 - On the Low Temperature and Low Pressure Regime Diagram of n-Heptane Droplet Burning in Microgravity

W. Zhang, Y. Liu

The present study investigates the n-heptane droplet burning with ambient conditions 600-1000 K and 0.1 - 2 bar through numerical simulations. Experimental data (initial droplet size 0.7 mm, pressure down to 1 bar) from microgravity experiments offer validation of our 1-D modeling for characteristic time scales identified throughout the droplet lifetime. The motivation of this study is the seemingly narrowing cool flame regime towards the low-pressure conditions presented by prior experimental and numerical works, as contrast to the diverging negative temperature coefficient region for lower pressures. Results for sub-atmospheric pressure show that the cool flame area on the regime diagram converges with decreasing pressure due to major contribution from the ceiling temperature effect. Moreover, the physics trigger at various chemical time scales are well bounded by the droplet lifetime such that very long ignition delay becomes irrelevant to droplet problems.

15:30 Explosion Safety 5

66 - Estimation of the Critical Conditions for Suppression of the Combustion and Detonation Waves

A. Vasil'ev

An attempt was made to estimate the criterion not partial attenuation of combustion and detonation waves with the help of dust particles or water droplets cloud, but to focus on the criteria for the complete suppression of blast waves. The simplest estimates are illustrated on the methane-air mixtures as typical example of mining explosives.

85 - Effects of fuel decomposition on the minimum ignition energy of n-decane/air

X. Chen, Z. Chen, Y. Wang

In scramjet combustion chamber, it is common to cool the engine with the inboard fuel in order to reduce the weight of cooling system and to get additional heat. During the cooling process, the hydrocarbon fuels undergo pyrolysis through endothermic reactions, and the liquid heavy hydrocarbons decompose into light gaseous species. Since the decomposed small fragments have shorter ignition delay and larger mass diffusivity, it is expected that fuel decomposition has a great impact on forced ignition. This motivates the present work, which aims to investigate numerically the effects of fuel decomposition on the minimum ignition energy (MIE). One-dimensional numerical simulation is conducted to investigate the effects of fuel decomposition and fuel stratification on the forced ignition in n-decane/air mixtures. For homogeneous n-decane/air mixture, fuel decomposition can greatly promote the ignition of fuel lean mixtures. With the increase of fuel decomposition, the MIE reduces greatly at fuel lean case while it remains to be nearly constant for the stoichiometric case. There is a lower limit of the MIE, around which further increase in fuel decomposition does not reduce the MIE. Furthermore, it is shown that the combination of fuel decomposition and fuel stratification can further promote forced ignition.

8:30 Detonation Propagation in Rough Wall Duct

91 - Change in Quasi-detonation Wave Propagation Mechanism with Obstacle Blockage*Q. Li, M. Kellenberger, G. Ciccarelli, C. Wang, S. Lu*

The intermittent detonation and failure of a combustion wave propagating in a partially obstructed channel has been observed to propagate by two distinct mechanisms. In this study, the interaction of the shock-flame structure with a series of repeated obstructions is investigated using a soot foils and high-speed schlieren photography technique. Experiments were conducted in a $h = 7.6$ cm by 2.54 cm cross-section aluminum combustion channel equipped with fence-type obstacles along the top and bottom surfaces, spaced equally at distances of h and $2h$. Obstacle heights of 1.27 cm and 2.54 cm were utilized, yielding blockage ratios of 0.33 and 0.66 respectively. The 3.66 m long channel includes a windowed section, providing optical access for a high-speed schlieren photography system. Stoichiometric hydrogen-oxygen at initial pressures of between 10 kPa and 50 kPa were tested. A technique to obtain simultaneous soot-foil and schlieren photography was implemented to provide additional insight to the interaction of the shock-flame structure with the obstacles. The objective of this study is to examine detonation initiation and failure of the discontinuous detonation over an obstacle in a variety of geometric configurations.

41 - The Computational Study of Gaseous Detonation Diffraction and Re-initiation by Small Obstacle Induced Perturbations*X. Yuan, X. Mi, H. Xu, J. Zhou, H. D. Ng*

In this study, numerical simulations using two-dimensional reactive Euler equations with a two-step induction-reaction kinetic model were performed to investigate the detonation diffraction phenomenon and re-initiation induced by small obstacle induced perturbations in the open area. The objective is to analyze the re-initiation mechanism of an unstable gaseous diffracted detonation wave and highlight the importance of cellular instabilities. The effect of the reflection process from the obstacle and the subsequent necessary interaction with the triple points along the original diffracted detonation wave leading to the formation of an explosion bubble are elucidated by the numerical results. A series of simulations were also carried out to examine the effect of obstacle location and its influence on the re-initiation process.

335 - Propagation of Near-Limit Gaseous Detonations in Rough Walled Tubes*Y. Yan, T. Ren, J. H. Lee, H. D. Ng*

In this study, experiments were carried out to investigate the detonation velocity behavior near limits in rough walled tubes. The wall roughness was introduced by using different spiral inserts in the 76 . 2 -mm-diameter, 50 . 8 -mm-diameter and 25 . 4 -mm-diameter tube. Different pre-mixed mixtures, $C_2H_2 + O_2$, $C_2H_2 + 2.5O_2$, $C_2H_2 + 2.5O_2 + 70\%Ar$ and $2H_2 + O_2$ were tested in the experiment. Different wire diameters of the spring inserts were used, and the pitch of each spiral is twice of the diameter to keep same level of roughness in all experiments for each test tube. Fiber optics were chosen to record the time-of-arrival of detonation to deduce the velocity from the trajectories. The normalized velocity V/V_{CJ} and the velocity deficit were computed and analyzed to describe the detonation behavior near the limit. The cellular structure near the limit was recorded by the smoked foils.

211 - Flame Acceleration in the Hydrogen-based Microfoam*B. Kichatov, A. Kiverin, I. Yakovenko, A. Korshunov*

The paper presents new results on the flame propagation through the aqueous microfoam bubbled with hydrogen-oxygen mixture. It is shown that such a flame is able to accelerate and even propagate with significantly high (nearly detonation) speed. This high-speed regime, however, occurs to be unstable and decays into the fast wave dragged by the flow generated in the transient process of flame acceleration. Presumably all the peculiarities are fully related to the structure of the foam so such a reactor can be used to analyze features of combustion independent on the reactor geometry.

8:30 Micro Combustor

62 - Combustion Instability Analysis in a Subscale Rocket Chamber with a Single Injector and Two Injectors*Y. Wang, J. Son, C. H. Cho, C. H. Sohn*

Combustion instabilities of a subscale rocket combustor mounted with gas-centered swirl coaxial (GCSC) injectors are investigated numerically and experimentally. The boundary conditions are divided into two conditions for propellants injection: fuel-lean and fuel-rich. When only single injector is installed on the combustor, stability enhances firstly and then degrades as the equivalence ratio increases from fuel-lean to fuel-rich condition. It means that when the equivalent ratio gets close to the stoichiometric value, the combustion in the combustor becomes stable, and when the equivalent ratio becomes a very small or large value, the combustion becomes unstable. When two injectors are installed on the combustor, effects of injector gap on combustion instability are studied numerically. When the injector gap is small, the local equivalence ratio between two injectors becomes larger. Therefore, stability degrades in the fuel-rich cases and enhances in the fuel-lean cases. When the injector gap becomes larger, the local equivalence ratio between two injectors decreases. Then, stabilities in fuel-rich and fuel-lean cases enhance and degrade, respectively.

226 - Standalone portable micro power generator using stepped micro combustor

B. Aravind, R. Varghese, S. Kumar, K. Hiranandani

In the present study, a dual combustor-based thermoelectric power generator with different modes of air cooling heat sinks, such as a cooling fin with natural cooling, fin-fan combination with forced convective cooling are investigated and presented. Detailed experimental investigations on flame stability limits in the micro-combustor systems are carried out initially to understand the effect of various heat sinks on thermal characteristics of the combustor. Further, two thermoelectric modules are integrated into the combustor along with different active and passive cooling sinks for electric power generation. Finally, a standalone micro power generator system has been developed consist of a power supply unit and mixture supply unit.

90 - A Numerical Investigation on Non-premixed Catalytic Combustion of CH₄/Air in a Symmetrical Planar Micro-combustor

L. Li, A. Fan

Non-premixed catalytic combustion in micro-combustors has not been reported so far. The present work numerically investigated the non-premixed catalytic combustion of CH₄/air in a symmetrical planar micro-combustor with detailed homogeneous and heterogeneous reaction mechanisms. The combustor was designed as a symmetrical structure with three inlet ports in order to provide a fuel rich atmosphere near the catalytic surfaces, which was validated to be beneficial to CH₄ adsorption and reaction in premixed catalytic combustion. The impacts of inlet velocity and nominal equivalence ratio on combustion characteristics were discussed. First, it is found that with the increase of inlet velocity, the maximum temperature, total heat release rate and radiant energy output increase, whereas the combustion efficiency and radiation efficiency decrease. Moreover, a steep decrease in the heat release of chemical reactions and a sharp increase in the surface coverage of O(s) on the catalytic wall are observed in fuel lean case, which means that fuel lean condition may be not suitable for non-premixed catalytic combustion. Furthermore, this combustor shows satisfactory performance in combustion efficiency and radiation efficiency in a wide operation range, which benefits from the fuel rich atmosphere near catalytic wall surfaces. Finally, the external wall surfaces of this micro-combustor have a high temperature level with relatively uniform temperature distribution, and thus this combustor may be fit for micro-TPV systems.

299 - Numerical Simulation of the Influence of Propellant Mixture Ratio on High Frequency Combustion Instability in a Kero/LOX Liquid Rocket Engine

K. Guo, W. Nie, Y. Liu, T. Shi

The topic of this paper is the effect of propellant mixture ratio on high frequency combustion instability (HFCl) in a Kero/GOX liquid rocket engine (LRE). There are 6 cases whose mixture ratio value (oxidant to fuel ratio, O/F) are 2, 2.5, 3, 4, 3.9, 4.4 and 6.044 investigated based on OpenFOAM. Results shows that propellant mixture ratio has great impact on the stability characteristic of LRE. When the propellant mixture ratio value are 2, 2.5, 3.4 and 3.9, there is no HFCl, although small amplitude oscillation occurs at 2 and 3.9, there is no thermo-acoustic coupling phenomenon. Once the value arrive at 4.4, HFCl begins to happen, and the value of pressure peak-to-peak amplitude is 17.2 atm, which equals 13.8% of average chamber pressure. When the mixture ratio value reaches 6.044, severe HFCl occurs whose pressure peak-to-peak amplitude is 119.8 atm,

which accounts for 92.2% of average chamber pressure. Numerical results demonstrate that higher value of mixture ratio tends to make chemical reaction heat accumulate closer to the injector face, which induces thermoacoustic coupling phenomenon.

8:30 Chemical Kinetics 5

328 - Methane combustion dynamics in non-adiabatic PSRs with detailed reaction mechanisms at low and high pressures

F. S. Marra, L. Acampora

The capability of a given reaction mechanism to include all the proper time scales required to reproduce unsteady conditions is the focus of this paper. It is shown that several information required for this assessment can be obtained from the analysis of the bifurcation maps representing the steady equilibrium points of a PSR. This analysis has been here conducted with reference to methane-air mixtures described adopting up-to-date detailed mechanisms, and including the effect of heat losses at the reactor walls. It is found that critical condition can be readily identified from the inspection of the bifurcation maps. The effect of the discrepancies arising even adopting detailed mechanisms on the unsteady behavior resulting from harmonic forcing is then illustrated. The dependency upon frequency and amplitude of the forcing is highlighted for both high and low pressure conditions. Finally, it is shown how conditions of mutual interaction between heat losses and chemical kinetics can produce even less reliable predictions of the dynamic evolution of unstable points.

189 - A reduced virtual chemistry model for soot prediction in hydrocarbon-air flames

H. M. Colmán, N. Darabiha, B. Fiorina

Virtual chemistry is a novel reduced chemistry approach which aims to reproduce detailed chemistry effects at a very low computational cost. The methodology consists in building-up an optimized reaction mechanism from scratch instead of simplifying a detailed mechanism. The reduced mechanism includes virtual species and virtual reactions whose thermodynamics and chemical properties are optimized using a genetic algorithm to capture user-specified target flames quantities. Chemical rate constants are also optimized to fit a given set of constraints such as the temperature profile, the heat release but also the pollutants formation. The present work aims at applying this technique to predict soot production. This is done in two steps: (I) by first looking for Polycyclic Aromatic Hydrocarbons (PAHs) separately and then coupling to a soot formation solver; and (II) in a more straightforward view of soot particles, by considering them as chemical species (BINs) and looking for the soot volume fraction. Here, soot virtual schemes are obtained by targeting a database including 1-D freely-propagating premixed flames. Even though PAH and soot formation are very complex phenomena, a large reduction of the detailed scheme was achieved and a good agreement in predictions was obtained.

80 - Laminar Flame Speed and Laser Absorption Measurements of Conventional and Alternative Kerosene-Based Liquid Fuels

C. Keesee, E. Petersen, B. Guo

Laminar flame speed experiments have been conducted on conventional and alternative kerosene-based liquid fuels, including Jet-A, RP-1, Diesel Fuel #2, Syntroleum S-8, and Shell GTL. Understanding the combustion characteristics of these synthetic fuels is an important step in developing new chemical kinetics mechanisms that can be applied to real fuels. The precise composition of these fuels is known to change from sample to sample. In addition, their low vapor pressures cause uncertainties in their introduction into gas-phase mixtures, hence leading to uncertainty in the mixture equivalence ratio. An in-situ laser absorption technique was implemented to verify the procedure for filling the vessel and to minimize and quantify the uncertainty in the experimental equivalence ratio. The diagnostic utilized a 3.39m HeNe laser in conjunction with Beers Law. These flame speed experiments were conducted over a range of equivalence ratios from 0.7 to 1.5 at an initial pressure of 1 atm and an initial temperature of 403 K. Laminar flame speed and Markstein length were calculated using the appropriate nonlinear method. Laser absorption results matched published data for absorption coefficients, and the results therefrom helped validate the mixtures used in the flame experiments. The laminar flame speed results for all fuels were very similar with the alternative fuels having a slightly faster flame speed than the conventional kerosene-based fuels.

8:30 Turbulent Flames 4**360 - Experimental Study of EGR Dilution and O₂ Enrichment Effects on Turbulent Non-premixed Swirling Flames***T. Boushaki, H. Zaidaoui*

The present paper reports some experimental results of the EGR dilution (CO₂, H₂O, CO₂+H₂O) and O₂ enrichment effects on CH₄-air flame characteristics. The burner used is swirled with a coaxial configuration and the flame is turbulent and non-premixed. The fraction of diluents varies from 0 to 20%, O₂ enrichment from 21 to 30% in volume and the swirl number from 0.8 to 1.4. Visualization of OH* chemiluminescence, LDV measurements and gas analysis of flue gases are conducted. Results showed that the dilution has a significant influence on flame behavior. With dilution the lift-off height increases but the flame remains stable. The O₂ enrichment decreases the lift-off height and enhances flame stability. The increase of dilution rate induces a decrease in NO_x emission and exhaust gas temperature and an increase in CO emissions. LDV measurements showed the axial velocity distribution of flow and its fluctuations in reactive and non reactive conditions. Note that the presence of the flame induces an increase in the axial velocity downstream of the flow due to the expansion of gases. The comparison of axial velocity of flow without and with dilution shows that the maximum velocity is slightly higher and the flow is narrower with presence of dilution.

235 - Measurements of High-Pressure/Temperature Turbulent Burning Velocities of Lean and Rich Iso-Octane/Air Mixtures and Their Various General Correlations*M. T. Nguyen, Y. Chen, S. Shy*

This note reports the turbulent burning velocity (ST) measurements of pre-vaporized liquid iso-octane/air mixtures over a range of the equivalence ratio ($\phi = 0.9 \sim 1.25$) with $Le > 1 \sim Le < 0.93 < 1$ and the r. m. s. turbulent fluctuating velocity ($u = 0 \sim 4.2$ m/s) under high pressure ($p = 1 \sim 5$ atm) and high temperature ($T = 358K$ and $373K$) conditions, where Le is the effective Lewis number. Experiments are conducted in a large dual-chamber, constant temperature/pressure, fan-stirred explosion facility capable of generating near-isotropic turbulence. Schlieren images of spherical expanding turbulent flames are recorded to obtain the growth of mean flame radii $R(t)$ and the observed flame speeds, SF and/or dR/dt . SF is the slope of $R(t)$ which is equal to the average value of dR/dt within 25 mm $R(t)$ 45 mm. After density correction and using Bradleys mean progress variable c -bar converting factor for Schlieren spherical flames, one can obtain ST at c -bar = 0.5, i.e. $ST = 0.5 (\rho_b/\rho_u) SF (Re = 0.1/Rc = 0.5)^2$, where the subscripts b and u represent the burned and unburned mixture. At any fixed p , T , and u , $Le < 1$ flames propagate faster than $Le > 1$ flames with large scattering of ST, $c = 0.5$ data.

317 - Characterization of soot in a co-annular ethylene diffusion flame when submitted to a dc electric field*A. S. Kassem, P. Gillon, M. Idir, V. Gilard*

An electric field applied to a flame promotes modifications in the burning process as remarked by researchers. The ionic wind was proved to influence the dynamics of the flame environment causing changes in flame shape, flame stability and emissions. However, the effect of electric field on soot characteristics is still an open topic. A stable non-premixed flame of ethylene is developed by the mean of a co-flow burner. The burner is connected to a high power supply, and a downstream electrode is mounted above the burner and grounded in order to generate a vertical dc electric field. The non-intrusive Scattering/Extinction method is implemented in this study to investigate the effect of the electric field on soot volume fraction and particles diameter formed during combustion. Interestingly, under a positive potential at the burner, the flame exhibited a reduction in flame height and an increase in diameter. This fact is attributed to the ionic wind modifications affecting the internal dynamic of gases, especially near the burner nozzle. The measurements of soot volume fraction, particles diameter and number concentration were taken at different HAB with 8 kV of potential applied to the burner.

8:30 Dust Combustion 1**323 - Radiation heat loss and solid combustion products characterisation of premixed Al-air flames***P. Laboureur, C. Chauveau, F. Halter, R. Lomba, C. Dumand*

Through an increasing global energy consumption based mainly on the use of fossil carbon products, the scientific community agrees that human activity is partly responsible for climate change and global warming. A process of decarbonizing our energies is necessary, however, despite existing clean energy conversion systems, our current incapacity to massively store energy is the main obstacle to the development of these alternative solutions to fossil fuels and pushes to study new energy carriers. The metallic energy vector can be a solution to answer this challenge, in which metal powders are used to store and convey the energy. Indeed, metal combustion is highly exothermic and oxides formed by this reaction can be recycled using processes powered by renewable energies. The energy carrier would thus be used in a closed loop without generating greenhouse gases over its entire cycle. Aluminum seems to be a potential candidate as a metallic energy vector with interesting energy properties (specific energy 31 MJ/kg), a quantity of raw material sufficient to meet global needs and the existence of a clean zero-carbon recycling industry of these oxides.

265 - Effects of Particle Size Distribution on Cell Size Prediction in Al-Air Detonation

Z. Zhang

Realistic reactive dusts involved in industries or experiments are always polydisperse in size. Previous studies have revealed the effects of particle size distribution on gas-particle detonation cell size. In this study, 2D Eulerian-Lagrangian simulations of Al-air detonation with a hybrid combustion model are conducted to construct the important quantitative relationship between detonation cell size and particle size distribution. Moreover, the effective particle diameter is formulated, which is proved capable of predicting polydisperse detonation cell size with high accuracy but still through monodisperse Eulerian-Eulerian simulations that save computational sources.

206 - Comparison on Laser Ignition and Combustion Characteristics of Nano- and Micron- sized Aluminum

X. Huang, X. Jin, S. Li

A comparative study was conducted on the ignition and combustion characteristics of nanometer aluminum (nano-Al) and micron-sized aluminum (micro-Al) powder stacks. It is pointed out that the nano-Al and micro-Al stacks are significantly different in ignition mode by laser heating. In the static air flow with atmospheric temperature and pressure, ignition delay time of nano-Al is much smaller than that of micro-Al. The combustion of nano-Al is more intense and the self-maintenance performance is better than micro-Al. A model is built to analyze the combustion difference of nano-Al and micro-Al. It is presumed that the ignition and combustion characteristics depends on particle size, oxide film thickness and porosity of powder stacks.

192 - Flame Inhibition of Aluminum Dust Explosion by Sodium Bicarbonate with different particle size

W. Gao, H. Jiang

Flame inhibition mechanism of sodium bicarbonate for aluminum dust explosions is investigated experimentally and computationally. NaHCO_3 with three particle size distributions is employed to determine the inhibition efficiency on aluminum flame propagation. Results show that flame morphology and flame colour change with the addition of NaHCO_3 . The average flame propagation velocity decreases with the concentration of NaHCO_3 ; increases. Meanwhile, fine NaHCO_3 particles within the range studied have a greater reduction in average flame propagation compared to the coarser one. Hence, the inhibition efficiency depends on the particle size of NaHCO_3 . The effect of SBC on gas and surface reaction of aluminum particles burning is further discussed. The simulations indicate that decomposition products of NaHCO_3 particles reduce the burning rate of aluminum flame and obstruct complete oxidation of aluminum particles through flame radical consumption. Additionally, the addition of NaHCO_3 can reduce the surface reaction rate, the vaporization rate of aluminum particles, and decrease the diffusion rate of oxidizers near Al droplet surface.

11:40 Flame Acceleration & DDT 3

277 - DDT Limits in H₂-Air Mixture In a Tube Filled With Obstacles

W. Rudy, A. Teodorczyk

The experimental research has been conducted in 4-m long, rectangular 0.08 x 0.11 m cross-section obstacle filled tube with constant blockage ratio $BR = 0.5$ to define deflagration to detonation

transition (DDT) limits in H₂-air mixture. Three geometrical configurations of obstacles spacing were considered: $S = H$, $2H$ and $3H$, where H is the unobstructed channel height. The results showed that the DDT limits highly depends on the obstacles spacing. The widest DDT limits and higher velocities were observed for largest spacing. This effect is due to lower heat and momentum losses behind the lower number of obstacles where detonation diffracts. It has been shown that criterion of Dorofeev et al. [4] for successful transition to detonation is valid with relatively large margin for the geometry and mixtures investigated. The criterion of Thomas [11] has not been confirmed however, the analysis was based on the velocity of the leading shock wave velocity only. The measured experimentally time difference between leading shock wave and following flame front points at the order of magnitude of ignition delay time that should be shorter to self-ignite the mixture before being consumed by the flame. That increases with the increase of spacing and therefore might partially explain the increase of DDT range.

45 - Effects of Unequal Blockage Ratio and Obstacle Spacing on Wave Speed and Overpressure During Flame Propagation in Stoichiometric H₂/O₂

C. B. Ahumada, M. S. Mannan, E. Petersen

Flame propagation and explosion behavior of hydrogen mixtures remain critical issues for explosion safety in nuclear power plants and refineries. Although extensive efforts have been made to understand the underlying mechanisms affecting flame acceleration and explosion severity in obstructed enclosures, most of the studies address obstacles with uniform distribution. This uniformity is characterized by constant obstacle spacing, shape, and blockage ratio, and may not be representative of the layout in actual industrial facilities. Therefore, the objective of this work was to investigate the influence of unequal area blockage and obstacle spacing on the leading shock wave speed and overall overpressure

during flame propagation. Experiments were performed in a closed pipe with 38-mm internal diameter and a total length-to-diameter ratio (L/D) equal to 73. Two ring-shaped obstacles with 5-mm thickness were used during each test. The arrangement between obstructions in the test vessel was changed in terms of blockage ratio (increasing, decreasing, and equivalent) and obstacle distance (1D, 2D, and 3D). Premixed hydrogen/oxygen mixtures at stoichiometric concentration were considered at 150 torr. The aim was to identify layout parameters that increase the overall overpressure and reduce run-up distance when detonation-to-deflagration (DDT) takes place. From the conditions tested, the increasing blockage ratio has a more significant impact on the overall maximum pressure and the run-up distance.

172 - Deflagration-to-Detonation Transition in Mixtures of the Pyrolysis Products of Polypropylene with Air

S. Frolov, V. Zvegintsev, V. Aksenov, I. Bilera, M. Kazachenko, I. Shamshin, P. Gusev, M. Belotserkovskaya

A new method for determining the detonability of a fuel is proposed: on the basis of the measured values of the length and time of the deflagration-to-detonation transition (DDT) in a pulsed detonation tube (PDT). Granulated polypropylene (GP) was used as a fuel. A test bench with PDT was designed and manufactured together with a gas generator for obtaining the pyrolysis products of GP at a decomposition temperature of up to 800 C. Experiments on the study of DDT in air mixtures of the GP pyrolysis products are conducted. It is shown that the pyrolysis products of GP have a detonability close to that of the liquefied petroleum gas (LPG) of the PBA (propane-butane automobile) brand; in a stoichiometric mixture with air under normal conditions.

267 - Two-Dimensional Numerical Simulation of Flame Acceleration and Deflagration-to-Detonation Transition in Channels with Obstacles: Effects of Blockage Ratio and Channel Size

K. Iwasaki, A. Ago, N. Tsuboi, K. Ozawa, K. Hayashi

This research investigates flame propagation and local explosions in channels filled with hydrogen/oxygen stoichiometric mixture and installed ten obstacles by using the two-dimensional simulation using a detailed reaction model. Furthermore, we estimate differences between the three-dimensional experiments performed in a past study and the present two-dimensional simulations. The simulations performed using the channels at one-twentieth the size of the experimental equipment with 5 m orthogonal grids for BR (blockage ratio) of 0.06, 0.12 and 0.18, and the channel at one-tenth the size of experimental one with 10 m orthogonal grids for BR of 0.18. As a result, higher

obstacles disturbed the flame propagation and induced the shock waves crossing the channel, which lead to the enhancement and acceleration of the combustion reaction. A small local explosion in the unburned gas compressed by flames was observed near the seventh obstacle at one-tenth the size. Unlike the experiments of the past study, the flames did not transit to detonation under any conditions of the height of the obstacles despite using a reaction model because of three-dimensional effects. The flame acceleration was larger in the experiment than in the numerical analysis.

11:40 RDE 7**251 - Effects of Combustor Size on Behavior of Rotating Detonation Waves**

K. Ishii, H. Kawana, W. Kurata, K. Ohno, D. Ikema

In the present work, tests were conducted using two types of combustors to study the effects of the combustors size on behavior of rotating detonation waves (RDWs). The combustor A had an outer diameter D of 50 mm and an inner diameter d of 42 mm forming a channel width of 4 mm, while the combustor B had D of 115 mm and d of 99 mm ~ 107 mm forming a channel width of 4 mm ~ 8 mm. The mass flux rate varied from 0. 10 to 0. 24 g/(s \cdot mm²). The experimental results show that the operating frequency slightly increases with the total mass flow rate for the combustor A, while the combustor B shows almost constant operating frequency under the condition of the same wave number. Regardless of the combustor size, discrepancy between the measured wave speed and the CJ speed increases together with increase in the wave number. The wave number is strongly dependent on the combustor size for the same mass flux rate. The critical mass flux rate at which the wave number jumps differs between the two combustors. As for the combustor B, the critical mass flux rate increases with decrease in the channel width. Concerning the height of the mixture ahead of RDW, there is an upper limit above which the wave number jumps. This upper limit shows almost the same value for the two combustors, except for the combustor B with the channel width of 8 mm.

185 - Experimental Research of Liquid Fueled Continuously Rotating Detonation Chamber

P. Wolanski, W. Balicki, W. Perkowski, A. Bilar

The aim of this research was to test new system of preparation of liquid fuel-air mixture which should allow stable continuously rotating detonation in cylindrical chamber. The newly designed and patented system utilize evaporation of liquid fuel in mixture with hot compressed air under very rich fuel-air conditions. Such mixture is then injected into main stream of air to form detonable mixture. ; Special system was designed and constructed to test this method of mixture creation. From conducted experiments it is clearly seen that if the fuel-air mixture is properly prepared, stable continuously rotating detonation in cylindrical chamber can be achieved. Evaporation of liquid fuel before injection to the detonation chamber is most important to provide appropriate conditions to support stable detonation in the chamber. Obviously, chamber/channel dimensions, initial pressure and rate of supply mixtures play also crucial role in supporting stable continuously rotating detonation. Stable detonation was achieved for commercial gasoline with air, and unstable detonation for Jet-A-air mixture, but nothing fundamental stands in the way of accomplishment of stable, continuously rotating detonation in cylindrical chambers of turbine or turbojet engines operating on typically available jet fuels.

353 - Mixed Detonation-Deflagration Behavior of Hydrocarbon-based Rotating Detonation Engines

T. Sato, V. Raman

Rotating detonation engines (RDEs) provide a promising approach to increasing efficiency in fossil-fuel based energy extraction, by utilizing detonative combustion processes as opposed to the deflagrations that drive conventional propulsion and energy conversion devices. However, this gain is realizable only when the detonation process can be stabilized and the associated pressure gain can be converted into useful work. Prior studies have shown that RDE behavior is highly sensitive to the fuel-air injection process, with the strength of the detonation determined by the level of stratification of the fuel-air mixture within the system. Many of these studies have focused mainly on hydrogen-air detonation, where the high detonability of hydrogen ensures more stable detonation process. In practice, RDEs will use hydrocarbon fuels (methane, ethylene or jet fuels), which are considerably less detonable, and may involve phase change as well. As a result, the behavior of hydrocarbon-based RDEs need to be understood in detail. Since the detonation behavior is highly sensitive to the mixing process, a detailed description of the complex injection process is necessary.

245 - Propulsive Performance of Rotating Detonation Engines in CH₄/O₂ and C₂H₄/O₂ for Flight Experiment

K. Goto, A. Kawasaki, K. Matsuoka, J. Kasahara, A. Matsuo, D. Nakata, R. Yokoo, J. Kim, I. Funaki, M. Uchiyumi

Detonative propulsion systems are promising candidates to replace deflagration in aerospace propulsion systems because of their high thermal efficiency and short combustor length to complete combustion. A rotating detonation engine (RDE) uses one or more detonation waves that continuously circle around its annular chamber to generate thrust. In particular, the application of RDE as rocket motors could enable smaller and more powerful propulsion system. Our research group in Nagoya University proposed a flight experiment of detonation engine systems in space in 2020. However, the primary parameter to determine propulsive performance of RDE to achieve a target thrust have not identified for various fuels, throat and injector geometry. In this study, thrust measurements of RDE of (1) methane / gas-oxygen and (2) ethylene / gas-oxygen with various throat geometries in a vacuum chamber to simulate different back-pressure conditions ranging from 1. 1-104 kPa were conducted. For throatless RDE, equivalent throat area was defined as the detonation channel area, and then four nozzle contraction ratios of 1, 1. 5, 2. 5, and 8 were tested. We measured the time-averaged RDE combustor pressure and revealed that it was almost proportional to the RDE throat mass flux regardless of contraction ratios and the combination of propellants. The specific impulse could achieve more than 80% of ideal specific impulse at the optimum expansion for each back pressure when RDE had a divergent nozzles for high pressure ratio cases.

10:30 Explosion Safety 6**369 - Towards Descriptive Scenario of a Burning Accident in an Obstructed Mining Passage: An Analytical Approach**

F. Kodakoglu, V. Akkerman, S. Demir, D. Valiev

A recent predictive scenario of a burning accident in a coalmining passage is extended to account for obstructions encountered in a coalmine such as the mining equipment, belt conveyor systems, pile of rubbles, etc. Specifically, the theory of globally-spherical, self-accelerating premixed expanding flames and that of ultrafast flame acceleration in obstructed conduits are combined to form a new analytical formulation. The coalmining geometry is imitated by a two-dimensional passage of high aspect ratio, with a comb-shaped array of tightly-placed obstacles attached to the walls. The passage has one extreme open such that a flame is ignited at a closed end and propagates to an exit. The key stages of the flame evolution such as the velocity of the flame front and the run-up distance are scrutinized for a variety of the flame and mining parameters. Starting with gaseous methane-air flames, the analysis is subsequently extended to gaseous-dusty environments. Specifically, the coal (combustible, i.e. facilitating the fire) and inert (such as sand, moderating the process) dust and their combinations are considered, with the impact of the size and concentration of the dust particles on flame acceleration quantified.

73 - Ignition Temperature of Combustible Liquids in Mixtures of Air with Oxygen or Dinitrogen Oxide

S. Zakei, B. Elisabeth, M. Mitu, W. Hirsch

A hot surface can become a potential ignition source in the presence of a combustible vapour/air mixture. Chemical and technical processes as well as cleaning operations are often carried out at temperatures high enough that such surfaces result. The autoignition temperature (AIT) is a safety characteristic used, on the one hand, to classify the combustible substances and, on the other hand, to classify the explosion-proof equipment according to the surface temperature. Under environmental conditions, the autoignition temperature is determined in accordance with standards such as DIN ;51794, ISO/IEC 80079-20-1, DIN EN ;14522 and ASTM E ;659-78. According to these standards, the autoignition temperature is measured at ambient pressure with air as the oxidizing gas. Oxidizing gases other than air may lead to significantly different ignition temperatures (IT). A considerable body of data has already been collected with pure oxygen as the oxidizer. Some substances show an ignition temperature in pure oxygen (ITOX) that is only a few degrees Kelvin lower than the AIT in air; however, for many other substances, it is lower by at least 100 ;K. For some substances that are not flammable in air at all, ITOX can be found in pure oxygen.

111 - Simulations of blast wave propagation in open space that require adaptive mesh refinement

T. Roh, J. Yoh

When detonation occurs in open space areas, the energy of reaction is released instantly in short time and high pressure dense product gas is produced and expanded. The impulsive energy released quickly reaches equilibrium with the environment by the expansion in the air while producing multiple shock waves in the form of blast wave. The blast wave travels in open space follows a Friedlander waveform: instantaneously increasing to a maximum peak pressure well above the ambient pressure and then decaying exponentially away from the source of explosion. Previous works in blast wave simulations provided an empirical equation for predicting peak pressure using explosive weight and standoff distance [1]. To accurately simulate and predict the effects of blast wave propagation pertaining to specific environments, a large-scale integrated hydrodynamic simulation that can handle very large spatial dimensions is required. The reaction length associated with a source detonator is typically a few orders of magnitude shorter than the open space domain, and thus the necessary mesh refinement suitable for blast wave propagation must be considered into ones numerical method.

63 - An adaptive flame-tracking shock-capturing scheme for industry-scale explosion simulations

J. Hasslberger, T. Sattelmayer, S. Ketterl

This paper presents an adaptive flame-tracking shock-capturing scheme for industry-scale explosion simulations. The multi-physics multi-scale problem poses several challenges which are met by special numerical techniques. As a key element, the hybrid flame-tracking shock-capturing scheme reduces grid dependency by treating the flame as a reactive discontinuity which is embedded in a compressible flow. The flame is propagated by a geometrical Volume-of-Fluid method and gas-dynamic discontinuities, especially shocks, are calculated by an approximate Riemann solver. Adaptive mesh refinement is additionally used to reduce overall computational cost. The spatial resolution is locally adapted according to the highly unsteady evolution of explosions. The advantages of the proposed method are demonstrated by multi-dimensional fundamental test cases for which analytical solutions are available.

10:30 Turbulent Flames 5

78 - Statistics of Two-Phase Coupling in Turbulent Spherically Expanding Flames in Mono-sized Fuel-Droplet Mists

G. O. Erol, J. Hasslberger, N. Chakraborty

Flame-droplet interaction in terms of the source terms associated with droplet evaporation in various gaseous carrier phase transport equations has been analysed using a three-dimensional DNS database of spherically expanding flames propagating in mono-sized fuel-droplet mists for different overall equivalence ratios and droplet diameters. It has been found that the slip velocity is significantly affected by the droplet size. Furthermore, evaporation contributions have significant influences on mass, momentum, energy and mixture fraction transport equations but this influence is relatively weak for the reaction progress variable transport equation.

64 - Numerical Simulation of Turbulent Flame Propagation in a Fan-Stirred Combustion Bomb at Elevated Pressures(64)

F. Zhang, T. Zirwes, P. Habisreuther, H. Bockhorn, N. Zarzalis, D. Trimis

239 - Experimental and numerical determination of Lewis number and Markstein lengths for a multi-component jet fuel surrogate and air mixtures

R. L. Dortz, C. Strozzi, J. Sotton, M. Bellenoue

Determining the conditions in which thermodiffusive instabilities of spherical premixed flames of kerosene/air are developed is necessary for a better understanding of this regime in conditions relative to aeronautic. Here, these instabilities are studied with the experimental and numerical evaluation of the Lewis number and the Markstein length for a mixture of a multi-component jet fuel surrogate and air in representative conditions. Experiments are realized using a spherical constant-volume combustion chamber. Numerical calculations are performed using Cantera chemical software, coupled with a reduced chemical mechanism dedicated to the jet fuel surrogate. An innovative numerical methodology for evaluating the Lewis number and the Markstein length of a multi-component surrogate and air mixture is proposed here and is able to reproduce the experimental measurements, excepted for the pressure influence.

10:30 Dust Combustion 2**133 - Experimental Study on the Ignition Temperature of Combustible Dust Clouds with the Effect of CH₄/CO/H₂**

X. Tan, W. Huang, M. Schmidt, D. Wu

Godbert-Greenwald furnace was used to investigate the ignition temperature (ITC) of dust clouds in air with the presence of flammable gas which is lower than its lower explosion limit (LEL). Three flammable gases (CH₄, H₂ and CO) and three dust (anthracite coal, bituminous coal and sweet potato starch) were tested. Experimental results showed that all flammable gases with different mole fractions have distinct effects on the ITC of the dust samples. The ITC of anthracite coal decreases from 610 to 560, 580 and 570 with 3% CH₄, 3% CO and 2.5% H₂, respectively. All three gases have an ignorable effect on the ITC of starch considering the experimental error 10. The presence of CO and H₂ slightly promoted the ignition of bituminous coal dust, but the addition of CH₄ showed a non-monotonic effect on the ITC of bituminous coal: the ITC decreased with 1% CH₄ while increased with 2% and 3% CH₄, showing a concentration effect. These results improve our understanding of the ignition behavior of dust clouds with the presence of small amount of flammable gas.

86 - Numerical study on a shock wave through dusty-gas layers with different particles

J. Yin, X. Yu

The gas seeded with small solid particles, which is called dusty gas, is widely investigated for its extensive industrial applications. The non-equilibrium effect caused by particle relaxation behaves differently for dusty gas flows with different characteristic time. Those former studies mainly focused on the simple dusty flow environments with a few interruptions and reflections. The phenomena of flow field will become much more complex with the number of contact surface increasing and thickness of dusty gas layer decreasing. This paper contains a detailed study of a shock wave through dusty-gas layers with different particle mass fraction. The wave patterns and the distributions of particles behind the shock are mainly focused. Especially, the influence of the strength of reflected wave on the interaction with contact surface. More studies about the wave patterns and density distributions with different shock strength, thickness of dusty gas layer, the material density and radius of particles are advancing. Due to limited space, they have not been mentioned here.

177 - Dynamics, Spectra, and Temperatures of Silicon Combustion in the pSi CO₂ System

V. Mironov, O. Penyazkov, Y. Baranyshyn, P. Krivosheyyev

The ability of porous silicon (pSi) to maintain oxidation reactions that lead to combustion and explosion allows treating it as a component of high-energy fuels. By virtue of this, it is of interest to study interaction of pSi with molecular oxygen, the most wide-spread oxidizer in nature. The experiments on pSi combustion were conducted in a sealed steel chamber that can resist an excess pressure of up to 35 bar. The sample was placed in the chute of recoverable module with its porous layer upward. For combustion initiation, a high-voltage electrode that provided a breakdown between the electrode and the pSi surface ($U_{break} > 16$ kV) was used. Samples of pSi with a length of up to 70 mm and widths, as a rule, 5 mm were used in the experiments. Scanning-electron microscopy and x-ray microanalysis were performed to identify pSi structure. Four regimes of pSi combustion in oxygen have been established and investigated. The velocity of combustion propagation V throughout the porous layer as a rule, increases with oxygen pressure and layer thickness. The results obtained show that the processes studied are high-power ones and that porous silicon is a promising material for creating solid fuels on its basis.

128 - Pyrolysis and Ignition of Branched-Chain Amino Acid Powders

W. Kim, T. Soga, T. Johzaki, T. Endo, T. Kato, K. Choi

The pyrolysis and ignition of branched-chain amino acid powders such as L-leucine, L-isoleucine and L-valine were experimentally investigated. For branched-chain amino acid, same tendency of TG was observed, and a number of flammable products were formed in the pyrolyzates. Minimum Ignition Energy (MIE) and Minimum Explosible Concentration (MEC) of branched-chain amino acid powders with two different particle size distributions were experimentally evaluated. The values of MIE and MEC of the branched-chain amino acid powders were much lower than that of glycine powder. These results demonstrated that the branched-chain amino acid powders have a high risk of dust explosion with lower MIE.

and MEC as compared to glycine powder, and the risk assessment is necessary in the field of powder handling.

13:50 Flame Acceleration & DDT 4

43 - Flame Acceleration and Transition to Detonation in Methane-air Mixtures with Composition Gradients

W. Zheng, C. Kaplan, R. Houim, E. Oran

This paper is part of a more comprehensive study of the effect of composition gradients on flame acceleration and DDT in methane-air mixtures. Here, we present four cases with two linear distributions and two nonlinear distributions of composition gradients. In all cases, the gradients are both perpendicular to the main direction of reaction propagation. The problem is addressed numerically by solving the unsteady, fully compressible, reactive Navier-Stokes equations. The solution method uses a calibrated, optimized chemical-diffusive model (CDM) that reproduces correct flame and detonation properties for methane-air mixtures over a range of equivalence ratios. The results show that the evolutions of flame velocity and total heat release are very similar for two inhomogeneous cases with reverse composition gradients. As the composition gradient is steepened, the maximum flame surface area increases and is reached at a longer distance. In this case, the distance to DDT also increases, resulting from the lower total heat release throughout the entire process.

341 - Numerical Analysis of Flame Acceleration and Onset of Detonation in Homogenous and Inhomogeneous Mixture

J. Wen

Numerical investigations have been conducted for flame acceleration and transition to detonation in a horizontal obstructed channel with 60 percent blockage ratio filled with hydrogen/air mixture. Both homogeneous and inhomogeneous hydrogen/air mixtures have been considered. The later has a vertical concentration gradient. The density-based solver within the OpenFOAM CFD toolbox developed by the present authors [1] is used. High-resolution grids are facilitated by using adaptive mesh refinement technique, which leads to 30 grid points per half reaction length (HRL) in the finest region near the flame and shock fronts. The forward and backwards jets which represent Richtmyer-CMeshkov (RM) instability, were found to impact on the shock front, resulting in the appearance of a secondary triple point on the initial Mach stem on the flame front. Moreover, since both the forward and backwards jet propagate in the shear layer, some small vortices can be found on the surface of the secondary shear layer, which represent the Kelvin-Helmholtz (KH) instability. Additionally, it has been found that the inhomogeneous mixtures cause higher shock and flame velocities compared to the homogeneous mixtures for 20 % hydrogen concentration. Some quantitative comparison with experimental measurements will also be presented.

197 - Flame acceleration and transition to detonation in a channel with triangular obstacles

H. Xiao, E. Oran

This work presents numerical simulations of flame acceleration and DDT in a highly reactive hydrogen-oxygen mixture in a channel with triangular obstacles. The unsteady fully compressible Navier-Stokes (NS) equations are solved using high-order schemes and adaptive mesh refinement (AMR). The influence of blockage ratio on DDT is also examined. In the early stage of flame acceleration, vortices are generated between triangles as the accelerating flow passes over the obstacles. The flame is stretched and convoluted when it approaches the obstacles and interacts with the vortices. The flame convection and corrugation further accelerates the flow and produces compression waves ahead of the flame front. Detonations are initiated in the corners between obstacles at upper and bottom walls. Blockage ratio has a significant influence on flame acceleration and DDT occurrence. One interesting phenomena is that although a full DDT does not develop at high blockage ratio, detonation initiation and failure repeatedly occur during the choking flame propagation. This detonation initiation and failure process repeats every time the shock-flame complex passes over a pair of opposite obstacles until the end of combustion.

25 - Numerical Investigation of DDT Mechanism in Cross-Section Abrupt Detonation Tube

X. Jia, N. Zhao, H. Zheng, X. Chen

Two-dimensional numerical simulation is conducted to investigate the DDT mechanism in a cross-section abrupt detonation tube which could realize fast detonation initiation. The temperature field and

pressure field is discussed in detail from three stages (flame acceleration, transition to detonation and detonation propagation). It is concluded that the existence of convex platform is helpful to DDT, which is validated comparing with the cases of annular tube and single tube: The DDT time and distance of cross-section abrupt tube are both shortest.

13:50 RDE 8**68 - Numerical study on two-dimensional detonation propagation across inert layers**

Y. Wang, C. Huang, R. Deiterding, Z. Chen

Due to its high thermal efficiency, detonation can be used in propulsion systems such as Pulsed or Rotating Detonation Engines (PDE, RDE). In these engines, the fuel and air might not be perfectly mixed and thereby spatial heterogeneity in terms of fuel concentration might occur. The spatial heterogeneity can affect the detonation propagation. Therefore, we need understand the propagation and instability of detonation propagation in non-uniform mixtures. In this study, 1D and 2D simulations considering detailed chemistry are conducted to investigate the effect of inert layers on detonation propagation and detonation structure. The objective is to examine how the appearance of inert layers affects gaseous detonation propagation in hydrogen/oxygen/nitrogen mixture. For successful detonation propagation across the inert and reactive layers, detonation quenching, autoignition, and detonation development and propagation occur alternatively. The critical inert layer thickness and global cell size are studied for different disturbance period lengths. It is found that successful detonation propagation occurs only at relatively small values of inert layer thickness and period. The critical inert layer thickness for the 2D case is much greater than that for the 1D case since multi-dimensional instability promotes detonation initiation.

181 - Experimental Research of Performance of Combined Cycle Rotating Detonation Rocket-Ramjet Engine

P. Wolanski, M. Kawalec

The aim of this work is to test experimentally operation of the combined cycle rocket-ramjet engine utilizing continuously rotating detonation. The experiments were conducted at the Institute of Aviation in Warsaw to verified advantages of combine cycle rocket-ramjet engine over simple rocket engine during atmospheric flight. It was found that for subsonic atmospheric operating condition specific impulse/thrust improvement, for combined cycle operating conditions, is ; over 40% as compared to conventional rocket engine mode.

36 - Chemical and Thermal-Chemical Non-Equilibrium Calculation of FIRE-II Vehicle

N. Hu

Chemical and Thermal-Chemical Non-Equilibrium flow field of FIRE II vehicle is simulated using three different gas models: FSST as base model; ESST with more gas components, and FSDT with vibration energy excited. Simulation results show that including more gas components yields larger differences on shock position and stagnation temperature than including vibrations energy. This suggests for the conditions considered, ionization has more impacts on flow dynamics than molecule vibration.

15:30 Detonations**280 - Coupled Shock Cluster - Reaction Front Structures during Detonation Transition in Narrow Channels Filled with Ethylene/Oxygen Mixtures***M. Wu, H. Su, W. Su, Y. Tseng*

Experiments show that a coupled shock cluster reaction front structure emerges prior to detonation transition in ethylene/oxygen mixture in small channels. The structure features checkered oblique shock pattern interweaved with reaction front. It is found that the angle between the parallel oblique shocks in the structure and the side wall, defined as w -angle, does not change over time in a certain mixture. However, the angle does vary with mixture equivalence ratio. Minimum w -angle is observed in $F = 1.2$ mixture, which happens to be close to the equivalence ratio at which DDT time and distance are the shortest. Shock cluster structure in the leanest $F = 0.6$ case is not as substantial as the other cases. Tests show that the final state of the reaction wave is low-speed detonation instead of near C-J detonation.

7 - The Impact of Spark-igniting Configuration on Detonation Onset in a Rapid Compression Machine*Y. Wang, W. Liu, Y. Qi, Z. Wang*

A combination of experimental and numerical method is used to analyze the impact of different spark igniting configurations on detonation onset. When auto-ignition occurs in unburned region, the oscillation intensity is not proportional to burning velocity as configuration changes. A moderate burning velocity is required for detonation suppression. Especially, 12 circumferential sparks will exaggerate the detonation intensity. The burned mass fraction at auto-ignition occurrence is relevant; to low temperature chemistry.

389 - Effect of initiation on detonation cells for a three step chain-branching scheme*H. Qiu, L. Bauwens, C. Xiong*

Cells obtained from simulations in relatively narrow channels typically adapt to the channel width even if weakly unstable, as shown in simulations in wide channels for single step kinetics [12-13]. The key feature of real kinetics that the single step model fails to represent even qualitatively is chain-branching. Furthermore, in many cases including hydrogen, the initiation mechanism is much slower than other steps. These aspects are at least qualitatively described in a model three step scheme originally proposed by Kapila [14] and used e. g. in [2, 3,15]. Here, results are presented from simulations in wide channels for the model three step scheme, with stiff and slow initiation, in which case it has been shown [15] that in the ZND wave, moving toward termination chain branching eventually no longer takes place, leading to a potentially significant concentration of reactants that only burn very slowly under the combined effect of initiation and termination, so that for a practical purpose the reaction effectively stops. Results below consider mainly increasing values of the initiation activation energy and an increasing initiation length, mainly for CJ waves. Size and pattern of detonation cell are shown as numerical smoke foils. Results typically show that stiffer initiation leads to more irregular cells.

24 - Numerical Investigation of the Direct Initiation Mechanism of Double Point Laser Ignition*G. Hongbo, N. Zhao, H. Zheng, Z. Li, C. Sun*

A two-dimensional numerical simulation has been performed to study the direct initiation of detonation with the lowest laser energy in premixed gas. A detailed elementary chemical reaction model with 9 species and 34 elementary reactions is used for a stoichiometric oxy-hydrogen mixture diluted with argon. The formation, development and initiation process of flame-core in two-point laser ignition under different static pressure conditions were simulated specially. The environmental pressure has an obvious influence on the development process of flame-core and blast wave after laser-ignition. A higher environmental pressure increases the activity of the mixture, resulting in frequent triple point collisions. If we use the interaction of high-power multi-lasers to form strong reflected shocks in the airflow, it will help to realize direct initiation of detonation in stationary combustible gases.

137 - Numerical Studies on the Effects of Ozone Addition on Flame Acceleration and Deflagration-to-Detonation Transition for Hydrogen/Oxygen Mixtures*W. Kong, D. Ning*

Study on flame acceleration and deflagration-to-detonation transition (DDT) is of considerable importance not only due to industrial safety concerns, but also the potential application to advanced engines. This paper numerically investigates the effects of ozone addition on flame acceleration and DDT for hydrogen/oxygen mixtures in a microchannel. The study showed that adding a small amount of ozone can greatly reduce the ignition delay time, but does not change the heat release rate in the detonation reaction zone. The flame accelerates in the microchannel due to thermal and kinetic enhancement. In addition, under the coupling of pressure waves and wall viscous effect, the mixtures near the wall surface auto-ignites due to the shortening of the ignition delay time by ozone addition. DDT occurs due to a local explosion at the tip of the accelerating flame caused by pressure pulse.

114 - Effect of molar ratio of H₂ to O₂ on gaseous detonation synthesis of graphene quantum dots

C. He, X. Wang

29 - Detonation cellular structure with inner tube of CH₄-O₂ pre-mixed mixture

H. Zhao, Y. Yan

In order to study on the cellular structure of spinning detonation, experiments were carried out in annular channels. The limit of detonation was measured as well as the detonation cellular structure was recorded under different pressure. Smoked foils were used in the experiments. They were fixed at the inner-wall and outer-wall of the plastic tube, and the inner wall of the steel tube. Another, round and annular smoked foils were fixed at the end of the plastic tube and the gap between the plastic tube and the steel tube respectively. The results show there are continuous trajectory along the big steel tube to the small plastic tube. Another, the cell size on outer-wall of the channel is larger than that on the inner-wall of the channel. Meanwhile, the cell size becomes smaller when the detonation goes into the inner tube. The change of the cellular structure is for the detonation self-maintain. Compared with records in 20 mm, 40 mm and 60 mm, the cell size decreases with the tube diameter decreasing. The boundary condition is important role in for the cellular structure. The compression by the tube wall on the detonation cannot be ignored.

248 - Propagation Mechanism of quasi-Detonation in Annularly Rough tube

N. Jianguo, J. Li, T. Yang

In the present study, the detonation propagation and limit in an annularly rough tube are studied to provide insight into the physics. In order to investigate the propagation mechanism of quasi-detonation in annularly rough tube, it is reliable to combine photodiode records and high speed camera video to measure the velocity of detonation wave in the annularly rough tube. In addition, a long length of smoked foil was stuck to the smaller tube near the end of the tube to record the cellular structure of the detonation front. On the basis of the present experimental results, it may be concluded that in annularly rough, detonation velocity can vary continuously from close to the theoretical C-J value far from the limit to about 40% VCJ where the detonation fails. The limit where the velocity abruptly drops indicates the transition from a quasi-detonation to a high-speed deflagration wave. For cases with very large or very small roughness, the abrupt velocity drop cannot be observed instead of a continuous decay in velocity. d_2 for the case in annularly rough tube, while d_1 . 5 for the case in circularly rough tube. From the observation in smoked foils, as the initial pressure decreases, a spinning detonation occurs until approaching the limit where cellular structures disappears.

93 - Flame evolution in shock accelerated flow under different reactive gas mixture distributions

Y. Zhu, L. Gao, K. Luo, J. Pan, Z. Pan, P. Zhang

The spherical flame instability and acceleration induced by incident shock and its reflected waves are numerically studied for an ethylene-oxygen-nitrogen mixture, with the same initial shock Mach number ($Ma=2.5$). In particular, the influences of different initial reactive gas mixture distributions on the shock-flame interaction are investigated. The results show that: (1) A detonation emerges in case 1 with uniform reactive mixture gas distribution in present study, which can consume the fresh reactive gas mixture rapidly. (2) For case 2 with negative reactive gas gradient, no detonation emerges, and the area of the distorted flame decreases, thus the chemical reaction speed is relatively slow. Besides, a distinct shock bifurcation emerges from the vicinity of the top wall owing to the leftward reflected shock wave propagates in a reverse flow with a high velocity gradient. (3) Different from case 2, the distorted flame expands quickly behind the leftward reflected shock wave in case 3 with

positive reactive gas gradient, and the heat release also increases distinctly. (4) Overall, the different reactive gas mixture distributions greatly affect the flame evolution in shock accelerated flow, and the combustion intensities in case 2, case 3 and case 1 correspond to the weak, medium, and strong combustion, respectively.

255 - Numerical Investigation of Cylindrical Detonation using a Multiscale Adaptive Reduced Chemistry Solver (MARCS)

H. Liang, L. Wang

This study carried out direct numerical simulations of hydrogen-air cylindrical detonation with a central ignition source at a stagnation temperature of 3000K and stagnation pressure of 5MPa, using a Multiscale Adaptive Reduced Chemistry Solver (MARCS). The MARCS was developed by integrating the Correlated Dynamic Adaptive Chemistry and Transport (CO-DACT) method with the Hybrid Multi-Timescale (HMTS) and the G-Scheme methods, and a full-speed flow solver to conduct the efficient combustion modeling with detailed chemical kinetics. In the final paper, two different reduced chemical kinetics mechanisms, a comprehensively reduced mechanism and a 2-step skeletal mechanism, are examined. Results from these computations are compared with experimental observations, enabling their reliable assessment through the detailed investigation of averaged velocities as well as pressure fluctuations. Several initial turbulence intensities are also considered. Importance of including accurate chemical kinetics in numerical simulations is demonstrated.

67 - Parallel Chemistry Acceleration Algorithm with Table Size Control Method for Gaseous Detonation Simulations

J. Wu, G. Dong

For the purpose of chemistry acceleration in the parallel computations of transient, compressible and reacting flows, a TP/DEP algorithm enhanced with ISAT table size control method is proposed and applied in the numerical simulations of two-dimensional gaseous detonation wave propagation. The effect of total size control of all tables on the computational efficiency and accuracy was investigated. The results show that chemical speedup ratios of all case in present study are ranged between 3.2 and 5.2. The total size of ISAT tables has an obvious influence on the computational efficiency (chemical speedup ratio). The appropriate choice of the table size can keep the favorable load balance among table operations and thus accelerate the chemistry computations of gaseous detonation simulations, without the loss of computational accuracy.

378 - Study on Simplified Model of Detonation Based on Wave Front Curvature

Y. Sun

A simplified model of analog system is considered for the dynamics of one-dimensional detonation with generic losses. The simplified model consists of only a single partial differential equation which can describe many properties of detonation waves at a qualitative level. The critical characteristic of detonation wave propagation can be captured by studying the influence of curvature on detonation dynamic using analytic method. Direct numerical simulation is used to observe the propagation of detonation wave and verify the analytic method. The simulation results show that the wave front curvature has decisive influence on the failure of detonation wave propagation.

37 - Theoretical Study on the Deflagration to Detonation Transition Process

W. Zhang, Y. Liu

DDT process is a complex non-linear physical process, which involves shock wave mechanics, thermodynamics and chemical reaction kinetics. To describe and predict DDT process completely, the coupling of shock wave interaction, combustion and turbulence should be considered. In this paper, a one-dimensional model describing DDT process is proposed. The critical criterion of DDT is obtained by theoretical analysis, which is in good agreement with the experimental results. The propagation state of quasi-detonation wave and the critical state of DDT are obtained by numerical simulation with simplified three-dimensional equation. The physical meaning of the proportional coefficient C in the simplified model is explained by a numerical example of two-dimensional detonation.

242 - Research on Detonation of Liquid Hydrogen-Oxygen by Numerical Simulation

Y. He

To investigate the high pressure peaks during the ignition phase of liquid hydrogen-oxygen combustors, 3D numerical simulations are performed by a Reynolds Average Navier-Stokes method in the framework of the commercial software ANSYS FLUENT, where discrete phase models and 6-species, 7-reaction (6s7r) chemical reaction models are involved. Simulation results show that the strong detonation wave is due to the combination of three main factors: low initial temperature, high initial pressure and appropriate mixing ratio.

15:30 Explosions

58 - Evaluation of the Effects of Coated Walls on Flame Stability of C1-C3 Alkane/air Mixtures in a Slit Burner

F. Li, H. Yang, D. Zhao, X. Wang

The development of good oxidation- and wear- resistance surfaces in small or micro-scale devices is receiving attention. With the common STS 304 wall as reference, the Al₂O₃- and AlCrN- coated STS 304 substrates are fabricated to experimentally evaluate the effects of these coatings on the flame stability of C1-C3 alkane/air mixtures in a slit burner, which is characterized by the flame position, quenching distance, and near-wall OH distribution. Results show that the flame-wall interactions are closely related to the properties of fuel and surface. Overall, the flame position and quenching distance decrease in the order of methane, propane, and ethane, which is correlated to the reactivity of each alkane fuel. Compared with the STS 304 wall, the flame formed between the AlCrN-coated walls has substantially the same variation tendency of the flame position as the gap and wall temperature decrease, and exhibits a slightly greater quenching distance. Conversely, the Al₂O₃-coated wall sustains a much lower flame position and shorter quenching distance. The chemical effect of different materials is very weak near the wall of 200, whereas the chemical effect and near-wall normalized OH intensity is strongly dependent on the surface material at 600. The captured OH intensity in the vicinity of the Al₂O₃-coated wall is the highest, followed by the STS 304 and AlCrN-coated walls.

215 - Finger Flame over the Heat Absorbing Surface

G. Viktor, V. Volodin, A. Gavrikov, A. Mikushkin, V. Petukhov

The work presents the results of experiments on flame propagation with heat absorption, numerical simulation and interpretation of the results using an analytical model of flame acceleration in a confined volume. The experimental part was carried out in a cylindrical shell with a volume of 4.5 m³ filled with 15% hydrogen-air mixture. Steel wool was used as heat absorbing material. The flame was visualized using an InfraTec ImageIR 8320 infrared camera with a spectral range of 2.0-5.7 μm. Numerical simulation was performed using the computer code CREBCOM (Criteria and Experimentally Based COMbustion). The computer code CREBCOM uses a semi-empirical approach based on identifying characteristic combustion regimes, applying criteria to determine the combustion regime for specific initial conditions and geometry, and developing appropriate three-dimensional models to describe flame propagation. Based on the experimentally obtained time-dependences of the flame front radius in the horizontal direction, an analytical model of the heat absorption in a steel wool was made.

60 - Experimental Study on Active Deflagration Suppression Technology in an Open Tube

W. Fan, H. Wu, Y. Huo

Research on active deflagration suppression technology in the tube is the precondition for formulating relevant industry standards and anti-explosion measures. The active deflagration suppression technology suitable for large diameter (more than 2m) tubes was studied in this work. This technology can automatically detect the deflagration fire within 10 ms and start the deflagration suppression system. And the deflagration suppression particles can be injected completely within 10 ms. A uniform particles barrier with an area of 3 m² and a certain thickness can be formed within 60 ms to prevent the development and propagation of deflagration. The experiments on deflagration and deflagration suppression of LPG/air premixed gas in an open tube with a diameter of 2.6m and a length of 25m was carried out. The experimental results showed that the deflagration suppression technology can effectively inhibit the flame propagation, reduce the degree of deflagration damage and reduce the temperature in the tube.

14 - Energy of the Explosion of Unit 3 Reactor Building of Fukushima Daiichi

T. Tsuruda

Three reactor buildings of the Fukushima Daiichi Nuclear Power Plant exploded following the Great East Japan Earthquake in March 2011, owing to core overheating after the station blackout. The two explosions of units 1 and 3 were recorded by a camera. Expanding flame, gas, and fragments are observed in these recorded images. The explosion of the unit 3 reactor building was examined in terms of a similarity solution. Plotting the height of the expanding gas from the unit 3 reactor building against the two-fifth power of time shows a line along the expanding gas front following the explosion near the reactor building. This line indicates the presence of a strong blast wave. The gradient of the line along the expanding gas front gives a constant that depends on the energy of the explosion, the air density, and a non-dimensional parameter that depends only on the ratio of specific heats. The obtained total energy is larger than the accumulated energies of the gas-phase systems in the reactor building. The accumulated energy in the liquid-phase system in the reactor building is considerably larger than the energy of the observed explosion of the unit 3 reactor building.

151 - Effect of impurities on thermal hazard of dimethyl 2,2'-azobis(2-methylpropionate) (AIBME) in industrial application

A. Yu, X. Pan, M. Hua

Dimethyl 2,2'-azobis(2-methylpropionate) (AIBME) is an azo initiator. The substance is unstable and easily decomposes after being heated. AIBME is inevitably in contact with impurities such as acids and alkalis in the process of initiating the reaction. Some impurities may change the thermal decomposition behavior of AIBME. Therefore, in this paper, the effects of common impurities (hydrochloric acid, sodium hydroxide, iron oxide) on the thermal stability of AIBME were studied by differential scanning calorimetry (DSC). The activation energy was determined by Kissinger method and compared with pure materials. The results showed that three impurities reduced the heat release of AIBME during the decomposition process. However, hydrochloric acid reduced the activation energy of AIBME, increasing the risk of AIBME, while sodium hydroxide was the opposite. So it is necessary to avoid contact between AIBME and hydrochloric acid in industrial production.

107 - Determination of the explosion characteristics of methanol -Air mixture in a 20-l sphere

H. Yu, X. Zang, X. Pan

In this work, the effects of ambient temperature and methanol temperature on the explosion characteristics of methanol droplet were investigated by performing experiments in a 20-l closed sphere at different equivalence ratios. The ambient temperature and methanol themselves temperature were varied from 298. 15K to 318. 15K, respectively. Results show that, the explosion range of methanol droplets in the 20-l closed sphere is 118. 8-594. 0 g/cm³. Compared with the explosion range of pure methanol vapor (78. 6-628. 6 g/cm³), the explosion range of methanol droplets is narrower, and the sensitivity of the droplets is lower than that of pure methanol vapor. As the ambient temperature in the 20-l closed sphere increases, the explosion range of methanol droplet becomes wider. When the methanol temperature or the ambient temperature in the 20-l closed sphere remains unchanged, the corresponding explosion characteristics firstly increase, and then decrease at the inflection point of $\lambda=1.8$. When $\lambda=1.8$, there is a maximum explosion pressure in the methanol droplet explosion. The increasing ambient temperature and methanol temperature can improve the evaporation and atomization of methanol, and then promote the transient physicochemical process in the 20-l closed sphere. However, the effect of ambient temperature is more significant than the factor of material temperature on the explosion characteristics of methanol droplet explosion.

260 - Exhaust Gas compositions and Hazardous Effect of Coal Dust Explosion

B. Nie

In order to analyze the explosion gaseous products compositions and its hazardous effect of different metamorphic grade coal dust, 14 coal samples with different metamorphic grade such as anthracite, bituminous coal, lignite explosion experiments were carried out by the self-designed pipeline explosion experimental system, the composition and concentration of explosion gaseous products were studied. The experimental results suggest that: After coal dust explosion, the concentration of N₂ is about 80%, the concentration of O₂ is generally lower than 16%, and the concentration of CO₂ ranges from 3. 89% to 8. 63%. Meanwhile, the lowest CO concentration is 100 ppm and the highest is 8449 ppm, beyond the human body's endurance capacity.

122 - Relation between the ignition point of a flame and the jet behavior in a gas explosion*K. Jindai, T. Tsuruda, T. Daitoku*

An explosion accident occurred at the Fukushima 1 nuclear power plant because of the Great East Japan Earthquake that occurred on March 11, 2011. A curing sheet, which deformed due to thermal influence, was found at the damaged part. In a previous study, we investigated the heat effect on thermally thin combustibles by performing a small gas explosion experiment. The behavior of the flame was observed by using the Schlieren system. From this, it was confirmed that the unburnt gas ejected accelerated going away from the experimental vessel, and the flame decelerated. In this study, we changed the ignition point of the experiment vessel, and its effect on the behavior of the flame was examined.

15:30 Energetics**8 - Propagation of the Explosion of a Solid Propellant in a Partitioned Structure***J. M. Pascaud*

The aim of this work is to present a theoretical study applied to the chain propagation of the explosion of solid propellants and the formation of overpressures inside a partitioned vessel. A calculation methodology is developed to simulate the transmission of the explosion from one compartment to another adjacent compartment by the means of the hot flow through the shared orifice and finally to generalise this methodology to complex multi-partitioned structures. The basic characteristics of the model have been developed for the ignition and the combustion of classical propulsive powders in a one compartment vessel and adapted to a solid propellant such as hexogen with appropriate parameters linked to simplified kinetics. A simple representation of the combustion phenomena based on energy transfers and the action of specific molecular species is presented. The model allows the study of various parameters such as the initial thermodynamic conditions, the location of the ignition energy, and the size of the inner openings or the vent areas.

208 - The effect of relative humidity on aging of zirconium-based energetic materials*B. Han, Y. Park, J. Yoh*

High energy metal particles have been extensively used in standard initiators for producing hot particles to ignite other, more difficult-to-ignite materials. In this study, naturally aged zirconium (Zr) and iron oxide (Fe₂O₃) compound, and zirconium-nickel (Zr-Ni) and potassium perchlorate (KClO₄) compound were prepared to analyze the effect of natural aging on performance behavior. Reaction kinetics were investigated using differential scanning calorimetry (DSC) and thermogravimetric analysis (TGA). Chemical composition changes with aging were determined using x-ray photoelectron spectroscopy (XPS). Additionally, transmission electron microscopy with energy dispersive x-ray spectroscopy (TEM-EDS) and scanning electron microscope (SEM) experiments were conducted to analyze the surface of Zr and Zr-Ni materials. Furthermore, on-going ignition delay time experiments related to aging effects is proposed.

72 - Study on Ignition and Combustion Characteristics of Zr-radical or ZrH₂-radical Propellant*Q. Liu*

In order to investigate the influence of Zr(ZrH₂) powder and Zr particle size on the ignition and combustion characteristics of composite propellant, the combustion process of Zr-radical propellant and ZrH₂-radical propellant with the same particle size and Zr-radical propellant with different particle size were studied. The propellant is ignited by a CO₂ laser igniter, and a high-speed camera is used to visualize the propellant combustion process. The spectral thermometer measures the real-time temperature of the combustion. Finally, the microstructure and particle size distribution of the propellant combustion products are analyzed by SEM and particle size analyzer. The experimental results show that as the particle size of the zirconium powder in the propellant increases, the ignition delay time and combustion time increase, and the combustion rate decreases. The combustion time of ZrH₂-radical propellant is significantly lower than that of Zr-radical propellant, and the burning rate is significantly higher than that of Zr-radical propellant. The addition of Zr(ZrH₂) powder to the propellant resulted in more intense side-burning, which indicates that the addition of Zr(ZrH₂) can significantly improve the ignition and combustion performance of the propellant. As the particle size of the zirconium powder increases, the particle size of the product decreases slightly, and the degree of particle agglomeration decreases during combustion.

286 - A Highly Integrated Conjoined Single Shot Switch and Exploding Foil Initiator Chip Based on MEMS Technology

C. Xu, Q. Zhang, Z. Yang, P. Zhu, R. Shen

In the letter, a highly integrated conjoined device, single shot switch and exploding foil initiator (S3-EFI) chip, was fabricated with microelectromechanical system (MEMS) scale fabrication methods. Photon Doppler Velocimetry (PDV) was utilized to characterize the behavior of the flyer at firing voltages ranging from 1.00 kV to 2.40 kV, and the fabricated device exhibits a terminal flyer velocity of 2967 m/s at 1.50 kV which is considered as an inflection point. Electrical characterizations were then performed on the conjoined chip to obtain some fundamental parameters such as current and voltage, a peak current of 1.73 kA was observed at 1.50 kV. Moreover, ultra-fine hexanitrostilbene (HNS) pellets were detonated over firing voltage range 1.80 kV to 1.40 kV. These results demonstrate the feasibility of the S3-EFI chip and pave the way to non-lead high-voltage discharge circuit. To the best of our knowledge, this is the first time to integrate exploding foil initiator with high-voltage switch.

357 - Experimental Study on The Reaction Evolution of Pressed Explosives in Long Thick Wall Cylinder Confinement

H. Hu, T. Li

The non-shock initiation reaction behavior of pressed HMX-based PBXs inside long thick wall steel tube is studied with detailed diagnostics of tube movement on different sampling sites along the tube and its two ends. The multi-stage reaction processes are revealed with transportation of reaction products, e. g. the convective flow of high temperature gaseous products driven by high pressure along the seam between the HE pellets and the inner wall of the confinement tube, the early stage burning of HE pellets on their surface with an induction time delay and uneven pressure growth along the tube, the late stage violent reaction with rapid expansion and rupture of the tube wall. These processes last nearly 10ms which is much longer than the corresponding detonation duration. The pressure measured by tube wall velocities is much less or about 1GPa for two tested HMX-based PBXs correspondently while the tube wall is accelerated to almost 200m/s during the last 200us -300us before the confinement rupture.

136 - Radiation Imaging Based Temperature Measurement Method for Aluminum Particles in NEPE Propellant Combustion

L. Huang, Z. Xia

Nitrate ester plasticized polyether (NEPE) propellant is a new kind of high-energy propellant and has attracted great attention. Given the advantages of high calorific value, stable performance and abundant reserves, aluminum is usually used as a good additive for NEPE propellant. Aluminum particle temperature is an important parameter for the characterization of aluminum particle and NEPE combustion and . As for the existing temperature measurement technologies based on radiation imaging, the temperature of aluminum or aluminum alloy is usually measured with an assumed emissivity, which is insufficient in theory and has no universality. Aluminum particle temperature measurement in NEPE reacting flows is needed on the purpose of investigating the combustion characteristics of NEPE propellants. In this study, a particle temperature measurement method in NEPE propellants under combustion chamber environment is proposed, based on aluminum particle images and Monte Carlo probability simulation.

288 - Thermal Decomposition and Microscopic Characterization of 8701 Explosive Subjected to Thermal Load

Z. Shao, Y. Wu, F. Huang, P. Jiang

In this paper, a heating apparatus has been designed, by which the cylindrical 8701 explosive charge (95% RDX, 3% Dinitrotoluene, 2% Vinyl acetate resin) was put inside undergoing long-term (~40h) heating at different temperatures (140C-180C) for investigating thermal damage at microscopic scale. >After heating and subsequent cooling of 8701 explosive, the microscopic morphology of the sample was characterized by optical microscopy, scanning electron microscopy (SEM) and computed Tomography (CT). Using CT technique we have quantitatively characterized the change of porosity and specific surface area of internal structure. The results show that with the increase of temperature, the pores and cracks increase, and the damage becomes more serious.

83 - High-Resolution Numerical Simulation of Dead Zones in the Insensitive Explosive Detonation

M. Tianbao, M. Fanjie, N. Jianguo

In this paper, the fifth-order WENO method is used to simulate air-corner turning of LX-17 in the hockey puck configuration with level set method, and the simulation result is compared with rigid-corner turning with the same configuration based on the desensitization model. In the result of weak-confinement corner simulation, the position and the size of dead zone are both consistent with the experiment result in Souers's work in LX-17 Corner-Turning.

15:30 Fire**152 - A Numerical Analysis on the Shedding Mechanism of Dripping Flame**

X. Huang, C. Xiong, P. Sun, Y. Jiang

Dripping of molten fuel is a widely observed fire phenomenon, which can often carry flames, ignite nearby combustibles, cause explosions and enlarge the dangerous scope of fire. By using high-speed camera, the detailed structure of dripping flame is shown to be a burning near-sphere combined with a flame-shedding process, i.e., continuous small explosions. This paper was therefore motivated to present a DNS study on the shedding mechanism of dripping flame. A parametric study by varying the acceleration of flame during falling is carried out to examine the evolution of shedding process, and a vorticity transport equation is utilized to discuss the corresponding shedding mechanism. It was found that the flame acceleration of 0.3 m/s² is the critical condition for triggering shedding, and the initial formation of vortical structure is mainly attributed to gravity. The DNS data further showed that baroclinic torque is the leading factor which dominates the development of vortex field, whereas the volumetric expansion of gas and viscosity both exert negative influences on the vorticity transport.

345 - Modelling the propagation of one-end-burning cylindrical firebrands based on the measured regression rates

H. Zhou, Y. Lai, Y. Li, Y. Zhang

Spotting phenomenon of a burning firebrand lofted in the flow field is the key mechanism of fire spread in a large-scale wildfire such as Forest Fire. Although many models have been developed to determine the maximum spotting distance of the burning firebrands under various conditions, few focused on the effects of volume regression rate. The combustion on a firebrand can be enhanced by its inclined surface, which further increases its regression rate. This effect is discussed even less. In this paper, experiments determining the volume regression rates of one-end-burning cylinders at different incident angles have been conducted. From the initial results, it is found that the angle of incidence can either weaken or strengthen the regression rate of burning cylinders, especially for the cylinders of large diameters. The effects of the incident angle on the flame spread is also enhanced by increasing diameters. Furthermore, basing on the measured volume regression rates, numerical models have been developed to estimate the maximum spotting distances of the burning cylindrical firebrands lofted in a constant flow field. The results demonstrate that both the improvement and the suppression of spotting distances due to volume regression are significant.

198 - Experimental investigation on the flame characterization and temperature profile of single/multiple pool fire in cross wind

Z. Chen, X. Wei, T. Li

An experimental study is carried out for investigate the flame characterization and temperature profile for single and multiple pool fire with the influence of cross wind. There are 13 test cases in total, categorizing circle and rectangle fuel pans, with diameter (or equivalent diameter) ranged for 50 mm to 300 mm. Kerosene is used for the fuel of pool fire. Some K-type thermocouples are arranged around the flame to monitor the flame temperature, while the flame tilt angle is measured base on the photograph of flame for different case. Firstly, it can be found that there are three phases, including preheating, steady burning and extinguishing phase, during the flame evolution. The temperature near by the fuel surface is higher than flame plume, with maximum temperature approximately 1040 K and 600 K, respectively, in the steady burning phase of circle single pool fire (D=300 mm), while the average burning rate is ~1.525 g/s. In addition, the burning rates of all cases are measured and compared with the current predicted method. Typically, the flame morphology of single/multiple pool fire at different cross wind speed (ranging from 0 to 3.5 m/s) is

analyzed, and it is found that the results for single pool fire is according to Thomas model and AGA model well, but not suitable for multiple pool fire.

200 - Heat and mass transfer of flame spread along a combustible slope

X. Huang, C. T. Daitoku, K. Hiyama, T. Tsuruda

Flame spread along an inclined surface is often seen in wild and residential fires. During the flame spread, upward and downward spread flames are seen. Under wild fire condition, the thin combustible locates near the ground. The presence of the ground may affect the flow and temperature fields. The flow and temperature fields are governing the heat and mass transfers in the spreading flame. The flame spread along combustible near the ground had been examined by Professor Torahiko Terada more than 80 years ago; He reported that downward spreading flame is only seen along combustible inclined around 35 degree near the ground. This phenomenon is called "Terada phenomenon". His report is not widely referenced by recent studies. In the previous study, The Terada phenomenon as shown in figure 1 was seen inclined angle = 25degree to 55 degrees when separation dL between combustible bottom and base was 3 mm. The range of inclined angle where the Terada phenomenon occurs decreases as gap height dL increases. The Terada phenomenon was not seen when $dL = 6$ mm. We considered that Terada phenomenon occurs because flow in between combustible bottom and base changes by gap height dL and inclined angle. In this study, flame spread vicinity of the thin combustible surface was observed using Schlieren equipment to investigate influence of the flow in between combustible bottom and base.

130 - Thermal stability of chemicals under fire conditions: the case of hydroxylamine sulphate

E. Danzi, G. Pio, E. Salzano, L. Marmo

In this work, the case of hydroxylamine sulphate $(\text{NH}_3\text{OH})_2\text{SO}_4$, which has been recently responsible for large scale explosion in a chemical warehouse is analysed. This substance is largely used as intermediate in the production of caprolactam, but also in pharmaceutical, food and textile industry (EU Risk Assessment Report, 2008). The substance is relatively stable at ambient temperature, while it decomposes explosively at higher temperatures, around 130 C; Accordingly, GHS and CLP (1272/2008) do not consider fire or explosion hazards. However, the classification of EU Directives 67/548/EEC and 1999/45/CE, recognized $(\text{NH}_3\text{OH})_2\text{SO}_4$ as R2 i.e.: risk of explosion by shock, friction, fire, or other sources of ignition. This paper investigates the explosive behavior of hydroxylamine sulphate, the chain of reactions that generate hydroxylamine (well-known unstable and hazardous chemical), also with experimental research on the heat of combustion of the different reactions involved. The paper underlines the poor consistency of GHS classification and its ineffectiveness to identify hazards related to fire conditions effects on substance like hydroxylamine sulphate. Finally, some results of a simulation code are reported, which attempts to estimate hydroxylamine sulphate amount involved in a warehouse explosion occurred in Italy, through damage and explosion crater analysis.

290 - Study on Characteristics of Ship Engine Room Fires

L. Cong

Fire is one of the main threats to ship safety, leading to heavy casualties and property losses. As the power source of the ship, engine room is the location of the highest frequency of fire with the presence of high temperature and inflammables. In this paper, we simulate the development process of full-scale ship engine room fire, and analyze the characteristics of ship engine room fire through related fire parameters. Under different opening sizes of ceiling vent, the results show that the quenching modes of engine room fire can be divided into oxygen control type and fuel control type according to the difference of fuel consumption rate and other fire parameters. Critical horizontal ventilation factor for two quenching modes are 2000. In the development of fire, the temperature field in cabin distributes evenly in the horizontal direction, while in the vertical direction it presents stratification phenomenon.

119 - AutoCAD inspired level-set algorithm for 3D simulation of industrial fire and explosion

K. Hyun-jun, J. Yoh

In a conventional method of defining an interface via the level set, an analytic function is required to initialize the material boundary [1]. It is often the case that a realistic material interface is never

circular or rectangular, rather it is complex and three-dimensional in its shape. Thus defining and initializing such material interface as a zero level-set has been a great challenge for multi-material hydrodynamic simulation. In this paper, we present a novel interface initialization algorithm for defining a zero level-set for constructing any complex 3D geometry that utilizes STL (Stereolithography) file format [2]. The algorithm is tested in the deflagration spreading problem associated with a complicated plant facility. The gas tank explosion by leakage of hydrocarbons is simulated as a process of catastrophic failure of gas storage in the industrial fires.

15:30 Kinetics and Flames

278 - Nonlinear large-eddy simulation of a Cambridge stratified swirling flame

X. Qian, H. Lu, C. Zou

Recently, numerical studies have been carried out for the flames under non-swirl conditions and swirling conditions. A recent large-eddy simulation (LES) study by Brauner et al. has shown the overestimation of the temperature in the central regions of swirling flames is very serious (~400K), and they and their co-workers have also shown that, at the 14th international workshop of measurement and computation of turbulent nonpremixed flames (2018), changes of the combustion model are not critical to solving this issue. In LES, subgrid-scale (SGS) model is one of the keys to accurately simulate turbulent flames. Modeling studies have shown that nonlinear SGS models can capture strong anisotropies in turbulent flows, thus yielding a more accurate set of results in flows with strong shears. A recent achievement in LES of MILD combustion has made an initial attempt to accurately capture the turbulent mixing under MILD combustion conditions using the gradient-type structural SGS models. Owing to the strong shear generated in high-velocity nozzles under high swirling configuration, nonlinear SGS models would be a better option to study the high-swirling case. The aim of this study is to investigate the influence of high swirl in the SwB3 case by using a gradient-type structural SGS stress model, which is one of the recently developed nonlinear SGS models. The following section describes our study's numerical framework, including a description of the case and the simulation details. Then the LES results are presented and discussed.

20 - Study of Oil Droplet ignition and its Induction for Pre-ignition under Different Environmental Conditions

S. Fei, Y. Qi, Y. Wang, Z. Wang, H. Zhang

The ambient gaseous mixture consists of iso-octane and oxygen with stoichiometric ratio, as well as nitrogen and argon. The impacts of pressure on the induction of pre-ignition of gas phase by the oil droplet have been analyzed under different temperature conditions. The introduction of lubricating oil droplet would decrease the ignition delay of the ambient gaseous mixture. Furthermore, the effect of pre-ignition induction shows different pressure dependence mechanisms under different temperature conditions. Under a relatively lower temperature condition, the ignition delay of the ambient gaseous mixture without an oil droplet decreases with the increase of pressure, while that with an oil droplet keeps almost constant. Under a relatively higher temperature condition, the values of ignition delay of the ambient gaseous mixture with/without an oil droplet both decrease with the increase of pressure when the pressure is in a relatively lower range. On the other hand, the ignition delay of the ambient gaseous mixture with an oil droplet keeps almost constant while that without an oil droplet continues to decrease with the increase of pressure when the pressure is in a relatively higher range. The different pressure-dependence mechanisms of pre-ignition induction by oil droplet under different temperature conditions could be attributed to the trade-off effect of pressure on droplet evaporation and gas-phase chemical reaction.

28 - Composition and Outlet Distribution of Pre-combustion Pyrolysis Products

F. Song, Y. Wu, D. Jin, X. Chen, S. Xu

In the experiment, the method of first-stage pre-combustion heating is used to achieve the required total temperature of incoming flow. At the same time, in order to simplify the system, the process of kerosene pyrolysis is required to be completed in the combustion chamber. When the temperature reaches 1060K, kerosene cracking reaction time is about 50 ms. The pyrolysis reaction rate of kerosene increases exponentially with temperature, and the higher the temperature, the faster the pyrolysis reaction. However, kerosene injected into the gas with too high temperature will be ignited. Therefore, there are several temperature zones in the combustion chamber to study the optimal

location of secondary refueling. In this paper, experiments have been carried out on existing pre-combustion pyrolysis experimental devices to study the effects of different experimental parameters on pyrolysis products. The circumferential distribution of 3 to 5 nozzles at different axial distances is used to study the effect of kerosene filling distance on pyrolysis products. The working pressure range of pre-combustion pyrolysis combustor is 0. 1-0. 5 MPa, the air flow rate is 0. 1-0. 4 kg/s, and the total outlet temperature is about 550 K. The pyrolysis products under each working condition are tested for different positions of kerosene replenishment, and the effects of temperature of kerosene replenishment position and the residence time on the pyrolysis products are studied.

118 - Genetic Algorithm Applied in Optimizing Reaction Mechanism Based on Reduced Reaction Mechanism

R. Yang

With the development of CFD, numerical simulations play a more and more important role in the study of combustion. However, the detailed chemical mechanisms describing the combustion process typically involve hundreds of species and thousands of reactions. Due to the computer's memory capacity and CPU speed limits, using detailed chemical reaction mechanism should be quite unrealistic in reality. A significant portion of the computation time in the simulation of combustion systems is used for the calculation of chemical reactions. Furthermore, the vastly disparate reactions of the various chemical species frequently induce chemical stiffness as an additional obstacle for numerical simulations. Therefore, reasonably choosing simplified reaction mechanism has become an effective way to acquire results with adequate precision and efficiency simultaneously. In this paper, genetic algorithm combined with sensitivity analysis method is applied to determine the ignite delay and final species concentration of mixture of methane combustion with premixed Perfectly Stirred Reactor(PSR) model. Compared with methane reduced reaction mechanism's result which were obtained through PSR model, the new methane mechanism based on genetic algorithm has high accuracy in computing the end temperature, ignite delay and species concentration.

264 - Two-dimensional frequency analysis of a diffusion methane jet flame under transverse acoustic excitations

J. Wang, X. Mei, Q. Wang

The paper investigates the response of diffusion methane jet flame under transverse acoustic excitation in atmospheric environment based on high speed color/schlieren imaging and image processing techniques. The excitation frequencies are set as 5 Hz, 10 Hz, 15 Hz, 20 Hz respectively and a case without excitation is set for comparison. The overall flame oscillating frequency has been evaluated based on the time-resolved color images, while the two-dimensional (2D) frequency of the flame and flow field have been analyzed based on the color flame and schlieren sequences respectively. It is found that the overall flame oscillating frequency is 10. 7 Hz in all cases. However, nonlinear responses have been found through the 2D frequency analysis based on the color flame and schlieren images. In all cases, the regions of double frequency (20. 5 Hz and 21. 4 Hz) can be found in both color flame and schlieren results. The excitation frequency has been found near the nozzle exit, which is mainly due to the disturbance on the unburned fuel.

79 - Numerical Study of OH*, CH* and C2* Radicals in a New Reduced Ethanol Kinetics

J. Zhng, Y. Zhang

The main objective of this research consists of developing a new reduced ethanol mechanism with excited radicals (OH*, CH* and C2*) so that the chemiluminescent emission of the ethanol flame can be simulated and compared with imaging based experimental data. This is an area worth of further investigation because the flame self-light emission can be readily imaged with modern digital cameras and analyzed with the ever increasing computing and processing power. The proposed reduced model, which was successfully validated with extensive experimental data of shock tube ignition delay times, jet-stirred reactor (JSR) species concentration, and premixed laminar flame species profiles by using Chemkin-pro, has extremely high accuracy compared to the detailed model. The simulated chemiluminescence emission were then compared to the relative experimental data. Furthermore, reaction paths analysis was carried out for good understanding ethanol oxidation process and the formation and decay reactions of the excited radicals. The new reduced ethanol model can be applied for the further study of ethanol flame. For example, the CFD simulation with chemiluminescence mechanism can be cross-validated using imaging based techniques. As a result, the experimental tests

can be more easily setup using imaging based technique and more expensive laser based diagnostics could be avoided.

16 - Effect of Hydroxyl Radical Precursors Addition on LTC-affected Detonation in DME-O₂-CO₂ Mixtures

Y. He, R. Mevel

In the present study, the effects of hydrogen peroxide (H₂O₂) and tert-butyl hydroperoxide (TBHP) as hydroxyl radical precursors on the characteristic length-scales of LTC-affected detonation propagating in DME-O₂-CO₂ mixtures were investigated using the ZND model. The effect of these two additives on the energy release dynamics and chemical kinetics have been also analyzed in details. The H₂O₂ addition induces a similar reduction of the different induction zone lengths, as well as an increase of the energy release rate. The addition of TBHP induces both a thermal and a chemical effect. Thermally, since the effective equivalence ratios of the mixtures are higher, higher Mach numbers and higher von Neumann temperatures are achieved. Chemically, there is a LTC chain propagation loop which leads to a significant decrease of the induction zone length along with a substantial increase of the energy release rate, especially for the first stage of energy release. Hence, TBHP seems to be a promising additive for experimentally observing LTC-affected detonation with multi-stage energy release.

69 - Kinetic Study on Nitromethane and its Application as Power Booster in Engines

K. P. Shrestha, F. Mauss, L. Seidel, T. Franken, T. Zeuch

162 - Advanced Dimension Reduction Methods for the Identification of Intrinsic Low-dimensional Manifolds in Composition Space

Y. Xia, Y. Jiang

Many species problem is one of the principal challenges of modeling the coupling of detailed chemical reaction kinetics with fluid dynamics. Manifold assumption suggests that low-dimensional manifolds exist in the composition space and dynamics models based on these manifolds only need to deal with much more less variables, usually 2 or 3, than the whole set of species. Recently, the idea of identification the low-dimensional manifolds from data of experiment or direct numerical simulation (DNS) was studied, and principal component analysis (PCA) and its related nonlinear methods have shown promise in accomplishment of this work. In this paper, a nonlinear dimensional reduction method, Isometric feature mapping (Isomap), as an alternative to PCA or its variant are investigated. Both the dimensional reduction methods are applied respectively on a result of a non-premix diffusion H₂/N₂ flame, based on ODT simulation, to get the reduced data set. And artificial neural networks (ANN) is involved to rebuild the full data set.

247 - Effect of Hydrogen addition on ignition of methane-hydrogen-air mixtures over a hot surface

S. Kumar, R. K. Velmati, S. Shashidharan

The present study involves investigations on hot surface ignition of hydrogen-air mixture using detailed H₂-air chemistry for ignition and combustion modelling. The hot surface is modelled as a commercially available glow plug with combustion chamber at 1 atm pressure. Numerical simulations were carried out for various equivalence ratios and heating rates. The results indicate that there is a change in the location of ignition point for lean and rich mixtures, with side-ignition occurring for rich mixtures and lean mixtures igniting only at the top of the heated surface (glow plug). Variation of heating rates appears to play a significant role for rich mixtures and ignition temperature of lean mixture does not show any considerable deviation. The role of the local equivalence ratios at the ignition point and reaction rates prior to the ignition process has been studied to help it better understand under different conditions. The phenomenon of puffing flame occurs at lean extinction limits. The effect of gravity and buoyant forces on the phenomenon has been investigated and highlighted for different heating rates leading to mixture ignition.

243 - Velocity Measurement Comparison of Traditional and Schlieren-equation Based optical flow methods

H. Cheng, Y. Wu, X. Mei, Q. Wang

An optimized schlieren motion estimation (SME) algorithm is developed in this study. Two constraint equations has been established: one is based on the relationship between schlieren luminance and

velocity gradient as well as continuity equation; the other one is a second-order div-curl regularizer. The velocity results are obtained through the minimization of energy function which derives two matrix equations by adopting variational method. In addition, multiple optimization method is introduced into SME method to offer better results. The performance of SME and traditional optical flow (OF) method on schlieren image velocimetry is compared. It shows that SME do has better results than OF in solving stability, continuity of velocity/vorticity and shows finer flow structures.

232 - Effects of Nitrogen on the Flammability Limits of Dimethyl Ether at Different Temperatures

Y. Zhang, Y. Liu

With the ever-increasing energy consumption, the traditional fossil fuels have become increasingly scarce and the environmental problems caused by overuse have become more serious. Therefore, it is urgent to seek a clean and efficient alternative energy source. Dimethyl ether (DME), which has the potential to be used as a substitute for fossil fuel, has attracted widely attention. And it has been demonstrated that the use of DME reduces nitrogen or sulfur oxides and carbon monoxide emissions. Due to its excellent combustion properties, scholars have carried out extensive experiments and theoretical research on the flammability characteristics of DME in recent years. Zhang et al. investigated the explosion characteristics of DME-nitrogen/argon and DME-methane using a 20L spherical device, and analyzed parameters such as P_{max} , explosion limit, and laminar flame speed. Zhang et al. investigated the explosion characteristic of DME diluted by five gases (CO₂, N₂, HCFC-22, HFC-134a, HFC-227ea) and analyzed the influences of flammability limit of DME by different dilution gases. Chen et al. tested the flammability data of binary mixtures DME/R134a with different volume ratios, and obtained corresponding flammability limits and critical flammability ratios. Mohammed et al. studied the effect of N₂/CO₂ dilution on laminar flame speed at different temperatures.

201 - A study of Combustion Characteristics of Heterogeneous Combustion Field by Impinging Injection and Multiple Fuel Injection

J. Liu, H. Aoki, T. Kawakami

Nowadays, global environmental problems become serious, and it is a common belief that the internal combustion engines are the main causes. Due to the depletion of natural resources and environmental problems, it is necessary to achieve low emissions and low fuel consumption for internal combustion engines, especially automotive diesel engines. From the viewpoint of improvement fuel consumption, the thermal efficiency, and the reduction of NO_x, CO, and HC emissions, DI (Direct Injection) has been widely used in internal combustion engines. Except DI, there are several techniques were developed, such as EGR, lean combustion, and HCCL. Previous researches indicated that impinging injection can help with the unburned components adhere to the wall surface by using the collision between the fuel spray. In this study, the experiments have been carried out to examine the influence of the injection type and injection timing difference to ignition on combustion characteristics such as maximum burning pressure, total burning time and ratio of heat release by using impinging injection and multiple fuel injections. The main conclusion are as follows: 1) It is possible to have combustion improvement at heterogeneous combustion field by change the combination of impinging injection and multiple fuel injection. 2) The most suitable conditions of combustion improvement exist for investigating the injection amount ratios under the multiple fuel injections.

170 - Burning of fuel droplets incorporating solid carbon particles

V. Nikitin, V. Tyurenkova, N. Smirnov

In the present paper the development of physical and mathematical models, allowing to consider the effect of multiphase fuel (hydrocarbon liquid + solid combustible material) on the conditions of ignition and modes of propagation of combustion in polydisperse nonuniform mixtures. In this case, the combustion of different droplet fractions occurs in different modes: the volatile fraction evaporates and burns in the gas-phase mode, and the solid fuel fraction reacts with the oxidizer in the heterogeneous mode. The effect of the presence of a solid fraction in droplets reacting in a heterogeneous regime on the evaporation rate of the volatile fuel component is studied. The effect of tightness due to the presence of other drops on the evaporation rate of each drop is taken into account. The results of computational modeling of flame propagation during ignition of polydisperse mixture of liquid hydrocarbon fuel droplets with solid fine carbon particles are presented.

370 - Structure and dilatation of perturbed flame interface during the reactive Richtmyer-Meshkov instability*D. Wang, G. Dong*

Richtmyer-Meshkov instability is common in engineering and disasters formed by the interactions between flame interface and shock wave (reactive RMI) enhancing the mixing and promoting combustion. The interface is continuously deformed under reactive RMI while in the late reactive RMI process the patterns of flame are stable and could be featured by dilatation effect. Under these circumstances, the dilatation is studied by the expansions resulted from the reaction heat release and the heat flux separately, both in three dimensional space and through correlation analysis. Furthermore, the relationship between dilatation and vorticity is also examined and forecast by the probability density function of the alignment between vorticity generations and the vorticity.

222 - A New Cylindrical Converging Shock Tube*D. Zheng, X. Luo, Z. Zhai*

A new shock tube facility for generating a strong cylindrical converging shock wave is developed in this work. Based on the shock dynamics theory, When a planar shock wave propagates forward along the curved wall, the disturbances produced by the curved wall would continuously propagate along the shock surface and bend the shock wave. A specific wall profile is designed for the test section of the shock tube to transfer a planar shock into a cylindrical one. And the Mach number near the center area will reach to around 8.

13 - Experimental study on the lower flammability limits of ammonia/methanol/air mixtures at elevated pressures and temperatures*W. Ji, Y. Wang, J. Yu, X. Yan*

An experimental apparatus based on the 20 L steel spherical vessel was set up, aiming to measure the flammability limits of gaseous mixtures at elevated temperatures and pressures. The lower flammability limits (LFLs) of ammonia/methanol/air mixtures were measured at ambient temperature up to 150 C and atmospheric pressure up to 4 bar. The results showed that the LFLs of ammonia/methanol/air mixtures decreased as the initial temperature and initial pressure rise. The pressure dependence of the LFL of ammonia/methanol/air mixture were found to be linear. Damping effect was found for ammonia, which would increase the LFL of ammonia/methanol/air mixture if improving the ammonia content in the mixture. The predicted results by LeChatelier's Law were slightly conservative than the experimental ones.

75 - Experimental and Numerical Study of Excited-state Radicals in Methane-air Jet Diffusion Flames*Y. Liu, J. Tan, L. Zhang*

Spatial distribution images of OH* and CH* chemiluminescence from methane co-flow laminar diffusion flames were acquired using intensified CCD cameras coupled with multiple lens and narrow-band-pass filters. A processing method was employed to subtract contributions from background emissions in CH* chemiluminescence and an Abel inversion method were introduced to obtain more accurate results of chemiluminescence radial distributions. To obtain deeper understanding, the detailed GRI-Mech3.0 mechanism combined with OH* and CH* reaction mechanism were used in the two-dimensional simulations. Results show that OH* distribution can be divided into three regions: intense section(I), transition section(II), secondary section(III), while CH* is distributed in only two regions: intense section, transition section. CH* generates near the fuel side, while the OH* is distributed outside the flame front. The intensity of reactions in zone I and II is also stronger in the numerical image.

145 - Characteristics of sub-standard liquid hydrocarbons combustion when interacting with superheated steam jet*E. Kopyev, I. Anufriev, O. Sharypov, A. Tsepenok*

This paper by the example of spent automobile transmission oil investigates the combustion of sub-standard liquid hydrocarbons in a straight-flow burner, implementing a promising method of liquid fuel dispersion by a superheated steam jet. The aim of the work is to study the influence of regime parameters on the thermal and environmental characteristics of the combustion process. Gas

composition of combustion and heat release products was measured. A flow calorimeter was used to measure heat release. The measurement of the amount of generated heat was based on determining the coolant temperature difference at the inlet and outlet as well as the flow rate of the coolant and fuel under stationary experimental conditions. TESTO 350 gas analyzer was used to control the composition of gaseous combustion products. Sampling of reaction products cooled to room temperature was carried out at the calorimeter output. Dependences of specific heat release on steam and fuel flow rates have been obtained. The regimes with low CO content in the combustion products have been found.

141 - Experimental study of substandard liquid hydrocarbons spraying by shadow photography method

I. Anufriev, E. Shadrin, E. Kopyev, O. Sharypov, Y. Osintsev, M. Mukhina

A promising method for spraying liquid hydrocarbons by a high-speed jet of superheated steam was studied experimentally. Information on the disperse composition and structure of the gas-droplet flow during the spraying of used transmission automotive oil was obtained using the method of shadow photography. Size distributions of fuel droplets were obtained in a wide range of operating parameters (flow rate and temperature of steam, fuel consumption).

4 - RANS Simulation of Turbulent Non-Premixed H₂/Air Combustion

H. Dong, J. Liu, X. Bai, Y. Wei

The velocity of the incoming air in the combustion chamber of the scramjet engine is very high ($M > 1$), and the residence time of the combustible gas in the chamber is on the order of milliseconds. In such a short period of time, the mixing and chemical reaction are completed, and therefore, it is very important to be stable with the flame. In addition, shock waves are generated in the supersonic flow field, and there are complex interactions such as shock/flame, shock/boundary layer, shock/turbulence in the combustion chamber. In summary, there are complex problems in self-ignition, partial flameout, re-ignition, shock and turbulent combustion in scramjet engines. Supersonic non-equilibrium chemical reaction flow has been showing great complexity in numerical simulations due to the complicate physics-chemistry interactive phenomena. Especially, the space-time multi-scale essentiality causes significant numerical difficulty, for instance, rigidity or stiffness of the Ordinary Differential Equation (ODE). A modified uncoupled method, which follows the idea of Strang splitting and has proved to be simple and efficient for solving the reactive flow system, is applied with using unstructured finite volume discretization and detailed reaction mechanisms.

144 - Investigation of characteristics of diesel fuel atomization by steam jet

W. Ji, Y. O. Sharypov, I. Anufriev, E. Shadrin, E. Kopyev, V. Leschevich

The disperse composition of the gas-droplet flow was studied experimentally when spraying diesel fuel by a jet of superheated steam in a burner device with good prospects. The studies were performed using the method of shadow photography (SP). In a wide range of operating parameters (steam and fuel flow rate) corresponding to the area of stable operation of the burner, size distributions of fuel droplets were obtained. Dependences of the droplet size in the flow on the steam and fuel flow rate were determined.

355 - Further investigation of hydrogen flame colour

M. Pan

Hydrogen flame colour is often commonly described as colourless. However, in a controlled laboratory condition with careful imaging, the flame appears reddish. There have been researches reporting a variety of colours generated from hydrogen flames. Nevertheless, there isn't a definitive conclusion to explain the phenomenon. This paper reports a very probable cause for the redness of hydrogen diffusion flame by means of spectroscopic imaging.

214- Effect of CO₂ dilution on combustion characteristics of a liquid fuel-fired flameless combustor

S. Sharma, S. Kumar, H. Lal, A. Chowdhury

Effects of CO₂ dilution on combustion characteristics such as temperature distribution and gaseous emissions are studied experimentally. The combustor operates in the flameless mode for the range of operating conditions studied here. Kerosene is used as fuel for the present study. Thermal input is

varied between 30 kW-53. 23 kW and the air preheat temperature is kept as 800 K. The dilution level is maintained at 9% by volume of the total air. CO₂ dilution results in reduced temperatures at all locations in the combustor. CO₂ dilution has a negligible effect on the CO emissions in flameless mode, however, NO_x emissions are observed to affect significantly.

195 - Study of ignition delay in mixtures of diesel, biodiesel and ethanol

S. Hanriot, D. Guimarães, O. Valente

This work aims to study the measurement of ignition delay in mixtures of diesel, biodiesel and ethanol. The demand for fuel that achieves higher engine energy efficiency and lower emissions of polluting gases is increasing in the academic and industrial areas. Therefore, there are several studies on the possibility of using blends of diesel, biodiesel and ethanol in compression ignition engines. However, the combination of fuels interferes with the ignition delay time according to the amount of each type of fuel. This delay is an important parameter to determine the quality of the burn. The shock tube is an instrument capable of quantifying this phenomenon, and the ignition delay is the time interval between the onset of the shock wave and the moment of ignition. This delay is greater in mixtures with a lower cetane number. In this work was designed a Data Control and Acquisition System that would guarantee the repeatability of the experiments and was analyzed the delays ignition of 5 types of fuel: diesel B7 (diesel mixed with 7% of biodiesel) and diesel B7 mixed with 5, 10, 15 and 20% of ethanol. The ignition delays measured in these mixtures should be known to determine the timing of injection of these types of fuel mixtures in the internal combustion engine so as not to damage it. These delays were higher as the addition of ethanol. The longest time of delay ignition measured occurred in the sample with the highest percentage of ethanol, corresponding to 23,48,17,10 milliseconds more than diesel B7.

308 - Kinetic modeling for PAH formation in a counterflow diffusion flame of isobutane

W. Chiu, H. Tao, K. C. Lin

In the purpose of understanding the complex chemistry of aromatic hydrocarbon formation in diffusion flames of isobutane oxidation, mechanism that consists of 300 species and 11790 reactions is employed for verifying experimental measurements. The kinetic mechanism is incorporated into a 1-D axisymmetric laminar finite-rate model of a counter flow flame to compute the species profiles. Furthermore, the reaction pathway diagram produced by rate of production analysis illustrates the correlation between the decomposition of isobutane and formation of the target species.

110 - Numerical studies of hydrogen-enriched partially premixed combustion on a model gas turbine combustor

J. Nam, J. Yoh

The most commonly used method for the operation of gas turbines is the combustion of natural gas, which is composed of several hydrocarbon mixtures. In this study, simulations are carried out on a hydrogen-enriched partially premixed model gas turbine combustor. Synthetic gas consisted of methane and hydrogen is considered as the working fuel and the influence of hydrogen composition in the reactive flow is investigated. For accurate simulation of the swirl-stabilized flame inside the combustor, large eddy simulation (LES) is applied within the OpenFOAM framework. Comparisons are made with experimental PIV and OH-Chemiluminescence data for verification of simulation. Changes in the hydrogen composition also affect the combustion instability, and such the related findings are also reported herein.

179 - A Numerical investigation of Combustion Characteristics of Biogas Fuel in a Spark Ignition Engine

M. Bassiouny, A. Ebrahemi, S. Ahmed

Biogas is formed from anaerobic deterioration of organic composites, and its main components are methane (CH₄) and Carbon Dioxide (CO₂) with variations in their proportions. Using biogas can reduce pollutant levels in exhaust gases, including emissions of solid particles and nitrogen oxides. Gasoline fuel and mixtures of CH₄ and CO₂ that represent biogas fuel were tested at different inlet air temperatures using AVL Boost Simulation model on a single-cylinder Spark Ignition Engine to investigate the combustion characteristics of biogas fuel in engine. The study was performed in control simulation with a general species chemistry. The fuel data input species contains gasoline, CH₄, CO₂, O₂, N₂, H₂O, CO, H₂, H, O, NO. The fuel species setting refer of volume based fraction from 10%

to 40% of CO₂. The results showed a reduction in the peak pressure inside the cylinder as well as the maximum pressure rise rate (dP/dt)_{max} with the increase in CO₂ concentration in the fuel. The maximum reduction was about 23% for the peak pressure and about 44% for dP/dt when the CO₂ ration increased to 40% comparing with those of gasoline fuel. Moreover, the brake power output decays and bsfc increases with the increase in the CO₂ volume fraction, while the effect of inlet air temperature was minor at all operating conditions.

32 - High Efficiency and Clean Combustion of Converter Gas

Y. Zhai, S. Li

The effects of water vapor concentration in air and inlet temperature of converter gas on converter gas combustion were investigated by numerical simulation. When water vapor concentration in air increases from 0 to 5%, the emission concentration of CO and NO and the peak flame temperature decreases. When the inlet temperature of converter gas is constant, water vapor concentration increases from 0 to 0.7%, CO concentration in converter gas decreases rapidly. When converter gas temperature varies from 1050 to 1150 K, the effect of water vapor on NO is more significant. When the inlet temperature of converter gas increases from 823 to 1153 K, CO emission concentration decreases, NO emission concentration and peak flame temperature increases. At water vapor occurrence, CO is mainly oxidized by OH free radical, it reduces the maximum flame temperature, thus the formation of thermal-NO_x is reduced.

158 - Dynamics of the Low-Temperature Auto-ignition Kernels in Turbulized Hydrogen-Air Mixture

S. Medvedev, S. Khomik, O. Maximova, G. Agafonov, A. Tereza, A. Betev, H. Olivier

The experiments on auto-ignition in turbulized hydrogen-air mixtures were performed at the shock tube operated at over-tailored conditions. The schlieren (shadow) image velocimetry technique was used for evaluation of turbulence intensity. It was shown that appearance and spreading of the autoignition kernel (hot spot) can increase intensity of turbulence in the unburned part of the reactive volume.

87 - Multiphase LES Analysis on Kerosene/H₂O₂ Combustion of a Slit Injector

J. Kang, Y. Yoo, H. Hwang, H. Sung

In this study, kerosene/H₂O₂ multiphase combustion characteristic of the slit type pintle injector is analyzed. To consider the pintle moving, conformal sliding mesh technique is employed. At the gas phase, the Eulerian approach is used to solve the gas phase physics, and at liquid phase, the Lagrangian approach is used to analyze the liquid phase physics for calculation efficiency. Also, a LISA-RT breakup model is implemented to predict the liquid film and ligament breakup process. And dynamic SGS model of an LES is implemented to simulate the turbulence effect. The flamelet model is employed for turbulent combustion model.

15:30 Dust

6 - Analysis of Explosion Dynamics from Dust Cloud Metal Particle using Thermal Infrared Imaging

S. B. Tombet, F. Marcotte, A. Huot, L. Yi

Many working environments are at significant risk of explosions. Dust cloud explosions are especially insidious, as powdered material in suspension in the air is exposed to a lot more oxygen than solid flammable materials, and thus burn extremely rapidly. Moreover, dust cloud explosions are often caused by ordinary and otherwise harmless materials, such as flour, coal or pollen, that can be ignited by an unsuspecting source of energy, such as an electrical spark or a hot surface. Many powdered metals, such as aluminum oxide and magnesium, can also be dangerous explosives when they are in suspension in the air. The understanding of dust cloud explosions therefore is critical to ensure the safety of workers. In order to study the thermodynamic processes involved in such explosions, scientists need to understand the characteristics of the ignition, the explosion and the propagation.

375 - Study on heating process of micro-sized aluminum particles in planar flame

J. Li, X. Gu

In order to understand heating process of aluminum particles in planar flame, a single aluminum particle heating model is established to analyze the heating process of the aluminum particles in the preheating stage. By comparing heating time of the model in the preheating stage with experimental results of literatures, the accuracy of heating model is verified. The heating model is used to study heating time variation of micro-sized aluminum particles in the preheating stage under different flame temperatures and different particle sizes. Results show that the single-particle heating model established in this paper fits well with the experimental results of literatures and can be used as a model for the preheating stage. According to analysis, preheat time is affected by flame temperature and particle size. For a particle size of 10 μ m aluminum particles, as flame temperature increased from 1000 K to 3300 K, heating time is reduced to 1/100. When flame temperature is 1500K, as particle size increased from 1 μ m to 100 μ m, heating time is increased by about 104 times. It's found that, during heating process of aluminum particles, convective heat transfer between flame and particles is the main source of heat transfer.

272 - Combustion Behavior of Acoustically Levitated Biomass Particle

T. Matsuoka, Y. Nakamura, T. Kajimoto

The acoustic levitation system using high intensity ultrasonic waves is developed to examine its applicability to a burning solid particle. The acoustic levitation system consists of a Bolted Langevin type transducer and a reflector and it enables to generate the acoustic standing wave in between the horn and the reflector. A cellulosic particle of 4 mm diameter is chosen as fuel sample. Byigniting the particle prior to placing it into the standing wave field, the combustion process of levitated particle without any supporting devices is successfully visualized. It was found that the combustion takes place only in a part of the particle while there remains an unburnt part until the end of the test. A series of experiment are then conducted under various input power conditions to investigate an effect of acoustic standing wave. From the result shows it is deduced that the combustion of the particle in the standing wave follows the d-square law and thus quasi steady, one-dimensional combustion is attained. It is also shown that Furthermore, the combustion rate constant increases as the input power increases for moderate input power.

262 - Explosion Characteristics of Coal Dust with Different Metamorphism Degrees

B. Nie

To study the propagation characteristics of coal dust uniform dispersion explosion under different metamorphism, 19 coal samples including anthracite, bituminous coal, lignite were selected, and explosion pressure distribution flame propagation velocity were studied. The experimental results suggested that: In the case of coal dust uniform dispersion, the reaction of coal dust with high metamorphism degree is slow at the initial stage of explosion. Moreover, the lower coal rank, the higher the explosion flame propagation velocity and the rising rate of pressure. Therefore, from lignite to anthracite, the maximum explosion pressure and flame propagation velocity of coal dust first increase and then decrease.

304 - Mechanisms of Silicon Combustion in the pSi-CO₂ and pSi-CNaClO₄H₂O Systems

V. Mironov, O. Penyazkov, P. Krivosheyev, E. Golomako

The behavior of pSi-CO₂ system at elevated pressure and spark ignition have been investigated. Analysis of dynamics of pSi-CO₂ combustion and post combustion cross-sectional SEM images of samples at small and medium pressures of oxygen give us the possibility to describe characteristics and to explain the physical essence of the phenomena that occur during the ignition of this system. Porous silicon layer is properly a block of densely packed elements of solid fuel. Such system at pressures of oxygen more than 15 bar and with supply of a small energy pulse is transformed, at the expense of destructive mechanical deformations, to suspension with multiple increase of the surface and jumpwise increase of the mass rate of combustion. Such behavior is caused by ejection of these elements to the gaseous medium with subsequent aerosol combustion of these particles. When replacing gaseous oxygen with a solid-state oxidizer, the energy efficiency and power of the system based on the material with such properties should increase many times. It was confirmed by experiments with spark initiation of the pSi-CNaClO₄H₂O system with various parameters of the structure of porous layers.

313 - TG-FTIR Study on Effects of Titanium Dioxide Nanoparticles on the Decomposition of HAN Aqueous Solutions

M. Wu, H. O. Yang, C. You, J. Chin

TG-FTIR measurements were performed to study the effects of TiO₂ addition to HAN aqueous solution. The test showed that with 0.657% mass loading, the decomposition temperature was reduced to 119°C from 178°C, and the decomposition rate was increased by ~ 31 times. Both heat flow measurements and FT-IR spectra of the evolved gas verified the reduction of decomposition temperature and the enhancement of decomposition rate. The absorption spectra also indicated that peak concentrations of N₂O and H₂O in the evolved gas became higher with the existence of TiO₂ nanoparticles in the liquid phase.

244 - Ignition and Combustion of Individual Aluminum Particles below 10µm at Different Laser Heating Rates

X. Huang, F. Hou

The ignition and combustion characteristics of individual aluminum particles below 10µm were investigated. A specific experimental setup and corresponding diagnosis method were presented to directly observe the ignition and combustion behaviors. Individual aluminum particles heated by laser at different power density undergo similar several stages, including thermal expansion, alumina shell rupture, molten aluminum core overflow, shell melt and aluminum evaporation, ignition and combustion of aluminum vapor. This work will be beneficial to further extend the investigation of submicron individual metal particles and reveal their combustion mechanism by direct observation.

331 - Determination of Burning Rate of Gas Generator Compositions Based on Sodium Nitrate

M. Atamanov, Z. Mansurov, S. Tursynbek, D. Bayseitov, F. Abdrakova, M. Tulepov

In this paper, we have studied methods for determining the burning rate which is easy and affordable, continuously measuring the current mass or linear burning rate. The results are presented after processing with the help of modern programs. And also we studied the effect of size components and their ratio in the burning rate.

120 - Propagation of a strong shock wave in a random bed of metal particles

S. Choi, J. Yoh

When a strong shock wave collides with a particle, complex flow structures are generated due to the distortion of the incident pressure wave and the mechanical deformation of the particles; the diffraction of the rarefaction waves develops in various forms due to the interactions between the shock wave and the downstream particles. In addition, metal particles which are combustible can burn and spherically expand into atmosphere, which is a complex phenomenon not easily understood due to the interactions between a large number of metal particles and the strong shock waves generated from an energetic material. Metal particle additives in an energetic material enhance the multiple reaction functionality due to the afterburning characteristics of the particles. Such secondary reactions following a primary detonation of an explosive allow for a longer duration of overpressure, which is an intended thermobaric effect. To understand the extended burning at high pressure condition of such metalized energetic materials, it is necessary to identify the detonation from the subsequent deflagration of the metal particles. Recently, Mehta et al. [1] compared and analyzed the interactions between a single particle of a cylindrical (or spherical) rigid body and a shock wave in a 2D geometry. Ling et al. [2] considered the deformation of a particle impacted by a shock wave. As the impact pressure was applied, the rounded particle was gradually deformed into a flat shape and vortex shedding occurred.

15:30 RDE

11 - Effect of Wall Viscosity on Flow Structures in 3-D Rotating Detonation Wave

P. Liu

Using hydrogen/air mixture with 7-species-and-8-reaction chemical model, four 3-D cases of rotating detonation simulation are performed with different numerical models and wall boundaries, in order to investigate the effect of wall viscosity on flow structures. Wall viscosity has notable effect on the flow structures in 3-D rotating detonation wave. It will lead to the extension of deflagration area and the occurrence of reactant deficit zone. The formation mechanism of reactant deficit zone is explained.

23 - Numerical prediction of the detonation wave number

Q. Meng, N. Zhao, H. Zheng, J. Yang, L. Qi

In this paper, three-dimensional numerical simulations are performed to investigate the transition boundary of propagating mode switch of rotating detonation wave (RDW). Considering the combustion efficiency, the transition line of single-wave to dual-wave mode is obtained. The numerical results show that low combustion efficiency reduces the height of RDW, leading the RDW easily locates in the single-wave mode region. Additionally, for current combustor, Case #4(=1. 2, total=0. 1036kg/s, wch=5mm) are close to the transition line, indicating that it easily switch to dual-wave mode when the total mass flow rate increases. Similarly, Case #1(=0. 6, total=0. 1018kg/s, wch=5mm) will switch to single-wave mode when the total mass flow rate decreases.

26 - Effect of Expansion Outlet on Continuous Rotating Detonation Combustor

C. Sun, N. Zhao, H. Zheng, J. Yang, G. Hongbo

Continuously rotating detonation combustion chambers should be coupled with downstream supersonic turbines in practical applications. In view of the fact that the size of a CRDC (continuously rotating detonation combustor) usually cannot directly match with turbine, a variable cross-section design of the outlet structure of CRDC is required. In this paper, the three-dimensional numerical simulation of CRDC with methane/air premixed air is carried out, which proves the feasibility of continuous rotating detonation wave propagation in the variable cross section outlet combustor, and then the CRDCs of different expansion angles are researched. The results show that changing the outlet section of the combustor for coupling with the turbine would sacrifice the pressure gain performance of CRDC, which would greatly reduce the attractiveness of detonation combustor, and at the same time, changes in the exit interface would reduce the static temperature and static pressure of the combustor outlet, and increases the outlet flow rate, which is beneficial to improve the outlet temperature distribution unevenness and the combustor outlet pressure load.

27 - Investigation for delay time of rotating detonation fueled by hydrocarbon-hydrogen mixture

Y. Zhong, Y. Wu, D. Jin, X. Chen, X. Yang

Experiments were conducted to investigate the effect of mixture components, flow rates and equivalence ratio on the delay time of the rotating detonation initiation. The results showed that the delay time decreased when the mixture activity increased and the equivalence ratio approached the stoichiometric ratio. The wider stable operating range at higher flow rates also could decrease the delay time of the initiation and the delay time in the stable operating range sustained at a low level.

44 - An Analysis of the Performance of a Continuous Rotating Detonation Engine

S. Huang

The engine needs to meet at least two conditions to produce the thrust effectively: a) transform heat energy into mechanical energy as high as possible; b) the converted mechanical energy is used to propel the engine as high as possible. If the mechanical energy converted from heat can't be effectively used to propel the engine, then high thermal efficiency will be meaningless. The stability of the detonation wave in the combustion chamber is artfully realized by the detonation wave moving along a circle. However it also pays for it, which has improved the difficulty of using mechanical energy to propel the engine. The circumferential motion of detonation wave causes some kinetic energy to be wasted on the circumferential motion, which is not helpful to increase the axial thrust of the engine. If the kinetic energy of the circumferential motion can not be reasonably utilized, it will inevitably cause the performance loss of the rotating detonation engine, and even cause the characteristics of high thermal efficiency of detonation engine can not be reflected at all. However, it is not easy to convert the kinetic energy of circumferential motion into that of axial motion. Because the circumferential motion will bring about strong non-uniformity of flow, the total pressure of flow loses very quickly in the process of downstream transportation. To reduce the loss, it is necessary to complete the transformation within as short a distance as possible, and the transformation must be carried out under the condition of strong non-uniformity of flow. The design difficulty of nozzle is greatly increased.

57 - Numerical Simulation of Reactive Gas Mixes Flows in the Detonation Engine

M. Sergey

Conservative mathematical models with accurate energetic balance are needed for correct numerical simulation of detonation wave appearing and propagation. Mathematical model of this type was used

for numerical simulation of flows of reactive gas mixes, namely model based on the full system of gas dynamics equations accompanied with the system of kinetics equations in the integral form. The state equations of real gas for every component of gas were used. Transition to characteristic variables of full system of the equations for any number of components of gas mixes is carried out. Numerical simulation of flows in the combustion chambers of detonation engine was carried out. Structure of flow for this engine was investigated. Boundary conditions for flow from Laval's nozzle for regimes with periodically closing, was discussed.

61 - Experimental Investigation of Pulse Compression Detonation System

K. Korytchenko, O. Sakun, C. Senderowski, D. Dubinin, V. Nikoluk, B. Maxwell

The PCD-system uses a phenomenon of a supersonic combustion where detonation inside a tube generates an impulse by compressing a reactive gas and whose products expand rapidly at the open end. A pulsed mixture compression at the closed end of the detonation tube is generated by a piston compressor in such a manner that the mass flow rate at the closed end of the tube exceeds the mass flow rate at the open end of the tube. This causes compression of the air-fuel mixture within the tube. Detonation is then initiated when the mixture is compressed. In this work, we found that by pre-compressing the reactive mixture in a detonation tube, detonation was much easier to achieve in practical tube sizes, owing to reduced cell sizes and increased sensitivity of the mixture to detonation. Moreover, consistent deflagration to detonation transition times were achieved. As a result, we believe the proposed PCD system can be used to improve detonation engine performance data such as efficiency, operating frequency, detonation tube size, fuel consumption, operating cost, etc. In this paper, we present the principle of the PCD-system operation in detail and present the results of the experimental investigation accordingly. A number of useful applications for the PCD-system have been proposed.

98 - Numerical Simulations of Compression and Detonation Strokes in a Pulse Compression Detonation System

B. Maxwell, K. Korytchenko, O. Shypul

At the National Technical University Kharkov Polytechnical Institute, Ukraine, an experimental pulse compression detonation (PCD) system was developed to operate on propane-air mixtures, while addressing potential issues with regards to efficiency, ignitability of the gas, and the critical tube diameter for detonation. In this PCD system, the reactive gas was pre-compressed within the detonation tube, prior to ignition. As a result, the mixture was easier to ignite, and the transition to detonation within the tube was much more reliable and consistent. To gain further insight, and to investigate the influence of pressure gradients on the detonation tube outflow process and cycle efficiency, a two-stage modelling procedure was adopted. First, a 3D inert simulation of the compression process of the PCD system was modelled using ANSYS.

109 - Numerical Investigation of a Non-premixed Rotating Detonation Engine with Different Number of Fuel Injectors

J. Sun, J. Zhou

Rotating detonation engine (RDE) is one type of the promising detonation-based engines. Propellants are injected at one end of the combustion chamber, and one or more detonation waves propagate circumferentially at the head end of the combustion chamber consuming the freshly injected propellants. The products exhaust from the combustion chamber at the other end with high axial velocities to produce thrust [1]. Compared to pulse detonation engine (PDE), an RDE can operate continuously once ignited, and the operating frequency is very high. Additionally, an RDE has a compact structure, and can operate under a wide range of Mach-number flighting conditions. Therefore, RDE has received much attention in the propulsion research field. Many countries performed experimental and numerical investigations on RDE, including Russia, Japan, France, America and China.

116 - Numerical Investigation on non-premixed Rotating Detonation Engine with Different Exhaust Nozzle Configurations

S. Xue

Three-dimensional numerical simulations were conducted on a non-premixed rotating detonation engine (RDE) with different exhaust nozzles (i.e. without a nozzle, with a divergent nozzle, with a

convergent nozzle, and with a Laval nozzle). Aside from describing the flow-field structure inside the chamber, the detonation wave height, the average propagation velocity of the detonation wave, and the outlet Mach number were also investigated. It is found that the minimum cross section reaches a critical state for the convergent nozzle and the Laval nozzle, but there is a subsonic region at outlet for the divergent nozzle. By the reflected shock waves, the convergent and Laval nozzles make the flow-fields more complex in chamber, but it makes the Mach number distribution more homogeneous in exit.

124 - Numerical Investigation of Effect of Wall Curvature on Detonation Propagation in an Annular Cylinder

M. Gui, H. Cui, H. Zhang

In rotating detonation engine (RDE), the curved wall can continuously make convergent/divergent effects. Hence, detonation propagation in an annular cylinder is more complicated than that in a straight tube. Detonation propagation in an annular cylinder with various inner and outer radii is numerically studied using the two-dimensional reactive Euler equations with detailed chemical kinetic mechanism. Effect of wall curvature on detonation propagation is analyzed based on detonation cellular structure for several rotations. The results show that decrease of the outer wall curvature and increase of the inner wall curvature are equivalent, which can both lead to weakness of detonation around the inner wall. Thus, the inner and outer radii should be appropriately chosen to keep a balance between inner rarefaction and outer compression in order to maintain self-sustaining detonation in the annular cylinder.

149 - Frequency Locking of Global Unstable Lean Premixed Bluff Body Stabilized Flame with Acoustic Excitation

P. Liu, J. Feng, X. Lv

In this study, the frequency locking response of a lean premixed flame in a duct combustor have been investigated in the presence of acoustic excitation. ;BVK flame does not respond significantly to low amplitude acoustic excitation, but higher amplitude excitation can make a BVK flame transition to large-scale symmetrical oscillations, and frequency locking is observed at high excitation amplitudes. The lock-in analysis reveals that the lock-in amplitude (A_{lock}) reaches the minimum value when the excitation frequency is close to the vortex shedding natural frequency. Consequently, it is found that lock-in amplitude rises monotonically as ff diverges from fn as the excitation frequency is near the natural BVK frequency. Furthermore, the lock-in amplitude drops suddenly at sub-harmonic and first harmonic of the natural BVK frequency.

161 - Influence of the combustion wave velocity in a mixture on the thrust of a pulsed detonation combustor

M. Assad, O. Penyazkov, I. Chernuho

The dynamics of the propagation of a combustion wave in the PDC and the thrust created by the jet flowing out of the combustor are studied. It is shown that the change in the PDC thrust has a direct dependence on the dynamics of the combustion wave velocity, with both characteristics having an inverse dependence on the degree of enrichment of the mixture with fuel. The maximum velocity of the combustion wave (2500 m/s), and accordingly, the maximum thrust (200 N) are reached by burning near-stoichiometric and slightly fuel-enriched mixtures ($f = 0.95$ C1. 20). The mixture enrichment up to $f = 2.57$ leads to a drop in the wave velocity to 500 m/s and below (80% of the maximum velocity and more), and in the thrust to 60 C50 N (70-75% of the maximum thrust).

178 - Investigation on Self-sustaining Mechanism of Wedge Supported Oblique Detonation Waves for equilibrium flow

A. Wang

Detailed equilibrium chemical reaction was used to improve the transition patterns model. Through detailed analysis and calculation, results show that the determining factors for the transition pattern include the initial inlet Mach number Ma, equivalence ratio, wedge or cone angle and static temperature T1. Critical transition pattern of ODW has been obtained when 1.

229 - Experimental Research on Ignition and the Stabilization Process in Rotating Detonation Chamber

Z. Ma, Y. Hao, S. Z. Zhang, J. P. Wang

This study presented experimental research on ignition and the stabilization process in hydrogen-air rotating detonation engine with an array of injection holes. The stabilization process can be divided into six sections, including deflagration, deflagration to detonation transition (DDT) process, the coexistence of detonation with deflagration, the coexistence of strong weak detonations, unstable to stable detonation transition and stable detonation.

246 - Wave Direction Studies in Rotating Detonation Engine

M. Kawalec

The article deals with the issue of wave directionality in RDE engines. Responding to the questions: Why is this important and why is it worth finding a way to point waves in the RDE engine? The tests were carried out in a detonation combustion chamber for a hydrogen-air mixture. The chamber has been adapted so that the direction of the wave spinning can be unambiguously determined. Three methods were tested: synchronized initiators, an element that hinders the formation of a wave in one direction, and an eccentric chamber. One of the methods achieved 100% effectiveness during experiments. An attempt was made to find the mechanism of operation of this method by numerical method.

249 - Numerical Simulation of the Rotating-Detonation Process with Nonpremixed Injection of Hydrogen and Air

D. Li, Y. Zhang, G. Liang

The rotating detonation engine (RDE) is an intriguing approach to achieving pressure gain combustion and higher thermal efficiency of cycle for propulsion and power systems. A large amount of experimental studies have fully proved the feasibility of RDE. In this study we design a rotating-detonation combustor (RDC) and calculate the mixing process of the air and hydrogen, then simulate the operation of the RDC with hydrogen and air supply separately and compared the differences of RDC under different injection pressures. The results indicate that as the injection pressure of fuel increases, the peak pressure and peak temperature and velocity of the DC and the total pressure along the distance of RDC increase.

276 - The Comparison of Detonation Diffraction and Re-initiation in the Static and Supersonic Inflow

L. Hongbin, J. Li, W. Fan

Supersonic propulsion systems based on detonation wave have attracted great interest in recent years. The initiation of detonation wave in the supersonic inflow is important to the application of detonation wave engines. In this work, the detonation diffraction and re-initiation processes in a confined channel (with the influences of reflections) were investigated, and the detonation is initiated by a pre-detonator that is transversely placed at the side of main channel. The differences of detonation diffraction and re-initiation in the static and supersonic inflow were quantitatively compared in this paper. In the static flow, the critical width w_d of initiation channel for a successful re-initiation was 5.5 (is the width of detonation cell), approximately. However, the critical width w_d of initiation channel is decreased to 3.0 in the supersonic flow. The reason is that the emerged flow is compressed at the upstream side by the supersonic flow, which results in the increase of the initiation energy. Hence, the generations of transverse waves can be occurred subsequently even though the width of initiation channel is less than 5.5.

294 - 3D simulations of a Non-Premixed Continuous Rotating Detonation Ramjet Engine Fueled by Hydrogen

D. Xiong, M. Sun, H. Wang, S. Liu

The continuous rotating detonation engine (CRDE) has drawn more and more attention because of its high efficiency and simple configuration. Many researchers have carried out in-depth research on the detonation wave, flow field structure and propagation characteristics of continuous rotating detonation. However, the existing literature of CRDE simulations are mostly based on idealized fully premixed gas. In practice, the air and the fuel enter the combustion chamber separately, hence the mixing of air and fuel has a significant importance on the performance of combustion and the sustainability of detonation wave. Three dimensional simulation is also necessary due to the three dimensional characteristics of the mixing process. The focus of the present work is to analyze the

mechanisms of mixing process and propagation characteristics of the detonation wave in a model continuous rotating detonation ramjet engine under the condition of Mach 2.5. 2 Numerical method the simulation Software is based on the STSCFD3D developed by the Science and Technology on Scramjet Laboratory, National University of Defense Technology. The LES method is adopted in this work. And the finite rate chemistry is employed to resolve the reacting flows with overall H₂/O₂ reaction mechanism. The basic size of the grid is 0.5mm meanwhile the total cell number is 6.75 million.

296 - Adaptive Mode Switching Process of Rotating Detonation Engine

S. B. Yao, M. Y. Luan, J. P. Wang

The mode switching process in the rotating detonation engine (RDE) due to the change of inlet conditions is numerically explored and analytically explained. Once a quasi-stable rotating detonation flow is obtained, the inlet total pressure of reactant reservoir is decreased and maintained at the low level for some time, in order to observe the feedback on the RDE. It shows that instead of being quenched immediately, the RDE adapts to the change of inlet conditions by a mode switching; it decreases the number of detonation waves and begins to run in a new operation mode. Overall, RDEs adapt to the fluctuation of inlet conditions successfully, and, what's more, swiftly, demonstrating high adaptivity. Theoretical analysis indicates that, for a stable multi-wave RDE, the characteristic parameters of rotating detonation waves are determined by both geometry of combustors and inlet conditions.

302 - Number Change Of Detonation Waves In Hollow Continuous Detonation Chamber

Z. J. Xia, M. Y. Luan, S. J. Zhang, Z. Ma, J. P. Wang

A three-dimensional numerical simulation of continuous detonation chamber (CDC) with hollow combustor is performed to analyze wave structure evolution systematically. Wave structure evolution is classified into three categories, namely two-wave collision (counter-rotating waves), abscission of detonation tail, and shock wave to detonation transition. Two-wave collision consists of symmetric detonation collision, asymmetric detonation collision, and detonation/shock collision. Two symmetric detonation waves turn into shock waves after collision. Collision of asymmetric detonation waves creates single detonation wave. The detonation/shock collision decreases the detonation wave intensity. Abscission of detonation tail and shock to detonation transition can both create single detonation wave or two opposite-direction detonation waves, depending on the wave hitting angle and the amount of fresh gas. All phenomena mentioned above affect the number of detonation waves in the combustion chamber.

307 - Numerical Simulation of Detonation Propagation in the Branch Tubes of the Detonation Wave Ignition System

H. Guo

Numerical simulation was carried out according to the same dimension of the experiment system. Results show the process of the detonation wave propagation in the tubes of the system. The numerical simulation results show that the detonation wave propagate stably along the ignition system with high speed about 3000m/s, high temperature about 2500K, high pressure (about 10 times initial pressure), and the detonation wave ignition system has excellent simultaneous time difference about 0.04ms between different ignition units by distance difference of 120mm. Same conclusion could be drawn from the experiments data.

312 - Control of Detonation Combustion of Hydrogen-Air Mixture in Plane Channels

V. Levin, T. Zhuravskaya

Using a detailed kinetic model of chemical interaction, numerical modeling of detonation combustion of a stoichiometric hydrogen-air mixture has been carried out with purpose of determination of mechanisms of detonation wave control both in a quiescent gas mixture and in a supersonic gas flow.

327 - Analysis of Fuel Mixing Characteristic in Supersonic Combustor with Injection Pressure and Existence of Cavity using Modal Decomposition Method

S. Jeong, J. Choi

In this paper, we were conducted a study to confirm the effect of cavity on fuel mixing in a supersonic combustor which has transverse fuel injection. DMD, a modal decomposition method that can capture

the dynamic behavior of the flow, was applied to analyze the mixing characteristics of the propellant. Through the computational results of the H₂ mass fraction were analyzed by the DMD method, we confirmed how the presence of the cavity according to the fuel injection pressure condition affected the propellant mixing.

352 - Experimental Study on 100 N-scale C₂H₄/GO₂ Small RDE

H. Han, J. Choi

A small-scale RDE is constructed and tested to understand the operational and performance characteristics. The measured thrust performance was compared with that of the ideal rocket engine calculated by the NASA CEA code. The results suggest that C-D nozzle or plug nozzle is essential to improve the thrust performance of RDE. This suggestion is also shown in the simple thrust comparison with conical center body and bluff body. The thrust with conical center body was improved by 10 ~ 30% than with bluff body in present experiment range. For more accurate comparison of the RDE and the conventional rocket engine, it would be necessary to conduct an experimental comparison with equivalent shape and operating condition. A technical issue arose during the experiments should be compensated for further experiments. The occurred ablation at around holes appeared to be prominent from the lean condition and the choking condition of the combustor. It would be necessary to minimize the inner diameter of the pre-detonator and other things to reduce the ablation.

13:20 Detonations/Explosions**178 - Investigation on Self-sustaining Mechanism of Wedge Supported Oblique Detonation Waves for equilibrium flow***A. Wang*

Detailed equilibrium chemical reaction was used to improve the transition patterns model. Through detailed analysis and calculation, results show that the determining factors for the transition pattern include the initial inlet Mach number Ma , equivalence ratio, wedge or cone angle and static temperature T_1 . Critical transition pattern of ODW has been obtained when $\lambda=1$.

407- Investigation on Damage Norm and Criterion of the Shock Wave in Underwater Explosion*J. Zhang, S. Wang*

In this study, the applicability of various forms of power parameters including peak pressure, energy flux density, and impulse of the shock wave in underwater explosion as damage norm and criterion was first examined, and universal damage norm and criterion of the shock wave in underwater explosion were proposed. Based on the explosion similarity law, the limits of peak pressure, energy flux density, and impulse of the shock wave in underwater explosion as the damage norm and criterion were analyzed, and a general form of the damage power parameter was proposed as, in which denotes the explosive charge, denotes the explosive distance, and is an undetermined coefficient. Through dimensional analysis, the functional relationship between and structure damage was derived. It was proposed as a general form of damage norm and criterion of the shock wave in underwater explosion. Next, using infinite element analysis software AUTODYN, the effects of the shock wave in underwater explosion on two target scircular plate and cylinder were simulated, and the iso-damage curves in which different damage power parameters were used as the damage norm and criterion were plotted and compared. The results show that the proposed general form as the damage norm and criterion of the shock wave in underwater explosion is scientifically reasonable, universal, and practical to use and can also be regarded as a combined damage norm and criterion of peak pressure and impulse.

410 - Numerical Study on the Oblique Shock Wave in a Surrounding Fluid and Detonation in a Cylindrical PETN*Y. Sugiyama, T. Homae, T. Matsumura, K. Wakabayashi*

In this paper, the oblique shock wave in a surrounding fluid and the detonation in a cylindrical PETN were studied, and the two-dimensional axisymmetric simulation of the detonation in the PETN with infinite length were conducted. The surrounding fluid is modeled as the ideal gas equation of state in which the specific heat ratio is a parameter. The detonation in a PETN showed the steady propagation with curved front. The oblique shock wave in a surrounding fluid is attached at the detonation wave at PETN/ideal gas interface when the specific heat ratio is smaller than a critical value. We measured the detonation/shock angle and the contact-surface angle between the detonation products and the ideal gas. To understand the flow properties near the detonation, we modeled the flow as the planar CJ detonation in a cylindrical charge and oblique shock wave in a surrounding fluid, and theoretically estimate

the flow properties behind them as 1) Prandtl-Meyer expansion of the detonation products from CJ state with zero degree of the deflection angle from the center axis, and 2) conical flow of a surrounding fluid by the Taylor-Maccoll equations. Detonation products reduce its pressure with increasing the deflection angle from the center axis.

414 - Experiment and Numerical analysis for H₂-air Rotating Detonation Engine with Water Cooling System*W. Koido, E. Dzieminska*

The goal of this study is to evaluate the stability of RDE (rotating detonation engine) thrust with water cooling system. Outer wall diameter of this RDE is 115 mm and inner one is 95 mm. The combustion chamber is 10 mm in width which satisfies conditions for detonation propagation. Initiator with a conventional spark plug is placed to ignite a stoichiometric mixture of hydrogen and oxygen as a pre-detonator (Figure 1). By using the detonation wave from initiator, RDE starts running. The gas mixture in the main chamber is air and hydrogen. Air is injected through a circumferential slit located on the outer wall of the combustion chamber, whereas hydrogen is injected through axial 80 orifice holes, which have 1 mm in diameter. There are 3 types of data which are measured, thrust of RDE, speed of

rotating detonation wave, and temperature of cooling water by using load cell, high speed camera and thermocouple respectively. By comparing data of cooled and not-cooled RDE, the effect of water cooling to RDE performance is obtained. At this stage, initiator and RDE need to be tested. In addition, numerical analysis is used to predict results of experiments and to evaluate not only temperature change but also pressure change in combustion chamber which is not measured in experiment.

415 - A Study on Operating Conditions of Disk-Type Rotating Detonation Engine

H. Kawana, W. Kurata, K. Ohno, K. Ishii, A. K. Hayashi, N. Tsuboi, K. Ozawa, T. Obara, S. Maeda, E. Dzieminska, T. Mizukaki

A disk-type rotating detonation engine was newly constructed to study its stable operating conditions. Hydrogen is introduced into the combustion chamber through orifice holes and is mixed with air which is supplied from a circumferential slit. This hydrogen-air mixture flows radially inward and consumed by rotating detonation. The combustion product is centralized and exhausted in the axial direction to atmosphere. A special attention was paid

in designing the combustion chamber so that its cross-sectional area along the flow path keeps constant up to the exhaust gas outlet. To estimate the operation frequency of rotating detonation waves, two pressure transducers (Kistler 603B1) were flushmounted on the chamber wall. From the obtained pressure histories, in which sharp pressure rises typical of detonation waves were detected, the operation frequency was measured for various mass flow rate. It is found that in the present test condition the operation frequency is insensitive to the mass flow rate, which is not the case with conventional rotating detonation engines. The equivalence ratio of the mixture is found to affect the operation frequency for the mass flow rate of 290 g/s. The maximum operation frequency is obtained around the equivalence ratio of 1.2.

416 - Effect of bluff bodies on DDT

L. Wang

We report an experimental investigation of detonation propagation in a tube filled with bluff bodies. Experiments were carried out in a 6m long rectangular cross-section (112mm 107mm) tube. Firstly, the effect of an array of cube bodies (60mmX60mmX60mm) on the detonation propagation characteristics were studied. Hydrogen, ethylene and acetylene mixed with air and hydrogen-oxygen diluted with argon were used as the test mixtures. Evenly spaced photodiodes were mounted on the top wall to recorded the optical signals, from which the detonation velocity could be determined. Soot foils were adopted in hydrogen-oxygen-argon mixture to record the evolution of the cellular structure. The results show that the flame accelerates rapidly in the obstructed tube. The critical conditions for deflagration to detonation transition (DDT) are found to be consistent with $L/d > 7$, where $L = (S+a+H)/2 / (1-(1-BR)^{1/2})$ is the modified characteristic geometrical size for the tube with repeated cubes and d is the detonation cell size.

417 - Influence of transversely supersonic inflow condition on the diffraction and re-initiation process for regular and irregular detonation wave

H. Li, J. Li

For the application of detonation wave in the supersonic propulsion, it is significant to initiate the detonation wave in the supersonic flow. In general, it is an effective and common way to initiate the detonation wave with the aid of a pre-detonator both in the static and supersonic flow. The outcome of detonation diffraction and re-initiation is not only decided by the geometry of confinement, but also decided by the characteristic of detonation wave, i.e. the stability between the detonation fronts in undiluted (unstable) and diluted (stable) mixtures. Moreover, the stability of detonation wave can be characterized as the observed degree of cellular regularity. Subsequent studies shown that the empirical correlation breaks down in the regular detonation wave whose critical diameter for successful re-initiation can be up to 25 or even bigger. d_c and refer to the minimum tube diameter above which a self-sustained detonation can transmit into an unconfined space without failure and the width of detonation cell respectively. Hence, the dominant mechanisms of detonation diffraction and re-initiation are different in two types of detonation waves. The diffraction and re-initiation processes have been widely investigated in the static and subsonic flows, however, the same phenomena have been little discussed in the supersonic flow.

419 - Numerical simulations of induction fronts with nearly-constant propagation speed

V. Robin, A. Chinnayya, S. Taileb, A. Karan

Despite the prolific literature on the deflagration to detonation transition, see among others [1,2], the identification and analysis of the various physical mechanisms involved in the development of a detonation from a subsonic flame is still a challenge. Whatever the physical mechanism that initiates the flame acceleration (turbulence, flame instabilities, heterogeneities, etc.), specific effects due to the multidimensional characteristics of the flow may yield pressure waves or enhance their effects on the upstream gas promoting deflagration to detonation transition. Thus, the main objective of this study is the identification of two-dimensional mechanisms that promote the thermal runaway from subsonic initial conditions. The study focuses on compressibility effects neglecting the influence of dissipative effects. A global step chemistry is also considered to facilitate physical analysis. The subsonic flame considered in the present study is an induction front for which the propagation speed is controlled by setting appropriate initial conditions, see the pioneering work of Zel dovich [3]. The interplay between these spontaneous ignition waves in a gradient of reactivity and pressure waves deserves to be further investigated. This key mechanism first needs to be analyzed in a one-dimensional configuration with initial conditions corresponding to a constant propagation velocity of the induction front. Depending on the ratio of this velocity with that of the sound speed, the analysis would lead to highlight a possible acceleration.

420 - Safety characteristics of hybrid mixtures for explosion protection - Determination methods capable for standardization (NEX-HYS)

W. Hirsch, U. Krause, M. Schmidt, S. Zake, E. Askar, D. Gabel, J. Kleinert, A. Krietsch, J. Meistes, A. Sachtleben, V. Schröder

In this joint project, standardized measurement methods for hybrid mixtures are developed, which serve to determine safety characteristics for explosion protection. A hybrid mixture is a multi-phase system consisting of fuel gas or vapor, as well as air and combustible dust. The results will be published in a final report and as a pre-standard of the German Institute for Standardization (DIN). This pre-standard enables test institutes and industry to assess explosion hazards when operating technical plants with hybrid mixtures and thus to control processes both more safely and more efficiently. Standardization at the international level is supposed to be initiated based on this pre-standard. The project is funded by the Federal Ministry of Economy as part of the WIPANO frame program, which promotes knowledge and technology transfer through patents and standards. For flammable gases, vapors and dusts, there are already standards that define procedures for determining the relevant characteristics. This ensures the comparability of measured values between different laboratories. However, these standards treat gaseous and solid flammable substances separately due to their different explosion properties. For example, the design of the ignition vessels, the ignition sources and the test procedure for fuel gases and dusts differ considerably.

422- Proper Orthogonal Decomposition (POD) Analysis of CFD Data for Two-Dimensional Cellular Detonations

M. Kim, X. Mi, H. D. Ng

Modal decomposition techniques are becoming standard post-processing methods in fluid dynamics to interpret either experimental or numerical data in term of the flow structures and characterize them spatially and temporally. These techniques reduce large amount of flow data into a set of spatial modes for building reduced model aimed to better understand complex flow evolution. In this study, Proper Orthogonal Decomposition (POD) is applied to high-resolution, two-dimensional, numerical simulation results obtained using the reactive Euler equations with one-step Arrhenius kinetics for examining compressible flow instabilities and understanding the underlying mechanisms on the dynamic of cellular detonation structure. CFD data computed using different values of activation energy E_a are analyzed. The results of such modal decomposition analysis help to identify events that contribute the most to the energy of the flow and any dominant or coherent features, ultimately to determine the hydrodynamic thickness of unstable cellular detonation based on the energy mode distribution. In such analysis, Mode 1 corresponds to the mean velocity field in the detonation structure in close agreement with the ensemble average. The higher modal structures describe the vorticity component and different degrees of hydrodynamic instabilities embedded in the two-dimensional cellular detonation wave.

424 - Flame acceleration in presence of polyurethane foam on the channel walls

G. Bivol, S. Golovastov

Flame acceleration in hydrogen-air, acetylene-air and methane-air mixtures and influence of polyurethane foam pore size on flame velocity were experimentally investigated in rectangular cross-section channels with solid walls and polyurethane foam on two channel walls. The combustion channel consisted of 200 mm long driver section with 20 mm inner diameter and a 400 mm long test section with rectangular cross-section. Top and bottom inner surfaces of the rectangular section were covered with porous material. Four types of polyurethane foam were used with a number of pores per inch ranging from 10 to 80. The equivalence ratio (ER) of the combustible mixture ranged from 0.25 to 1. High-speed schlieren image sequences of flame propagation in hydrogen-air, acetylene-air and methane-air mixtures with polyurethane foam on the walls were presented. It was discovered that the flame starts to propagate in turbulent manner earlier when using polyurethane foam with biggest pores. The acceleration of the flame front was the highest in polyurethane foam with biggest pores (10 pores per inch) acceleration was lower in polyurethane foam with 20 pores per inch for all mixtures used in the experiments. Flame acceleration in polyurethane foam with 40 and 80 pores per inch was found to be similar.

425 - Analysis of coupling characteristics between RDE nozzle and combustion

H. Xia, Y. Huang

The rotating detonation engine (RDE) is a new type of dynamic propulsion device based on detonation combustion, which has high thermal cycle efficiency and complex flow characteristics. The efficient utilization of the energy generated by detonation is a major problem in the study of RDE. Therefore, it is important to study the coupling characteristics between RDE nozzle and combustion to solve this problem. In this study, the influence of rotating detonation structure on the nozzle flow and the effect of the nozzle internal flow characteristics on the rotating detonation mode are analyzed, which represents the difference between detonation nozzle and traditional steady nozzle. The governing equations are the N-S equation with the hydrogen-air finite chemical reaction rate model. The explicit scheme solving method was used to control the model and ignore the affection of viscosity, heat conduction and component diffusion transport in the simulation. The inlet boundary of the model is the mass flow inlet with a steady inflow about 0.144kg/s and the outlet boundary is far field boundary (under Mach 4). As shown in Fig 1, the oblique shock wave in the downstream of the detonation combustion chamber is spread into the flow field of the nozzle, and a spiral shock wave system is formed around the nozzle wall surface in the nozzle.

426 - Numerical simulations on ignition using NRPD under high-speed flow conditions

Y. Morii, H. Nakamura, K. Maruta

The lean burn would be one of the solutions to improve the thermal efficiency of SI engines. The advantage of lean burn is that it has a high specific heat ratio and low heat loss. However, ignition becomes quite difficult as high-intensity turbulence is required to enhance flame speed under lean burn conditions. Therefore, a new concept of the ignition system is necessary. In this study, we focused on nanosecond repetitive pulse discharge (NRPD), which is one of the ignition methods using non-equilibrium plasma. Since the ignition phenomenon using non-equilibrium plasma is instantaneous and local, and it is difficult to understand it in detail experimentally. Therefore, numerical simulations were performed on the ignition problem using NRPD under high-speed flow conditions. First, zero-dimensional simulations were performed to determine one-dimensional simulation conditions. The initial conditions of mixture gas were stoichiometric methane/air, pressure 1 atm, and temperature 300 K. The frequency of NRPD was 100 kHz and the discharge time is 100 ns. The reduced electric field was assumed as a sine function of time and maximum reduced electric field were 120, 140, and 160 Td. As a result, in the case of 160 Td, ignition occurred after one pulse, and in the case of 140 Td, ignition occurred after two pulses.

427 - Study on Flame Development using the External Excitation in Baffled Combustion Chamber

W. Song, J. Koo

Since the technology of the liquid rocket engine advances, the high efficiency and high performance is important in the development of the space launch vehicles. The swirl coaxial injector has problems such as the high frequency combustion instability. In order to prevent and detect the combustion instability, the stability rate test has been performed with the external excitation. There are numerous

methods of the dynamic stability, and the pulse gun is a typical measurement method for dynamic assessment. Structural baffle has been widely used as a means to decrease the intensity of the combustion instability. Liquid rocket engines applied this technology to prevent the combustion instability in the combustion chamber. Typically, an injector-forming baffle that the injector inserted in the baffle has been used to protect the combustion chamber from the heat load. However, the baffle injector affects the pressure field in the combustion chamber during the combustion. The objective of this study is to observe effects of the baffle on the flame development using the external excitation in baffled combustion chamber. The hot firing test was to verify the performance of the dynamic characteristics of a flame using the external excitation in the baffled combustion chamber. CH* chemiluminescence images were recorded using the high-speed camera.

428 - A low cost microwave detonation velocity measurement system

F. Vivot

Since 1960's, microwaves systems are known to be able to measure continuously the detonation front velocity with a very good accuracy. Indeed, high ionized detonation fronts reflect standing electromagnetic waves but with a Doppler shift in frequency generated by the front displacements. This is then post processed to retrieve the front velocity. First systems used klystron tube as emitter which are not produced anymore. Nowadays, technology developments have replaced these items by Gunn diodes and, more recently, by transistors which can be found in various all-day equipment and thus are very affordable. New and current design of microwave system for detonation front measurement will be addressed. Moreover, results will show the detonation velocity evolution in a 52mm detonation tube for C3H8+5 O2+xN2 mixtures with varying dilution x from 0 to 3.76. Use of microwave systems in detonation experimental devices is quite simple and they have the great advantage not to be intrusive.

432- Numerical Simulation of Reactive Gas Mixes Flows in The Detonation Engine

M. Sergey

Accurate mathematical model is needed for correct numerical simulation of detonation wave appearance and propagating in spin detonation engine, in particular, for ones using hydrogen as the fuel. As the matter of fact such engine does not exist. Detonation wave is connected with appearance of point explosion of gas mix. The origin of such explosion is mechanism of chain reaction in hydrogen-oxygen mix. In contradiction, in propagation of detonation wave chain reaction doesn't play significant role, as influence of temperature failure inside of shock wave.

435 - Simulation of a Detonation Propagation in a Two-phase Gas/Liquid Cross Flow Injection

N. Jourdaine, N. Tsuboi, K. Hayashi, X. M. Tang, K. Ozawa

Gaseous detonations for propulsive application or energy generation are studied around the globe with the promise to increase the engine or energy production efficiency. However, for real engine utilization where the volume and weight are limited, increasing the energy density by using liquid fuel is required. Liquid fuel detonation introduces more complications than gaseous detonation such as droplets distribution and size effects, partial evaporation, and poor oxidizer/fuel mixture. If a few simulation studies were carried out on the subject, the field still suffers a lot of unknown. The purpose of this research is to create a simulation code to study detonation in a liquid fuel injection cross-flow for rotating detonation engine. The two-phase liquid-gas flow simulation applies an Eulerian/Eulerian approach with an adaptive mesh refinement (AMR) method to reduce the computation cost. The governing equations are the two dimensional Navier-Stokes equations with nine species mass conservation equations. The detailed chemical reaction model for hydrogen combustion is the UT-JAXA model. For the code construction, the current condensed phase is water and the spray is represented by a single droplet size owing to the locally monodisperse formulation of the employed mesoscopic Eulerian/Eulerian approach.

436 - Generation of shock wave in a tube by detonation of spherical high explosive

E. Anderzhanov, S. Medvedev, A. Tereza, S. Khomik, B. Khristoforov

The aim of the present study is experimental investigation and numerical simulation of blast generator based on detonation of spherical high explosive placed axially symmetric inside a tube. In the experiments, thick-walled metal pipes with a radius of $R = 15$ and 19 mm were used in which PETN

spherical charges of 0.8 and 2.5 g (density 1600 kg/m³) were exploded. The motion of the shock front in air or xenon was recorded by the shadow technique through longitudinal windows in the tube. Details of a complicated flow pattern cannot be revealed on the basis of the experimental dependence of the velocity of the shock front on time (distance). To overcome this difficulty 3D numerical simulation were performed using GAS DYNAMICS TOOL package (Zibarov, 2000) with implemented procedure for detonation of high explosive. For the sake of validation of numerical method the shock-front arrival time t_A at a distance of 200 mm from the charge was chosen as a reference parameter. The calculated values of t_A was found to be (1.6-1.8) times shorter than that experimentally determined. It should be noted that in the present experimental arrangement the scaled distance Z from the center of the charge to the tube wall is varied from $Z = 0.11$ to $Z = 0.2$, where $Z = R/M^{1/3}$ and M is the charge weight (in units of mass). Such a short distance can set limits on the accuracy of calculations of incident and reflected shock parameters. Meanwhile, the intensity of the reflected shock has a great impact on the velocity of shock propagated along the tube.

437 - Lower Explosion Points of selected reference substances under Non-Atmospheric Conditions

A. Lucassen

The lower explosion point (LEP) is an important safety characteristic parameter in explosion protection. It is defined as the temperature of a combustible liquid at which the concentration of the saturated vapour equals the lower explosion limit. This makes it a much more accurate safety measure than the longer used and more widely known Flashpoint. For atmospheric conditions there is an European standard (EN 15794) for the determination of explosion points (lower and upper). Also the Chemsafe database at PTB already various holds data for various substances. However, modern industrial processes often use non-atmospheric conditions to enhance the yields. For instance, for partial oxidation of alcohols to aldehydes or carboxylic acids higher pressures or pure oxygen are used. Our work aims to expand the standardised determination method for higher pressures and non-air oxidizers. A theoretical method using the vapor pressure and temperature dependence of the lower explosion limit can be employed to estimate pressure dependence of the LEP, but in many cases, there is a lack of reliable input or LEP validation data. Therefore, an apparatus to measure the LEP at pressures from a 100 mbar up to 6 bars was designed and constructed. The apparatus does include optical access to ensure the connection to the optical detection of the LEP defined in the standard.

440 - Experimental Investigation and Modeling of Oxidizer Size and Concentration Effects on Composite AP/HTPB Propellant Burning Rates

J. Thomas, C. Dillier, E. Petersen, G. R. Morrow

The effects of altering ammonium perchlorate (AP) particle size or loading in composite AP/HTPB solid propellants are well documented. Existing propellant datasets include these variations, but they have significant holes in their current data span. In the current study, IPDI-cured composite AP/HTPB propellants were manufactured with AP loadings between 70-85% and AP sizes between 20-200 μm , and propellant burning rates were evaluated between pressures of 2,250-5,000 psi. Decreasing the AP particle size or increasing the AP loading yielded increases in burning rate, as expected from known results from the literature. The AP particle size effect is more drastic than that of the AP loading. The developed dataset was coupled with several existing propellant datasets to develop a simple empirical correlation that captures these effects. The developed correlation accurately predicts propellant burning rate for a large span of AP particle sizes and loadings, as well as test pressure. The classical three-flame model is derived from first principles, coupled with the latest available thermophysical data, and implemented to predict burning rates. The model is compared to experimental results and shows good agreement.

441 - Performance Enhancement of HTPB Fuels burning in Gaseous Oxygen by Metallic Additives

J. Thomas, F. Rodriguez, E. Petersen, A. J. Tykol

Low regression rates in hybrid rockets have limited their capability and application. Addition of metallic particles to hybrid rocket fuel systems has been shown to increase the regression rate specific energy of the fuel. This behavior has been widely explored for aluminum additives, but relevant data is lacking for alternative metal fuels. In the current study, HTPB fuel grains were loaded with aluminum, magnesium, titanium, and zirconium micro-particles; aluminum and boron nano-particles;

and magnesium-coated boron nano-particles to study their relative effects on the combustion behavior. Ballistic experiments were conducted in gaseous oxygen crossflow at moderate pressure (<1 MPa) and oxidizer mass fluxes up to 300 kg/m²-s. Accumulation of the metals on the fuel surface is observed to reduce heat feedback from the diffusion flame to the virgin fuel. The combustion efficiency of all motors is observed to vary with residence time of the fuel in the combustion chamber. Fuels loaded with micro-zirconium outperformed all other in terms of theoretical performance and experimental regression rate.

442 - Burning Rate Characterization of Ammonium Perchlorate Pellets Containing Energetic and Catalytic Additives

F. Rodriguez, E. Petersen, J. Thomas, C. Dillier, E. Petersen

Ammonium perchlorate (AP) is a common oxidizer utilized in composite propellant applications ranging from military use to space exploration. The regression rate of AP in composite propellants relative to the binder can have significant impacts on the global burning rate, and thus is important to evaluate on its own. Gaining a deeper understanding of the underlying mechanisms of AP combustion can enhance the ability to properly control these effects in composite propellants. The combustion behavior and burning rates of baseline AP pellets with high purity have been evaluated in a constant-volume bomb at pressure of 3. 4-34. 4 MPa (500-5,000 psi) and compare well with the available literature. AP pellets manufactured with AP particles coated in TCP were observed to deflagrate slower, and exhibited a significantly higher low pressure deflagration limit. AP pellets containing metal oxide and energetic additives are currently being evaluated for their combustion behavior and burning rates. Preliminary results indicate that the burning rate of AP can be selectively tailored by the incorporation of proper catalysts.

444 - A review of the effect of particle size and particle concentration on burning velocity calculation in FLACS-DustEx: a simplified approach

M. Ghaffari, T. Skjold, K. V. Wingerden, A. Hoffmann, R. Eckhoff

Storage and handling of combustible dusts in many industries, e. g. metal ore processing, plastics and elastomers, pharmaceuticals, food and agricultural grains, involve a serious hazard of dust explosions. Powders and granular materials consist of distribution of particle sizes. In particle combustion problems, the particle size plays arguably the most important role in determining the relative contribution of chemical and transport processes. (Eckhoff, 2003; Ogle, 2016). This paper reviews the flame modelling and the effect of particle size and its concentration on burning velocity, with particular emphasis on numerical modelling of dust explosions in the process industries. In the computational fluid dynamics (CFD) tool FLACS-DustEx, the turbulent burning velocity is calculated using an empirical correlation that incorporates turbulent flow conditions and the laminar burning velocity. Building on a previous study (Ghaffari et al. , 2018), this paper examines a new formulation for the laminar burning velocity that takes into account the effect of particle size and its concentrations with a new methodology, i.e.adapting Williams (1985) approach for liquid mist for dust flames. Particle concentration (loading) is also considered as an important factor in flame propagation. In case of lean mixtures of fuel particles, the particles will burn to completion while in case of rich fuels, some particles will be found in the combustion products with diameter smaller than the original diameter (Ogle, 2016). Using the aforementioned simplified approach, a new formulation for the laminar burning velocity tailored for our large-scale simulation software will be derived.

451 - Effect of impurities on thermal hazard of dimethyl 2,2'-azobis (2-methylpropionate) (AIBME)

A. Yu, X. Pan, M. Hua

Dimethyl 2,2'-azobis(2-methylpropionate) (AIBME) is an azo initiator. The substance is unstable and easily decomposes after being heated. AIBME is inevitably in contact with impurities such as acids and alkalis in the process of initiating the reaction. Some impurities may change the thermal decomposition behavior of AIBME. Therefore, in this paper, the effects of common impurities (hydrochloric acid, sodium hydroxide, iron oxide) on the thermal stability of AIBME were studied by differential scanning calorimetry (DSC). The activation energy was determined by Kissinger method and compared with pure materials. The results showed that three impurities reduced the heat release of AIBME during the decomposition process. However, hydrochloric acid reduced the activation

energy of AIBME, increasing the risk of AIBME, while sodium hydroxide was the opposite. So it is necessary to avoid contact between AIBME and hydrochloric acid in industrial production.

452 - Determination of the explosion characteristics of methanol -Air mixture in a 20-l sphere

H. Yu, X. Zangö

In this work, the effects of ambient temperature and methanol temperature on the explosion characteristics of methanol droplet were investigated by performing experiments in a 20-l closed sphere at different equivalence ratios. The ambient temperature and methanol themselves temperature were varied from 298. 15K to 318. 15K, respectively. Results show that, the explosion range of methanol droplets in the 20-l closed sphere is 118. 8-594. 0 g/cm³. Compared with the explosion range of pure methanol vapor (78. 6-628. 6 g/cm³), the explosion range of methanol droplets is narrower, and the sensitivity of the droplets is lower than that of pure methanol vapor. As the ambient temperature in the 20-l closed sphere increases, the explosion range of methanol droplet becomes wider. When the methanol temperature or the ambient temperature in the 20-l closed sphere remains unchanged, the corresponding explosion characteristics firstly increase, and then decrease at the inflection point of equivalence ratio=1. 8. When equivalence ratio=1. 8, there is a maximum explosion pressure in the methanol droplet explosion. The increasing ambient temperature and methanol temperature can improve the evaporation and atomization of methanol, and then promote the transient physicochemical process in the 20-l closed sphere. However, the effect of ambient temperature is more significant than the factor of material temperature on the explosion characteristics of methanol droplet explosion. The ambient temperature and equivalence ratio both affect the explosion index of methanol droplet explosion. When equivalence ratio=1. 8 and the ambient temperature is 303. 15K, the intensity of methanol droplet explosion is greater than the intensity of methanol gas explosion.

456 - Experimental study on the detonation propagation behaviors through a single orifice plate in hydrogen-air mixtures

X. Sun, Q. Li, S. Lu, L. Wang

In this study, the regimes of detonation transmission through a single orifice plate were investigated systematically in a 6-m length and 90-mm inner diameter round tube. A single obstacle with different orifice size (d) from 10 to 60 mm was adopted to study the effects of the induced perturbations on the detonation propagation. Here, particular attention was paid to the cases for which the blockage ratio (BR) is greater than 0. 9, i.e., the cases of small hole diameter of $d < 25$ mm. Because it is a more practical and important problem in industrial safety. Detonation velocity was determined from the time-of-arrival (TOA) of the detonation wave recorded by eight high-speed piezoelectric pressure transducers (PCB102B06). Detonation cellular size was obtained by the smoked foil technique. The characteristic of detonation velocity evolution were quantitatively analyzed after it passes through a single obstacle. The experimental results showed that with the increases of BR from 0 to 0. 96, the effect of BR on the upper limit of detonation propagation is more serious. Once the detonation wave fails in the fuel-rich side, it is difficult to be re-initiated due to the larger sound speed of products. As the BR values are further increased to 0. 972 and 0. 988, no detonation wave can be observed, indicating the perturbation induced by orifice plates has exceeded the critical condition of detonation formation. Of note is that the detonation is easier to be produced in the fuel-lean side when the BR values are greater than 0. 802. This can be explained and the specific reasons are as follows: Firstly, the stronger shock wave is easier to be formed at the fuel-lean side due to the smaller products speed of sound. Secondly, the hydrogen-air mixture is unstable with highly irregular detonation cellular structures, which is easier to induce a detonation wave. Finally, the disturbance is sharply enhanced in the larger BR cases, which facilitates the fast mixing of combustible gases. Moreover, the critical condition for detonation propagation through an orifice plate can be quantified as $d/\lambda > 1$ where λ is the detonation cell size.

459 - Experimental Study of the Spray Characteristics of Liquid Jets in Supersonic Crossflow

C. Li, Q. Li

The spray characteristics of a water jet in Mach 2. 85 air crossflow were investigated experimentally using a Phase Doppler Anemometry (PDA) system. The droplet diameter and velocity of liquid jets with various nozzle diameters were measured and analyzed. Experiments with liquid jets positioned ahead of a cavity were performed to investigate the effects of the cavity on the spray characteristics. For the liquid jet distributed from a nozzle positioned from the plane wall, the SMD distribution

presented a C shape, and the u presented a mirrored C shape. The maximum u did not appear at the maximum height of the spray, due to the interaction between the air crossflow and the spray boundary. An inverse tendency was observed, in that the SMD became larger downstream at $y/h > 0.5$. A reasonable explanation was proposed based on the motion of the droplets. Large droplets were more prone than small droplets to move from the lower layer to the upper layer of the liquid jet, which resulted in an increase in the SMD downstream. For the liquid jet distributed from a smaller nozzle positioned from the plane wall, the secondary atomization was accomplished earlier, and the final SMD had a lower value. The SMD distribution was related to the x-component velocity, because the small nozzle resulted in a shorter acceleration process with the same condition of the airflow. Consequently, the leeward region of the liquid column injected from the nozzle receded somewhat. That led to a difference in the u of the liquid jets injected from the three nozzle diameters tested.

460 - Comparison of OH-PLIF visualization of the supersonic combustion in partly premixed and diffusion hydrogen-air flow

Q. Yang, X. Xu

As the promising power device for hypersonic vehicle in the future, the dual-mode scramjet has attracted more and more attention from all over the world. Strut fuel injection and flame stabilization is a desirable configuration for the dual-mode scramjet because of the higher penetration depth. Supersonic combustion visualization is of great significance to the development of scramjet, particularly for the premixed and the diffusion combustion system. Planar laser-induced fluorescence (PLIF) of the OH radical is employed to visualize the supersonic combustion field in a strut-based hydrogen fueled scramjet. Experiments are carried out in the scramjet test facility at Beihang University. The hydrogen combustion heater was employed to simulate Mach 2 flight conditions. The stagnation temperatures 1230 K and additional oxygen was injected into the airflow to keep a 0.21 O₂ mole fraction in the heated products. The scramjet which consists of an isolator and a combustor has a total length of 1310mm. The cross section area of the isolator is maintained at 32mm (height) × 54mm (width), as shown in Fig. 1. The OH-PLIF system employed in the research is based on the method outlined by Cai et al. The strut locating at the central isolator can realize the hydrogen side injection and post injection, corresponding to the partly premixed and diffusion combustion respectively.

462 - Effects of fluidic jet angle on detonation propagation in Rotating Detonation Engines

Z. Luan, Y. Huang

In recent years, the potential benefits of applying rotating detonation engine (RDE) to modern propulsion systems to revolutionize current engines have generated significant interest, because RDEs have high thermodynamic efficiency, short burning time and relative mechanical simplicity. Most of the researches now focus on the propagation of detonation waves under premixed atmosphere, but in a practical RDE, local variations in reactant homogeneity and species concentration have significant impacts on the propagation of detonation waves. The detonation wave propagates in a non-premixed atmosphere, which have few researches yet. A numerical simulation in the paper is performed to study the effects of fluidic jet angle on detonation propagation in the RDEs. The Reynold Average Navier-Stokes (RANS) equations are used as the governing equations in the paper. Turbulence model is Two-Equation k-ε model. Roe Riemann solver is used to construct inter-cell numerical upwind fluxes. The continuous TVD limiter is used for construct a second-order method in space. A H₂/O₂/N₂ reaction mechanism including 7 species and 7 elementary reactions is used. The computational domain includes pre-detonation tube and combustor as shown in Figure 1.

470 - Effect of molar ratio of H₂ to O₂ on gaseous detonation synthesis of graphene quantum dots

C. He, X. Wang

Graphene quantum dots (GQDs) have attracted growing interest due to their interesting electrochemical and photoluminescent properties. However, it is still a challenge to establish a solvent-free and rapid method to prepare GQDs on a large scale. In this study, GQDs are fabricated using a one-pot gaseous detonation approach with benzoic acid (BA) as the carbon source and H₂-O₂ mixture as the explosion source. Furthermore, through altering the molar ratio of H₂ to O₂, three types of GQDs are obtained. Their morphology, composition and optical properties characterized by Transmission electron microscope (TEM), X-ray diffractometer (XRD), Raman spectra, Fourier

transform infrared (FTIR) spectra, Elemental analyses, UV-Vis spectroscopy and Photoluminescence (PL) spectra suggest that all the GQDs possess multilayered structures and multitudes of sp² subdomains with oxygen-containing functional groups. Meanwhile, higher molar ratio of H₂ to O₂ is beneficial to formation of more oxygen-containing groups and has little effect on optical properties.

471 - Theoretical Study on the Deflagration to Detonation Transition Process

W. Zhang

DDT process is a research hotspot in the field of detonation at present. It is a complex non-linear physical process which involves shock wave mechanics, thermodynamics, chemical reaction kinetics, etc. In this paper, A quantitative criteria of DDT is obtained by theoretical analysis, which is in good agreement with experimental results. By introducing an expansion term in Euler equation, the quasi-detonation state is simulated successfully with one-step overall model or detailed chemical reaction model. A physical model of DDT is proposed. In this model, the detonation wave surface and the flame surface are transonic in the laboratory coordinate. The supersonic and subsonic flow region of the flame surface will produce different flow behavior, which directly affects the DDT process of the detonation wave. This model can explain the physical mechanism of DDT process and decoupling process of detonation explicitly.

13:20 Kinetics/Flames

392 - Propagation of Symmetric and Non-symmetric Flames in Channels

V. Kurdyumov, C. Jiménez, A. Dejoan

Symmetry loss of premixed flames propagating in narrow channels, planar and circular, is investigated. It is found that, depending on the flow rate, the Lewis number, the thermal expansion and the heat loss intensity, a bifurcation phenomenon can appear, leading to the existence of multiple solutions at the same set of parameters. In particular, the parametric influence on the critical bifurcation values is presented. Time-dependent simulations reveal that, as a general rule, symmetric flames are unstable with subsequent formation of non-symmetric flames. These results can be very important for practical applications, affecting, for example, the point of flashback.

393 - Investigation of flame measurement characteristics on multiple ion-probes

N. Miura

Ion probes are widely used in detonation and deflagration measurement for detecting the arrival of a flame front. The multiple ion-probe method we developed can record the shape and instantaneous acceleration / deceleration of the flame front by using multiple ion-probes installed on the inner wall surface of the combustion vessel. An investigation was performed to reveal the flame measurement performance of the multi-ion probe using a 58 mm diameter combustion tube with 120 points (12 rows x 10 rows) of multiple ion-probes installed at intervals of about 10 mm. The length of combustion tube was 1800 mm, and the multiple ion-probes was located 1640 mm from the ignition end. The combustible mixture was a stoichiometric mixture of methane and oxygen diluted with nitrogen. Flame propagation velocity was varied by the dilution rate of nitrogen. Three types of combustible mixture were used. The mixing ratio of them were CH₄: O₂: N₂ = 1: 2: 0, 1: 2: 0. 45, 1: 2: 0. 71. When the mixture of CH₄:O₂:N₂ = 1:2:0 was used, a fully developed detonation was observed at the multiple ion-probe measurement section. The observed flame front was macroscopically planar shape and perpendicular to the combustion tube axis. In the microscopic view point, the propagation velocity measured by adjacent ion-probes fluctuates the range of about 200 m/s with respect to the CJ detonation velocity of 2394 m/s. This is considered that the velocity fluctuation derived by micro-explosion was captured.

394 - Effects of projection length and diameter of ion-probe on flame detecting characteristics in 2-stroke gasoline engine

R. Kamei, T. Yatsufusa

In the present study, effects of the shape of ion-probe on flame detection characteristics in 2-stroke gasoline engine was investigated. Tested parameters of the shape in ion-probe were projection length and diameter of ion-probe wire. Projection length was changed as 0, 0. 5, 1. 0, 1. 5mm. Test results say that projection length has positive effects for flame detection. Longer projection length has higher sensitivity for flame detection. However, longer projection should be avoided because long projected ion-probe disturbs the flame itself and it becomes negligible. Diameter of ion-probe wire was changed

as 0. 3, 0. 5, 0. 7, 1. 0mm. Experimental results indicate that the size of diameter has negative effects on mean strength of detected flame signal. Although the detailed reason is still investigated, one possible reason is as follows. Combustion in piston engine varies widely in general. Ion-probe with larger diameter detects the weaker flame, and this makes mean value of detected flame signal small.

395 - Effects of flame detection performance on wire diameter of ion-probe

H. Yamamoto

In this study, the influence of the diameter of the ion probe on the flame detection characteristics was investigated by using four types of ion probes: 0. 1, 0. 5, 1. 0 and 2. 0 mm in ion-probe wire diameter. The tested gas was the stoichiometric mixture of methane-oxygen diluted with argon. Two types of combustible mixture were used. The mixing ratio of them were CH₄: O₂: Ar = 1: 2: 0, 1: 2: 0. 45. In the case of CH₄: O₂: Ar = 1: 2: 0, the output signal of the ion current tends to increase as the wire diameter became larger. However, comparing 1. 0 mm and 2. 0 mm, it cannot be said that the output signal is larger at 2. 0 mm than 1. 0 mm. In the case of increasing the wire diameter in expectation of an increase in the output signal, the optimum value exists in the ion-probe wire diameter. In the case of using CH₄: O₂: Ar = 1: 2: 0. 45, an increase in the output signal was observed as the wire diameter increased to 2. 0 mm. However, when the wire diameter was increased, the variation of the output signal got large. Same tendency was also observed in CH₄: O₂: Ar = 1: 2: 0. From the above, it is clarified that the smaller the diameter of the ion probe brings the smaller the signal output, but the smaller diameter is advantageous in the output stability.

396 - Laminar flame propagation and instability investigations of transportation fuels in a high-pressure constant-volume cylindrical combustion vessel

Y. Li

A high-pressure constant-volume cylindrical combustion vessel was designed to ensure the investigation of laminar flame propagation and instabilities over 298-500 K, 1-20 atm and a wide range of equivalence ratios for transportation fuels. A dual-direction-protection and self-sealing strategy was proposed to avoid quartz window damage and leakage at the static pressure up to 200 atm. Schlieren method with a high speed camera was applied to record the flame images. The nonlinear extrapolation method proposed by Kelley and Law was applied to obtain the laminar burning velocity (LBV). With this new apparatus, the laminar flame propagation of high boiling point fuels, such as aromatic fuels (benzene, toluene, ethylbenzene, n-propylbenzene), cycloalkane fuels (decalin), alkanes (n-heptane), alkenes (1-hexene and 1-heptene), alcohols (methanol, propanol isomers and butanol isomers) has been investigated under engine-relevant conditions. Apparent fuel molecular structural effects have been observed.

397 - A Study of Oxy-Combustion of Palm Empty Fruit Bunch with Coal

F. H. Wu, G. B. Chen, H. Lin, Y. C. Chao, C. Peng

In this study, the combustion characteristics of PEFB, Australian coal and their blend with various blending ratios are investigated. First, the feedstock is analyzed via proximate analysis, elemental analysis and calorimetry. The pyrolysis and combustion behavior of PEFB in the air and Oxy-fuel conditions are then investigated by thermogravimetric analysis (TGA). The combustion characteristic parameters (ignition temperature, burnout temperature and the comprehensive combustion characteristic index) are calculated from the TGA results and the synergistic effects of blends with various blending ratios are also studied. Evolved species in the flue gas are analyzed through Fourier-transform infrared spectroscopy (FTIR Analysis). A single pellet free-drop furnace is also used to investigate fuel ignition delay, fuel combustion time and burning rate. The current results indicated that replacing N₂ by CO₂ in the combustion atmosphere with 21% of O₂ caused increase in the ignition temperature and burnout temperature. When the O₂ concentration was increased to 30%, the ignition temperature and burnout temperature were lower than the air case. A slight decrease in the ignition temperature and a significant reduction in the burnout temperature were observed after the addition of PEFB. This trend became more obvious as the blending ratio was increased. The emissions of NO_x and SO₂ during oxy-combustion were lower than under air-firing conditions.

401 - Numerical study of the propagation of lean hydrogen-air flames in Hele-Shaw cells

A. Dejoan, D. Fernandez-Galisteo, V. Kurdyumov, J. Meguizo-Gavilanes

The premixed propagation of lean hydrogen-air flames (equivalence ratio 0.3) in adiabatic Hele-Shaw cells (i.e. two parallel plates separated by a small distance h) is investigated using numerical simulations with detailed chemistry and transport. We focus on the effect of the distance between plates, h , for a semi-closed system of size $50f$, where $f = 3.45$ mm is the flame thickness of the planar adiabatic flame. The mixture is ignited at the open end and a reactive front propagates towards the closed end. The simulations compare three cases, $h=0.1f$, $h=f$ and $h=3f$, in which the flow field is driven by viscous effects. Hydrodynamic and diffusive-thermal instabilities wrinkle the flame front to form small cellular structures that increase the overall propagation velocity. Symmetric and non-symmetric shapes are seen to emerge in the third dimension (i.e. along h).

404 - Effects of the Different Injection Delay on the Combustion Characteristics for the Propagation Flame in a Tube

Z. Luoyu, T. Kawakami, A. Yukiya

A lean burn mode is a way to reduce throttling losses. The engines designed for lean-burning can employ higher compression ratios and thus provide better performance, efficient fuel use and low exhaust hydrocarbon emissions than those found in conventional gasoline engines. The main conclusions are as follows: 1) The flame shape of turbulent premixed flame shows that the upper part of the flame is disturbed first, and the flame advances to the upper part as it is. There are also clear differences in the flame propagation velocity and measured values. 2) By focusing on the period during which the injection equivalence ratio and the flame propagation speed increase, it was observed that the injection timing at which the flame propagation speed increase effect appears is delayed as the injected pre-mixture shifts to lean. 3) When the injection equivalence ratio is less than the import equivalence ratio, comparing the influence of injection equivalence ratio and the mixtures injection timing it has been observed that the increase and decrease of the heat input does not greatly affect the maximum value of the flame propagation speed, but the pre-mixture injection timing has a significant effect.

406 - Influence of low hydrocarbon fuel addition on exhaust characteristics for small gas engines

Y. Hong, T. Kawakami, H. Matsunaga

In recent years, including petroleum, the reduction of fossil fuels is a serious problem. Natural gas and petroleum gas have attracted attention as environmentally friendly fuels. In terms of fuel shift from coal to natural gas, including not only passenger cars but also generators, both production and share rates are increasing compared to other alternative fuels. Due to the shale gas revolution in the United States, shale gas is noticed as a new fuel replacing petroleum, based on data of world oil consumption in 2000. Shale gas will become the main fuel, in addition, the price gap between oil and gas has shrunk and the linkage between markets has dramatically increased. So it is expected that demand will expand for practical use. Applications include natural gas vehicles, cogeneration systems, etc. Gas fuel is expected to penetrate daily life in a wide range from commercial to home use. And it is a research using a large gas engine for industrial use. There are a few research examples using small gas engines for domestic use. This study has investigated the combustion characteristics of a small gas engine, the effect of the addition rate and the combustion characteristic on the reduction effect of combustion products (NO_x, CO and HC) by adding low hydrocarbons to fuel. The main conclusions are as follows: 1) By adding a low hydrocarbon fuel to the small gas engine, there is an effect on reducing NO_x. 2) In small gas engines, the addition rate of low hydrocarbon fuel is limited to about 15%. 3) CO emissions decrease with increased engine load. 4) The results are linked to the CO results, and it is confirmed that CO₂ emissions are increasing under the condition that the complete combustion ratio increases.

408 - RANS Simulation of Turbulent Non-Premixed H₂/Air Combustion

H. Dong

The velocity of the incoming air in the combustion chamber of the scramjet engine is very high ($M > 1$), and the residence time of the combustible gas in the chamber is on the order of milliseconds. In such a short period of time, the mixing and chemical reaction are completed, and therefore, it is very important to be stable with the flame. In addition, shock waves are generated in the supersonic flow field, and there are complex interactions such as shock/flame, shock/boundary layer, shock/turbulence in the combustion chamber. In summary, there are complex problems in self-ignition, partial flameout, re-ignition, shock and turbulent combustion in scramjet engines. Supersonic non-equilibrium chemical

reaction flow has been showing great complexity in numerical simulations due to the complicated physics-chemistry interactive phenomena. Especially, the space-time multi-scale essentiality causes significant numerical difficulty, for instance, rigidity or stiffness of the Ordinary Differential Equation (ODE). A modified uncoupled method, which follows the idea of Strang splitting and has proved to be simple and efficient for solving the reactive flow system, is applied with using unstructured finite volume discretization and detailed reaction mechanisms. In order to further improve the efficiency of the uncoupled method, a chemical reaction detection criterion is designed to adaptively turn off chemical reaction computation. Numerical tests have shown significant efficiency improvement and satisfactory accuracy of the presented method.

409 - Ignition by electrical discharges - Interaction of the hot gas kernel with self-generated vortices

J. Kummer, S. Essmann, D. Markus, U. Maas, H. Grosshans

Electrical discharges in combustible atmospheres represent a safety relevant risk in several industries. The determination of minimum energies using capacitive sparks is a classical method to examine ignition hazards of combustibles. The minimum ignition energy (MIE) depends on the characteristics of the ignition source i.e. electrode types, spark gap and the characteristics of the electrical source. The MIE of a given combustible is not characterized by a single threshold value but is rather of a statistical nature. After the end of the energy coupling by the electric spark with a duration of 50 ns, the transition into a self-sustained combustion is hindered by various factors as the ignition process is a combination of physical and chemical effects comprising flow effects. In this work, numerical results are assessed to identify and quantify the processes influencing the ignition and early flame propagation, especially two-dimensional flow effects of hydrogen/air and methane/air mixtures at energy levels close to the MIE. An in-house tool for two-dimensional unsteady flames was employed which includes detailed transport and chemical kinetics models. The results are compared to Schlieren images from experiments. Our investigations reveal that the hot gas kernel produced by the electrical discharge interacts with vortices produced by the expansion of the gas kernel and the shedding shock wave. Therefore, the temperature and hence the ignition process are significantly influenced by enhanced mixing and cooling. The results of this work help understanding of processes relevant to the ignition by electrical discharges near the MIE.

411 - Optimizing Mixture Properties for Accurate Laminar Flame Speed Measurement from Spherically Expanding Flame: Application to H₂/O₂/N₂/He mixture

Y. Zhang

The uncertainty of laminar flame speed due to the extrapolation method can be diminished by using large radii data for spherically expanding flames. However, the wrinkling and subsequent development of cells at the spherically expanding flame surface caused by the hydrodynamic and thermo-diffusive instabilities might limit the range of usable large radii data. In the present study, the method of adding helium to reactive mixture was used to optimize the mixture property and mitigate the development of cellular instabilities. The flame stability theory developed by Matalon was utilized to obtain the optimized mixture composition for which onset of cellularity occurs at a predefined large radius. The laminar flame speed of optimized H₂/O₂/N₂/He mixtures with equivalence ratios ranging from 0.6 to 2.0, pressures of 50/80/100 kPa and initial temperature of 300 K was measured. For all the experimental cases performed, the extrapolation-induced uncertainty was below 2% in the error diagram which depends on Markstein length (L_b), the lower ($R_f;L$) and upper ($R_f;U$) flame radius bounds of the extrapolation range. Unstretched laminar flame speed and Markstein length were used to evaluate the performance of four chemical mechanisms. For unstretched laminar flame speed, it was shown that the deviation between the predictions of four chemical mechanisms and experimental data is less than 10% except for one model for a lean mixture at 50 kPa. Overall, the dynamical response of the flame to stretch rate could not be well reproduced by the mechanisms. The present work indicates that an appropriate framework based on Matalon's flame stability theory to improve laminar flame speed by optimizing the mixture properties was feasible. Nevertheless, the uncertainty of some required parameters like activation energy (E_a) and Zeldovich number (β) that lead to over-estimated critical radius should be explored and minimized.

412 - Micro-explosion effect of Bio-oil Spray Combustion

S. Yang

Biomass oil is converted from cellulose biomass by thermochemical process. The fuel has low heating value, high moisture and high viscosity multi-component fuel, so it cannot be used alone in existing power equipment. Most will be mixed with fossil fuels. In this study, the spray characteristics of bio-oil blended with kerosene were investigated experimentally. In the combustion of a single droplet, the kerosene droplets of some bio-oil were added to cause micro-explosion phenomenon. Therefore, this study uses synchronous image method. The effects of micro-explosion on the fracture frequency of liquid film and the characteristics of upstream turbulence field were discussed. The results show that adding a low ratios of bio-oil in kerosene changes the frequency of liquid film breakup and the length of liquid film. This is mainly because the kerosene added with bio-oil increases the viscosity and causes the surface tension of the liquid Film and thus change the characteristics of the breakup. In addition, the bio-oil contains a lot of volatile substances and water, so in the emulsified liquid droplets, it is easy to cause a micro-explosion phenomenon. The micro-explosion phenomenon affects the characteristic frequency of the flow field, however, the higher ratio of the bio-oil increases the viscosity of the fuel, and the characteristic frequency disappears. It is shown that adding only the biomass oil below a certain proportion range will affect the characteristic frequency of the flow field. In addition, the jet flow field itself has a low frequency characteristic frequency, and after the addition of the bio-oil, the high frequency characteristic frequency changes due to the micro-explosion phenomenon.

413 - High Efficiency and Clean Combustion of Converter Gas

Y. Zhai, S. Li, W. Yan

The effects of water vapor concentration in air and inlet temperature of converter gas on converter gas combustion were investigated by numerical simulation. When water vapor concentration in air increases from 0 to 5%, the emission concentration of CO and NO and the peak flame temperature decreases. When the inlet temperature of converter gas is constant, water vapor concentration increases from 0 to 0.7%, CO concentration in converter gas decreases rapidly. When converter gas temperature varies from 1050 to 1150 K, the effect of water vapor on NO is more significant. When the inlet temperature of converter gas increases from 823 to 1153 K, CO emission concentration decreases, NO emission concentration and peak flame temperature increases. At water vapor occurrence, CO is mainly oxidized by OH free radical, it reduces the maximum flame temperature, thus the formation of thermal-NO_x is reduced.

421 - Assessment of Chemical improvers for the oxidation of heavy fuels

A. M. Rayaleh, A. Comandini, S. D. Persis, N. Chaumeix, S. Abid

The aim of this work is to determine the effect of sensitizer achieved by the addition of promoters on the oxidation of hydrocarbons representative of kerosene. First, the addition of IPN to ethylene will be investigated. The work will focus on the transition from shock to detonation (TDD) in a 78mm diameter tube to reduce the distance and transition time associated the shock to detonation transition, over a given temperature and pressure range relevant to PDE application.

423 - Minimum ignition temperature of hybrid mixtures

D. Gabel, U. Krause, Z. Abbas

The minimum ignition temperature is an important safety value for handling gases, liquids and dust. The European regulation only provides standards to measure single-phase values. That poses a problem to industries where different phases occur at the same time, as there is no way to prove that the mixture does not have an ignition temperature that is not below the single values. Partial aim of the joint research project NEX-HYS is to provide an extension to the standard for the minimum ignition temperature of dusts (IEC 80079-20-2). Therefore, the Godbert-Greenwald oven is modified to allow testing dust, liquid and gas alone and in mixture with each other. Various experimental setups and combinations of dusts, liquids and gases and the single-phase values in comparison to the standardized values are tested and presented for discussion. The proposed experimental setup is only a slight modification to the furnace mentioned in the standard. Main changes are a solvent reservoir and an additional gas supply. First results are already published as a proof of concept. To provide a reliable base for a standardization the influence of these changes according to the ignition behaviour is tested in detail.

429 - Experimental Research about Combustion of Multi-hole Pintle Injector Using LO_x/GCH₄

K. Lee, J. Koo, J. Nam

Pintle injector can control injection velocity optimally at any combustion conditions with moving pintle parts. In addition, pintle injector can replace many injector elements to single element. For this reason, Pintle injectors have recently been adopted in rocket engines due to the advantages of combustion performance and weight savings [1]. Methane is researched as liquid rocket fuel in Europe recently [2]. Methane has advantages of higher specific impulse and cocking temperature compared to kerosene. Furthermore, NASA [3] is researching about Mars in-situ resource utilization technology for in-situ production. For this reason, LOx/GCH₄ combustion has been researched in DLR recently [4]. The objective of this work is to analyze the combustion efficiency depending on geometric parameter, like number of pintle hole and pintle opening distance. The experimental system was designed for 500N of thrust and 20 bar of chamber pressure. Cryogenic liquid oxygen and gaseous methane was adopted as main propellant, and gaseous oxygen and methane was used for torch ignitor. The cross-section view and dimensions of a pintle injector are shown in Table 1.

430 - Unsteady Dynamics of Impinging Jet with Swirl and Premixed Combustion Studied by PIV and PLIF

L. Chikishev, V. Dulin, L. Aleksei, R. Tolstoguzov, D. Sharaborin

Impinging jet-flames have wide applications in industrial and domestic heating purposes, in particular for intensive heating of solid materials. The present work focuses on experimental study of flow structure and coherent structures in impinging jets with strong swirl and combustion by a combined application of OH PLIF, HCHO PLIF and PIV. To reveal coherent structures, the experimental data were processed by proper orthogonal decomposition (POD). The jet flow was produced by a swirl burner, oriented vertically, and impinged normally on a flat metallic plate. The burner consisted of an axisymmetric contraction nozzle with a vane swirler mounted inside. The inner diameter of the nozzle was $d = 15$ mm. The swirl rate was 1.0 to induce vortex breakdown. The impinged plate represented bottom of a steel cylindrical tank (with the diameter of 300 mm) installed above the nozzle. This work was funded by Russian Science Foundation (Grant No 16-19-10566).

431 - Structure of premixed flames of H₂/CO mixtures at atmospheric pressure: experimental and numerical study

D. Knyazkov, A. Dmitriev, T. Bolshova, A. Shmakov, V. Dulin

In this work we report new experimental data for chemical speciation in the atmospheric pressure burner-stabilized premixed flames diluted with Ar and fuelled with H₂/CO (1:1) mixture at equivalence ratios of 1 and 2. In atmospheric pressure conditions we were able to span a wide range of equivalence ratios and therefore to reveal the tendencies observed with the change in the unburnt mixture composition. The goal was to ascertain how the available models for syngas combustion reproduce these tendencies, particularly for labile flame intermediates. This will allow a formulation of guidance for further development of predicative kinetic schemes of syngas combustion. Flame sampling molecular beam mass spectrometric setup with soft electron impact ionization was used in this work to examine laminar premixed flames of H₂/CO/O₂/Ar mixtures stabilized on a Botha-Spalding burner. Argon mole fraction in the mixtures was 0.75. The flames were sampled by a sonic quartz probe with 0.07 mm orifice diameter. Spatial variations above the burner of mole fractions of reactants (H₂, CO, O₂), major flame products (H₂O, CO₂) and intermediates (H, O, OH, HO₂, H₂O₂) were measured.

433 - An adaptive multiresolution framework applied to turbulent compressible reacting flows

M. Sroka, J. Reiß

In the current work the adaptive multiresolution technique is applied to three dimensional reactive flow problems. The aim of this work is to provide a new code, which is able to speed-up combustion computations for practical applications while controlling the errors due to the mesh adaptation and reach high performances in massively parallel processing.

438 - A new miniature shock tube for kinetic studies

S. Abid, N. Chaumeix, A. Comandini, S. Nagaraju, R. Tranter

Conventional shock tubes have been widely used to carry out chemical kinetic studies using numerous complementary detection techniques 1-3. Nevertheless, these shock tubes do not allow access to the most recent advanced techniques based on Synchrotron light due to physical and operational

constrains. Recently, miniature shock tubes have been designed and constructed to overcome such limitations thanks to their small dimensions (around one meter in length) and high-repetition rates (up to 4 experiments per second) 4-5. The coupling between miniature shock tubes and Synchrotron based techniques provides a powerful tool for performing complex kinetic studies at engine-like conditions with the potential to finally bring light on long-standing problematics. In this work, we will discuss the design of a new miniature shock tube. The shock tube which has been developed at ICARE, based on the original design by Tranter and Lynch1, has a driven section of 1.05 m length and an internal diameter of 8 mm. Five pneumatically operated valves are used to evacuate the exhaust gases from the driven section and fill the shock tube with fresh gas mixture before each experiment.

439 - Entropy and Exergy Analysis of Syngas Premixed Flames with a Detailed Mechanism

L. Acampora, F. S. Marra

The entropy production (second law-based) and exergy loss analysis, from historical point of view, were developed to evaluate and optimize the performance of energy conversion systems [1]. For those systems involving a combustion process, it has been concluded that the major part of the exergy loss is due exactly to the combustion process [1]. Therefore, entropy production has been investigated in several combustion processes, for example: droplet combustion [2]; spray combustion [3]; coal/carbon combustion [4]; laminar premixed flames [5, 6]; diffusion flames [7]. Four irreversible processes are responsible for entropy production during combustion: viscous dissipation, heat conduction, mass diffusion, and chemical reaction [6]. The scope of this work is to study the local entropy production due to these processes in premixed syngas laminar flames taking into account detailed chemical kinetics and transport data.

446 - Spontaneous Combustion of Hydrogen/Oxygen Mixtures in Nanobubbles

S. Chakraborty, L. Qiao, S. Jain

Loyal to the scaling law, we would expect combustion to be impossible at nanoscale because heat loss would profoundly dominate chemical reactions. Svetovoy et al. [1, 2], though an accidental discovery, however, claimed that the hydrogen and oxygen gases (generated by water electrolysis) could be ignited spontaneously in nanobubbles with sizes smaller than 150 nm. If this is true, the nanobubbles would be the first nanoscale device in which combustion took place. Motivated by this, we developed an experiment similar to that of Svetovoy to see if we could get same results. Moreover, a microfabricated thermal sensor was employed to measure the change in the temperature (and the amount of heat produced), which would provide important insights on whether combustion of H₂ and O₂ in nanobubbles took place or not. A chip consisting of several pairs of micro-electrodes was fabricated. Bubbles were generated by electrolysis of a 1M solution of Na₂SO₄ in deionized water. In addition to the experiment, we also performed reactive molecular dynamic simulations to understand the mechanism that contributes towards the spontaneous combustion of H₂/O₂.

447 - A detailed computational model of a wood-fired cookstove for determining the effect of geometric parameters on thermal efficiency and emissions

R. K. Velmati, V. Sankar, C. Tighe, M. Serrar

Improving the thermal efficiency and reducing harmful emissions of biomass-fuelled cookstoves has long been of interest to researchers. Millions of families in India and developing countries worldwide use simple wood-fired stoves for cooking. The emissions from the incomplete combustion of wood, including soot, volatile hydrocarbons and carbon monoxide all have health effects, which become evident only in the long term. Thus there is a global challenge to improve cook stove design to reduce harmful emissions without reducing the efficiency. The development of new designs of cook stoves, which produce less emissions, is imperative and a better understanding of biomass combustion inside the stove is essential for improvements in stove design. The present work focuses on the development of a detailed CFD model of a natural draft cook stove, using the commercially available CFD software ANSYS FLUENT 19.3.

448 - Methane Number model based on a Deep Neural Network

A. Jach, K. Malik, M. Zbikowski, A. Teodorczyk, L. Kapusta

The Methane Number, just as the Octane Number, provides an indication of knock propensity of a fuel. It is an important metric for manufacturers of reciprocating engines, as high efficiency, fuel flexibility and low emissions are highly desirable. However, the range of fuels, which customers are

willing to utilize in the engines is increasing, i.e. due to an idea of energy storage in fuels (Power-to-Ammonia, Power-to-Hydrogen, etc). The motivation for this work is to extend widely available Methane Number calculators and enable assessment of knock propensity of new fuels, not present in the calculators. The Methane Number model is developed using a Deep Neural Network. The model takes as an input physicochemical properties of a mixture (e. g. , ignition delay time and laminar burning velocity at certain condition, activation energy, molar mass) instead of a name of this mixture. In order to develop the model firstly an extensive dataset of methane numbers for variety of mixtures has been collected from the Cummins Fuel Quality Calculator.

449 - Experimental Study of combustion syngas released from gasification of agriculture waste in a downdraft gasifier

B. Sarh

The main objective of this research is to investigate the combustion and emission characteristics of syngas by using an atmospheric flame burner. The syngas produced by gasification of olive waste particles in a small pilot scale 5 kWth downdraft fixed bed gasifier, where the oxidizing agent is a air, was combusted in a combustor through a burner. The gasifier has an inner diameter of 0.190 m lined with refractory cement and a height of 0.682 m. The throat diameter is 0.047 m. The gasifier and burner are made of stainless steel. The nozzle exit inner burner diameter is 25 mm. The fuel nozzle consists of a center body fuel injector, a radial air swirler, and a mixing area. Thermocouples type-K were used for recording temperature profiles at different parts of the gasifier and at different sections of air/syngas flame. Air flow at the inlet of the gasifier is regulated via mass flow controller while the syngas is regulated by high temperature vortex flow meter. For syngas and exhaust analysis, gas chromatograph and exhaust gas analyzer were used, respectively. Syngas combustion emissions measured include NO, CO, O₂ and CO₂. In this work, we compared the performance of olive waste and wood pellet as fuels for downdraft gasification to reveals the influences of the operating parameters such as reactor temperature and equivalence ratio on the hydrogen rich-syngas composition. The composition of syngas and gasification performance for olive waste and wood pellet were analyzed comparatively. Physicochemical characterization were checked through ultimate and proximate analyses as well as energy content measurement.

450 - A Study on the Combustion Characteristics of Non Class 1E Cables with Accelerated Deterioration

M. Kim, H. J. Seo, E. H. Jang, M. C. Lee, S. K. Lee, Y. S. Moon

A nuclear power plant (NPP) demands in-depth defense systems as they can cause serious accidents related to radioactivity leakage. However, a NPP is complex and large in scale and has a lot of combustible materials, such as complex devices and facilities and large amounts of cables. Therefore, in the event of a fire, fire spread by combustible materials can cause damage to the cables and cause malfunction of the safety system. In addition, the smoke with hazardous combustion products can have negative effects on the evacuation of occupants and manual actions of operators for safe shutdown. A NPP uses class 1E cables for the system connected inside the containment unit, and non-class 1E cables used for the other areas. The sheath and insulation of cables account for the largest number of combustible materials in NPP. In this study, Non-class 1E cables, which is mostly used in NPP, were selected as test specimen. In this study, combustion characteristics and composition of combustion product gas are investigated with respect to the lifetime of these cables according to the standard code of KS F ISO 5660-1 and ISO 19702.

453 - Flickering of Momentum-driven Jet Diffusion Flames

X. Xia, Y. Gao

This work was motivated by our recent progress in studying the buoyancy-driven instability of jet diffusion flames [J. Fluid Mech. , vol. 855, pp. 1156-1169], where we have demonstrated the effectiveness of vortex dynamics in calculating the formation of the toroidal vortex, which is outside of the flame sheet and responsible for the periodic dynamics of the flame, and derived a theoretical scaling relation for the flame flickering phenomenon. In an attempt to extend the theory to momentum-driven jet diffusion flames, we employed the particle image velocimetry (PIV) technique to experimentally investigate the additional physics associated with high-momentum fuel jet. By focusing on the small vortices inside the flame, which are primarily initiated by the Kelvin-Helmholtz instability, we expect to understand the associated instability mechanism and eventually identify the

nature of the interactions between the inner and outer vortices. The understanding gained from this work would further assist the considerations of the inner vortices effect as well as the baroclinic vorticity generation mechanism in analytically modeling the flickering of momentum-driven jet diffusion flames.

454 - Large eddy simulation of the response of turbulent non-premixed flame to acoustic perturbation

Y. Cheng, K. Luo

Combustion instability is a major challenge in the development of low-emission advanced gas turbine. The mechanism of combustion instability in practical combustion devices involves very complex interactions between acoustic, combustion and hydrodynamic. In the present study, the effects of inflow perturbations on the turbulent swirling non-premixed C₁₂H₂₃-air flame in a combustor are investigated via fully compressible Large Eddy simulation (LES). Subgrid turbulence is modelled by the Wall-adapting local eddy-viscosity (WALE) sub-grid model and Dynamic Thickened flame model is applied to handle turbulence-combustion interaction. The Navier-Stokes characteristic boundary condition (NSCBC) method is used to handle acoustic reflection at the boundary. A reduced two-step kerosene-air chemical reaction scheme is used to describe chemical reaction.

455 - Experimental Study on Intrinsic Thermoacoustic Instability from a Lean-Premixed Swirl Combustor with Tunable Acoustic Liners

L. Xu, S. Wang, J. Zheng, G. Wang, X. Liu, L. Li, F. Qi

In present work, a lean premixed swirl combustor with a tunable acoustic liner is built. A length of quartz tube is also mounted at the bottom of the chamber to capture the heat release signal with fast speed camera and photomultiplier (PMT). A hot-wire anemometer is set at the upstream of the flame and synchronized with the PMT to obtain the flame transfer function. The results show that: (1) in most cases, the ITA mode would arise as the 1/4 wave mode becomes stable. (2) The ITA mode is more unstable at relatively higher equivalence ratio, while the 1/4 wave mode is more prone to be triggered at lower equivalence ratio. (3) Within the scope of the present experiment, for the ITA mode, the HRR (Q') are always out of phase with the acoustic velocity perturbation U' . However, for the 1/4 wave mode, Q' are in phase with U' . (4) The ITA mode could be triggered with the increase of the bias flow Mach number. The pressure amplitude of the ITA mode would almost increase with the bias flow Mach number. (5) Changing the axial position of the acoustic liner and the rows of the small holes might have some influence on the ITA mode.

457 - A New Aerosol Shock-Tube Facility for the Study of Mixtures with Large Hydrocarbons

S. Cooper, O. Mathieu, E. Petersen, B. Guo, J. Hargis

A new shock-tube facility for the study of gas and condensed-phase measurements is discussed. The facility was constructed for use at the Doha, Qatar campus of Texas A&M University. The facility is modeled after prior experiences by the authors and recent developments from the literature. This shock tube has many of the same features in other facilities used by the authors, but it also has some additional features to enhance the utility of the present shock tube as compared to other versions. For the purposes of the current project, the shock-tube facility will be used to study combustion properties of long-chain hydrocarbon fuel components and mixtures at realistic engine conditions. To this end, an aerosol generation and entrainment facility is utilized along with an enlarged driver section and double-diaphragm interface between the driver and driven sections.

458 - Effect of char combustion reactions on drag force coefficient

H. Zhang, K. Luo, T. Jin, J. Fan

In this study, a particle-resolved simulation is performed using the ghost cell immersed boundary method to analyze the effect of char combustion reactions on the drag force. The effect of heterogeneous and gaseous reactions and the particle temperature are considered. The flow pattern is observably changed due to the Stefan flow induced by the heterogeneous reaction. The wall normal velocity is non-zero and therefore the boundary layer is thickened. As a result, the viscous stress is influenced. The recirculating wake becomes shorter and detached to the particle and the exact separation point doesn't exist. The heterogeneous and gaseous reactions change the species distribution around the particle and cause a considerable effect on the drag force. The particle with only heterogeneous reactions is compared with the particle with outflow. It shows that the effect of

Stefan flow is offset by the larger pressure drop caused by the species distribution. The drag force is even slightly aggravated by the heterogeneous reactions and this result is opposite to the effect of the Stefan flow. The gaseous reaction significantly aggravates the drag force.

463 - Single-pulse shock tube investigation on the pyrolysis of n-heptane and benzene

S. Abid, N. Chaumeix, A. Comandini, A. Hamadi, W. Sun

Among the different detection techniques used to perform kinetic studies with conventional shock tubes (ST), gas chromatography (GC) and mass spectrometry (MS) have been widely implemented for the measurement of stable intermediates from the pyrolysis and the oxidation of fuel components and mixtures¹⁻². In the present work, the single-pulse operation of a new ST-GC/MS facility is tested. First, the effects of the dump tank and the buffer gas on the pressure profiles will be presented. The facility was also used to study the thermal decomposition of n-heptane behind reflected shock waves under highly-diluted, pyrolytic conditions (100 ppm of n-heptane in argon bath gas), for temperatures between 900 K and 1900 K, nominal pressures of 10 bar, and reaction times of around 4 ms. The experimental profiles for both the decomposition of n-heptane and the formation of the main intermediate compounds are in good agreement with the simulation results obtained with recent chemical kinetic models. n-Heptane chemistry has been widely studied for decades now and the kinetic models have reached high level of accuracy, thus this first part of the study constitutes a validation of our experimental set-up. Additional experiments were performed on the pyrolysis of benzene at similar conditions to the ones considered for n-heptane. In particular, the work will focus on the formation of polycyclic aromatic hydrocarbons (PAHs), including biphenyl, acenaphthylene, indene, and naphthalene. The data will be analyzed using kinetic modeling and mechanisms for the PAH formation will be tested and proposed.

464 - Droplets autoignition simulations of ethanol mixtures with a reduced kinetic mechanism

A. M. Merino, E. F. Tarrazo, M. Sánchez-Sánz, F. A. Williams

Droplet ignition and combustion is a very relevant problem in combustion applications. Many studies have been conducted in the past, both theoretical [1, 2] and experimental [3, 4]. In view of the increasing use of biofuels, either as pure fuels or mixed with hydrocarbons, accurate modelling of vaporization and chemistry of such fuels is needed in order to optimize the systems to be used with biofuels and thus, facilitate their introduction. Ethanol is, by large, the most used biofuel, because it is easy to produce and because it is adequate to be used with present-day systems, considering both engine technology and fuel storage aspects. In typical combustion applications involving liquid fuels, the fuel is injected, in the form of a spray, in the combustion chamber, where the prevailing conditions include recirculated exhaust gases at high temperatures. In these conditions, heat transfer from the produces fuel vaporization and a fuel mixture evolves in the gas phase until either ignition is forced or autoignition is achieved. In this work we will focus on the vaporization and autoignition of a single multi-component droplet in realistic high temperature ambient conditions, in the absence of microgravity. With the aim of obtaining realistic autoignition times, accurate submodels for the different inter-coupled physical phenomena are required.

465 - High-Speed OH* and CH* Chemiluminescence Imaging and OH-PLIF Diagnostics in Spherically Expanding Flames

P. Parajuli, M. Turner, E. Petersen, W. Kulatilaka, T. Paschal, Y. Wang

To the best of our knowledge, the present work is the first-time demonstration of these diagnostics for spherically expanding flames. A high-speed CMOS camera coupled with a high-repetition-rate intensifier was used to acquire the volume-averaged OH* and methylidyne (CH*) chemiluminescence signals at 2 kHz frame rate during the flame propagation. The OH* emission represents the reaction zone and CH* is the marker of the flame front with its spatially resolved form obtained after Abel inversion. Subsequently, a 10-Hz, nanosecond, Nd:YAG laser pumped tunable dye laser was used to perform phase-locked OH PLIF, and images were acquired using an ultraviolet, intensified charge-coupled device (ICCD) camera. These OH PLIF images acquired from the sequential experiments show the temporal distribution of flame diameter and OH radical distribution ensuing the Q1(5) rotation of the AX (1,0) transition. In addition, an adiabatic Hencken burner calibration was used to calculate the OH number density from the images of OH fluorescence. Further studies will involve

the use of these diagnostic techniques as an extension of research on current laminar and turbulent flame conditions as well as the detailed kinetics modeling of spherically expanding flames.

467 - Effect of a DC electric field on the flame stability and soot emissions in an ethylene diffusion flame

A. S. Kassem, P. Gillon, M. Idir, V. Gilard

. First of all, the transmitted signal was used to derive the natural frequency of instability using a Fast Fourier Transform (FFT). Then, the maximum, minimum and mean signal intensities were recorded in each cycle and averaged during the acquisition time. These values were compared to the signal intensity in a stable flame at the same fuel flow rate. A stable flame was obtained with the addition of an air co-flow. Figure 1 presents an FFT of a signal collected during flame instability. As shown, the natural frequency of flame instability was close to 11 Hz. This value is in accordance with the values mentioned by Shaddix & Smith [1]. Figure 2 shows the radial distribution of soot volume fraction (f_v) for both stable and unstable flames at $HAB = 40$ mm. In this graph, the values of maximum, minimum and mean soot emissions for an unstable flame are exhibited in addition to the corresponding values in a stable flame case.

468 - A GPU Accelerated Filtered Density Function Discontinuous Galerkin Large Eddy Simulator

A. Kaltayev, M. Inkarbekov

A new GPU accelerated solver is presented and utilized for large eddy simulation (LES) of turbulent reacting flows. In this solver the effects of chemical reactions are modelled via the filtered density function (FDF) model. The base filtered transport equations are approximated via discontinuous Galerkin (DG) scheme and the FDF transport equation is solved numerically by Lagrangian Monte Carlo (MC) scheme. Computational performance tests show that the GPU algorithm can outperform the sequential CPU algorithm by factors of 156 and 212 times for DG and MC procedures, respectively. The consistency and the overall performance of the solver, and the realizability of the simulated results are demonstrated by LES of a temporally developing mixing layer under both non-reacting and reacting conditions. This brings LES of turbulent flows to a new level, facilitating efficient simulation of more complex turbulent flows.

477 - Exploring Flame dynamics of lean, diluted hydrogen mixtures

N. Chaumeix, N. Kouame, L. Wartski

The aim of the present work is to investigate the behavior of lean hydrogen/air flames diluted by steam. ENACCEF 2, a new vertical facility has been built at ICARE laboratory and will be used to study the flame propagation regimes of hydrogen diluted mixtures in closed, obstacle laden tube. The effect of the initial temperature and of dilution with steam is investigated. The combustion regimes, in terms of flame velocity profile and pressure loads, are characterized using a series of photomultiplier tubes.

